DIRECTED EVOLUTION OF ANGIOPOIETIN-BINDING PROTEINS BY SOMATIC HYPERMUTATION AND CELL SURFACE DISPLAY

Thesis submitted for the degree of

Doctor of Philosophy

at the University of Leicester

by

Kathryn Helen Steele BMedSci BMBS MRCSEd

Department of Cardiovascular Sciences

University of Leicester

2013

ABSTRACT

Directed Evolution of Angiopoietin-Binding Proteins by Somatic Hypermutation and Cell Surface Display

Kathryn H Steele

Angiopoietin-2 (Ang2) is a secreted ligand that promotes blood vessel destabilisation, remodelling, leakage and inflammation in response to pro-inflammatory activators. In binding to its primary receptor, Tie2, it functions as a competitive antagonist of the anti-inflammatory and pro-quiescent agonist angiopoietin-1 (Ang1). Ang2 is markedly elevated in conditions associated with vascular dysfunction and therefore development of an Ang2 inhibitor has multiple potential clinical applications. Ligand traps are developed from native receptor ectodomain fragments and offer improved pharmacokinetics over monoclonal antibodies. However production of an Ang2-trap requires manipulation of the endogenous Tie2 receptor to permit Ang2 but not Ang1 binding, and this objective formed the inspiration for this study. The aim was to test whether the somatic hypermutation (SHM) gene diversification activity of B cells could be combined with cell surface display to create a streamlined system for evolving binding proteins. The data presented demonstrates that a cell surface-expressed Tie2 mutant library can be generated via single transfection of a chimeric Tie2 ectodomain-cell surface display construct into the hypermutating DT40 cell line. Subsequently selection of Ang2-binding phenotypes via fluorescently labelled-angiopoietin binding assay and Fluorescence Activated Cell Sorting (FACS) was repeated iteratively prior to sequencing of Tie2 from recovered cells. This approach was successful in isolating mutant forms of Tie2 with altered binding characteristics. Directed evolution is one of the most powerful approaches for manipulating binding properties of proteins but traditionally has involved laborious techniques including iterative cycles of mutagenesis, expression and selection with inter-species translation issues. This combination of vertebrate 'in-cell' diversification and 'on-cell' binding and selection demonstrates a sustainable approach for evolution of any protein.

ACKNOWLEDGEMENTS

I am first and foremost sincerely grateful to my supervisor Professor Nicholas Brindle, who is a constant source of support and encouragement. The conception, logistics and continued investment in this research would not have been possible without his efforts.

I thank the Brindle group and associates, past and present, for technical assistance and entertainment. In particular I must mention Shikha Sharma, Tariq Tahir, Djalil Baiou, Nisha Patel, Julie Chamberlain, Ankur Karmokar and Christoph Boes.

Finally I am grateful to all involved with Plastic Surgery training in the Trent region, especially those at Leicester Royal Infirmary, for their assistance and understanding during this period of research.

DEDICATION

To Nick in New York

CONTENTS

CONTENTS

TABLES

FIGURES

CHAPTER ONE

CHAPTER THREE

CHAPTER FOUR

CHAPTER FIVE

ABBREVIATIONS

A *(nucleotide)*	Adenine
AICDA	Activation-induced cytidine deaminase
AID	Activation induced cytidine deaminase
Alpha-MEM	Minimum essential medium, alpha modification
Ang	Angiopoietin
APOBEC1	Apolipoprotein mRNA editing enzyme, catalytic polypeptide-like
APS	Ammonium persulphate
ASGPR	Asialoglycoprotein receptor H1 subunit
BER	Base excision repair
B_{max}	Maximal receptor binding sites
bp	Base pair
C *(nucleotide)*	Cytosine
cDNA	Complementary DNA
CSD	Cell surface display
C-terminus	Carboxy-terminus
Cy2	Cyanine-2
D *(nucleotide)*	Guanine, adenine or thymine
ddH_2O	Double-distilled water
DEPC	Diethyl pyrocarbonate
DMEM	Dulbecco's modified eagle medium
DMSO	Dimethyl sulfoxide
DNA	Deoxyribonucleic acid

DNA pol	DNA polymerase
dsDNA	Double-stranded DNA
DTT	Dithiothreitol
ECD	Extracellular domain
EDTA	Ethylenediaminetetraacetic acid
eEF1α	Eukaryotic translation elongation factor 1α
EGF	Epidermal growth factor
eGFP	Enhanced green fluorescent protein
EGTA	Ethylene glycol tetraacetic acid
ELISA	Enzyme linked immunosorbent assay
ExoI	Mismatch repair exonuclease I
FACS	Fluorescence activated cell sorting
FCS	Foetal calf serum
FGF	Fibroblast growth factor
FI	Median fluorescence intensity
FITC	Fluorescin isothiocyanate
FN	Fibronectin
F_r	Ratio of mutant fluorescence to wild-type fluorescence
FReD	Fibrinogen-related domain
FSC	Forward scatter
Fv	Antibody variable domain
G *(nucleotide)*	Guanine
GFP	Green fluorescent protein
GMFI	Geometric MFI

G_1 phase	Gap 1 phase
G_2 phase	Gap 2 (pre-mitotic) phase
GPI	Glycophosphatidylinositol
gpt	Guanine phosphoribosyl transferase
H *(nucleotide)*	Adenine, cytosine or thymine
HEK	Human embryonic kidney
HRP	Horseradish peroxidase
IC50	Half maximal inhibitory concentration
Ig	Immunoglobulin
IRES	Internal ribosome entry site
K_d	Dissociation constant
K_{off}	Dissociation rate
K_r	Ratio of wild-type K_d to mutant K_d
LB	Luria Bertani
MerCreMer	Mutated oestrogen receptor-Cre recombinase double fusion protein
MFI	Mean fluorescence intensity
MMR	Mismatch Repair
MPA	Mycophenolic acid
M-phase	Mitotic phase
mRFP	Monomeric red fluorescent protein
mRNA	Messenger ribonucleic acid
MSH	MutS homologue
N-terminus	Amino-terminus
OD	Optical density

4-OHT	4-hydroxytamoxifen
PAGE	Polyacrylamide gel electrophoresis
PBS	Phosphate-buffered saline
PCR	Polymerase chain reaction
PDB	Protein data bank
PDGF	Platelet derived growth factor
PDGFR	Platelet derived growth factor receptor
PE	Phycoerythrin
PlGF	Placental growth factor
ψV	Pseudo variable gene
R *(nucleotide)*	Purine
Rev1	Y-family DNA polymerase
RFP	Red fluorescent protein
RNA	Ribonucleic acid
RPA	Replication protein A
RSV	Rous sarcoma virus
RT	Room temperature
RTK	Receptor tyrosine kinase
RT-PCR	Reverse transcriptase-PCR
SDS	Sodium dodecyl sulphate
SEM	Standard error of mean
SHM	Somatic hypermutation
SOC	Super optimal broth with catabolite repression
S-phase	Synthesis phase

S_r	Ratio of maximal fluorescence to cell autofluorescence
SSC	Side scatter
ssDNA	Single-stranded DNA
SV40	Simian virus 40
T *(nucleotide)*	Thymine
TAE	Tris-acetate-EDTA
TBS	Tris-buffered saline
TEM	Tie2 expressing monocyte
TEMED	Tetramethylethylenediamine
Tie	Tyrosine kinase with immunoglobulin-like and EGF-like domain
TGF	Transforming growth factor
TLS pol	Translesion synthesis polymerase
TNF	Tumour necrosis factor
tRNA	Total RNA
TSA	Trichostatin A
U	Uracil
UNG	Uracil DNA glycosylase
UV	Ultraviolet
VDJ	Variable Diversity Joining
VEGF	Vascular endothelial growth factor A
W *(nucleotide)*	Adenine or thymine
Y *(nucleotide)*	Pyrimidine

CHAPTER ONE

Introduction

The angiopoietin family of growth factors and Tie receptors play a central role in regulation of vasculature and represent an attractive therapeutic target due to involvement in inflammation, angiogenesis and lymphangiogenesis. Angiopoietin-1 (Ang1) is constitutively expressed and involved in maintenance of vessel structure and integrity, whereas Angiopoietin-2 (Ang2) is dynamically regulated and provides a key destabilising signal to potentiate vessel permeability and sprouting in combination with Vascular Endothelial Growth Factor A (VEGF) at sites of vascular remodelling (Thomas, Augustin 2009). Both ligands share a common Tie2 binding site although the mechanisms responsible for their differential actions are not understood. A ligand trap for Ang2, comprising a mutant form of Tie2 ectodomain with the ability to bind Ang2 specifically and not Ang1, would be an ideal molecule to block pathologically elevated Ang2.

1.1 Angiopoietin-Tie system

1.1.1 Angiopoietins

Four members of the angiopoietin family have been identified to date. Ang1 and Ang2 are the most widely studied, whilst Ang3 and Ang4 are mouse and human orthologs respectively. The structure of the secreted 70kDa glycoprotein is highly conserved between all group members and composed of an N-terminal superclustering domain, a coiled coil homo-dimerisation domain, a short linker and a carboxy-terminal receptor binding fibrinogen-related domain (FReD) sequence (Procopio et al. 1999, Barton, Tzvetkova & Nikolov 2005) (Figure 1.1).

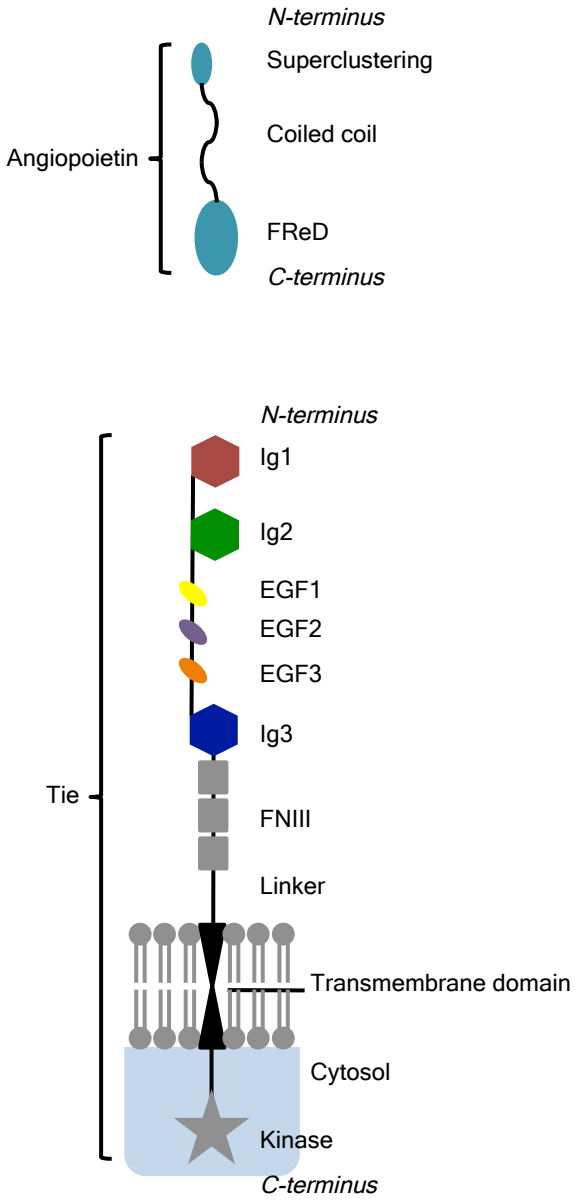

Figure 1.1: Angiopoietins & Tie receptors. Schematic diagrams illustrating modular structure of angiopoietins and Tie receptors. Structures adapted from Barton et al. 2006.

Overall there is 65% amino acid identity between Ang1 and Ang2 FReD sequences and 71% in their specific C-terminal receptor-binding portions (Davis et al. 1996, Maisonpierre et al. 1997).

1.1.2 Tie receptors

Tie (Tyrosine kinase with Immunoglobulin-like and EGF-like domain) receptors are type-1 transmembrane proteins (Davis et al. 1996, Maisonpierre et al. 1997, Suri et al. 1996). There are two family members, Tie1 and Tie2, which share 76% amino acid identity overall but only 33% in the extracellular ligand-binding domain (Schnurch, Risau 1993). The extracellular portion, from the amino terminus, is composed of two immunoglobulin loops, three EGF-like domains, a third immunoglobulin loop and three fibronectin type-III domains. The intracellular domain contains a tyrosine kinase domain, which is split by a kinase insert sequence, and followed by the carboxy-terminus tail (Dumont et al. 1992, Barton et al. 2006, Sato et al. 1995, Partanen et al. 1996) (Figure 1.1).

1.1.3 Angiopoietin-Tie interactions

Ligand-receptor interactions of the Ang-Tie family are shown in Figure 1.2a.

No specific Tie1-activating ligand or pathway has been proven. Conversely, the role of Tie2 is well documented. Angiopoietins 1-4 all interact with Tie2 (Maisonpierre et al. 1997, Davis et al. 1996, Valenzuela et al. 1999). Functional analyses indicate that the initial 210 N-terminal residues of Tie2 ectodomain, or

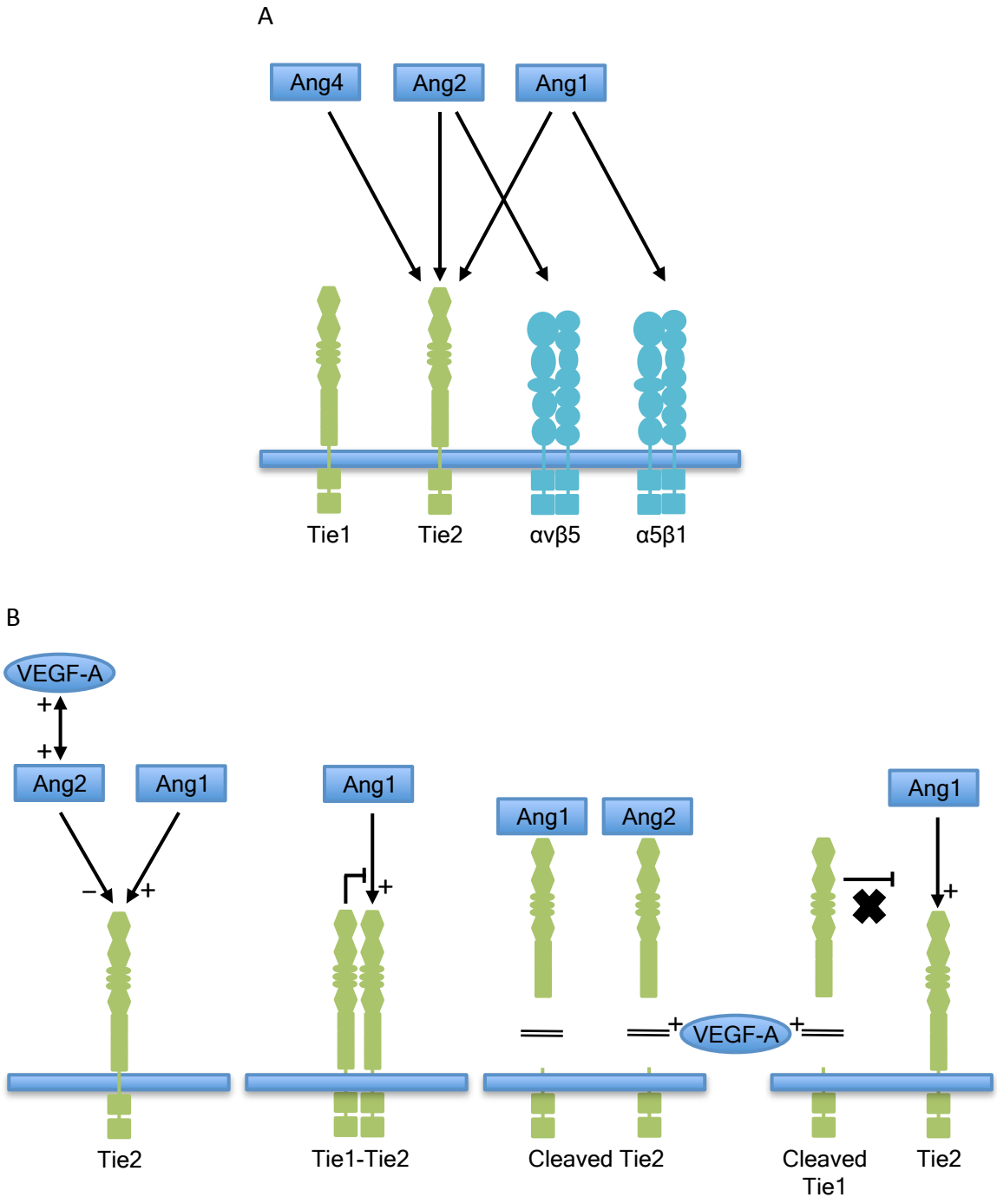

Figure 1.2: Angiopoietin-Tie ligand-receptor systems.
Schematic representation.

a) Angiopoietin ligand-receptor interactions. Documented ligand-receptor interactions are shown for the angiopoietin growth factors. *αvβ5/α5β1= integrins.*

b) Regulation of angiopoietin-Tie interactions. The interaction of Ang1 and Ang2 with Tie receptors and possible effects of VEGF are shown.

Ig1 and Ig2 domains, are sufficient for Ang1 binding (Macdonald et al. 2006). Crystal structure analysis of the Ang2-Tie2 interaction revealed that the Ig2 domain is the only part of Tie2 to contact Ang2 during binding (Barton et al. 2006) (Figure 1.3).

The structure of the Ang2-Tie2 complex suggests potential molecular mechanisms responsible for ligand:receptor binding (Barton, Tzvetkova & Nikolov 2005, Barton et al. 2006, Macdonald et al. 2006). These mechanisms and the roles of amino acids at and flanking the binding interface have not been tested to date. Sequence homology between Ang1 and Ang2 and the ability of Ang2 to competitively antagonise Ang1-Tie2 binding (Fiedler et al. 2003, Maisonpierre et al. 1997) support the theory that both ligands bind to Tie2 in a similar manner. Of thirteen Ang2 residues that contact the Tie2 Ig2 domain according to crystal structure analysis, six are conserved and only three have significantly different properties between Ang1 and Ang2 (Barton et al. 2006).

The majority of published studies estimate similar binding affinities of Ang1 and Ang2 for Tie2 receptor *in vitro*. Immobilised protein assays and surface plasmon resonance produced dissociation constants (K_d) of 3.7nM and 3nM respectively for both ligands (Davis et al. 1996, Maisonpierre et al. 1997). Conversely a more recent ELISA based study reported that Ang2 has twenty times lower affinity than Ang1 (Yuan et al. 2009).

The stochiometry of angiopoietin-Tie2 binding is 1:1 (Barton, Tzvetkova & Nikolov 2005, Barton et al. 2006, Davis et al. 2003). However ligand oligomerisation is

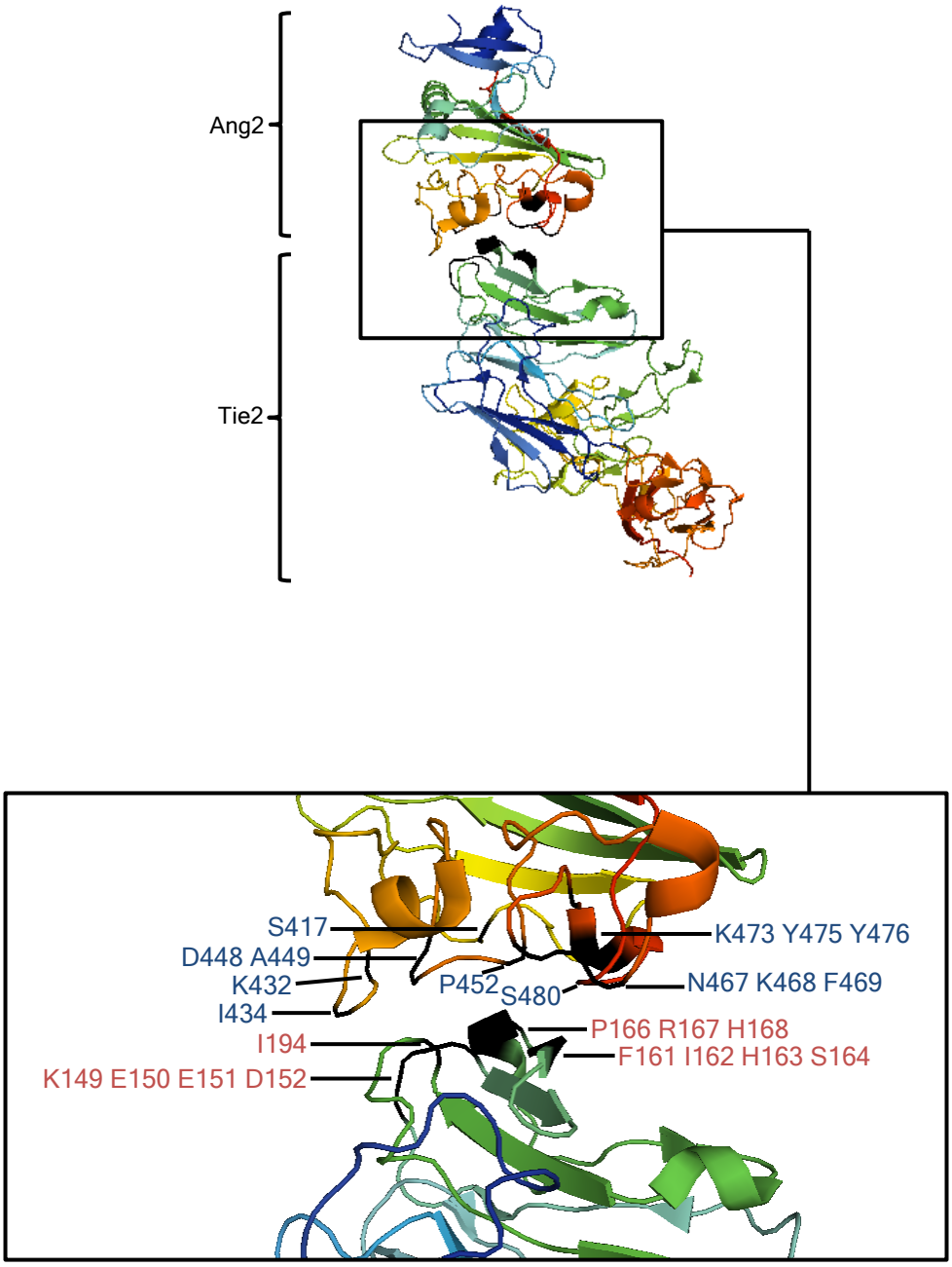

Figure 1.3: Crystal structure of Ang2-Tie2 binding interaction. Illustrates modular structure of Ang2-Tie2 binding interface. Modelled on PDB accession 2GY7. Interacting residues are coloured black and labelled (*blue=Ang2; red=Tie2*) (Barton et al. 2006).

essential for receptor activation, which proceeds via receptor dimerisation and autophosphorylation to activate various intracellular signalling pathways. Native Ang1 exists as a mixture of tri-, tetra- and penta- homo-oligomers and must present as a tetramer or higher order oligomer to activate Tie2 (Cho et al. 2004, Kim et al. 2005). Native Ang2 primarily exists as a disulfide-linked dimer (Kim et al. 2005, Kim et al. 2009, Procopio et al. 1999), and inability to form higher order multimers may limit its ability to activate Tie2 receptor (Brindle, Saharinen & Alitalo 2006).

1.1.4 Angiopoietin-Tie function

The Tie2 receptor and its ligands, Ang1 and Ang2, are crucial for blood vessel formation and maintenance (Davis et al. 1996, Maisonpierre et al. 1997, Dumont et al. 1994, Sato et al. 1993). Transgenic mouse models demonstrate the developmental roles of Ang-Tie family members. Tie2 or Ang1 deficiency precipitates vessel remodelling defects and embryonic lethality (Sato et al. 1995, Suri et al. 1996), whereas Ang2 overexpression produces a similar phenotype (Maisonpierre et al. 1997). Ang2 deficiency however produces severe vascular and lymphatic defects and impairs the inflammatory response (Maisonpierre et al. 1997, Gale et al. 2002) and knockout of the orphan Tie1 receptor also generates severe oedema and haemorrhage (Sato et al. 1995).

The effects of Ang-Tie signalling are also significant in mature vasculature. Tie2 is constitutively expressed in endothelial cells, haematopoietic stem cells and a sub-population of monocytes (Dumont et al. 1992, Sato et al. 1995, De Palma et al.

2005). When activated its downstream pathways influence cell migration, survival and cytoskeletal organisation (Brindle, Saharinen & Alitalo 2006). Spatial orientation of the receptor is relevant in determining the context-dependent effect (Saharinen et al. 2008).

Ang1 is continuously expressed by peri-vascular cells and activates Tie2 in a paracrine fashion to induce receptor oligomerisation and autophosphorylation (Suri et al. 1996, Davis et al. 1996). It is a potent inhibitor of vascular leakage, inflammation, and regression due to cell junction stabilisation and survival effects of downstream signalling pathways (Jones 2003, Peters et al. 2004).

In contrast Ang2 is dynamically regulated and functions as a context dependent antagonist of Ang1 (Maisonpierre et al. 1997). Inflammatory and other activators stimulate its rapid release from endothelial cells, where it binds but fails to activate Tie2 and impedes the tonic stabilising activity of Ang1 (Fiedler et al. 2004). The vasculature is consequentially rendered permeable, adaptable and responsive to environmental triggers (Fiedler et al. 2006).

However Ang2-mediated Tie2 agonism has been demonstrated in some circumstances and appears to be influenced by cell type, endothelial confluence, duration and concentration of Ang2 exposure and presence of co-receptors and other mediators (Fiedler et al. 2003, Brindle, Saharinen & Alitalo 2006, Bogdanovic, Nguyen & Dumont 2006, Yuan et al. 2009). Both Ang1 and Ang2 can also bind integrins and induce Tie-independent effects (Carlson et al. 2001, Cascone et al. 2005, Hu et al. 2006, Felcht et al. 2012).

The balance between Ang1 and Ang2 is critical in determining the activation state of the endothelium. Tissue hypoxia, thrombin, VEGF and other stimuli stimulate rapid release of Ang2 in both physiological and pathological situations to suppress Ang1 and consequently destabilise the vasculature (Fiedler et al. 2004, Scharpfenecker et al. 2005). Subsequent outcomes include vessel regression, angiogenesis and coagulation cascade activation depending on the influence of other vasoactive molecules including VEGF.

Ang-Tie2 signalling is also regulated at a receptor level. Full-length Tie1 heterodimerises with Tie2 and autophosphorylates (Marron et al. 2000), inhibiting Tie2-Ang1 binding. When Tie1 ectodomain is cleaved, as occurs rapidly under the influence of VEGF and Tumour Necrosis Factor-α (TNFα), the residual Tie1 endodomain is no longer able to modulate Tie2-ligand binding (Tsiamis et al. 2002, Marron et al. 2007, Singh et al. 2012). VEGF also stimulates Tie2 cleavage, albeit over a longer time course than Tie1 cleavage, which abolishes cellular angiopoietin binding and allows sequestration of free circulating angiopoietin by the soluble ectodomain (Singh et al. 2012).

The interactions of Ang1, Ang2, Tie1 and Tie2 and reported effects of VEGF are depicted in Figure 1.2b.

1.1.5 Angiopoietin-Tie in pathology

Elevated circulating Ang2 levels are associated with a number of primary malignancies, metastasis, inflammatory arthritides and mortality in sepsis (Zhou et al. 2007, Kuboki et al. 2008, Park et al. 2007, Helfrich et al. 2009, Orfanos et al. 2007). In contrast Ang1 appears to be protective in sepsis, ischaemic disease and certain tumours, though it can stimulate tumour growth in some circumstances and may be involved in inflammatory diseases (Cho et al. 2004, Witzenbichler et al. 2005, Imanishi et al. 2007, Yu, Stamenkovic 2001). In addition Ang2 is involved in recruitment of Tie2 Expressing Monocytes (TEMs) to tumours. TEMs express an aggressive proangiogenic phenotype on stimulation (Coffelt et al. 2010) and promote vascular ingrowth in therapy damaged hypoxic tumours (Kioi et al. 2010), which may be implicated in tumour recurrence.

In pre-clinical studies the administration of Ang1 to counteract pathologically elevated Ang2 inhibits progression of sepsis, diabetic retinopathy and ischaemia (Joussen et al. 2002, Witzenbichler et al. 2005, Nambu et al. 2004, Shyu et al. 1998, Novotny et al. 2009), but the effect on tumour growth is variable and dependent on dose, tumour type and concurrent Ang2 concentration (Shim et al. 2002, Machein et al. 2004, Ahmad et al. 2001, Tian et al. 2002, Hayes et al. 2000). The usefulness of therapeutic administration of Ang1 is also limited in a clinical context due to effects on vessel remodelling (Baffert et al. 2004, Cho et al. 2005) and possible involvement in pulmonary hypertension (Sullivan et al. 2003).

Animal models of angiopoietin blockade are more encouraging. Selective Ang2

blockade inhibits ocular neovascularisation whilst concurrent Ang1 blockade does not provide additional benefit (Oliner et al. 2004, Rennel et al. 2011). Selective Ang2 antagonism reduces tumour vascularity, normalises vasculature, produces sustained growth inhibition and inhibits metastasis (Falcon et al. 2009, Mazzieri et al. 2011, Holopainen et al. 2012). It also prevents upregulation of Tie2 expression in TEMs and reduces TEM association with tumour vessels, therefore inhibiting their proangiogenic activity (Huang et al. 2011, Mazzieri et al. 2011). A more potent reduction in tumour vascularity has been demonstrated with simultaneous Ang1 and Ang2 blockade compared with Ang2 blockade alone, but it does not induce vessel normalisation (Coxon et al. 2010, Falcon et al. 2009). However selective Ang1 antagonism does not inhibit tumour growth or vascularity (Falcon et al. 2009), confirming that Ang2 is the key familial effector molecule in tumour angiogenesis.

As alluded to previously, the molecular control of vasculature is an intricate system involving multiple players other than angiopoietins, including VEGF. Anti-VEGF therapies are more advanced in development than angiopoietin blockade, but despite positive pre-clinical reports they have only generated a moderate benefit in terms of overall cancer survival (Hurwitz 2004, Iwamoto et al. 2009). As with conventional chemotherapeutic agents, resistance to anti-VEGF therapies is emerging as a key issue (Fischer et al. 2007). Proposed mechanisms of resistance include upregulation of other vascular growth factors and proangiogenic cytokines, enhanced tumour cell activity and recruitment of proangiogenic bone marrow derived cells to the tumour (Bergers, Hanahan 2008). This therefore remonstrates the argument for combination anti-angiogenic therapy and suggests

that Ang2 is a suitable target.

The combination of VEGF and angiopoietin blockade further reinforces anti-angiogenic activity in tumour models. A chimeric decoy receptor for VEGF, Placental Growth Factor (PlGF), Ang1 and Ang2 produces more potent anti-angiogenic effects compared with VEGF-Trap (Koh et al. 2010) and synergistic use of Ang2 antagonist peptibodies with anti-VEGF agents suppresses growth and vascularity compared with either therapy alone (Hashizume et al. 2010, Huang et al. 2011).

The benefit of selective Ang2 blockade versus simultaneous Ang1 and Ang2 blockade remains debatable and may be contextual. Normalisation of vessels enhances the efficacy of synergistic cytotoxic and radiation therapies (Fischer et al. 2007, Falcon et al. 2009). It is not known whether tumour vessel normalisation or reduction in absolute vascularity is more effective, nor are the wider consequences of each method apparent. Initial reports of AMG386, a peptide-Fc fusion protein binding both Ang1 and Ang2, suggest anti-tumour activity in clinical trials for ovarian cancer (Karlan et al. 2012).

Minimal interference with normal physiology in terms of selective Ang2 blockade in preference to complete angiopoietin antagonism may theoretically be beneficial in reducing systemic toxicity. Adverse effects of peripheral oedema and hypokalaemia have been observed in human studies of the pan-angiopoietin blocking AMG386 (Karlan et al. 2012). Use of the chimeric VEGF-angiopoietin decoy receptor or VEGF-Trap in mice produces higher rates of thrombosis,

hypertension and microalbuminaemia than independent Tie2 blockade via Tie2-Fc (Koh et al. 2010). Therefore it is possible that angiopoietin blockade has a preferable side effect profile to that of VEGF generally.

1.2 Ligand traps

Whilst use of monoclonal antibodies has improved the specificity profile of anti-angiogenic and other drugs, polypeptides or endogenous peptides are likely to become the safest and least toxic therapy (Nakamura, Matsumoto 2005). In the case of ligand blockade, a soluble native receptor ectodomain is generally utilised as a 'ligand-trap' to sequester the target ligand (Economides et al. 2003). These small molecule agents offer improved tissue penetration, particularly through permeable tumour vasculature, and can be packaged such as by fusion to the immunoglobulin constant region (Fc) to improve pharmacokinetic properties (Huang 2009). The conjugated Fc domain prolongs the serum half-life and often improves the solubility and stability of the protein (Roopenian, Akilesh 2007). In addition all components are derived from endogenous molecules, which generally produces an excellent immunogenicity profile. Examples of clinically approved ligand-traps include Etanercept, a soluble form of tumour necrosis factor-α receptor, and Aflibercept, which contains fragments of VEGF receptors 1 and 2 and binds both VEGF and placental growth factor (Huang 2009).

Whilst a Tie2 ectodomain-Fc fusion protein could be produced to sequester both Ang1 and Ang2, selective Ang2 blockade would be more desirable in terms of

safety and toxicity. Efforts to create selective Ang2 antagonists to date have focused on RNA aptamers and antibodies (Oliner et al. 2004, White et al. 2003). The presence of natural agonist and antagonist ligands for a single Tie2 receptor binding site and as yet unravelled complexity of the Ang-Tie system create particular challenges in producing an Ang2-specific ligand trap. In order to do this it is necessary to explore the possibilities for engineering Tie2 ectodomain for differential Ang1 and Ang2 binding.

1.3 Protein engineering

Proteins have an extremely diverse role in the body, encompassing form and structure, transport, cell signalling and reaction catalysis. It is estimated that the number of distinct proteins in the human body is significantly higher than the 25,000 – 40,000 genes identified when post-translational modifications and splice variants are considered (Lander et al. 2001, Venter et al. 2001). The high degree of complexity and specificity in these naturally evolved molecules poses a challenge in synthetic mimicry.

Protein engineering involves manipulation of an amino acid sequence for desired functional gain. Proteins can be engineered to replace a protein that is deficient or abnormal, to augment existing pathways, to provide novel functions, to antagonise endogenous molecules, to deliver compounds in a site-specific manner and to produce vaccines. Modification of efficacy, stability, specificity, immunogenicity and pharmacokinetic properties may be necessary to convert a natural protein

into an effective drug. Although fusion of the immunoglobulin Fc domain may be sufficient to create an effective generic angiopoietin ligand trap, engineering of Tie2 for altered ligand binding properties requires adjustment of the native sequence.

Incremental single mutations are sufficient to achieve many desirable properties (Romero, Arnold 2009). Between 30% and 50% of mutations are strongly deleterious, generating truncated, unstable or inactive proteins. Approximately 50% to 70% are neutral, and only 0.01 to 0.5% are beneficial (Axe, Foster & Fersht 1998, Shafikhani et al. 1997, Guo, Choe & Loeb 2004). Multiplicity in mutations will not necessarily lead to functional gain and therefore only small modifications are often required.

So called 'promiscuous functions', those that can be improved by sequential beneficial mutations, are often present in the natural protein or a result of neutral mutations (Romero, Arnold 2009). Presence of stabilising mutations also compensates for the effects of more destabilising mutations, allowing greater diversity to be tested. As such, some proteins are intrinsically more evolvable than others (Bloom et al. 2007, England, Shakhnovich 2003, Tokuriki, Tawfik 2009).

Advancements in molecular biology, from the development of X-ray crystallography and site-directed mutagenesis to recombinant DNA technology, have led to huge expansion in the available approaches for protein engineering, which can be grouped into rational design or directed evolution techniques. Rational design involves generation and testing of specific amino acid substitutions

based on protein structure and function data. Directed evolution emulates natural selection by iterative screening and selection of randomly mutated libraries until the desired function is achieved or no further improvement is found (Figure 1.4). In practice a combination of strategies is often employed.

1.3.1 Rational design

Hypothesis driven manipulation of a protein sequence for specific functional change is only possible when the structure-function relationship is well defined. Non-covalent interactions including van der Waals and electrostatic forces, hydrogen bonds, hydrophobic effects and interactions associated with the tightly packed condensed interiors within proteins are relatively well understood. However the combinatorial complexity of subtle energetic changes is difficult to calculate and the difference in stability between active and inactive unfolded forms of a protein is often very small (Tokuriki, Tawfik 2009).

A combinatorial approach is often required, where undesired states are actively avoided by 'negative design' and the lowest possible free energy is ensured for the 'target state' (Hellinga 1997). This process can be augmented by computational design in which alternative natural fold sequences are utilised whilst maintaining compatibility and preservation of other protein functions (Orengo, Jones & Thornton 1994, Koga et al. 2012).

Despite these complexities, several rationally designed protein therapeutics are in continuous use. Many of the successes, including insulins, are based on fusion

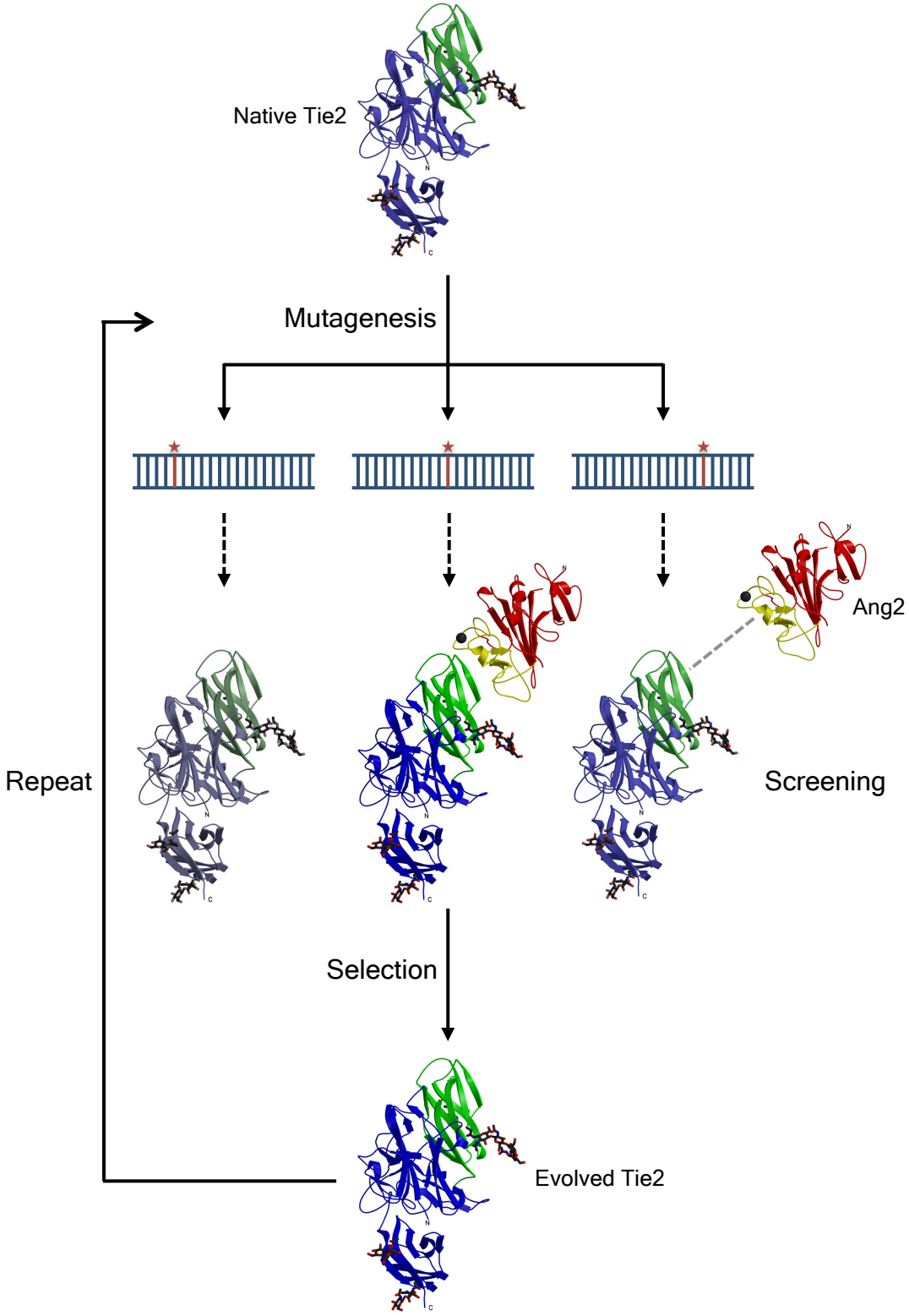

Figure 1.4: Directed evolution.
Schematic representation of a typical directed evolution experiment. The example depicts evolution of Tie2 receptor for increased angiopoietin-2 binding affinity. The native protein is subjected to mutagenesis, followed by screening and selection for improved ligand binding. The process is repeated iteratively until no further improvements are made. Structure of Tie2 and Ang2 adapted from Barton et al. 2006.

partners or changes to the oligomerisation state rather than modification of binding specificity (Brannigan, Wilkinson 2002). The outcome of such changes is more predictable than subtle changes to a binding interface, as would be required to differentially manipulate the binding of multiple ligands to a single receptor site as in the case of the angiopoietin-Tie2 interaction. In addition the crystal structure of Ang1 has not yet been defined and therefore there is limited data on which to base predictions of mutational outcome. An obvious limitation of rational design is that the number and combination of mutations tested is finite, and therefore the optimal molecule may never be realised.

1.3.2 Directed evolution

Directed protein evolution is one of the most powerful and successful approaches for altering molecular properties of proteins, including binding and recognition characteristics (Yuan et al. 2005). Generation of large mutant gene libraries is possible through a variety of methods, including error prone PCR (Mullis, Faloona 1987), DNA shuffling (Stemmer 1994) and sequence saturation mutagenesis (Wang et al. 2004a). A high throughput, sensitive and specific screening method is subsequently required to retrieve desired phenotypes from the pool, and the encoding DNA of each screened protein must remain identifiable.

Traditionally a mutant DNA library has been screened by laborious cycles of protein expression and selection. Therefore transformation efficiency and capacity of the screening method limit the realistic library diversity and multiple rounds of

mutagenesis are impractical. However up to 10^{10} variants can be screened with a high-throughput screening method (Daugherty, Iverson & Georgiou 2000).

If the mutant phenotype relates to a normal cellular function or can be assayed by means of a reporter gene, a single copy transformation is sufficient to enable selection. Alternatively phage- or cell- surface display can be utilised to allow rapid selection of binding characteristics via Fluorescence Activated Cell Sorting (FACS) or other methods.

DNA is generally expressed in non-mammalian host cells including *E. coli*, *S. aureus* and yeast. However for mammalian proteins these species are of limited utility due to differences in protein folding and post-translational modification that may crucially affect function. It is however difficult to achieve efficient transfection with single genomic integration of mutant DNA in mammalian cells and subsequent expression levels are variable (Majors, Chiang & Betenbaugh 2009).

Strategies for streamlining the evolution process have included *in vitro* translation and combination of the diversification and selection stages into a single format. Ribosome and mRNA display both negate the need for transformation and therefore permit screening of larger mutant libraries (Roberts, Szostak 1997, Zahnd, Amstutz & Pluckthun 2007, He, Taussig 2007, Grimm, Salahshour & Nygren 2012). Bacterial hypermutator strains have also been utilised to permit 'in-cell' diversification and selection (Orencia et al. 2001). However several groups have now utilised vertebrate hypermutating lymphocyte cell lines to mutate and select

fluorescent proteins following a single transfection (Wang, Yang & Wabl 2004, Wang et al. 2004b, Arakawa et al. 2008).

The choice of screening assay depends on the desired change in function, but sensitivity is crucial in detecting rare improved mutants and *in vitro* techniques are relatively insensitive in comparison with nature. The selection of mutants in each round of screening for use as the next parent population is generally based on a percentage with the best function (Daugherty, Iverson & Georgiou 2000). This process markedly reduces genetic diversity of the new parent population and limits the ability of a gene harbouring neutral or deleterious mutations to proceed, despite the possibility of epistasis whereby a particular combination of individually unremarkable mutations is ultimately beneficial (Romero, Arnold 2009). An alternative strategy is the neutral drift approach, where a high mutation rate and low selection pressure are applied to generate a more diverse and stable library as a starting point for positive selection (Bershtein, Goldin & Tawfik 2008).

For reasons outlined above evolutionary dynamics are not fully recapitulated by current methods of directed evolution. Although the protein 'fitness landscape' is not fully explored, affinity-enhancing mutants are often achieved and failure of the process is often due to an overambitious target, for example generation of a novel function (Bloom, Arnold 2009). Therefore whilst directed evolution offers vast scope for protein engineering it is limited by time-consuming and laborious techniques, inter-species translation, sampling of full potential and issues of screening and selection.

Of the methods described above, exploitation of somatic hypermutation (SHM) in vertebrate hypermutating cell lines has potential to address several difficulties. Its development had been limited to evolution of intrinsically fluorescent proteins until recently when an anti-apoptotic protein was evolved using the same method via intrinsic 'in-cell' screening (Majors et al. 2012). Theoretically this approach could be applied to evolution of any gene if a viable screening and selection method were designed. As the subtleties of the difference between Ang1 and Ang2 interactions are not well defined it is likely that directed evolution by such a method offers more opportunity for success than rational design techniques.

1.4 Somatic Hypermutation

The primary antibody repertoire is formed by immunoglobulin Variable-Diversity-Joining (V-D-J) recombination in which germline segments are recombined in different permutations. The resulting library size is species-specific and dependent on the number of available V, D and J segments and degree of imprecision at the sites of integration. However it is not sufficient to form a high affinity antigen response (Neuberger, Rada 2007).

Further diversification and affinity maturation occurs subsequently by somatic hypermutation (SHM), with or without gene conversion. SHM is the primary method of expansion in man and mouse and produces multiple single nucleotide substitutions at a frequency of 10^{-3} mutations per base pair per generation (McKean et al. 1984, Rajewsky, Forster & Cumano 1987), approximately 10^{6} times

greater frequency than other somatic cells. Gene conversion supplements the process in some vertebrates including chickens, which possess fewer VDJ segments and require insertion of upstream pseudo V gene donor sequences to increase diversity. Both mechanisms are triggered by the action of Activation-Induced Cytidine Deaminase (AID) (Muramatsu et al. 2000).

The targeting of AID-mediated mutation is not random. SHM occurs over a 1.5-2kb segment of the Ig V region beginning approximately 185 bases downstream of the transcription initiation site (Rada et al. 1997, Lebecque, Gearhart 1990). Hypermutation 'hotspots' are mutated with higher frequency than surrounding bases and regions of Ig V genes that are crucial for functional diversity are intrinsically more mutable than surrounding sequences. There is no known mechanism of SHM targeting for bases located outside of hotspots. Therefore the resulting library is not infinite but is sufficient for the intended purpose.

In man and mouse, SHM targets C:G and A:T base pairs with equal probability (Neuberger, Rada 2007). The most commonly referenced target 'hotspots' are R<u>G</u>YW and W<u>A</u> for G:C and A:T base pairs respectively, with the underlined base indicating the mutable position (Rogozin, Kolchanov 1992). There is no apparent strand bias in the case of R<u>G</u>YW and hence its inverse WR<u>C</u>Y is also included, but mutations at W<u>A</u> are more likely to occur if A is on the coding strand (Rogozin et al. 2001). However further analysis of a broader range of data suggests that D<u>G</u>YW, and its inverse WR<u>C</u>H, is a better descriptor of the G:C base pair hotspot (Rogozin, Diaz 2004); in this study adenine is most likely to be located at the 'D' position and the most mutable sequence overall is A<u>G</u>CT.

SHM occurs in two phases. In the first phase AID targets single stranded DNA and deaminates deoxycytidine residues to deoxyuracil, producing a U:G mismatch (Di Noia, Neuberger 2002). As summarised in Figure 1.5 the nature of the resulting mutations is dependent on the subsequent action of DNA repair machinery. Replication without repair results in C to T and G to A transition mutations, and transitions are responsible for around half of substitutions in germinal center B-lymphocytes (Rogozin et al. 2001, Neuberger, Rada 2007). Processing of the U:G lesion by Base Excision Repair (BER), Mismatch Repair (MMR) and translesion synthesis accounts for other mutations (Neuberger, Rada 2007). A:T base pair mutations are mediated by the action of the enzyme mutShomologue2 (MSH2) in the second phase of repair (Rada et al. 1998).

1.4.1 Activation Induced Cytidine Deaminase (AID)

Exploitation of SHM as a means of mutant library generation is dependent on utilisation of AID. AID is a 24kDa enzyme and part of the cytidine deaminase family with closest homology to the RNA-editing enzyme APOBEC1. The majority of AID is located in the cytoplasm due to its strong C-terminal nuclear export signal although AID is active in the nucleus (Magari et al. 2010). The mechanisms of AID regulation and targeting have only been partially delineated.

AID is expressed at high levels in murine and human germinal center B-lymphocytes (Muramatsu et al. 1999) during antibody affinity maturation. Crucially overexpression of AID can also induce SHM in Ig and non-Ig sequences

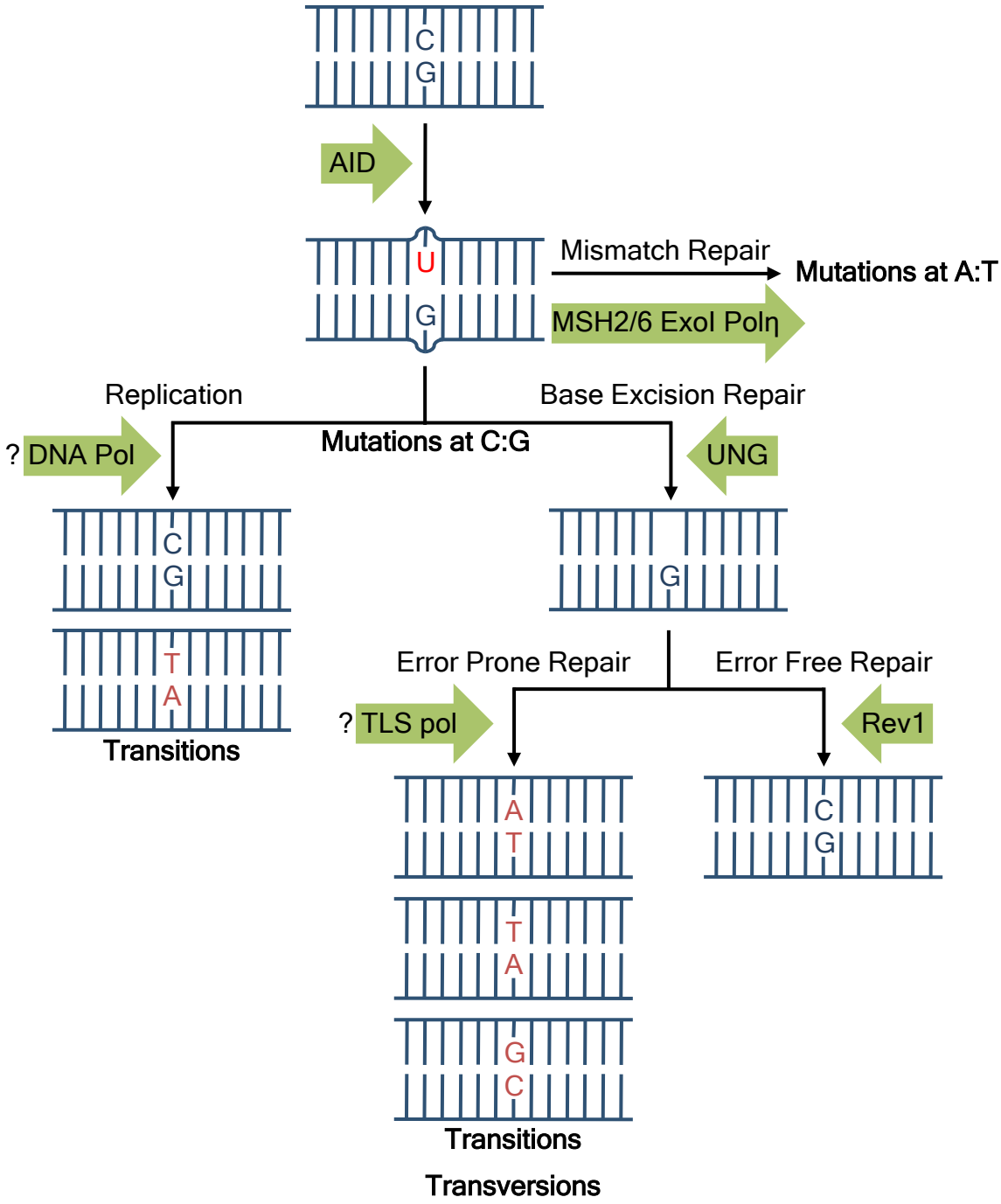

Figure 1.5: DNA repair pathways in somatic hypermutation.
Schematic representation of somatic hypermutation (SHM) featuring DNA deamination and repair pathways. Mismatch repair introduces mutations at A:T base pairs adjacent to the U:G lesion. *AID= activation-induced deaminase; ExoI= mismatch repair exonuclease I; MSH2/6= mismatch recognition proteins; Pol= polymerase; Rev1= Y-family DNA polymerase; TLS= translesion synthesis; UNG= uracil-DNA glycosylase*. Adapted from Neuberger, Rada 2007.

both within and outside the Ig locus in hypermutating and non-B cell lines (Martin, Scharff 2002, Wang, Harper & Wabl 2004, Wang, Yang & Wabl 2004, Wang et al. 2004b, Arakawa et al. 2008, Blagodatski et al. 2009, McConnell et al. 2012). Hence the AID expression level appears to be significant for the occurrence of SHM, although there are no published studies correlating this with mutation frequency.

Target gene transcription is required for SHM (Lebecque, Gearhart 1990) and the rate of SHM is also proportional to the transcription rate (Bachl et al. 2001). Accessibility of single-stranded DNA is presumed to be a major factor for SHM to occur via AID. Possible routes of access include the association of AID with replication protein A (RPA). AID may also interact with RNA polymerase II and therefore the transcription complex, although action of AID is not confined to the transcribed strand (Basu et al. 2005, Nambu et al. 2003). It has also been suggested that stem loop structures of single stranded DNA may influence base mutability, with transcription differentially stabilising stem-loop structures and exposing unpaired bases vulnerable to mutation (Wright, Schmidt & Minnick 2004).

The specificity of SHM for the Ig locus in B-lymphocytes suggests that *cis*-elements and *trans*-factors are involved. The endogenous Ig promoter is not required for immunoglobulin SHM (Rada et al. 1997, Yang, Fugmann & Schatz 2006). However the eEF1α promoter, for example, does not support SHM in hypermutating cell lines despite increased Ig expression levels relative to the endogenous Ig promoter (Yang, Fugmann & Schatz 2006). Transcription regulators, including a *cis*-acting 3' regulatory region located downstream of the Ig constant region, are reported to be vital for SHM (Kothapalli, Norton & Fugmann 2008, Blagodatski et al. 2009) and

disruption of the E2A transcription factor gene reduces mutation frequency despite unchanged AID expression (Schoetz et al. 2006).

1.5 Directed evolution and B cells

AID transfection has been utilised to perform SHM-mediated diversification of transgenes in vertebrate non-B cell lines, although the mutation rates are inferior to that of hypermutating cell lines (Yoshikawa et al. 2002, Martin, Scharff 2002, McConnell et al. 2012, Arakawa, Saribasak & Buerstedde 2004). Recently published studies have also combined AID co-transfection with cell surface display to evolve immunoglobulins in mammalian cell-based systems (Bowers et al. 2011, McConnell et al. 2012). Theoretically the combination of cell surface display with a hypermutating B cell line should provide a more efficacious technique for evolution of proteins for binding characteristics.

1.5.1 Hypermutating cell lines

The majority of SHM studies are in the context of immunoglobulin diversification in B-lymphocytes, where the frequency, distribution and regulation of mutation are not necessarily representative of the situation for transgenes in hypermutating cell lines. Three principal hypermutating cell lines, which constitutively express AID, have been utilised for evolution of fluorescent proteins. Ramos takes origin from human Burkitt's lymphoma, 18-81 from murine pre-B cells and DT40 from avian leukosis virus induced chicken bursal lymphoma.

Whilst Ramos and 18-81 only support SHM, DT40 is additionally capable of gene conversion (Arakawa, Buerstedde 2004, Arakawa, Hauschild & Buerstedde 2002). However modification of the DT40 genome by deletion of pseudo V donors (ψV^-) or RAD51 paralogues abolishes gene conversion and directs AID activity toward SHM.

Fluorescent proteins have been utilised both as reporter genes and as evolutionary models in each of the above cell lines. Efficient assay and selection of phenotype was achieved via Fluorescence Activated Cell Sorting (FACS) following single transfection of the fluorescent gene and propagation of a mutant population. C. Wang *et al.* demonstrated that a low fluorescence intensity mutant of enhanced green fluorescent protein (eGFP) could be mutated by SHM to varying levels of improved intensity after one month of culture and single selection in 18-81 cells (Wang, Yang & Wabl 2004). L. Wang *et al.* produced mutant forms of monomeric red fluorescent protein (mRFP) with improved photostability, termed mPlum and mRaspberry, after 23 rounds of sorting in Ramos (Wang et al. 2004b). Arakawa *et al.* improved the fluorescence intensity of eGFP after two months of cell culture and three rounds of selection in DT40 (Arakawa et al. 2008). These data demonstrate that the required iteration may be protein-specific and dependent on the desired functional gain.

A major consideration in utilisation of hypermutating cell lines for protein evolution is rate of SHM and control over the system. Estimates of mutation rate are expressed as a function of generation time. The limited available data for 18-81

suggests a mutation rate in excess of 10^{-5} per bp per generation (Wabl et al. 1985). Ramos mutate their Ig V region at a frequency of 2×10^{-5} per bp per generation although this may not be sustained during prolonged culture (Sale, Neuberger 1998, Zhang et al. 2001). Modified DT40 cell lines that do not support gene conversion yield Ig V mutation rates of $2\text{-}4 \times 10^{-5}$ per bp per generation (Sale et al. 2001, Arakawa, Saribasak & Buerstedde 2004). Therefore Ig V appears to be mutated at a comparable frequency across all three cell lines.

Given that mitosis requires DNA synthesis it seems reasonable to assume that mutation rate would correlate with cell division. The doubling times for hypermutating cell lines are in the region of 5 hours for 18-81 (Wang, Wabl 2005), 7 to 16 hours for DT40 (Simpson, Sale 2003, Seo et al. 2007) and 24 hours for Ramos (Cumbers et al. 2002). Variability in generation time for DT40 is related to culture temperature, cell density and genetic modifications (Simpson, Sale 2003, Nakamura et al. 2010). However Wang reported that chronological time is a more accurate descriptor in 18-81 cells and observed variation in AID and transgene expression levels depending on passaging conditions (Wang, Wabl 2005). There is some evidence to suggest that SHM occurs during the G_1 and G_2-M phases of the cell cycle, rather than the S phase where error-free repair is predominant (Faili et al. 2002). It does not seem sensible to discriminate between these cell lines based on their relative generation times in view of this evidence.

A distinct advantage of the DT40 cell line is the possibility of homologous recombination. Single copies of exogenous genes can be inserted at the desired location, the Ig locus in this case. Transgenes located in the rearranged Ig locus of

modified DT40 mutate at a frequency of 1×10^{-5} per base pair per generation and the Ig locus offers a preferable transgene mutation rate when compared to alternative genomic locations (Blagodatski et al. 2009). Insertion of transgenes into Ramos and 18-81 is frequently achieved with retroviral carriers, where the genomic location and number of copies cannot be controlled as readily. DT40 can also be manipulated to express exogenous rather than endogenous AID, which allows control of AID expression via an inducible promoter or Cre recombinase system (Arakawa, Hauschild & Buerstedde 2002).

Unlike B-lymphocytes, hypermutating cell lines preferentially mutate C:G base pairs (Bachl, Wabl 1996, Sale, Neuberger 1998, Sale et al. 2001) and transitions account for less than one third of mutations in DT40 cells (Sale et al. 2001, Arakawa, Saribasak & Buerstedde 2004, Barreto et al. 2003, Blagodatski et al. 2009). RGYW hotspot bias is however maintained (Sale, Neuberger 1998, Arakawa, Saribasak & Buerstedde 2004, Wang, Yang & Wabl 2004). Therefore the resulting SHM-mediated library diversity is inferior to that produced by traditional methods such as error-prone PCR. However given that screening capacity is often the rate-limiting step in directed evolution, this may have limited impact on success.

The frequency with which different point mutations accumulate in DT40 cells according to the available literature is recorded in Table 1.1. Arakawa *et al.* report that 51.9% of all mutations occur within the RGYW/WRCY hotspot motif in their sequencing of the Ig light chain of ψV knockout DT40 clones cultured for 5 - 6 weeks (Arakawa, Saribasak & Buerstedde 2004). This figure is based on mutation at any position within the RGYW/WRCY motif. If the published sequence is

Table 1.1: Mutation frequency in DT40 cell lines. The study of SHM has focused on two principal genetic modifications of DT40, pseudo V donor* and RAD51 paralogue§ deletion. Relevant examples of the frequency of SHM in existing literature are tabulated.

Cell line = genetic modification of DT40
Gene = gene sequenced
bp = number of base pairs in gene sequenced
n = number of cells sequenced
tbp = total number of base pairs sequenced (bp × *n*)
G = number of generations in culture prior to cell sequencing
M = total number of mutations observed
M rate = mutation rate per bp per generation

	Reference	Cell line	Gene	bp	*n*	tbp	G	M	M Rate
*	Arakawa04	$\psi V^- AID^R$	VJ	476	95	45,220	84	133	0.36×10^{-4}
	Schoetz06	$\psi V^- AID^R$	VJ	500	376	188,000	100	592	0.31×10^{-4}
	Blagodatski09	$\psi V^- AID^{R1}$	GFP	723	250	180,750	100	224	0.12×10^{-4}
§	Sale01	$XRCC2/3^-$	Vλ	427	191	81,557	60	131	0.27×10^{-4}
	Arakawa04	$XRCC3^-$	VJ	476	94	44,744	92	55	0.14×10^{-4}

analysed for G:C position only as per Rogozin's report (Rogozin et al. 2001) the frequency is reduced to 42.1%. However when the DGYW/WRCH consensus is considered, the total increases to 54.9%, of which the 'D' position is occupied by adenine, guanine and thymine in a ratio of 8:1:3 respectively and the 'Y' position occupied by cytosine or thymine in a ratio of 8:1 respectively. To put this in context, the forty C:G positions within DGYW/WRCH hotspots represent only eight percent of the examined sequence space. Therefore it will be necessary to consider the hotspot distribution in target genes, particularly at the binding site, before embarking on SHM as a diversification strategy.

The ability of B cells like DT40 to mutate exogenous transgenes provides a method for generating libraries of mutant protein. As discussed above this has been exploited to perform directed evolution of fluorescent proteins. However, in theory, gene diversification in B cells could be used to evolve other protein activities, such as specific binding activities. If SHM of transgenes could be coupled with cell surface display, altered binding affinities of mutant protein could be selected in viable B cells by fluorescent-labelled binding assay and Fluorescence Activated Cell Sorting (FACS).

1.5.2 Cell Surface Display

Cell surface display allows expression of a protein with a distinct function on the cell surface so that it is freely accessible to the soluble binding partner in binding assays. The technique has been used most extensively in yeast (Boder, Wittrup 1997, Kieke et al. 1999) and prokaryotes including *E. Coli* (Georgiou et al. 1997)

although it can equally be applied to mammalian cell lines (Heine, Muller & Brusselbach 2001, Ho, Nagata & Pastan 2006). Cell surface display would be a suitable method of permitting selection of an 'in cell' SHM-generated library of proteins based on binding affinities. To do this it would be necessary to create a genetic fusion of the protein in question to a membrane anchor in order that it is displayed on the cell surface correctly for FACS-mediated selection.

In addition to anchorage of the protein, the host cell must also express the protein in a format that allows the screening assay to be performed. It must therefore be competent to produce the protein in the correct conformation, and the associated transmembrane anchor must be amenable to fusion with foreign sequences, resistant to proteases, compatible with the host cell membrane and capable of orientating the protein correctly on the cell surface.

Prokaryotic cells display thousands of copies of a protein on the cell surface enabling high affinity FACS-based discrimination, but they lack essential foldases and chaperones required for human protein folding in the endoplasmic reticulum. Protein production in yeast approximates more closely to that of mammalian cells and rapid and quantitative library screening is possible, although there are some differences in glycosylation between yeast and mammalian cells (Boder, Wittrup 1997).

As previously discussed the most ideal system for engineering of mammalian proteins would be a vertebrate cell line, to ensure correct folding and post-translational modifications (Kieke et al. 1997, Lofblom et al. 2007). Clearly B cells,

including DT40, could be used for surface display. The remaining difficulty lies in ensuring that only a single copy of mutant DNA is integrated into the genome to guarantee that a single mutant form of the protein is displayed on the cell surface. Liposomal, electroporation and retroviral infection techniques of DNA transfection do not guarantee this eventuality. An additional advantage of using DT40 for gene diversification coupled to surface display for evolving binding proteins is that targeted genome integration by homologous recombination in the DT40 cell line is more likely to result in single copy transfection (Buerstedde, Takeda 1991).

Both native transmembrane proteins and glycophosphatidylinositol lipid (GPI) have been utilised as membrane anchors in mammalian cell surface display. Type I transmembrane (TM) proteins such as human platelet-derived growth factor receptor β chain (PDGFR) (Gronwald et al. 1988) and murine B7-1 (Freeman et al. 1991) can be used to orientate proteins whose N-terminus must face outward, whereas the type II TM human asialoglycoprotein receptor H1 subunit (ASGPR) (Spiess, Schwartz & Lodish 1985) bnenables location of the C-terminus of a protein toward the extracellular environment. GPI signal sequences produce acceptable cell surface protein expression levels but can also release from the cell membrane and anchor onto neighbouring cells (Chou et al. 1999), negating their usefulness in a directed evolution context.

1.5.3 Fluorescence Activated Cell Sorting

The combination of flow cytometry and FACS offers a high throughput, robust method of screening and selecting cell surface displayed proteins for differential

ligand binding characteristics. The library of cells is incubated in solution with fluorescently labelled ligand to perform 'on cell' binding assays. The concurrent use of a fluorescent protein expression tag and two-channel flow cytometry allows normalisation of ligand binding as a function of protein expression per cell. Desirable cells can be recovered by FACS to permit DNA extraction or further culture in the case of 'in cell' mutagenesis. Improved affinity single chain Fv antibodies and T-cell receptors have been produced using this method in *E. coli* and yeast (Daugherty et al. 1998, Boder, Wittrup 1997, Kieke et al. 1999).

When the intention is to modify the binding affinity of an existing interaction the target cell frequency in mutagenic libraries is low and demands a highly sensitive and specific screening assay. The issues particular to flow cytometric screening include signal to noise and signal to background ratios and specific sorting parameters. Noise occurs due to staining in non-viable cells and non-specific reagent binding and can be controlled experimentally. The choice of binding assay and gating regime are dependent on the characteristics of the binding interaction and the desired evolutionary outcome (Daugherty, Iverson & Georgiou 2000, Lofblom et al. 2007). In view of the principles of evolution previously outlined, multiple rounds of low stringency selection are often required to enrich the frequency of target cells and maximise population diversity prior to introduction of high purity conditions.

The principal methods of FACS-based screening for binding interactions are based on kinetic and equilibrium parameters (Lofblom et al. 2007). The equilibrium constant (K_d) for each interaction is dependent on the association and dissociation

rates. Association tends to be rapid and is therefore difficult and impractical to improve upon within the limits of *in vitro* detection. Selection based on slower dissociation rate is a more achievable option. Alternatively an equilibrium screen can be performed, in which ligand binding is detected at sub-dissociation constant concentrations in higher affinity mutants (Figure 1.6).

Equilibrium screens are generally utilised when K_d is in excess of 10nM where the ligand incubation volume required to prevent ligand depletion is practical, whereas kinetic selection is particularly sensitive for lower K_d interactions (Boder, Wittrup 1998). Therefore the baseline binding parameters must first be established before deciding on a selection regime.

1.6 Rationale and hypotheses

Directed evolution is one of the most powerful approaches for manipulating and creating novel protein functions. However the method requires multiple rounds of mutagenesis, expression and selection and this is both laborious and often difficult to perform. Furthermore, there are limited options for directed evolution of proteins that require the post-translational modifications found in vertebrates. In theory it should be possible to combine gene diversification activity of B cells with cell surface display to establish a facile method for directed evolution of binding proteins. This study seeks to test whether combining somatic hypermutation-driven diversification of an exogenous gene coupled with surface display in a

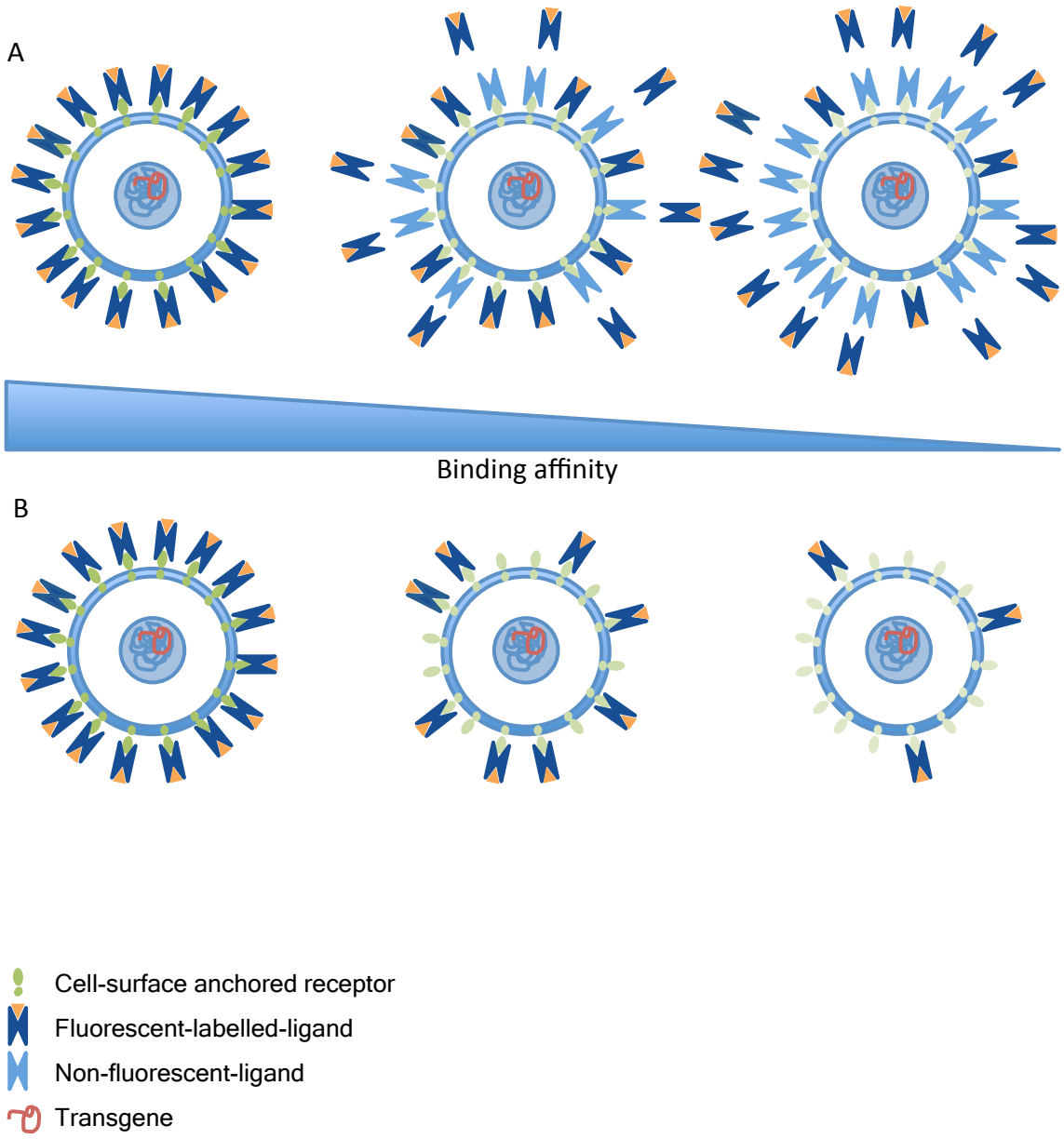

Figure 1.6: Screening methods for binding affinity.
Schematic representation of 'on-cell' binding assays.

a) Kinetic screening. Fluorescent-labelled ligand is bound at excess to 'on-cell' receptor prior to dissociation in the presence of unlabelled ligand. Brightest cells represent higher affinity secondary to prolonged dissociation rate (K_{off}).

b) Equilibrium screening. Fluorescent-labelled ligand is bound at sub-K_d concentration to 'on-cell' receptor. Brightest cells represent higher affinity secondary to lower dissociation constant.

hypermutating cell line can be used to evolve Tie2 ectodomain and change its binding specificity.

If successful this approach would ideally allow a single transfection of wild-type target protein into the hypermutating B cell line where it would localise to the Ig locus by recombination. Stable transfectants would then be grown allowing SHM to diversify the sequence, generating cells each with multiple copies of a specific mutant form of the protein on their surface. Cells with the desired binding properties would then be selected from the population by incubation under selective binding conditions with fluorescently-labelled binding partner and recovery using FACS. The selected cells would then be cultured to induce further mutations. Cycles of mutagenesis, binding and selection would be repeated iteratively until mutants with desired binding characteristics are derived.

In order to begin establishing this method, therefore, this study seeks to test the following hypotheses:

1. Somatic hypermutation can be utilised to generate a mutant Tie2 ectodomain library in a vertebrate cell line.
2. Tie2 cell surface display will permit discrimination of function via 'on-cell' fluorescent angiopoietin binding assays.
3. Tie2 ectodomain can be evolved 'in-cell' for angiopoietin binding properties via FACS-based iterative selection.

CHAPTER TWO

Materials & Methods

2.1 General reagents

The majority of reagents were of analytical grade and supplied by Sigma-Aldrich (Poole, UK) or Fischer Scientific (Loughborough, UK) unless otherwise stated. Experiments were conducted at room temperature (RT) except where indicated. Tissue culture plastics were obtained from NUNC (Denmark).

2.1.1 Buffers

Solutions were prepared with ddH_2O and pH was adjusted with 1M NaOH & 1M HCl.

1× TAE: 40mM Tris-acetate, 1mM EDTA

6× DNA loading buffer: 0.25% bromophenol blue, 40% w/v sucrose in water

TE buffer: 10mM Tris-HCl, 1mM EDTA (pH 7.5)

EB buffer: 10mM Tris-HCl (pH 8.5)

RNase-free H_2O: 0.1% Diethyl pyrocarbonate (DEPC)

2× sample buffer-DTT: 50mM Tris (pH 6.8), 10% glycerol, 2% SDS, 0.1% bromophenol blue, 5mM EDTA, 100mM DTT

Lysis buffer: 50mM Tris-HCl (pH 7.4), 50mM NaCl, 1mM NaF, 1mM EGTA, 1mM Na Orthovanadate, 1% TritonX-100, complete protease inhibitor cocktail

Running buffer: 2.5mM Tris (pH 8.3), 192mM glycine, 0.01% Na Dodecyl Sulphate (SDS)

Transfer buffer: 25mM Tris-HCl (pH8.3), 192mM glycine, 20% methanol

TBS-TX-100: 50mM Tris, 150mM NaCl, 0.1% TritonX-100

Blocking buffer: 5% non-fat dried milk in TBS-TX-100

Developer: 198µM p-Coumaric acid in DMSO, 1.25mM Luminol (5-amino-2,3-dihydro-1,4-pthalazinedione) in DMSO, 1:3333 H_2O_2, 0.1M Tris-HCl (pH 8.5)

PBS: 140mM NaCl, 2.7mM KCl, 10mM Na_2HPO_4, 1.8mM KH_2PO_4 (pH 7.4)

2.1.2 Media

Media were prepared under sterile conditions or autoclaved at 120°C for 20 min at 15-lb/in^2.

LB: 1% Tryptone, 0.5% Yeast Extract, 200mM NaCl (pH 7.4)

LB Agar: 1% Tryptone, 0.5% Yeast Extract, 200mM NaCl, 2% Agar (pH 7.4)

SOC: 2% Tryptone, 0.5% Yeast Extract, 10mM NaCl, 2.5mM KCl, 10mM $MgCl_2$, 10mM $MgSO_4$, 20mM glucose

Complete DT40: DMEM F12 (Lonza 12-719F), 10% foetal calf sera (FCS), 1% Chicken sera, 100µM β-mercaptoethanol

Complete Alpha-MEM: Alpha-MEM, 2mM L-glutamine, 10% FCS

Serum-free Alpha-MEM: AlphaMEM, 2mM L-glutamine

2.1.3 Commercial Kits

BIOTAQ™ DNA Polymerase (Bioline; London, UK)

Finnzymes Phusion™ High Fidelity DNA Polymerase (NEB; Hitchin, UK)

Ambion® RETROscript® (Invitrogen; Paisley, UK)

QIAquick® Gel Extraction Kit (Qiagen; Crawley, UK)

Generation Capture Column Kit (Qiagen; Crawley, UK)

RNeasy® Mini Kit (Qiagen; Crawley, UK)

QIAprep® Spin Miniprep Kit (Qiagen; Crawley, UK)

EndoFree Plasmid Maxi Kit (Qiagen; Crawley, UK)

pcDNA™3.1 Directional TOPO® Expression Kit (Invitrogen; Paisley, UK)

TOPO® TA Cloning® Kit For Sequencing (Invitrogen; Paisley, UK)

Lipofectamine™2000 tranfection reagent (Invitrogen; Paisley, UK)

Lightning Link® Biotin (Innova Biosciences; Cambridge, UK)

2.2 Preparation & storage of plasmid DNA

2.2.1 Transformation of XL1 competent cells

Competent cells were thawed on ice and gently mixed with 10-20ng plasmid DNA. The suspension was initially incubated on ice for 30 minutes, followed by a 42°C heat shock for 90 seconds and subsequent incubation on ice for 2 minutes. 500µl LB broth was added and the culture incubated at 37°C for 1 hour with 225rpm shaking. Between 10 and 100 percent of each culture was spread on LB agar plates, which contained the appropriate selective antibiotic. The plates were incubated overnight at 37°C in 5% CO_2.

2.2.2 Plasmid DNA preparation: Miniprep

A single colony was inoculated into 5-10ml of LB medium containing 50µg/ml ampicillin and grown at 37°C with 225rpm shaking for 12-16 hours. Cells were pelleted by centrifugation at 6000g for 10 minutes and the supernatant discarded. Miniprep was carried out as per the manufacturer's instructions (Qiagen). DNA was resuspended in EB buffer or sterile water, depending on downstream application, and assessed by absorbance and/or agarose gel electrophoresis. Plasmid was stored at −20°C.

2.2.3 Plasmid DNA preparation: Maxiprep

A single colony was inoculated into 2ml of LB medium containing 50µg/ml ampicillin and grown at 37°C with 225rpm shaking for 6-8 hours. 500µl of the starter culture was then inoculated into 100ml LB medium containing 50µg/ml ampicillin and grown at 37°C with 225rpm shaking for 12-16 hours. Cells were collected by centrifugation at 6000g for 10 minutes and the supernatant discarded. Maxiprep was carried out as per the manufacturer's instructions (Qiagen). DNA was resuspended in TE buffer and assessed by absorbance and/or agarose gel electrophoresis. Plasmid was stored at −20°C.

2.2.4 DNA & RNA quantification: absorbance

Absorbance at OD_{260} & OD_{280} was determined using a Shimadzu UV-1601 UV-Visible spectrophotometer. One unit of optical density was presumed equal to

50µg/ml dsDNA and 40µg/ml tRNA. OD_{260}: OD_{280} ratio was utilised to estimate purity.

2.2.5 Agarose gel electrophoresis

The appropriate mass of agarose (Melford, Chelsworth, UK) was dissolved in 1× TAE buffer by heating. 1:25000 ethidium bromide was added when it had cooled to approximately 50°C and it was poured into a gel tray with comb. When solidified, the gel was immersed in 1× TAE buffer within an electrophoresis tank. DNA samples were mixed with 0.2 volumes 6× loading buffer and loaded into the wells, with 10µl DNA ladder (TrackIt 1kb Plus, Invitrogen or Hyperladder IV, Bioline) as a reference. Gels were resolved at 100–120V until appropriate separation of bands was achieved. Images were captured on a Multimage light cabinet (Flowgen, Shenstone, UK).

2.2.6 Purification of DNA: gel extraction

DNA was resolved on agarose gel with 1:50000 ethidium bromide. DNA bands were excised under brief UV visualisation, except when the following application was ligation. In this case DNA was resolved on plain agarose gel with one extra 'guide lane' of DNA, followed by longitudinal division of the gel to incorporate the ladder and 'guide lane' in one part and the purification samples on the other. The guide segment was stained with 1: 10000 ethidium bromide for 15 minutes and the DNA band in the guide lane excised under UV visualisation. The guide segment was then realigned with the remaining unstained gel and required DNA bands

were excised by correlation of position with the guide lane. Purification was performed as per the manufacturer's guidelines (Qiagen). DNA was resuspended in EB buffer or sterile water, depending on downstream application, and assessed by absorbance and/or agarose gel electrophoresis.

2.2.7 Purification of DNA: chloroform phenol extraction

An equal volume of Phenol-Chloroform-Isoamyl alcohol was added to the DNA sample and vortexed to produce an emulsion. Following centrifugation at 12000g for 15 seconds, the aqueous phase was pipetted into a clean tube. An equal volume of chloroform was then added to the aqueous phase and vortexed to produce an emulsion. Following centrifugation at 12000g for 15 seconds, the aqueous phase was again pipetted to a clean tube and further treated by ethanol precipitation.

2.2.8 Purification of DNA: ethanol precipitation

2.5 volumes of 100% ethanol and 0.1 volumes of 3M sodium acetate pH5.2 were added to the DNA sample. Following incubation at −20°C overnight, the DNA was collected by centrifugation at 13400g, 4°C for 20 minutes. The supernatant was removed and the pellet was washed with 70% ethanol. After centrifugation at 13000rpm, 4°C for a further 5 minutes, the supernatant was removed and the pellet air-dried for a few minutes. DNA was resuspended in an appropriate volume of sterile water.

2.2.9 Glycerol stocks

Bacterial cultures were propagated for 12-16 hours following inoculation of a single colony into LB medium containing the appropriate selective antibiotic. Glycerol stocks were created using a mix of 850µl culture and 150µl sterile 99% glycerol in cryovials. The vials were snap-frozen in liquid nitrogen prior to storage at −80°C.

2.3 PCR & Cloning

2.3.1 PCR: plasmid DNA

PCR was conducted with BIOTAQ DNA polymerase (Bioline) in the case of analytical applications or high-fidelity Phusion DNA polymerase (Finnzymes) for cloning and sequencing. A master mix was prepared and distributed into thin-walled DNase-free tubes followed by addition of DNA and a mineral oil overlay. The reaction components, primers and cycles are specified in Appendix 2.1. PCR products were analysed by agarose gel electrophoresis.

2.3.2 Directional TOPO cloning

PCR primers were designed to amplify the required product, incorporating the required 5' CACC sequence for cloning and considering in-frame plasmid transcription. PCR was performed using proofreading polymerase and the product

was gel-purified (section 2.2.6). The cloning reaction was performed as per the manufacturer's instructions (pcDNA™ 3.1 Directional TOPO® Expression Kit). 2µl PCR product was typically added to 1µl TOPO® vector, 1µl salt solution and 2µl sterile H_2O and incubated at RT for 15 minutes. 2µl of cloning reaction was transformed into TOP10 cells (see below).

2.3.2.1 Cloning of Tie2ECD into pcDNA ™3.1D/V5-His-TOPO®

Tie2ECD was amplified from plasmid DNA containing full-length human Tie2 receptor (Dr H Singh, University of Leicester) with primers Tie2fwd and Tie2rev, which also incorporated restriction sites (Appendix 3.1). The reaction conditions are specified in Appendix 2.1. The product was cloned as described above to create pTie2-TOPO.

2.3.2.2 Cloning of cell surface display system (CSD) into pcDNA ™3.1D/V5-His-TOPO®

The transmembrane domain of PDGF receptor was amplified from plasmid DNA containing full-length human PDGFβ receptor (Prof N Brindle, University of Leicester) with primers PDGFRfwd & PDGFRrev, which also incorporated restriction sites, a linker and the FLAG-eiptope (Appendix 3.1). PCR conditions are specified in Appendix 2.1. The product was cloned as described above to create pCSD-TOPO.

2.3.3 Transformation of TOP10 chemically competent cells (Invitrogen)

Vials of TOP10 cells were thawed on ice and gently mixed with 2-5µl cloning reaction. Following incubation on ice for 30 minutes, the cells were heat-shocked at 42°C for 60 seconds and immediately transferred to ice for 2 minutes. 250µl RT SOC medium was added followed by incubation at 37°C for 1 hour with 225rpm shaking. 60-100% of each culture was spread on LB agar plates, which contained the appropriate selective antibiotic. The plates were incubated overnight at 37°C 5% CO_2 and colonies were analysed by plasmid miniprep (Qiagen), restriction analysis and sequencing.

2.3.4 Restriction digestion of DNA

Restriction enzymes were obtained from Roche Applied Sciences, UK. Reactions comprised 1-2U each enzyme per 1µg DNA and 1× buffer, made up with ddH_2O to give a final reaction volume of at least 12.5µl per 1µg DNA. All reactions were incubated at 37°C, for 2 hours in diagnostic studies and for 16 hours when the downstream application was cloning or transfection.

Enzyme(s)	Buffer
BglII	M
EcoRI	H
HindIII	B
NotI	H
XbaI	H
BglII/NheI	M
EcoRI/EcoRV	B
NheI/XbaI	A

2.3.5 DNA & RNA quantification: agarose gel

1µl purified vector & insert were resolved on 1% agarose gel with three different reference quantities of DNA ladder. The quantity of vector and insert was estimated in comparison with the intensity of ladder bands. The molar concentration was then calculated according to molecular weight.

2.3.6 Ligation of DNA

The reaction consisted of a 3:1 molar ratio of purified insert to vector, 1× ligase buffer, 1µl T4 DNA ligase (Roche Applied Science), made up to 30µl total volume with ddH_2O. The reaction was incubated for 16 hours at 8°C followed by heat inactivation at 65°C for 10 minutes. A proportion was then transformed into XL10 gold ultracompetent cells (Stratagene) (see below).

2.3.6.1 Cloning of pTie2ECD-CSD-TOPO

PCR of the cell surface display (CSD) segment was performed with proofreading polymerase (Phusion, Finnzymes) as previously described and the blunt-ended product was gel-purified. The 5' end of the PCR product was cut with EcoRI and again gel-purified. pTie2-TOPO was digested with EcoRI and EcoRV. The CSD segment was then ligated into pTie2-TOPO. Transformed colonies were assessed by colony PCR, restriction digestion of miniprep DNA, sequencing and protein expression following transfection.

2.3.6.2 Cloning of pTie2ECD-CSD-Hypermut2

NheI and BglII were used to digest both pTie2ECD-CSD-TOPO and Ang2-ASGPR-pHypermut2 (Dr S Sharma, University of Leicester). The Tie2ECD-CSD insert and the open pHypermut2 vector were gel-purified without exposure to ethidium bromide or UV light. The insert and vector were ligated and transformed. Colonies were assessed by colony PCR, restriction digestion of miniprep DNA and protein expression following transfection.

2.3.7 Transformation of XL10 gold ultracompetent cells (Stratagene)

Ultracompetent cells were thawed on ice and 50µl aliquots were transferred to pre-chilled 14ml Falcon tubes. 2µl β-mercaptoethanol was added to each aliquot, followed by a 10 minute incubation on ice with periodic swirling. 2-5µl ligation reaction was added followed by incubation on ice for 30 minutes. Tubes were heat-

shocked at 42°C for 30 seconds, followed by incubation on ice for 2 minutes. 500µl 42°C SOC medium was added to each tube followed by incubation at 37°C for 1 hour with 225rpm shaking. 40-100% of each culture was spread on LB agar plates, which contained the appropriate selective antibiotic. The plates were incubated overnight at 37°C 5% CO_2.

2.3.8 Colony PCR

A BIOTAQ master mix was prepared and distributed into thin-walled DNase-free tubes. Individual colonies were picked on pipette tips and exposed to the PCR mix before being inoculated into LB medium for overnight culture. PCR was performed as previously outlined with lengthening of the initial denaturation step to 10 minutes, and analysed by agarose gel electrophoresis.

2.3.9 Sequencing

Plasmid DNA was purified by miniprep and eluted in EB buffer. DNA and appropriate primers were supplied to the University of Leicester Protein Nucleic Acid Chemistry Laboratory Sequencing Service or Macrogen Inc., South Korea.

2.4 Cell culture & transfection

2.4.1 Culture of HEK293 cells

Cells were originally obtained from ECACC and maintained in complete AlphaMEM at 37°C in 5% CO_2. Passaging was performed at confluency by tapping of the flask to dislodge cells, centrifugation at 200g for 7 minutes and resuspension in an appropriate volume of media. Six-well plates were seeded and grown to 60% confluency prior to transfection.

2.4.2 Transient transfection of HEK293 cells

One aliquot of 250µl serum-free Alpha-MEM was combined dropwise with 5µl Lipofectamine™ 2000 (Invitrogen) and another was combined with 2µg plasmid DNA per well to be transfected. Following an initial 5 minute RT incubation, the two components were combined dropwise and incubated for 20 minutes at RT. Medium was removed from the plate and cells were washed in sterile PBS. 2ml serum-free Alpha-MEM was added to each well followed by dropwise addition of the Lipofectamine-DNA complex. The plate was incubated at 37°C in 5% CO_2 for 5 hours prior to removal of the media, PBS wash and replacement with 2ml complete Alpha-MEM. Cells were incubated overnight prior to assays.

2.4.3 Culture of DT40 cells

The DT40 cell line 'ψV^{-} AID^{R} Cl4' was a kind gift from Arakawa *et al.* (GSF Institute for Molecular Radiobiology, Munich, Germany). Cells were cultured in flasks of complete DT40 medium at 41°C in 5% CO_2. Stably transfected cell lines were also maintained in the appropriate antibiotic. When a density of 1 × 10^6 cells/ml was reached, cells were passaged at a ratio of between 1:3 and 1:30 depending on future application.

2.4.4 Stable targeted transfection of DT40 cells

Cloned pTie2ECD-CSD-Hypermut2 vector was linearised with NotI and purified by chloroform-phenol extraction and ethanol precipitation. 40µg DNA was resuspended in sterile water at a concentration of approximately 1µg/µl for each transfection. 10 × 10^6 cells were collected by centrifugation at 1500rpm for 5 minutes and resuspended in 800µl sterile PBS. The cell suspension and DNA were placed in a 4mm electroporation cuvette (Cell Projects, Harrietsham, UK) and mixed by brief vortexing. Electroporation was performed immediately at 25µF, 700V (BioRad GenePulser). Cells were then transferred to a pre-warmed 80cm^2 cell culture flask containing 14.2ml complete DT40 medium and incubated at 41°C 5% CO_2. After 24 hours, 15ml complete DT40 medium containing 2× puromycin (1µg/ml) was added to give a final puromycin concentration of 0.5µg/ml. Cells were plated out in 96-well plates at 200µl per well and incubated until colonies appeared. At this stage colonies were picked and grown up in culture flasks.

2.4.5 Stable non-targeted transfection of DT40 cells

pAIDblast^r vector (Ms T Numachit, University of Leicester) was purified and concentrated by ethanol precipitation. 30-50µg DNA was resuspended in 20µl sterile water for each transfection. 20 × 10^6 Tie2-DT40 cells were collected by centrifugation at 250g for 5 minutes, washed once in cold PBS, and resuspended in 700µl cold PBS. The DNA was pipetted into a 4mm electroporation cuvette (Cell Projects; Harrietsham, UK) followed by the cell suspension. The cuvette was gently vortexed and incubated on ice for 10 minutes prior to electroporation at 950µF, 250V (Biorad GenePulser). Following a further 20 minute incubation on ice, the cells were transferred to a pre-warmed 80cm^2 cell culture flask containing 29.3ml complete DT40 medium and incubated at 41°C 5% CO_2. After 24 hours 30 ml complete DT40 medium containing 2× puromycin (1µg/ml) and 2× blasticidin (40µg/ml) was added to give final concentrations of 0.5µg/ml puromycin and 20µg/ml blasticidin. Cells were plated out in 96-well plates at 200µl per well and incubated until colonies appeared. At this stage colonies were picked and grown up in culture flasks.

2.4.6 Mycophenolic acid treatment in DT40 cells

0.5µg/ml mycophenolic acid (MPA) (Sigma) was added to complete DT40 medium for three days of cell culture. Cells were then collected by centrifugation at 250g for 5 minutes and resuspended in complete DT40 medium.

2.4.7 Trichostatin A treatment in DT40 cells

Trichostatin A (Sigma) was added to complete DT40 medium at a concentration of 5nM for continuous cell culture.

2.4.8 Excision of floxed cassettes from DT40 cell genome

4-hydroxytamoxifen (4-OHT) (Sigma) was added to complete DT40 medium at a 1μM concentration for six days of cell culture. Cells were then collected by centrifugation at 250g for 5 minutes and resuspended in complete DT40 medium. Excision of the floxed Activation-Induced Cytidine Deaminase (AID) cassette was confirmed by RT-PCR from total RNA, against AID-positive control cells. Excision of the puromycin resistance gene was confirmed by cell death in 0.5μg/ml puromycin. On occasions where 4-OHT treatment did not produce a congruent cell population phenotype, subcloning and selection were employed.

2.4.9 Subcloning of puromycin-sensitive Tie2-DT40

4-OHT treated Tie2-DT40 cells were serially diluted and plated at less than 5 cells per 200μl medium in 96-well plates. When sufficiently grown, half the contents of each well were transferred to a duplicate plate containing 100μl 1μg/ml puromycin medium per well. Populations undergoing 100% cell death in puromycin were selected.

2.4.10 Freezing and storage of DT40 cells

Cells were grown exponentially to a density of approximately 1 × 10^6 cells/ml and collected by centrifugation at 250g for 5 minutes. Pellets were resuspended in freeze-mix (50% FCS, 10% DMSO, 40% complete DT40 medium) at a density of approximately 10 × 10^6 cells/ml. 1ml aliquots were frozen gradually to −80°C and later stored in liquid nitrogen. For retrieval, vials were thawed at 41°C and made up to 10ml volume with complete DT40 medium. Cells were then collected by centrifugation at 250g for 5 minutes and resuspended in complete DT40 medium.

2.4.11 Estimation of generation time of DT40 cells

Clonal Tie2 DT40 populations were cultured by passaging in a ratio of 1:3 or centrifugation with medium replacement (refeeding). Cells were counted daily on a haemocytometer. Generation time was calculated according to the formula:

$$T_d = t \times \frac{\log(2)}{\log\left(n_2/n_1\right)}$$

where T_d = doubling time; t = culture time; n_2 = final number of cells & n_1 = initial number of cells.

2.4.12 Kill curves

Equal suspensions of Tie2-DT40 cells were incubated in a range of concentrations of the reagent in question and counted daily on a haemocytometer with trypan blue staining.

2.5 Protein

2.5.1 Preparation of whole cell lysates for SDS-PAGE

In HEK293 cells, medium was removed from plated cells followed by two washes with PBS. Cells were incubated in 50µl lysis buffer per well for 5 minutes on ice and the cell lysate was collected with a cell scraper. In DT40 cells, 1×10^6 cells were collected by centrifugation at 250g for 5 minutes followed by two washes with PBS. Cells were incubated in 35-50µl lysis buffer for 5 minutes on ice.

Lysates were centrifuged at 13400g 4°C for 10 minutes in a microcentrifuge tube, and the supernatant was collected. An equal volume of 2× sample buffer-DTT was added to whole cell lysate and incubated at 95°C for 6 minutes prior to centrifugation at 13400g for 1 minute to pellet debris. Samples were stored at −20°C if not used directly for SDS-PAGE.

2.5.2 SDS-polyacrylamide gel electrophoresis (PAGE)

The appropriate percentage resolving acrylamide gel was prepared and topped with a 5% stacking acrylamide gel (see below). The gel was immersed in a tank of running buffer and loaded with 10µl protein ladder (Precision Plus Kaleidoscope Standards; BioRad; Hemel Hempstead, UK) in addition to samples. Gels were resolved at 120V until the molecular weight of the target protein was at the desired location.

	Resolving			Stacking
	7.5%	10%	12%	5%
30% Acryl/Bis (ml)	5.0	6.7	8.0	3.3
ddH_2O (ml)	10.9	9.6	7.9	13.7
Tris (ml)	3.7 (2M pH 8.8)			2.5 (1M pH 6.8)
20% SDS (µl)	100			100
10% APS (µl)	134			200
TEMED (µl)	14			20

2.5.3 Western blotting

Resolved acrylamide gel was sandwiched next to Hybond™ ECL™ nitrocellulose membrane (Amersham; GE Healthcare; Little Chalfont, UK), between filter paper and foam pre-soaked in transfer buffer, within a cassette. The cassette was treated in a tank of transfer buffer at 150mA RT for 14-16 hours or 200mA 4°C for 3 hours.

2.5.4 Immunoblotting

All incubations and washes were performed with agitation. For details of conditions used for specific antibodies see below. Nitrocellulose membrane was blocked in blocking buffer for 1 hour prior to immunoblotting. The membrane was immersed in antibody and 5% non-fat milk /TBS-TX-100 within a sealed bag during incubations. In some cases the primary and secondary reagents were combined in a single incubation. The membrane was washed three times in TBS-TX-100 for a total of 30 minutes following each incubation and finally exposed to

developer for 1 minute. Light emission from bound antibody was detected by exposure of the membrane to Kodak imaging film and enhanced chemiluminescence (ECL) system (Amersham Pharmacia Biotech; UK).

Primary Ab	**Incubation**	**Secondary Ab**	**Incubation**
Anti-FLAG M2 monoclonal Ab (Sigma Aldrich)	1:1000 RT 45 min	Anti-mouse IgG HRP (GE Healthcare)	1:2000 RT 30 min
Anti-human Tie2 Ab (R&D systems)	1:1000 4°C 14-16 hrs	Polyclonal anti-goat Ig HRP (Dako)	1:1000 RT 60 min
Anti-α-tubulin monoclonal Ab (Sigma)		1:10000	
Anti-mouse IgG HRP (GE Healthcare)		1:5000 RT 20 min	
Anti-AICDA polyclonal Ab (Abcam ab59361)	1:500 4°C 14-16 hrs	Anti-rabbit IgG HRP (GE Healthcare)	1:1000 RT 60 min
Anti-His Ab (Cell Signaling)	1:2000 RT 1 hr	Anti-rabbit IgG HRP (GE Healthcare)	1:1000 RT 30 min
Streptavidin biotinylated HRP (Amersham)		1:2000 RT 30 min	

2.5.5 Stripping nitrocellulose membranes

Previously probed membranes were immersed in 1× Stripping Mild (Millipore) for 15 minutes with agitation and washed in TBS-TX-100 prior to immunoblotting.

2.5.6 ImageJ analysis

Immunoblotting films were scanned as black and white 8-bit electronic files of 300dpi or higher. Calibration was performed for uncalibrated optical density. Protein bands were selected and area under the intensity curve was digitally calculated. Relative optical density was calculated by comparison of sample values with a ubiquitous loading control.

2.5.7 Biotinylation

Recombinant Ang1 was treated as per the manufacturer's instructions (Lightning-Link® Biotin). The product was analysed by SDS-PAGE, immunoprecipitation and immunoblotting.

2.5.8 Immunoprecipitation

Two 20µl aliquots of streptavidin beads (Sigma, Poole, UK) were centrifuged at 1250g and washed in PBS. One aliquot was resuspended in 1:40 recombinant Ang1/PBS and the other in 1:40 Ang1-biotin product/PBS, and both were incubated rolling for 20 minutes on a Spiramix (Denley). The suspension was

centrifuged at 1250g for 1 minute. The beads were resuspended in 20µl reducing sample buffer and the supernatants transferred to a fresh set of streptavidin beads. The process was repeated for the second set of beads and recovered beads were combined with the first set. Equal quantities of recombinant Ang1 and Ang1-biotin product were also prepared in reducing sample buffer as a control. All samples were denatured by incubation at 95°C for 6 minutes. The dissociated protein was collected by centrifugation at 13400g for 1 minute and the supernatants analysed by SDS-PAGE and immunoblotting for His-tag and biotin.

2.6 Analysis of cell genome

2.6.1 Total RNA isolation (RNeasy Minikit, Qiagen)

Cells were counted on a haemocytometer. Between 1×10^6 and 5×10^6 cells were collected by centrifugation at 250g for 5 minutes and washed once with PBS. RNA isolation was performed as per the manufacturer's instructions. RNA was resuspended in RNase-free water and assessed by absorbance. RNA was generally used immediately for downstream application, but if storage was required 1:50 RNase inhibitor (Ambion) was added prior to freezing at −80°C.

2.6.2 Reverse transcription

Total RNA was reverse transcribed to cDNA using the Ambion RETROscript™ kit. 2µg total RNA was mixed with 2µl oligo dT or random decamers and made up to

12µl with RNase-free H_2O. This was incubated at 85°C for 3 minutes followed by immediate cooling on ice. A mastermix was prepared to incorporate 4µl dNTPs, 2µl 10× RT buffer, 1µl RNase inhibitor and 1µl MMLV-RT per reaction. The required 8µl of mastermix was added to each sample, followed by incubation at 50°C for 1 hour and 92°C for 10 minutes. The cDNA product was stored at −20°C if not used directly for PCR.

2.6.3 TA cloning for sequencing (TOPO TA Cloning® Kit for Sequencing, Invitrogen)

PCR was performed using proofreading polymerase. Addition of 3' adenine overhangs to the PCR product was achieved using the BIOTAQ PCR kit (Bioline). 30µl gel-purified PCR product was incubated at 72°C for 15 minutes with 9µl ddH_2O, 5µl NH_4 buffer, 4µl $MgCl_2$, 1µl dNTPs & 1µl Biotaq. The cloning reaction was performed as per the manufacturer's instructions. 4µl of PCR product was added to 1µl pCR4-TOPO® vector and 1µl salt solution and incubated at RT for 20 minutes. 2µl of cloning reaction was transformed into TOP10 cells.

2.6.4 Sequencing

96-well plates of individual fresh colony agar stabs were supplied to Macrogen Inc., South Korea and sequenced using M13 Forward & M13 Reverse priming sites.

2.6.5 Genomic DNA isolation (Generation Capture Column Kit, Qiagen)

5×10^6 cells were collected by centrifugation at 250g for 5 minutes and resuspended in 200µl of the supernatant. Genomic DNA isolation was performed as per the manufacturer's instructions. The eluted DNA was assessed by absorbance and/or agarose gel electrophoresis. Samples were stored at −20°C.

2.6.6 PCR: genomic DNA

PCR was conducted as described for plasmid DNA with the following modifications: the initial denaturation step was lengthened to 5 minutes and DMSO was included in the reaction.

2.7 Flow cytometry & Fluorescence Activated Cell Sorting (FACS)

2.7.1 Binding and fluorescent cell labelling reagents

Biotinylated Recombinant Human Angiopoietin-2, Recombinant Human Angiopoietin-2 and Recombinant Human Angiopoietin-1 were all obtained from R&D Systems (UK) and diluted in PBS to the required experimental concentration.

Dilution of staining reagents, washes and incubations of cells were performed in PBS with 1:10 FCS additive.

Detection	Reagent	Dilution
FLAG	Anti-FLAG M2 monoclonal Ab (Sigma) & Anti-mouse Cy2 Ab (Amersham) *or* Anti-FLAG M2-FITC monoclonal Ab (Sigma)	1:50 1:100 1:100
Ang1	Polyclonal Ab to 6× His tag-Biotin (Abcam) & Streptavidin-R-phycoerythrin conjugate (Sigma) *or* Anti-His PE monoclonal Ab (Abcam)	1:50 1:25 1:25
Biotinylated Ang2	Streptavidin-R-phycoerythrin conjugate (Sigma)	1:25

2.7.2 On-cell binding and labelling procedure

Cells were collected by centrifugation at 250g and washed. Angiopoietin binding was performed at RT for 1 hour, whilst all other incubations were performed at 4°C for 30 minutes. All incubations were performed on a shaker and followed by washes. Fluorophores were shielded from light throughout. The sequence followed for multiple incubations was: angiopoietin; primary antibody (anti-FLAG & anti-His); secondary agent (streptavidin-R-PE, anti-mouse Cy2).

2.7.3 Flow cytometry

Cells were labelled, washed and resuspended in approximately 500µl volume PBS/FCS in a 5ml Falcon polystyrene tube and stored on ice without light exposure prior to analysis by flow cytometry. Unstained cells were included in each assay to

quantify autofluorescence. A BD FACSAria™ II cell sorter was utilised with an 85μm nozzle. Excitation lasers and emission bandpass filters were employed for the various fluorophores as stated below. Live cells were gated according to forward and side scatter characteristics and data was recorded for 10000 events per sample. FCS files were analysed with BD FACSDiva™ software.

Fluorophore	**Excitation laser (nm)**	**Bandpass filter (nm)**
Cy2 FITC	488	530/30
Phycoerythrin	561	582/15
Propidium iodide	561	610/20 *or* 582/15

2.7.4 Cell viability in flow cytometry

Cells were resuspended in 1μg/ml propidium iodide (Sigma Aldrich, Poole, UK) five minutes prior to flow cytometry.

2.7.5 Flow cytometry reagent optimisation

In the case of Tie2 detection, one cohort of wild-type DT40 cells and another of Tie2-DT40 cells were labelled with differing concentrations of fluorophore at 4°C for 30 minutes. In the case of angiopoietin labelling, one cohort of unbound Tie2-DT40 cells and another with pre-bound angiopoietin were labelled with differing concentrations of fluorophore at 4°C for 30 minutes. Flow cytometry was performed as outlined.

2.7.6 Flow cytometric analysis of specific binding parameters

Flow cytometry was performed as outlined following the procedures described below.

2.7.6.1 Dissociation constant (K_d)

Serial dilution of the ligand, recombinant Ang1 or biotinylated recombinant Ang2, was performed to produce the desired concentration points (Appendix 2.2). 1×10^6 cells per data point were collected by centrifugation at 250g for 5 minutes and washed once. Each aliquot of cells was resuspended in a ligand dilution and incubated shaking at RT for 1 hour. Cells were collected by centrifugation at 700g 4°C for 1 minute and washed once. In the case of Ang1, an additional subsequent step of incubation in 50µl cold anti-His biotin at 4°C shaking for 30 minutes was required prior to repeat washing and proceeding. For both Ang1 and Ang2, each aliquot was then resuspended in 50µl cold streptavidin-RPE and incubated shaking at 4°C for 30 minutes. Cells were collected as previously, followed by two cold washes.

2.7.6.2 Dissociation rate (K_{off}) Ang2

5×10^5 cells per time variable were collected by centrifugation at 250g for 5 minutes and washed once. Cells were resuspended together in 20nM biotinylated-Ang2, allowing 25µl per time variable, and incubated shaking at RT for 1 hour.

Cells were collected by centrifugation at 700g 4°C for 1 minute and washed once. Cells were then resuspended in cold streptavidin-RPE, allowing 25µl per time variable, and incubated shaking at 4°C for 30 minutes. Following incubation one aliquot of 25µl (representing t=0) was removed and transferred to a clean microcentrifuge tube. This separate aliquot and the remaining cells were collected as previously and washed twice. The t=0 aliquot was stored in 1ml 4°C PBS/FCS as described prior to flow cytometry. The remaining cells were resuspended together in 200nM RT Ang2, allowing 35µl per remaining time variable, and a 30µl aliquot was removed and transferred to 5ml Falcon polystyrene tube containing 1ml 4°C PBS/FCS at each specified time point. Flow cytometry was performed on completion of the time course.

2.7.6.3 Dissociation rate (K_{off}) Ang1

5×10^5 cells per time variable were collected by centrifugation at 250g for 5 minutes and washed once. All cells were resuspended together in 10nM Ang1, allowing 50µl per time variable, and incubated shaking at RT for 1 hour. Cells were then collected by centrifugation at 700g 4°C for 1 minute and washed once. Cells were resuspended in cold anti-His PE, allowing 25µl per time variable, and incubated shaking at 4°C for 30 minutes. Following incubation one aliquot of 25µl (representing t=0) was removed and transferred to a clean microcentrifuge tube. This separate aliquot and the remaining cells were collected as previously and washed twice. The t = 0 aliquot was stored in 1ml 4°C PBS/FCS as described prior to flow cytometry. The remaining cells were resuspended in 100nM RT Ang1 (section 3.4.5) or RT PBS/FCS (section 5.2.4), allowing 35µl per remaining time

variable, and a 30µl aliquot was removed and transferred to 5ml Falcon polystyrene tube containing 1ml 4°C PBS/FCS at each specified time point. Flow cytometry was performed on completion of the time course.

2.7.6.4 Association rate (K_{on}) Ang2

5×10^5 cells per time variable were collected by centrifugation at 250g for 5 minutes and washed once. Cells were resuspended in 2nM RT biotinylated-Ang2, allowing 250µl per time variable. A 250µl aliquot was removed at each time point, cells were collected by centrifugation at 1960g for 10 seconds, and resuspended in 50µl 100nM 4°C Ang2. When the time course was completed cells were collected by centrifugation at 700g 4°C for 1 minute and washed once. Cells were resuspended in 50µl cold streptavidin-RPE and incubated shaking at 4°C for 30 minutes. Cells were again collected as previously and washed twice.

2.7.6.5 Competitive equilibrium Ang1/Ang2

Aliquots of 125µl serially diluted recombinant Ang1 were each combined with 125µl 4nM biotinylated recombinant Ang2 to produce the desired concentration points. 5×10^5 cells per data point were collected by centrifugation at 250g for 5 minutes and washed once. Each aliquot of cells was resuspended in a ligand dilution and incubated shaking at RT for 1 hour. Cells were then collected by centrifugation at 700g 4°C for 1 minute and washed once. Each aliquot was resuspended in 50µl cold streptavidin-RPE and incubated shaking at 4°C for 30 minutes. Cells were again collected as previously, followed by two cold washes.

2.7.7 Fluorescence Activated Cell Sorting

Cells were labelled under sterile conditions, resuspended at a density of approximately 25 × 10^5 per ml in 5ml Falcon polystyrene tubes and stored on ice without light exposure prior to analysis. A BD FACSAria™ II cell sorter was utilised with an 85μm nozzle and cleaned with BD FACSClean™ solution and sterile PBS prior to each use. BD FACSFlow™ sheath fluid was utilised and the stream was adjusted and drop delay calibrated. 10000 events per sample were recorded and sort gates were specified for the acquired live cell data. Sorting was performed in 2-way purity mode at a maximum speed of 2000 events per second. Cells were collected directly into 4°C sterile complete medium and returned to incubator culture flasks as soon as practicable.

CHAPTER THREE

Characterisation of Tie2 extracellular domain in the DT40 'ψV^{-} AID^{R} Cl4' cell line

In order to perform directed protein evolution by somatic hypermutation and iterative fluorescence-activated cell sorting, the gene of interest must be integrated into the genome of a hypermutating cell line and the characteristics of the translated protein must be discernable by fluorescent assay.

Evolution of intrinsically fluorescent proteins by somatic hypermutation has been achieved in hypermutating B cell lines (Wang et al. 2004b, Wang, Yang & Wabl 2004, Wang, Harper & Wabl 2004, Arakawa et al. 2008, Blagodatski et al. 2009). Following stable transfection of the transgene and a period of cell culture fluorescent properties of cells were assessed and selected by FACS, yielding mutant phenotypes.

Fluorescent assay for characteristics of binding proteins requires use of fluorescently labelled binding partners and therefore extracellular accessibility of the protein of interest. Cell surface display, whereby the protein of interest is fused to a membrane anchoring protein, is an established method for permitting such fluorescent binding analyses (Chao et al. 2006).

The creation and characterisation of a system to allow evolution of the protein of interest, Tie2, is illustrated in Figure 3.1 and described in this chapter, to include:

- Cloning of chimeric Tie2ECD-cell surface display gene in pHypermut2;
- Stable targeted transfection into DT40;
- Confirmation of integration into rearranged Ig locus;
- Confirmation of cell surface expression and Ang1/Ang2 binding;
- Assessment of baseline binding parameters for Ang1/Ang2 binding.

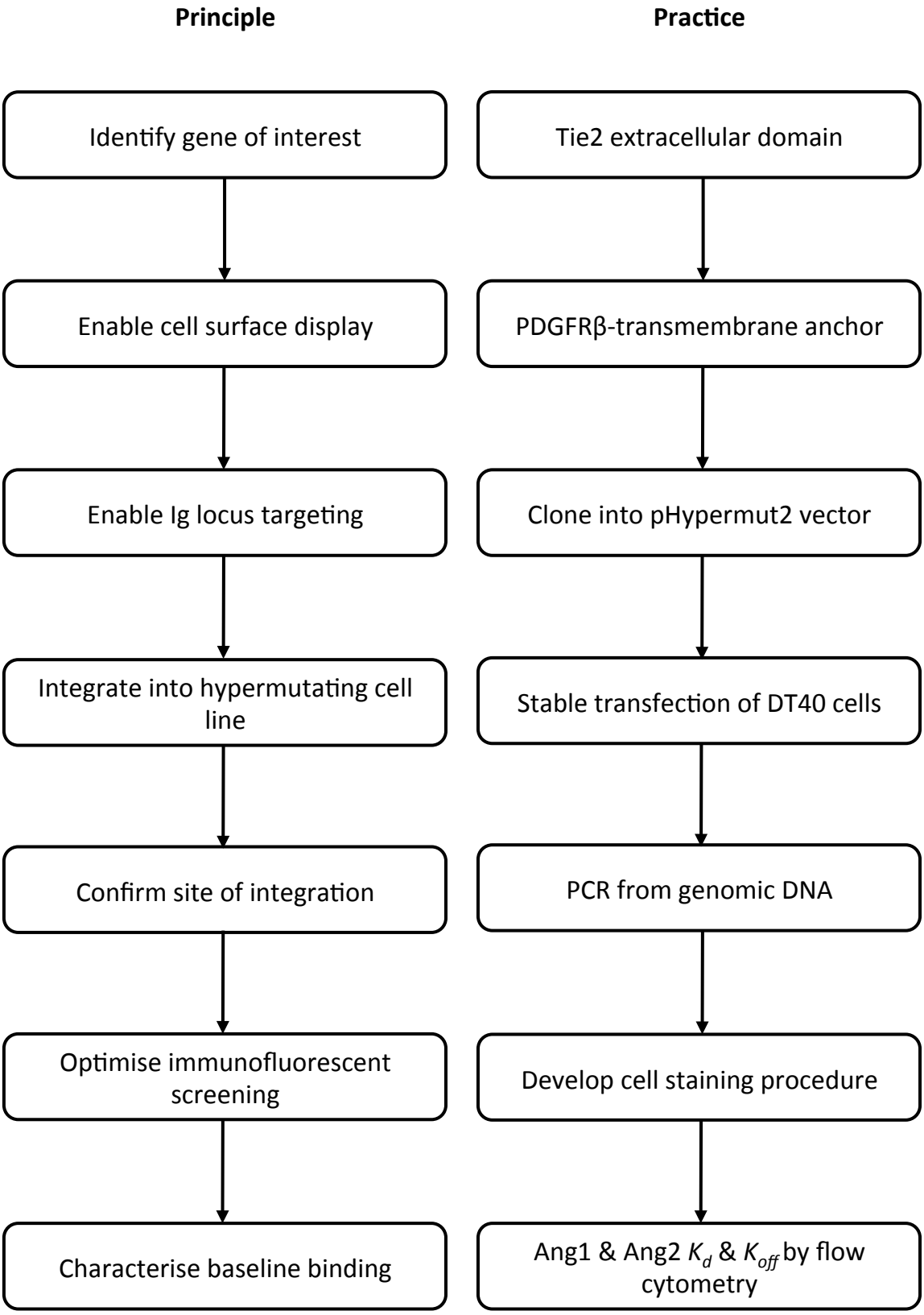

Figure 3.1: Approach to system design for evolution of binding proteins. General principles considered (left) and translation for this application (right).

Introduction

Only the Ig2 domain of Tie2 contacts Ang2 during binding, and Ang1 is thought to bind Tie2 in a similar manner (Barton et al. 2006). Evolution of Tie2 to explore Ang1 and Ang2 binding characteristics could therefore be limited to the Ig2 domain only. However mutations in residues outside the active site, or ligand-binding domain, can also modify binding characteristics (Shimotohno et al. 2001, Spiller et al. 1999). Functional studies have demonstrated that truncated Tie2 proteins encompassing residues 23-210 and 23-442 exhibit similar Ang1 binding affinity (Macdonald et al. 2006), and residues 1-360 and 1-440 produce comparable Ang1 and Ang2 binding (Fiedler et al. 2003).

An advantage of directed evolution over rational protein design is the ability to screen a range of mutations, many of which may modify binding affinity despite predictions to the contrary. To maximise the potential of the investigation, Tie2 residues 1-441 were selected for mutagenesis and will be referred to as Tie2ECD, encompassing the majority of the extracellular domain of Tie2 receptor and comprising the secretory leader sequence, $Ig1_{23\text{-}120}$, $Ig2_{122\text{-}209}$, EGF1, EGF2, EGF3 and $Ig3_{348\text{-}441}$.

The transmembrane domain of the PDGF receptor β (PDGFRβ-TM) has been successfully used as a means of anchoring proteins for cell surface display (Chesnut et al. 1996, Kontermann, Muller 1999, Heine, Muller & Brusselbach 2001, Ho, Nagata & Pastan 2006). Both PDGFRβ and Tie2 are type-1 transmembrane proteins (Shim et al. 2010, Ramsauer, D'Amore 2002), enabling fusion of PDGFRβ-

TM downstream of Tie2ECD to form a correctly orientated cell surface display construct.

The planned Tie2ECD-cell surface display (CSD) chimeric gene is illustrated in Figure 3.2. A FLAG epitope tag is included to enable detection of Tie2ECD on the DT40 cell surface and normalisation of angiopoietin binding as a function of Tie2 expression.

Hypermutating cell lines such as Ramos and DT40 express the enzyme Activation-Induced Cytidine Deaminase (AID), which induces mutations in single-stranded DNA (Ramiro et al. 2003). Ramos and DT40 both have B-lymphocyte characteristics due to their origins from human Burkitt's lymphoma and chicken avian leukosis virus induced bursal lymphoma respectively. Somatic hypermutation occurs in B-lymphocyte variable immunoglobulin light chain regions at a rate of approximately 10^{-3} mutations per base pair per generation in antibody affinity maturation (McKean et al. 1984, Rajewsky, Forster & Cumano 1987). The mutation frequency is highest in but not limited to the Ig locus (Martin, Scharff 2002, Blagodatski et al. 2009).

In comparison to Ramos cells, DT40 cells offer two distinct advantages as a vehicle for somatic hypermutation: exogenous genes can be more successfully targeted into the Ig locus, and a shorter cell doubling time is potentially conducive to more efficient gene diversification (Buerstedde, Takeda 1991, Sale et al. 2001, Arakawa et al. 2008). In order to target the gene of interest into the Ig locus upon transfection, it must be situated between regions of Ig locus homology within an

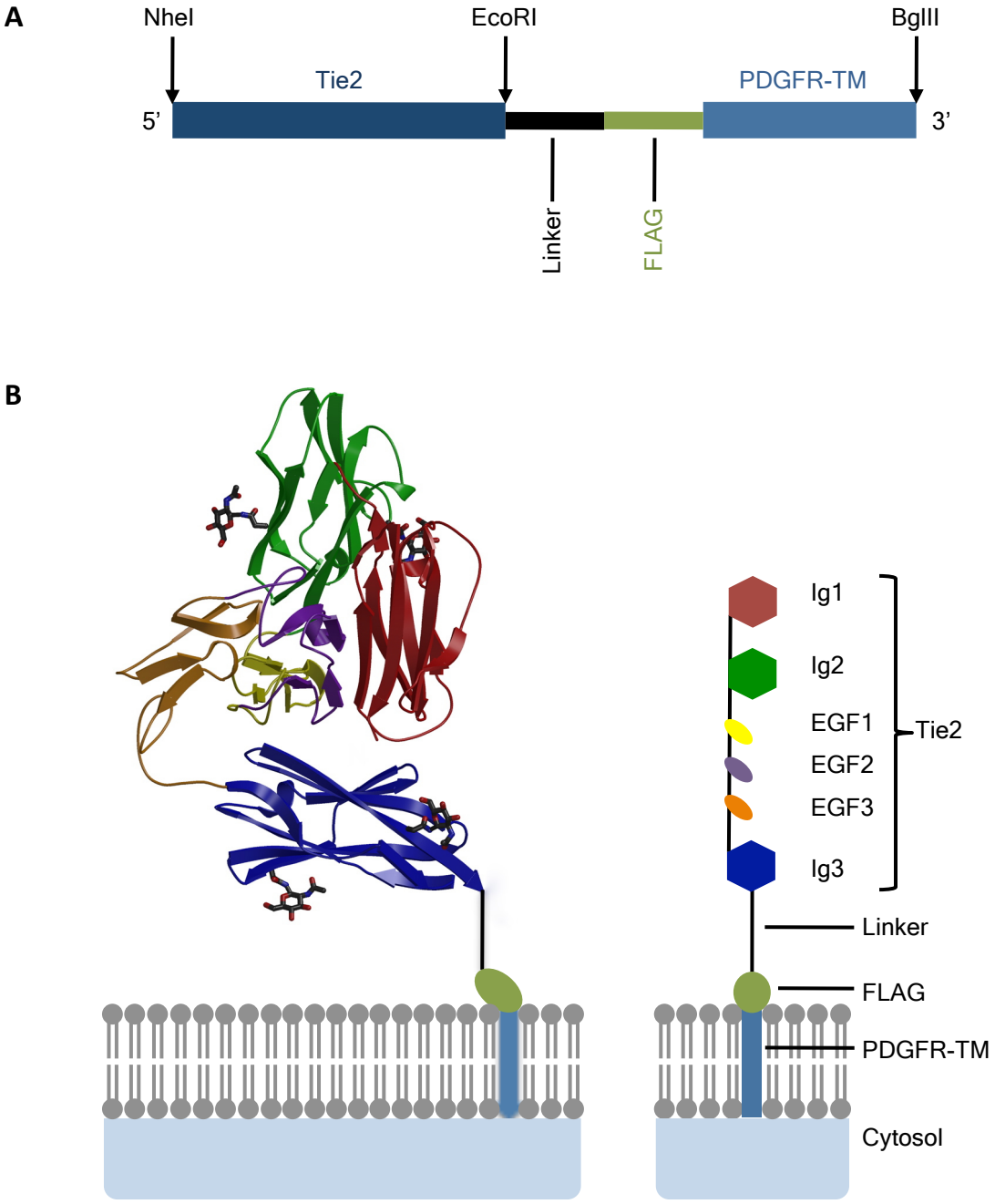

Figure 3.2: Schematic diagrams of Tie2ECD-CSD chimera.

a) Gene. Depicts orientation of construct and location of restriction sites included to facilitate cloning.

b) Expressed protein. Illustrates modular structure of Tie2ECD and its position when anchored to cell membrane. Structure of Tie2ECD adapted from Barton et al. 2006.

expression vector. A modified DT40 cell line, 'ψV^{-} AID^{R} Cl4' DT40, and pHypermut2 vector were kindly provided by JM Buerstedde *et al.* for use in this project (Arakawa et al. 2008).

A schematic diagram for the planned fluorescent staining procedure for cell surface anchored Tie2ECD is depicted in Figure 3.3. Dual fluorescent assays for expression and angiopoietin binding will be used to verify intact orientation and confirmation of Tie2ECD.

Initial studies into the binding affinities of Ang1 and Ang2 for Tie2 reported comparable dissociation constants (K_d) of between 3nM and 4nM for each interaction (Davis et al. 1996, Maisonpierre et al. 1997). A recent study has contradicted those findings, estimating a twenty-fold lower binding affinity for Ang2 at K_d 40.2nM in contrast to 1.9nM for Ang1 (Yuan et al. 2009). All of the studies utilised different methodologies, illustrating that baseline binding parameters need to be established for every system. Flow cytometry is an accepted technique for quantification of dissociation constants and rates (Lofblom et al. 2007) and is utilised here to determine the binding affinity of recombinant Ang1 and Ang2 for cell surface expressed wild-type Tie2ECD.

3.1 Generation of an Ig locus targeting vector for cell surface displayed Tie2

The cloning strategy is illustrated in Figure 3.4. It was necessary to clone Tie2ECD and the cell surface display domain (CSD) separately into expression vectors prior

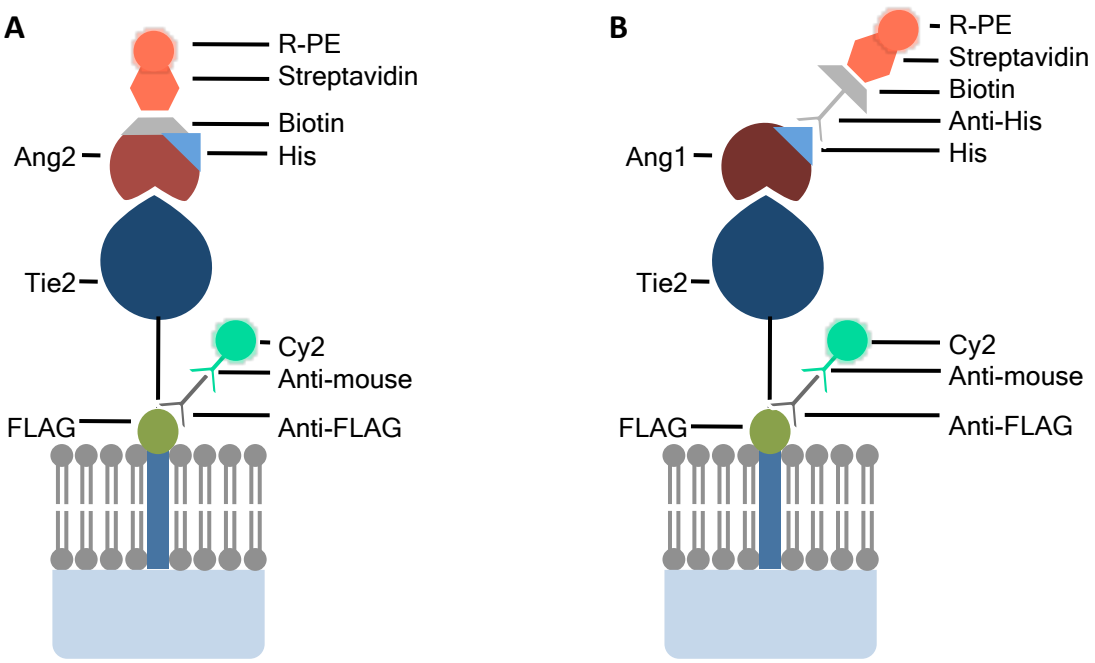

Figure 3.3: Immunofluorescent staining of cell surface expressed Tie2ECD.

a) Ang2 dual stain. Depicts immunofluorescent FLAG detection and biotinylated Ang2 detection via streptavidin-R-phycoerythrin.

b) Ang1 dual stain. Illustrates immunofluorescent FLAG detection and Ang1 detection via anti-His biotin and streptavidin-R-phycoerythrin.

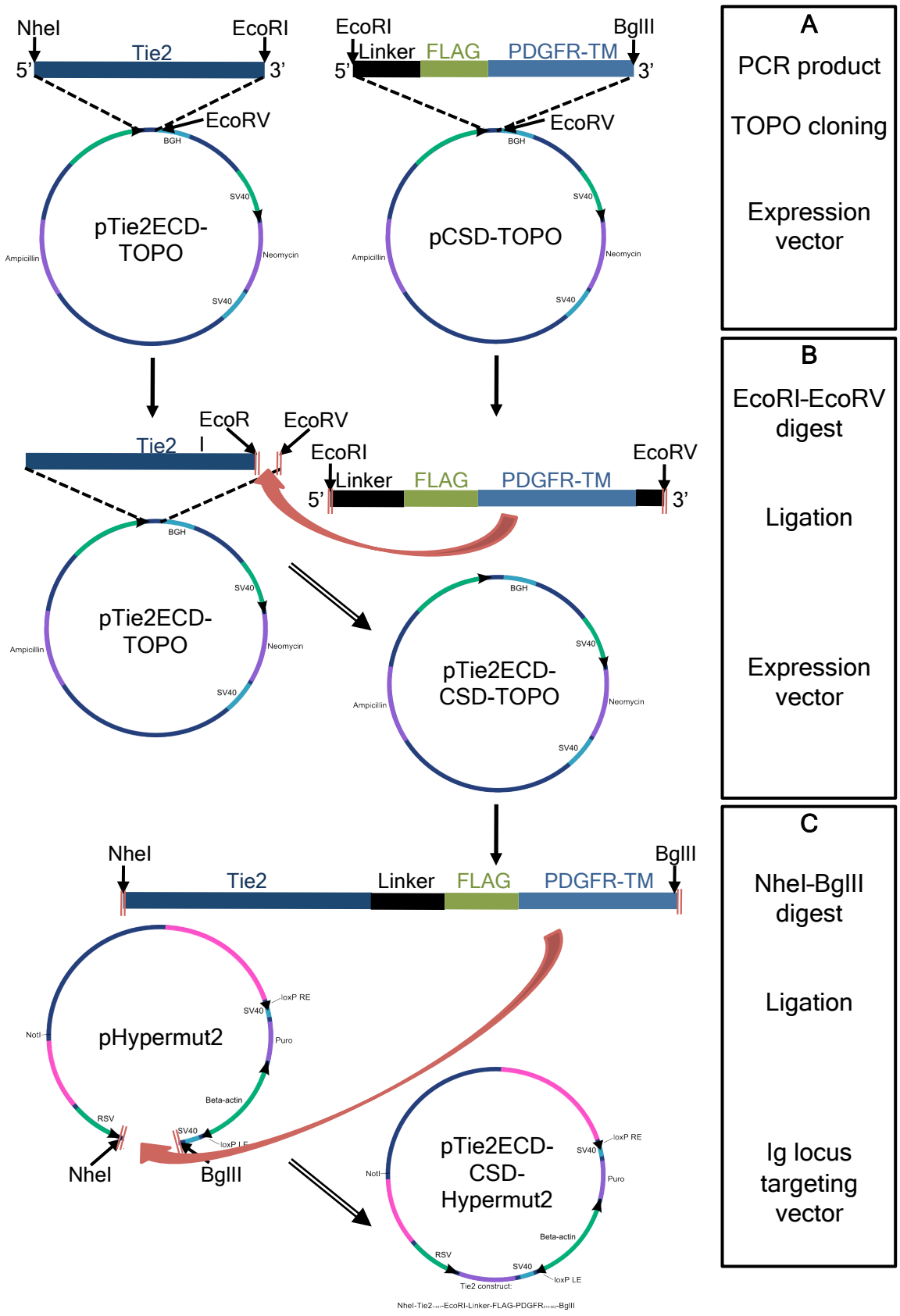

Figure 3.4: Cloning of Tie2ECD-CSD in pHypermut2. See Appendix 3.1.

a) **Cloning of Tie2ECD and cell surface display system (CSD) into TOPO expression vector.** Section 3.1.1 & 3.1.2.

b) **Ligation of CSD into Tie2ECD-TOPO expression vector.** Section 3.1.3.

c) **Ligation of Tie2ECD-CSD into pHypermut2 vector.** Section 3.1.4.

to their combination as a chimeric gene and finally transfer into the Ig locus-targeting vector, pHypermut2.

3.1.1 Cloning of Tie2ECD into pcDNA™3.1D/V5-His-TOPO® expression vector

Full-length human Tie2 receptor DNA was obtained from Dr H Singh (University of Leicester). Primers were designed to amplify residues 1-441 only, with consideration of Kozak's rules. In order to facilitate onward cloning of Tie2ECD, NheI and EcoRI restriction sites were included 5' and 3' respectively (Appendix 3.1). The Invitrogen pcDNA™3.1 Directional TOPO® Expression Kit was selected as a cloning strategy, which optimises efficiency by preferentially orientating the PCR product in the desired 5' to 3' direction. The recommended primer design guidelines were considered, including the addition of the 5' CACC motif.

The PCR product was amplified using proofreading polymerase under the conditions specified in Appendix 2.1 (Figure 3.5a). Cloning was performed as described in section 2.3.2. Resulting plasmid DNA, designated pTie2ECD-TOPO, was analysed by restriction with HindIII as described in section 2.3.4 and displayed the predicted restriction pattern (Figure 3.5b). The sequence was confirmed by sequencing with T7 and BGH reverse priming sites.

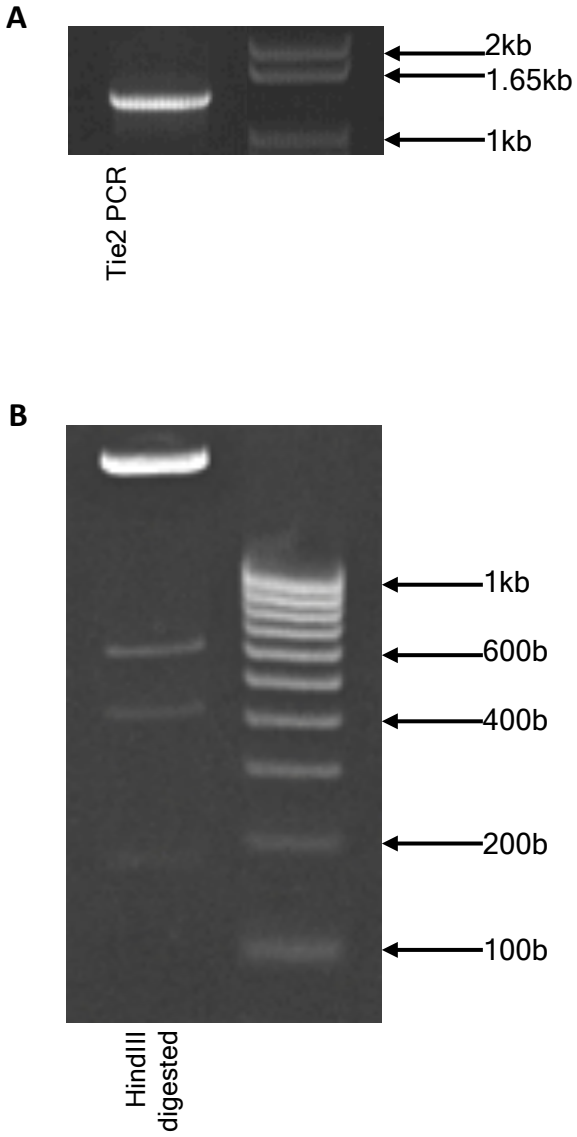

Figure 3.5: Verification of pTie2ECD-TOPO cloning.

a) PCR of Tie2ECD. PCR was performed as described in section 2.3/ Appendix 2.1. The 1342bp product was resolved by electrophoresis on 0.8% agarose gel and visualised by UV illumination as described in section 2.2.5. The position of molecular size markers are indicated.

b) Restriction digest of positive clone. Cloning was performed as described in section 2.3.2.1. Miniprep DNA was digested with HindIII as described in section 2.3.4. HindIII cuts the Tie2ECD PCR product at positions 372, 944 and 1122 and the TOPO vector at position 903, giving product sizes in pTie2ECD-TOPO of 178bp, 404bp, 572bp and 5.7kb. The products were resolved by electrophoresis on a 1% agarose gel and visualised by UV illumination as described in section 2.2.5. The position of molecular size markers are indicated.

3.1.2 Cloning of cell surface display system (CSD) into pcDNA™3.1D/V5-His-TOPO® expression vector

In order to anchor Tie2ECD to the cell surface with the N-terminus facing outward, a construct was designed for ligation to its 3' end. This comprised, from 5' to 3', EcoRI restriction site, short linker, FLAG peptide, PDGFRβ residues 514-562, BglII restriction site (Appendix 3.1).

Full-length human PDGFβ receptor DNA was obtained from Prof N Brindle (University of Leicester). Primers were designed to amplify residues 514-562 only (Gronwald et al. 1988), along with the additional elements detailed above. The required amendments were made to allow cloning with the Invitrogen pcDNA™3.1 Directional TOPO® Expression Kit.

The PCR product was amplified using proofreading polymerase under the conditions specified in Appendix 2.1 (Figure 3.6a). Cloning was performed as described in section 2.3.2. Resulting plasmid DNA, designated pCSD-TOPO was analysed by restriction with EcoRI/EcoRV as described in section 2.3.4 and exhibited the correct restriction pattern (Figure 3.6b). Subsequently the sequence was verified using T7 and BGH reverse priming sites.

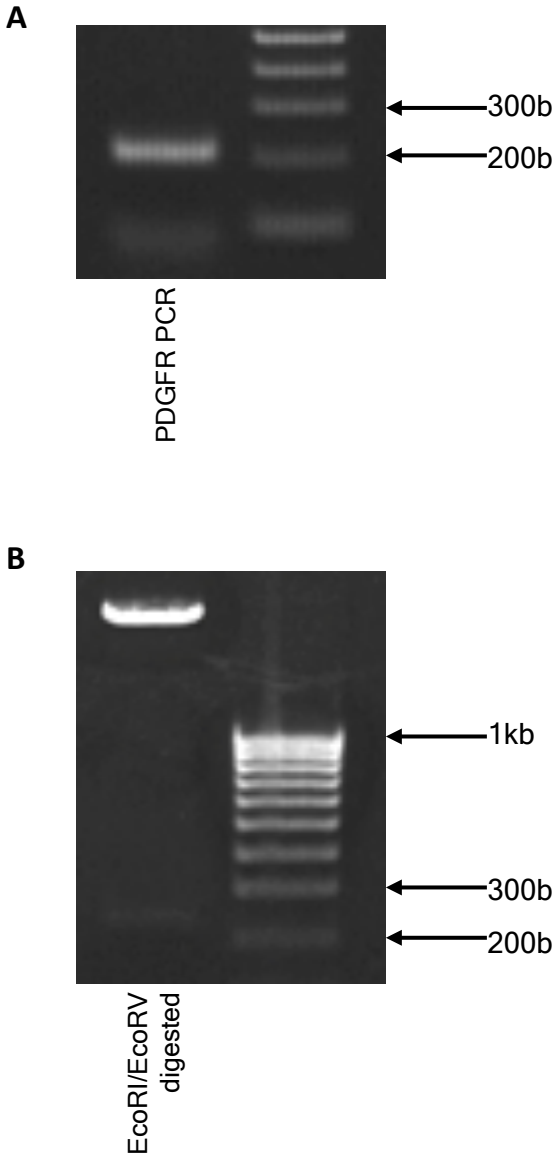

Figure 3.6: Verification of pCSD-TOPO cloning.

a) PCR of CSD. PCR was performed as described in section 2.3/Appendix 2.1. The 217bp product was resolved by electrophoresis on 1.25% agarose gel and visualised by UV illumination as described in section 2.2.5. The position of molecular size markers are indicated.

b) Restriction digest of positive clone. Cloning was performed as described in section 2.3.2.2. Miniprep DNA was digested with EcoRI & EcoRV as described in section 2.3.4. EcoRI cuts the CSD PCR product at position 7, and EcoRV cuts the TOPO vector at position 958, giving product sizes in pCSD-TOPO of 234bp, and 5.5kb. The products were resolved by electrophoresis on a 1% agarose gel and visualised by UV illumination as described in section 2.2.5. The position of molecular size markers are indicated.

3.1.3 Cloning of cell-surface displayed Tie2ECD in pcDNA™3.1D/V5-His-TOPO®

The initial strategy was to digest both pTie2ECD-TOPO and pCSD-TOPO with EcoRI and EcoRV, followed by purification and ligation of the open pTie2ECD-TOPO vector and CSD insert. However, achieving the 3:1 molar ratio of insert:vector for ligation required optimisation and a more expedient strategy was employed.

Comparison of double-digested CSD insert and PCR product revealed that the PCR product had far higher concentration (Figure 3.7a). The blunt-ended PCR product was digested with EcoRI only, enabling ligation with the complimentary EcoRI site and the blunt-ending EcoRV site in the double-digested pTie2ECD-TOPO vector (Appendix 3.1). Ligation was performed as outlined in section 2.3.6. The product, designated pTie2ECD-CSD-TOPO, was analysed by colony PCR (section 2.3.8; Appendix 2.1) and NheI/BglII restriction of the PCR-positive plasmids (section 2.3.4), which yielded the expected products (Figure 3.7b&c). Sequencing was again utilised as confirmation.

3.1.4 Cloning of cell-surface displayed Tie2ECD into pHypermut2 vector

The strategy was to digest both pTie2ECD-CSD-TOPO and pAng2-ASGPR-Hypermut2 (Dr S Sharma, University of Leicester) with NheI and BglII, followed by purification of the required segments and ligation (Appendix 3.1). Initial attempts at ligation were unsuccessful despite use of a 3:1 insert:vector molar ratio as per the manufacturer's guidelines.

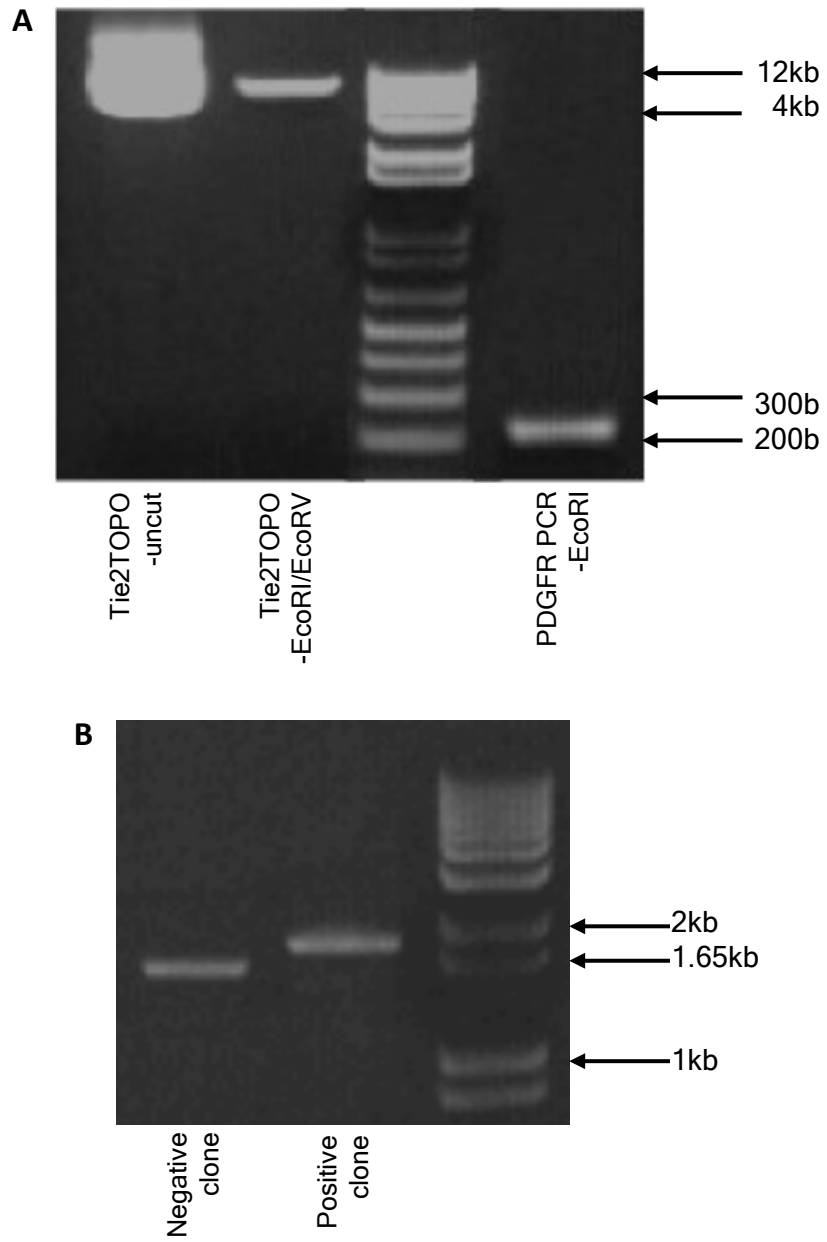

Figure 3.7: Verification of pTie2ECD-CSD-TOPO cloning.

a) Ligation components. The CSD PCR product (Fig. 3.6a) was digested with EcoRI. pTie2ECD-TOPO was digested with EcoRI and EcoRV. The products were gel purified. Purity and quantity was verified prior to ligation by 1% agarose gel electrophoresis of a small aliquot. The position of molecular size markers are indicated and uncut pTie2ECD-TOPO vector was included as a reference.

b) Colony PCR of positive clone. Cloning was performed as described in 2.3.6.1. Individual colonies were inoculated into aliquots of PCR mastermix prior to DNA preparation. PCR was performed as described in 2.3.8. Positive pTie2ECD-CSD-TOPO clones produce a 1779bp product, whereas pTie2ECD-TOPO produces a 1599bp product. The position of molecular size markers are indicated.

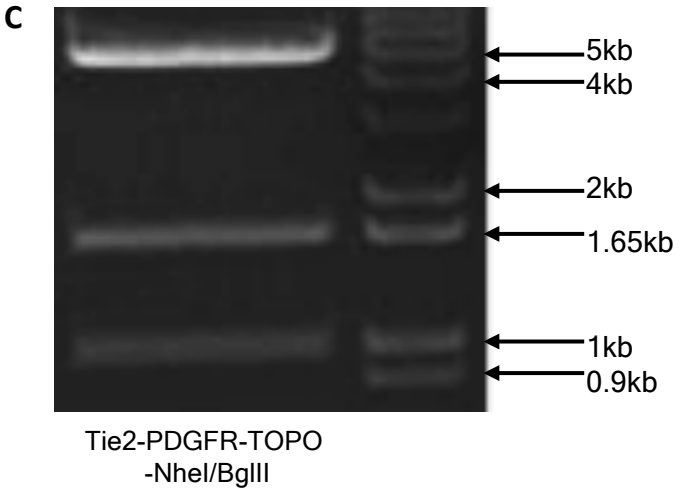

Figure 3.7: Verification of pTIe2ECD-CSD-TOPO cloning.

c) Restriction digest of positive clone. Miniprep DNA was digested with NheI & BglII as described in section 2.3.4. pTie2ECD-TOPO is cut by NheI at position 939 and BglII at position 12. BglII also cuts the EcoRI digested CSD insert at position 205, giving digestion product sizes of 927bp, 1536bp, and 4.5kb in pTie2ECD-CSD-TOPO. The products were resolved by electrophoresis on a 1% agarose gel. The position of molecular size markers are indicated.

A transformation efficiency of 30% was recorded for XL-10 ultracompetent cells using 0.01ng pUC18 plasmid as per the manufacturer's guidelines. Modification of the number of cells used and heat shock time did not have any significant effect on efficiency.

Ligation efficiency was assessed by testing a variety of conditions and visualising the completed reaction by agarose gel electrophoresis. Of those tested, optimal parameters comprised 8°C incubation, 3:1 molar ratio of insert to vector, 1 unit of ligase and avoidance of DNA exposure to ethidium bromide and UV light (Figure 3.8).

Ligation of pHypermut2 and the Tie2ECD-CSD insert was achieved using the protocol outlined in sections 2.3.6. The product was analysed by colony PCR (section 2.3.8; Appendix 2.1) (Figure 3.9a) and restriction of the PCR-positive plasmids with NheI/BglII (section 2.3.4) yielding the expected restriction fragments (Figure 3.9b).

3.1.5 Expression of cell-surface displayed Tie2ECD in HEK293 cells

In order to confirm correct translation of the chimeric Tie2ECD gene, positively screened pTie2ECD-CSD-Hypermut2 was transiently transfected into HEK293 cells by lipofection as outlined in section 2.4.2. Whole cell lysate was subjected to SDS-PAGE and Western blotting followed by immunoblotting with anti-FLAG antibody (section 2.5). Expression of the FLAG-tagged construct was confirmed (Figure 3.10).

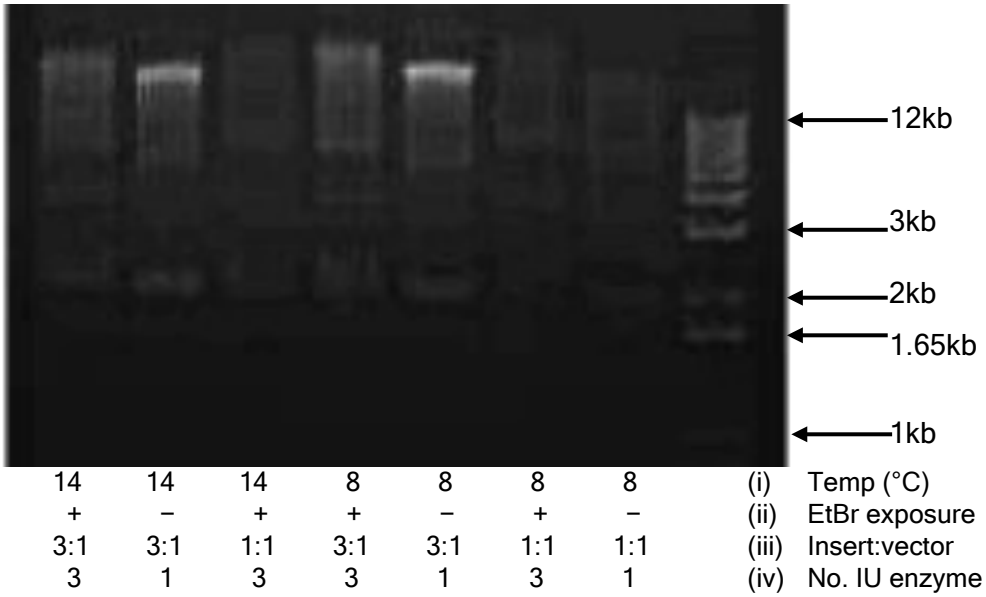

Figure 3.8: Optimisation of ligation. Miniprep DNA was digested with NheI & BglII as described in section 2.3.4. Insert and vector were gel purified and quantified by agarose gel electrophoresis against known quantities of molecular weight marker. Reactions were allowed to proceed for 16 hours prior to visualisation of products by agarose gel electrophoresis. The position of molecular size markers are indicated. The composition and temperature of ligation reactions is indicated in the legend:

(i) Temperature of ligation reaction
(ii) Exposure of digested DNA to ethidium bromide prior to ligation
(iii) Molar insert to vector ratio in ligation reaction
(iv) Number of units of ligase in ligation reaction

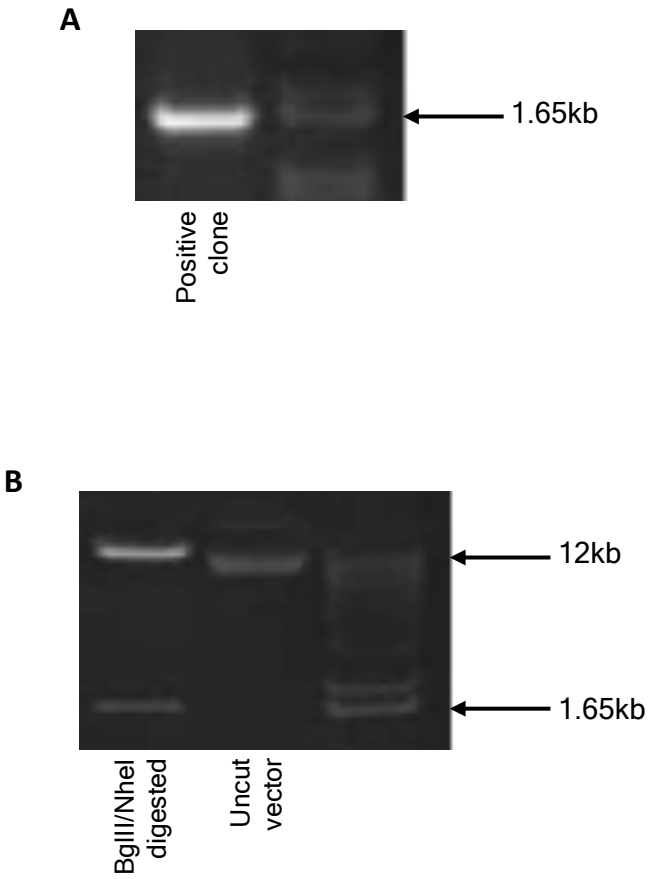

Figure 3.9: Verification of pTie2ECD-CSD-Hypermut2 cloning.

a) Colony PCR of positive clone. Cloning was performed as described in 2.3.6.2. Individual colonies were inoculated into aliquots of PCR mastermix prior to DNA preparation. PCR was performed as described in 2.3.8. Positive clones produce a 1546bp product. The position of molecular size markers are indicated.

b) Restriction digest of positive clone. Miniprep DNA was digested with NheI & BglII as described in section 2.3.4. The 1536bp Tie2ECD-CSD insert is excised from the vector in positive clones. The products were resolved by electrophoresis on a 1% agarose gel. The position of molecular size markers are indicated.

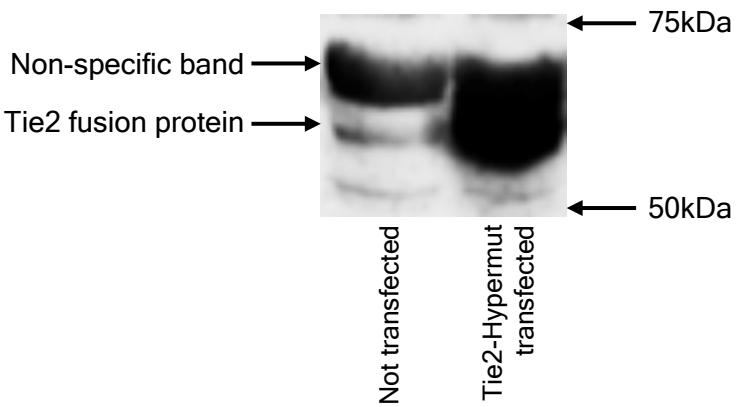

Figure 3.10: Expression of Tie2 construct in HEK293 cells. HEK293 cells were transfected with pTie2ECD-CSD-Hypermut2 as described in section 2.4.2. Whole cell lysate was prepared from transfected and untransfected cells, and subjected to SDS-PAGE and Western blotting as described in section 2.5. Immunoblot analysis was performed with anti-FLAG monoclonal antibody. The position of molecular weight markers are indicated.

3.2 Cell-surface displayed Tie2ECD can be integrated into the rearranged Ig locus of the DT40 'ψV^{-} AID^{R} Cl4' cell genome

In order to produce an optimal system for 'in-cell' mutagenesis of Tie2ECD it was necessary to integrate a single copy of the Tie2ECD-CSD gene into the rearranged Ig locus of an 'ψV^{-} AID^{R} Cl4' DT40 cell.

3.2.1 Optimisation of parameters for stable targeted transfection

Electroporation usually introduces a single copy of the gene at a single site. Electroporation parameters for stable transfection of DT40 cells have been previously described (Buerstedde, Takeda 1991, Zimmermann et al. 2002, Saribasak, Arakawa 2006). In pHypermut2 regions of homology flank the genes of interest, promoting targeted integration. In the absence of a readily accessible pHypermut2-fluorescent protein vector, non-targeted transient transfection of eGFP was initially used to explore electroporation parameters.

RSV promoter-driven eGFP plasmid was obtained from Dr S Sharma (University of Leicester). Conditions producing highest transfection efficiency and cell viability, as assessed by fluorescent microscopy of transiently transfected cells on a haemocytometer, were avoidance of washes, resuspension in PBS as electroporation buffer and higher DNA concentration. Conditions that had no significant effect included pre- and post-electroporation incubations and electroporation voltage (Table 3.1).

*Wash	§Suspension	vDNA (µg)	★Voltage (V)	˜Post-incubation	Survival (%)	GFP expression (%)
–	PBS	4	700	+	60	50
+	PBS	4	700	+	20	<5
–	PBS	4	700	–	65	60
–	PBS	4	550	+	80	40
–	PBS	1	700	+	55	<5
–	Serum-free medium	4	700	+	30	30
+	Serum-free medium	4	700	+	20	30
–	Complete medium	4	700	+	30	<5

Table 3.1: Exploration of electroporation parameters for transfection of DT40 cells. Cells were transfected as per the conditions set out in notes below. Percentage of cells surviving, and percentage of live cells expressing GFP at 24 hours is shown.

Notes:
1×10^6 DT40 cells were harvested by centrifugation at 200g 5 minutes.
*Wash step: cells were resuspended in 1ml PBS and centrifuged at 200g 1 minute.
§Suspension: cells were suspended in 200µl PBS or medium as stated.
vDNA: stated quantity A_{260}:A_{280} >1.8 DNA added to cells.
★Electroporation: 4mm cuvette at stated voltage, 25µF capacitance.
˜Post-incubation: incubated in cuvette 10 minutes 4°C following electroporation.
Cells were resuspended in 10ml complete medium and incubated for 24 hrs prior to microscopy.

3.2.2 Stable targeted transfection

pTie2ECD-CSD-Hypermut2 was linearised outside and adjacent to Tie2ECD-CSD and surrounding homologous regions with NotI to promote integration of the desired construct (Figure 3.11a). The linearised vector was transfected into DT40 'ψV^{-} AID^{R} Cl4' cells by electroporation with consideration of the above parameters and as described in section 2.4.4. After 24 hours of culture, puromycin was added and the cells were aliquoted into 96-well plates at limiting dilution to enable isolation of single stably transfected clones. Approximately ten days following transfection, colonies were visible at an average concentration of 0.8 colonies per well. Wells containing single colonies were picked and grown up progressively into 80cm^{2} flasks.

Total RNA and whole cell lysate were prepared from apparently transfected cells, referred to as Tie2-DT40, to confirm expression of the Tie2ECD-CSD construct by RT-PCR of Tie2ECD and by SDS-PAGE and Western immunoblotting with anti-FLAG detection respectively (sections 2.5 & 2.6) (Figure 3.12).

3.2.3 Transfected Tie2ECD integrates into the Ig locus

Targeted integration into the Ig locus is encouraged by the regions of homology on either side of the target gene in pHypermut2. In order to examine the site of genomic integration, genomic DNA was extracted from Tie2-DT40 clones A, B & C and PCR for correct integration was performed using the conditions specified in Appendix 2.1. The forward primer (GWFwd) anneals just upstream of the

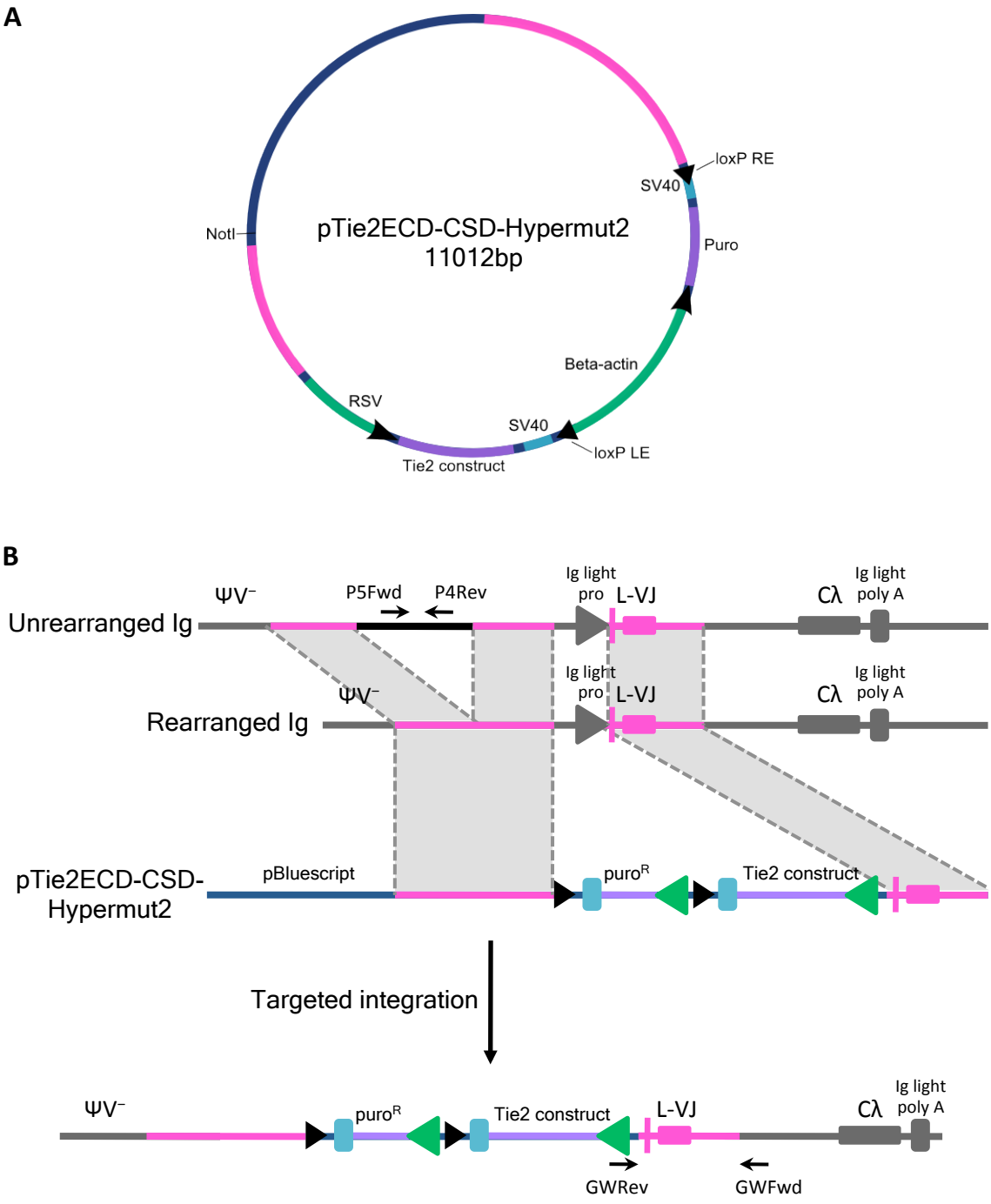

Figure 3.11: Targeted integration of pTie2ECD-CSD-Hypermut2 into the DT40 Ig locus.

a) Tie2ECD-CSD-Hypermut2 plasmid. Plasmid map depicting regions of Ig locus homology (coloured pink) and site of linearisation for transfection (NotI).

b) Schematic diagram of Ig locus and mechanism of targeted integration. Shaded areas identify regions of homology between unrearranged and rearranged Ig loci and pHypermut2. Primer pair P4Rev & P5Fwd ampliflies a 493bp segment of the unrearranged allele only. Primer pair GWFwd & GWRev amplifies 1189bp segment of integrated pHypermut2.

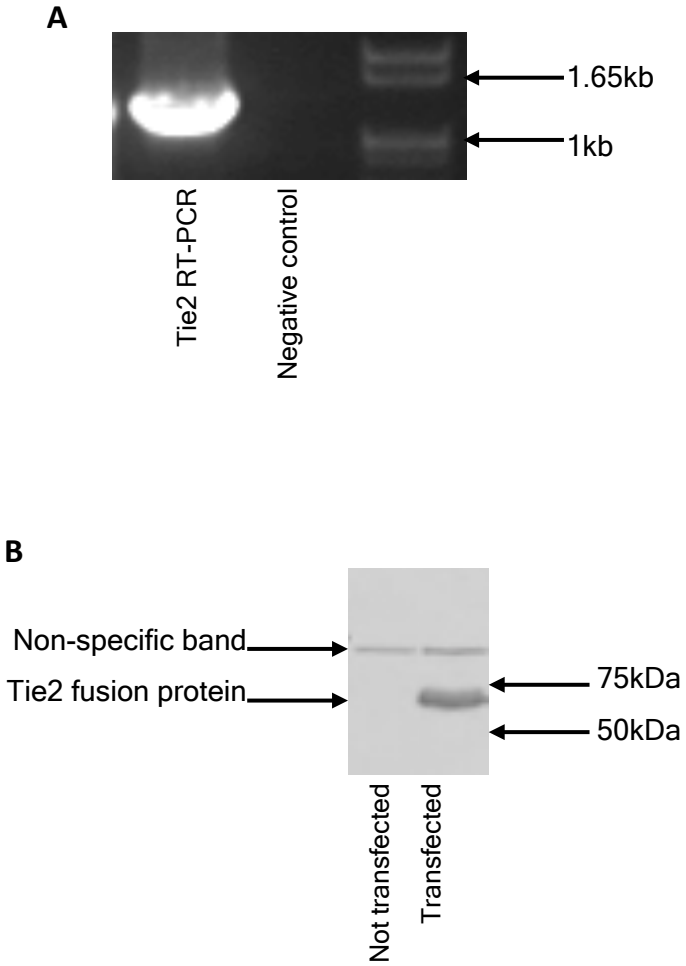

Figure 3.12: Stable transfection of Tie2ECD-CSD construct in DT40 cells. DT40 cells were stably transfected with pTie2ECD-CSD-Hypermut2 as described in section 2.4.4.

a) **RT-PCR of Tie2.** Total RNA was extracted and subjected to RT-PCR as described in section 2.6. The 1342bp product was resolved by electrophoresis on 1% agarose gel and visualised by UV illumination as described in section 2.2.5. The position of molecular size markers are indicated.

b) **Tie2 expression probe.** Whole cell lysate was prepared from transfected and untransfected cells, and subjected to SDS-PAGE and Western blotting as described in section 2.5. Immunoblot analysis was performed with anti-FLAG monoclonal antibody. The position of molecular weight markers are indicated.

homologous 5' region in the chicken Ig locus and the reverse primer (GWRev) anneals to the RSV promoter in pHypermut2, downstream of the homologous region, amplifying a 1189bp segment (Figure 3.11b).

If incorrect integration has occurred, the product would be incorrect in size or not present. Correct targeted integration was confirmed in all three clones by obtaining the 1189bp product (Figure 3.13).

3.2.4 Transfected Tie2ECD integrates into the rearranged Ig locus

The pHypermut2 vector can target the rearranged or unrearranged allele of the Ig locus. In order to proceed with somatic hypermutation, the vector must integrate into the rearranged locus. Arakawa et al described a greater than 70% incidence of pHypermut constructs undergoing targeted integration into this site (Arakawa et al. 2008).

Therefore to identify clones containing the vector in the rearranged Ig locus, genomic DNA was extracted from three separate Tie2-DT40 clones, A, B & C. PCR was performed using a primer pair (P4Rev & P5Fwd) designed to amplify a 493bp segment of the unrearranged allele which would be lost if integration occurred in this allele (Arakawa et al. 2008). The conditions are specified in Appendix 2.1 and it is illustrated schematically in Figure 3.11. Integration of the pHypermut2 vector into the unrearranged allele would result in inability to PCR the 493bp segment.

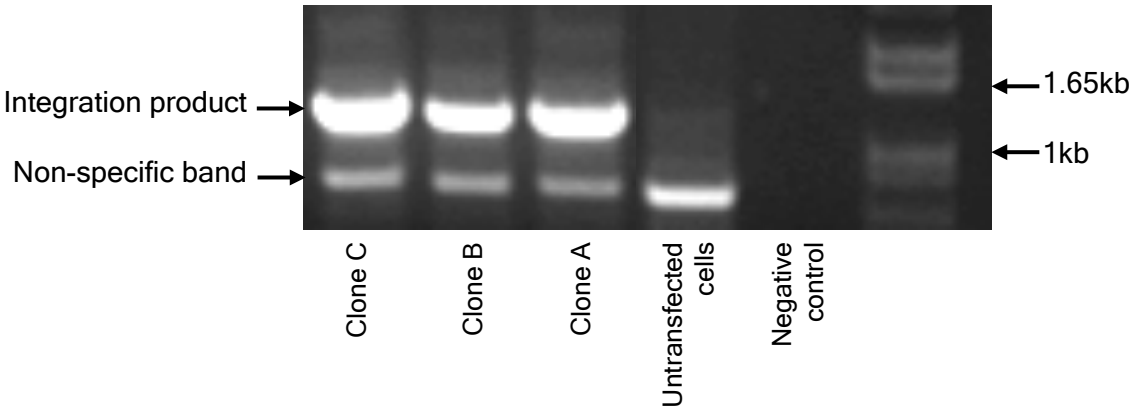

Figure 3.13: Targeted integration of Tie2 construct at the Ig locus. Genomic DNA was extracted from stably transfected Tie2-DT40 and subjected to PCR as described in section 2.6.6. The 1189bp product was resolved by electrophoresis on 1% agarose gel and visualised by UV illumination as described in section 2.2.5. The position of molecular size markers are indicated.

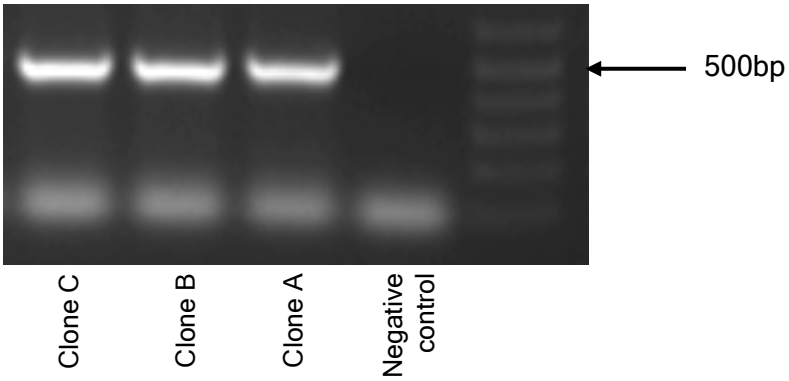

Figure 3.14: Targeted integration of Tie2 construct into the rearranged allele. Genomic DNA was extracted from stably transfected Tie2-DT40 and subjected to PCR as described in section 2.6.6. The 493bp product was resolved by electrophoresis on 1.2% agarose gel and visualised by UV illumination as described in section 2.2.5. The position of molecular size markers are indicated.

As shown in Figure 3.14, integration of pTie2ECD-CSD-Hypermut2 into the rearranged allele was confirmed by obtaining the 493bp PCR product in all three clones.

3.3 Immunofluorescent staining & angiopoietin binding in the Tie2-DT40 cell line

Following generation of a mutant Tie2 library 'in cell', the translated 'on-cell' Tie2 proteins require screening for angiopoietin binding characteristics via flow cytometry. It was therefore necessary to confirm that the expression of Tie2ECD on the Tie2-DT40 cell surface and associated angiopoietin binding could be detected by flow cytometry.

3.3.1 Characterisation of live Tie2-DT40 cells

Non-specific binding of angiopoietins and reagents will occur in permeable cells and therefore it is vital to exclude dead cells from flow cytometry assays. Propidium iodide fluoresces at a wavelength of 617nm when bound to DNA and excited at 535nm. To confirm the forward and side scatter characteristics of live and dead populations, Tie2-DT40 cells were incubated with 4°C 1µg/ml propidium iodide and assessed by flow cytometry as described in section 2.7. Propidium iodide staining confirmed the expected characteristics of dead cells (Figure 3.15). This data indicates that only 0.1% of dead cells will not be excluded based on

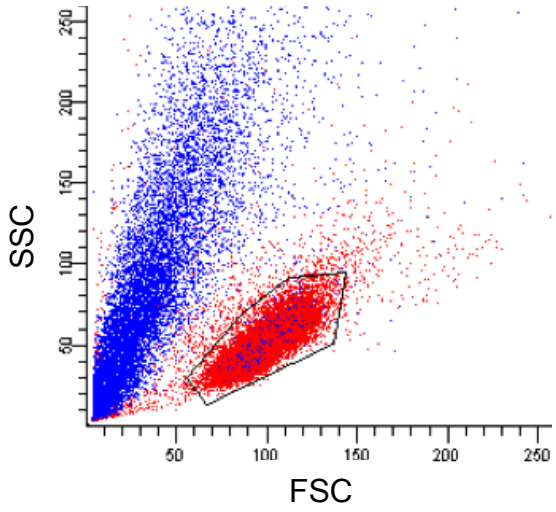

Figure 3.15: Characteristics of live Tie2-DT40 cells. Tie2-DT40 cells were incubated with propidium iodide and subjected to flow cytometry as described in section 2.7. Cells emitting fluorescence intensity above that of unstained control cells were considered lysed and coloured blue. Remaining cells are coloured red. The polygon gate illustrates the selected live cell population.

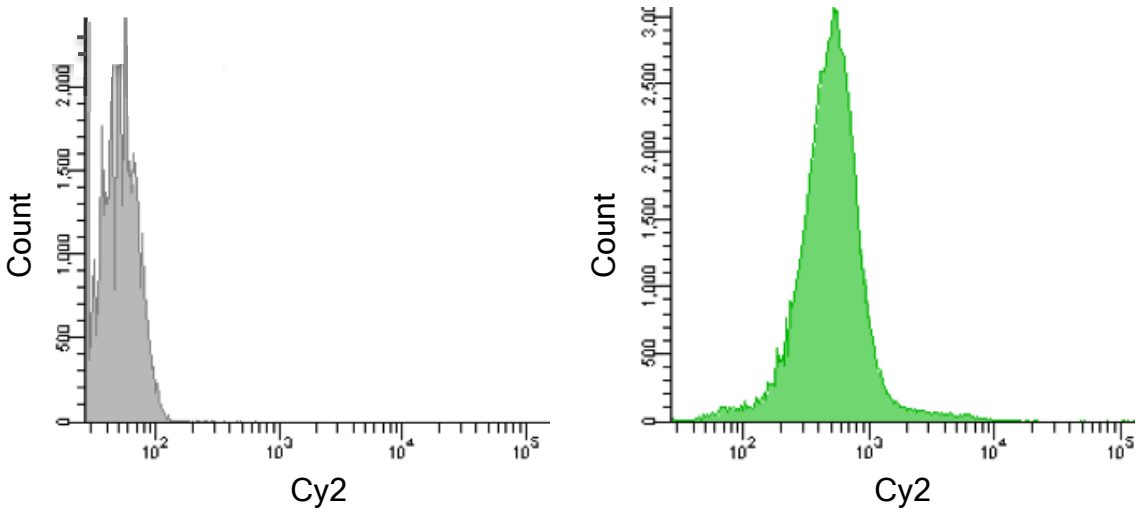

Figure 3.16: Cell surface expression of Tie2ECD. Tie2-DT40 and wild-type DT40 cells were stained by immunofluorescence for FLAG-peptide as described in section 2.7. Histograms of Tie2-DT40 (green) versus untransfected cells (grey) are shown.

forward & side scatter alone and cell parameters are therefore a suitable method for minimising non-specific signal during assays and cell sorting.

3.3.2 Tie2ECD is expressed on the DT40 cell surface

Tie2 cell surface expression can be detected via the FLAG epitope on live Tie2-DT40 cells, by incubation of cells with anti-FLAG monoclonal antibody and subsequent labelling with a fluorescent antibody as described in section 2.7. A suitable anti-FLAG concentration for binding had already been established in the laboratory (Dr S Sharma). The optimal anti-mouse-Cy2 secondary antibody concentration was established by staining Tie2-DT40 cells at concentrations above and including the recommended 1:400 dilution, with and without preceding anti-FLAG binding, and analysis by flow cytometry. 1:100 Cy2-Ab dilution produced the maximum signal without presence of significant background fluorescence and verified Tie2 cell surface expression. As expected staining of untransfected DT40 produced only background low level staining (Figure 3.16).

3.3.3 Angiopoietin-2 binds to cell surface expressed Tie2ECD

Biotinylated-Ang2 can be bound to cell-surface expressed Tie2 receptor on live Tie2-DT40 cells and fluorescently labelled with streptavidin-R-PE. The dissociation constant for Ang2 binding to Tie2 is reported to be as low as 3nM (Maisonpierre et al. 1997). A suitable streptavidin-R-PE concentration for labelling DT40 cells had previously been established in the laboratory (Dr S Sharma). To confirm binding, Tie2-DT40 cells were labelled with streptavidin-R-PE, with and

without prior incubation with an excess of biotinylated-Ang2, and analysed by flow cytometry as described in section 2.7. As shown in Figure 3.17, a clear signal was detected in Tie2-DT40 without any significant background. Identical staining of untransfected DT40 cells produced fluorescence intensity equal to unstained control cells. These data confirm that Ang2 binds specifically to DT40 expressing surface-expressed Tie2ECD.

3.3.4 Angiopoietin-1 binds to cell surface expressed Tie2ECD

His tagged-Ang1 can be bound to cell-surface expressed Tie2 receptor on live cells, and subsequently bound to anti-His biotin to enable labelling with streptavidin-R-PE. Ang1 is reported to have a similar Tie2 binding affinity to Ang2 (Maisonpierre et al. 1997, Davis et al. 1996). A suitable anti-His biotin concentration for use with DT40 cells had previously been established in the laboratory (Dr S Sharma). To confirm binding, Tie2-DT40 cells and untransfected DT40 cells were labelled with anti-His biotin and streptavidin-R-PE sequentially, with and without prior incubation with an excess of Ang1, and analysed by flow cytometry as described in section 2.7. A clear signal was detected for Tie2ECD expressing cells, in contrast to the background levels obtained in untransfected DT40 cells (Figure 3.18). These data confirm that Ang1 also binds specifically to DT40 expressing surface-expressed Tie2ECD.

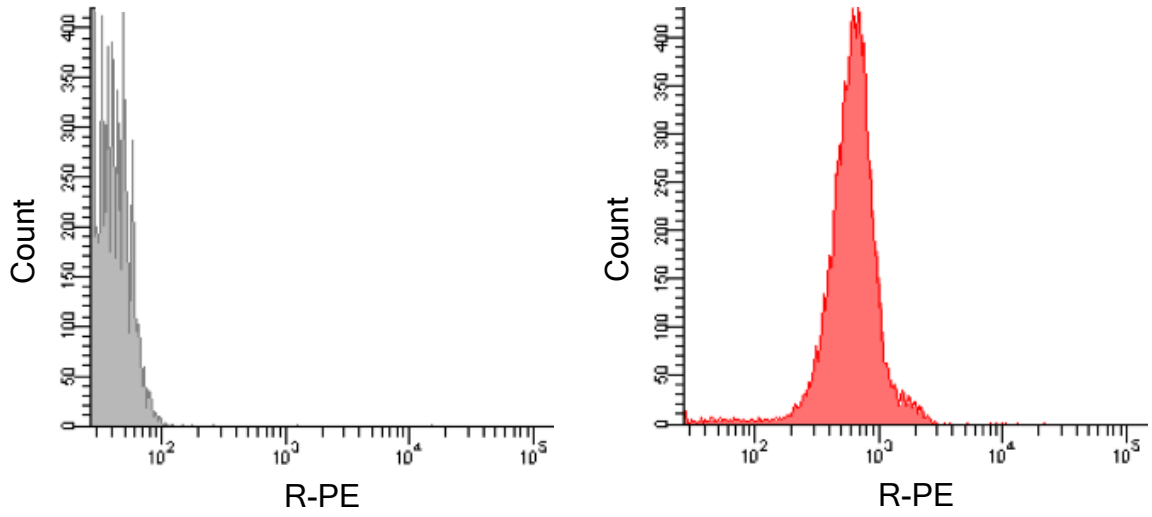

Figure 3.17: Angiopoietin-2 binding to cell surface expressed Tie2ECD. Tie2-DT40 cells were incubated with biotinylated Ang2 prior to streptavidin-R-PE labelling and flow cytometric analysis, as described in section 2.7. Parallel histograms of Ang2-R-PE (red) versus untransfected cells (grey).

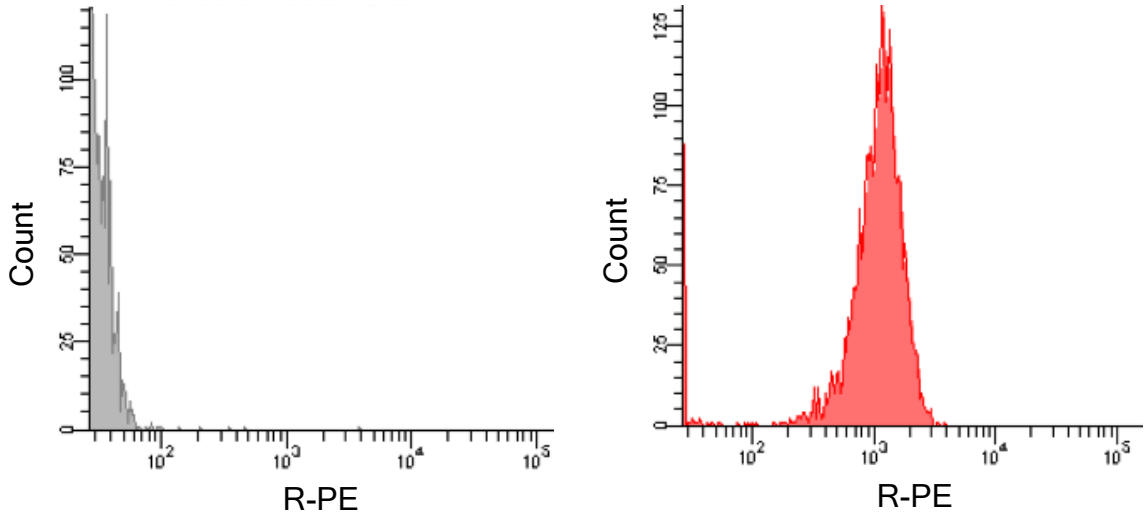

Figure 3.18: Angiopoietin-1 binding to cell surface expressed Tie2ECD. Tie2-DT40 cells were incubated with His-tagged Ang1 prior to anti-His biotin and streptavidin-R-PE labelling and flow cytometric analysis, as described in section 2.7. Parallel histograms of Ang1-R-PE (red) versus untransfected cells (grey).

3.3.5 Angiopoietin binding can be normalised for Tie2 expression level

In order to have capacity to normalise angiopoietin binding as a function of Tie2 expression it is necessary to perform simultaneous staining for angiopoietin binding and Tie2 expression. This involves detection of biotinylated or His-tagged angiopoietin and concurrent FLAG epitope detection (Figure 3.19a).

To establish the most concise protocol for cell staining various protocols for dual staining were tested. Use of pre-incubation of primary and secondary agents or simultaneous Ang2 binding and FLAG detection reduced the total Ang2 binding signal, indicating that when the maximal fluorescence intensity is of paramount importance such as to differentiate between levels of angiopoietin binding, staining should be done sequentially (Figure 3.19b).

3.4 Binding properties of wild-type Tie2ECD in DT40 cells can be determined by flow cytometry

Before designing screening assays for selection of angiopoietin binding properties in mutant Tie2-DT40 it is necessary to establish the quantitative binding characteristics of Tie2ECD in this cell system. In order to do this ψV^{-} AID^{R} Cl4 DT40 cells with undetectable AID expression (section 4.1.1) were stably transfected with pTie2ECD-CSD-Hypermut2 as described in section 2.4.4. A single clonal population was selected and cultured for all wild-type experiments.

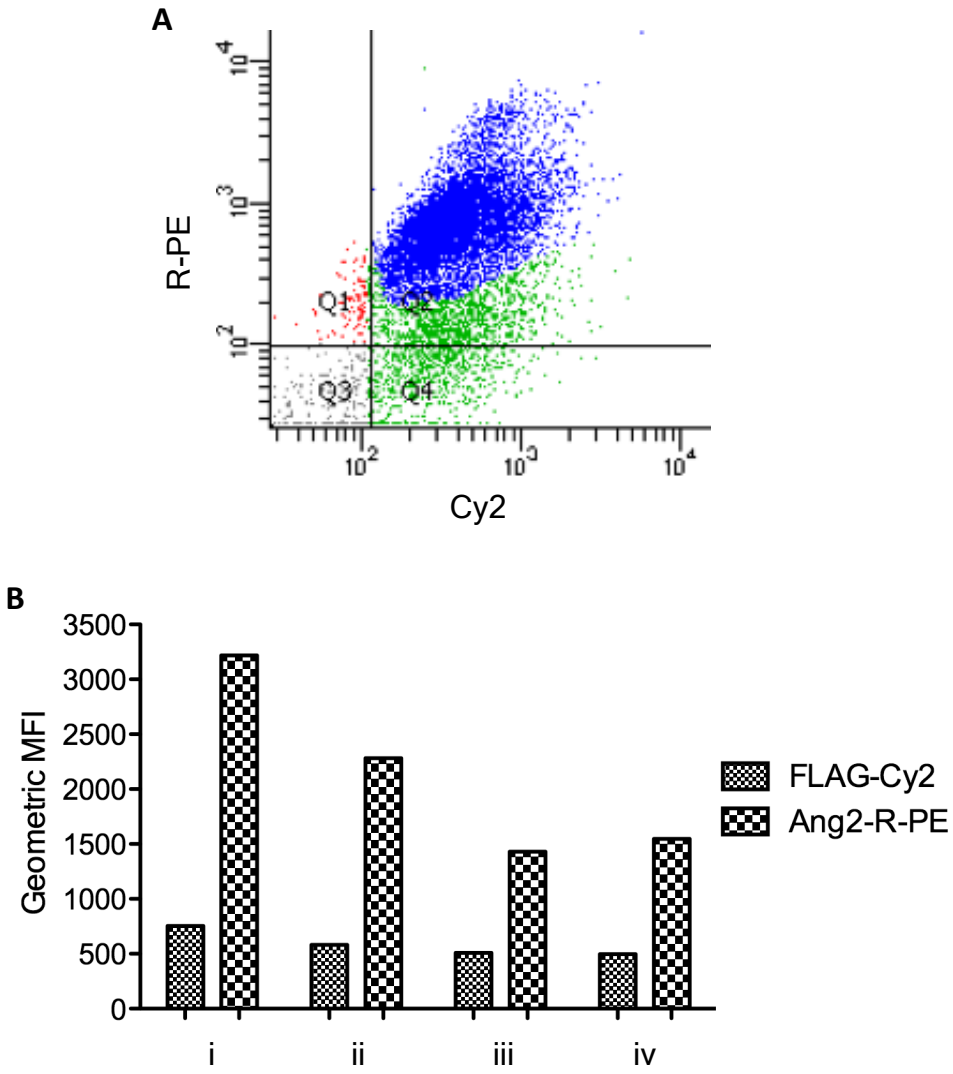

Figure 3.19: Dual staining of angiopoietin-2 binding cell surface expressed Tie2ECD.

a) Dual stained dot plot. Tie2-DT40 cells were incubated with biotinylated Ang2 prior to streptavidin-R-PE labelling and immunofluorescent detection of FLAG-peptide via Cy2. Flow cytometry analysis was performed as described in section 2.7. The principal dual stained population is coloured blue.

b) Dual staining methods. Detection of Ang2 binding and FLAG expression was performed using a variety of sequences to establish the most concise technique (*n*=1). Flow cytometry was performed as above. The absolute geometric mean fluorescence intensity (MFI) is graphed for each protocol:

(i) Ang2 binding → anti-FLAG binding → R-PE & Cy2 labelling;
(ii) Ang2 & anti-FLAG binding → R-PE & Cy2 labelling;
(iii) Ang2 & R-PE binding → anti-FLAG & Cy2 binding;
(iv) Simultaneous Ang2, anti-FLAG, R-PE & Cy2 binding.

3.4.1 Determination of Angiopoietin-2 K_d

In order to determine the dissociation constant (K_d) for Ang2 binding to cell-surface displayed Tie2, the geometric mean fluorescence intensity for several concentrations of streptavidin R-PE-bound biotinylated recombinant Ang2 was determined by flow cytometry.

Previous K_d estimations (Davis et al. 1996, Maisonpierre et al. 1997, Yuan et al. 2009) dictated the concentration range of Ang2 to be tested. To ensure that binding was not limited by the number of angiopoietin molecules present in the reaction volume relative to the number of Tie2ECD receptors, a ten times excess of ligand molecules over cell surface-bound receptor molecules was used. An assumed maximum of 5×10^4 cell surface-expressed Tie2 molecules per cell combined with a 1×10^6 cell requirement per fluorescent stain required at least 5×10^{11} molecules of ligand at each concentration to be tested. For lower ligand concentrations this required expansion of incubation volumes to maintain the desired concentration (Appendix 2.2).

Binding of ligand to cells was performed at room temperature. All subsequent steps were performed at 4°C without light exposure, to reduce the off-rate by 50 to 100 times (Boder, Wittrup 1998) and prevent photobleaching of the fluorescent R-PE. Labelling with streptavidin-R-PE was undertaken subsequent to Ang2 binding to prevent any interference with ligand-receptor interaction.

The assay was performed in triplicate as outlined in section 2.7.6.1. This yielded mean K_d ± SEM of 1.026 ± 0.23 nM for three independent experiments (Figure 3.20).

3.4.2 Determination of Angiopoietin-1 K_d

In order to determine the K_d for Ang1 binding to cell-surface displayed Tie2, several concentrations of His-tagged recombinant Ang1 were incubated with cells prior to anti-His biotin and streptavidin R-PE labelling and determination of geometric mean fluorescence intensity by flow cytometry.

The assay was performed as outlined in section 2.7.6.1, with consideration of the ligand quantity and conditions as outlined above. The resulting K_d ± SEM was 0.456 ± 0.17 nM for five independent experiments (Figure 3.21).

3.4.3 Methodological comparison of Ang1 and Ang2 K_d determination

It is possible that the difference between calculated dissociation constants for Ang1 and Ang2 is due to methodological variation, as Ang1 was detected by virtue of His-tag and secondary fluorescent label whereas Ang2 was labelled via conjugated biotin and streptavidin-R-PE. Utilisation of biotinylated ligand provides a more robust method due to the strong interaction between streptavidin and biotin. However biotinylated Ang1 was commercially unavailable at the time of investigation.

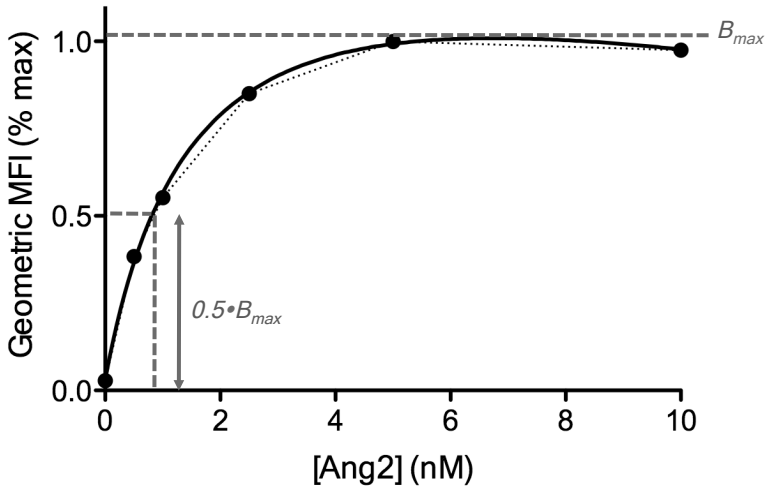

Figure 3.20: K_d determination for Ang2 binding to Tie2ECD. The geometric Mean Fluorescence Intensity (MFI) for various concentrations of R-PE labelled Ang2 bound to wild-type Tie2-DT40 cells was determined by flow cytometry in triplicate as described in section 2.7.6.1. Data from a single representative experiment is shown (*n*=3). Non-linear regression (solid line) was modelled on a one site-specific binding principle (Prism). K_d was presumed equal to the Ang2 concentration at half B_{max}.

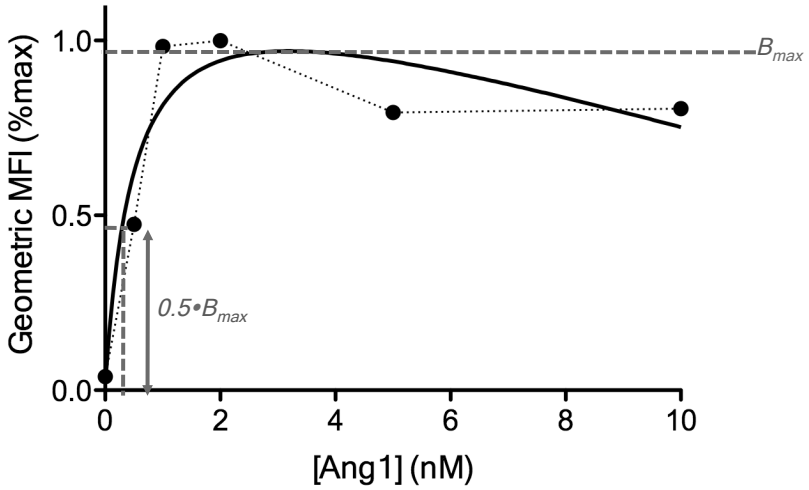

Figure 3.21: K_d determination for Ang1 binding to Tie2ECD. The geometric Mean Fluorescence Intensity (MFI) for various concentrations of R-PE labelled Ang1 bound to wild-type Tie2-DT40 cells was determined by flow cytometry in quintuplicate as described in section 2.7.6.1. Data from a single representative experiment is shown (*n*=5). Non-linear regression (solid line) was modelled on a one site- specific binding principle (Prism). K_d was presumed equal to the Ang1 concentration at half B_{max}.

In order to assess the comparability of results, Ang2 K_d was also estimated via the same process as Ang1, using His-tagged recombinant Ang2 (section 2.7.6.1). On this occasion the estimated Ang2 K_d was greater than with biotinylated ligand, at 1.951 nM in a single experiment (Figure 3.22). The higher Ang1 binding affinity is therefore not likely to be overestimated, but the difference in His-tagged Ang1 and biotinylated Ang2 binding affinities is not statistically significant (p=0.09).

3.4.4 Determination of Angiopoietin-2 K_{off}

In order to determine the off rate for Ang2 binding to cell surface-anchored Tie2, Tie2-DT40 cells were incubated with a biotinylated recombinant Ang2 concentration of more than ten times K_d at room temperature, and subsequently labelled with streptavidin-R-PE at 4°C. Dissociation of R-PE labelled-Ang2 was permitted by further room temperature incubation for fixed time points and stopped by significant dilution at 4°C. Significant reassociation of dissociated R-PE-Ang2 was prevented during the dissociation process by the presence of excess recombinant Ang2. Mean fluorescence intensity was assayed by flow cytometry for each time point sample (section 2.7.6.2).

In each of three independent experiments an apparent two-phase dissociation was observed (Figure 3.23). The majority of dissociation occurred during the first phase, which when analysed produced a K_{off} ± SEM of 0.578 ± 0.118 min^{-1}.

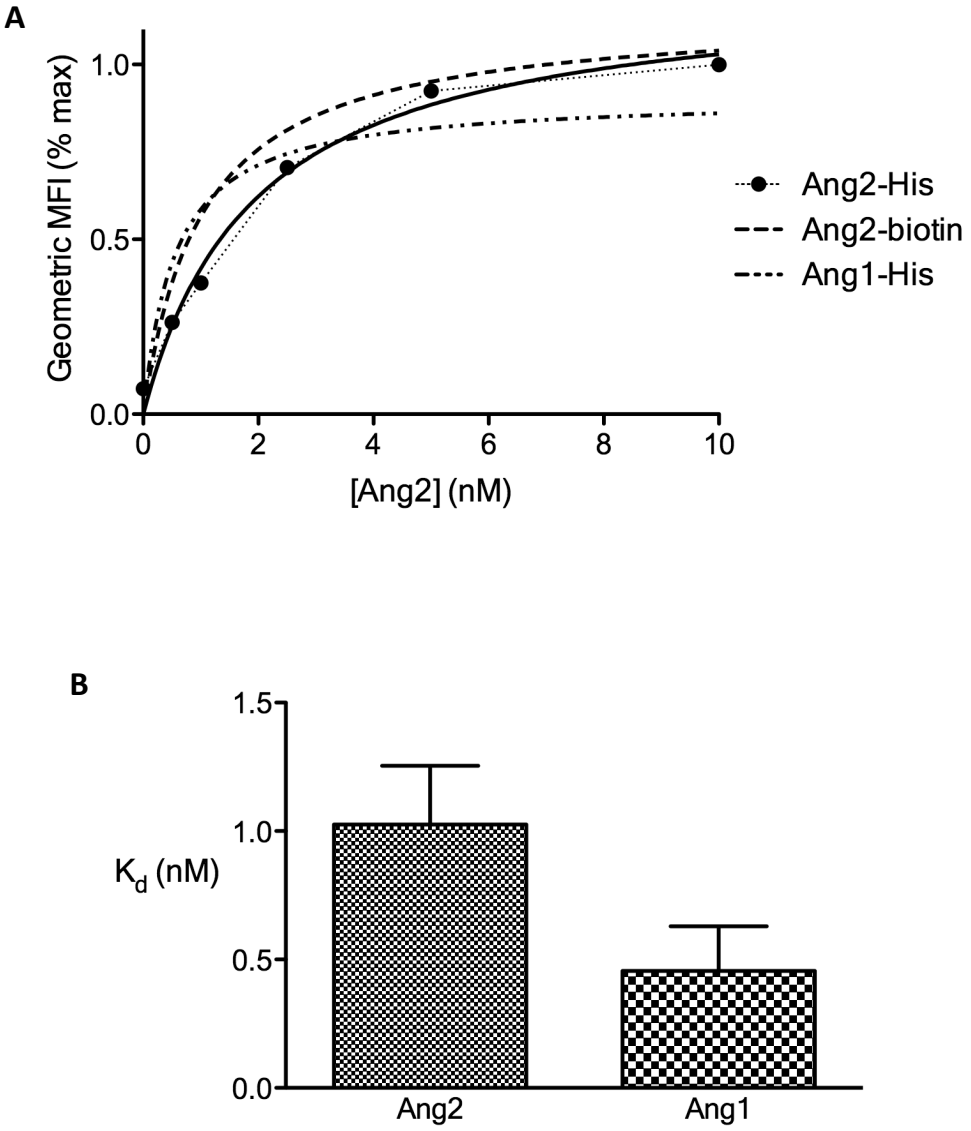

Figure 3.22: Comparison of Ang1 & Ang2 K_d.

a) Methodological comparison. The geometric Mean Fluorescence Intensity (MFI) for various concentrations of R-PE labelled Ang2 bound to wild-type Tie2-DT40 cells was determined in a single experiment by flow cytometry as for Ang1 (*n*=1). Non-linear regression, labelled 'Ang2-His', was modelled on a one site- specific binding principle (Prism). Regression analyses from Figs. 3.20 & 3.21 are overlaid and labelled 'Ang2-biotin' and 'Ang1-His' respectively.

b) Value comparison. Bar values represent mean for Ang2 (*n*=3) and Ang1 (*n*=5) flanked by SEM error bars, as determined in Figs. 3.20 & 3.21 respectively.

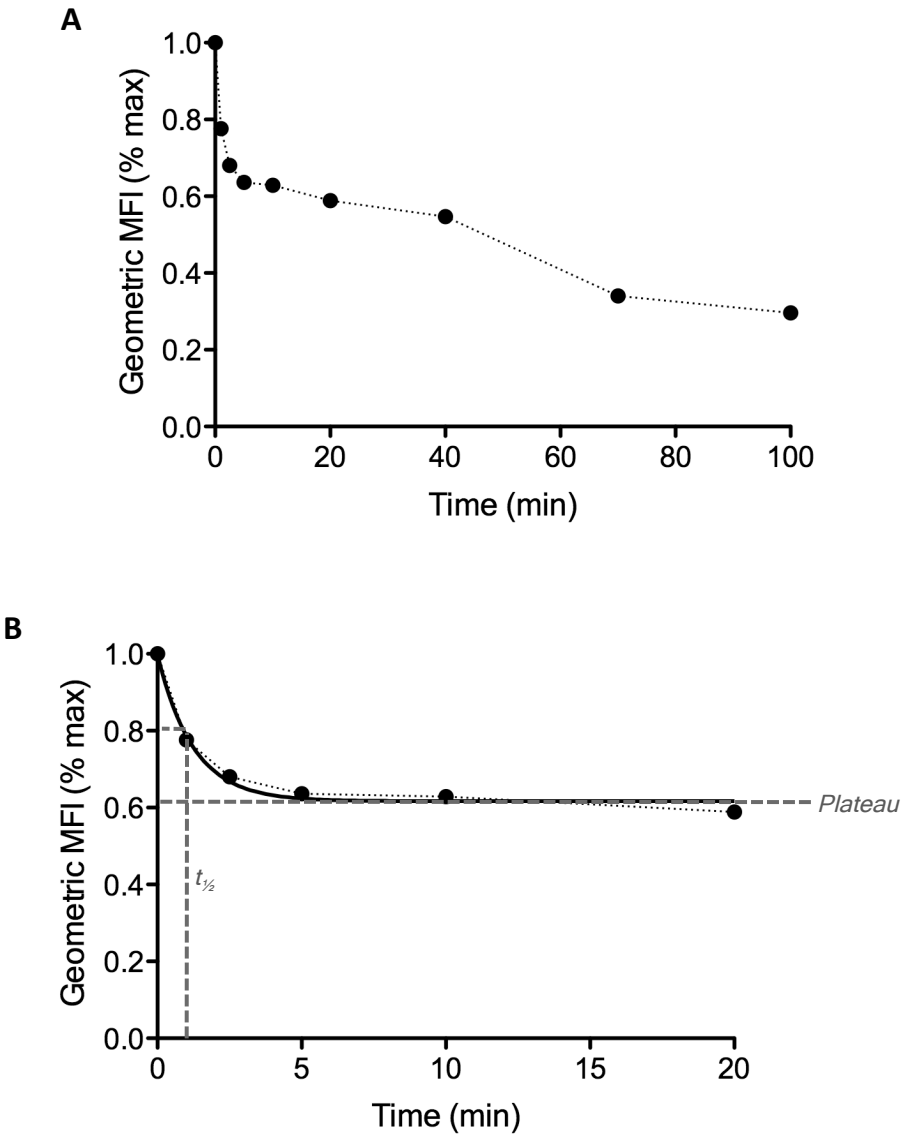

Figure 3.23: K_{off} determination for the Ang2-Tie2ECD binding interaction.

a) Observed dissociation. R-PE labelled Ang2 was bound at excess to wild-type Tie2-DT40 cells and allowed to dissociate for varying time points, as described in section 2.7.6.2. The geometric Mean Fluorescence Intensity (MFI) was determined by flow cytometry. Data from a single representative experiment is shown (*n*=3).

b) Estimation of K_{off}. Data gained in the first twenty minutes of dissociation of (a) was subjected to non-linear regression analysis (solid line) on a one-phase decay principle (Prism). Half of this exponential first phase of dissociation had occurred after 52 seconds.

3.4.5 Determination of Angiopoietin-1 K_{off}

Although anti-His biotin proved successful as a method of immunofluorescent staining for estimation of K_d, an equilibrium reaction, it is possible that measurement of the kinetic parameter K_{off} using anti-His is affected by dissociation of the anti-His antibody from angiopoietin. The off-rate for the anti-His biotin antibody used in section 3.4.3 has not been published, but K_{off} estimations for other anti-His antibodies are in the region of 3–60 × 10^{-4} s^{-1} (Bates, Quake 2009, Nieba, Krebber & Pluckthun 1996) compared with 3 × 10^{-7} s^{-1} (Hyre et al. 2000) for the streptavidin-biotin interaction, introducing the possibility that a proportion of apparent Ang1 dissociation could be attributed to anti-His dissociation.

Anti-His–PE was utilised in K_{off} experiments as opposed to separate primary anti-His-biotin and secondary fluorescent agent in an attempt to simplify and shorten the required staining steps. A further limitation is that recombinant Ang1 was not available without His-tag from the chosen supplier (R&D Systems), and so prevention of Ang1-anti-His-PE reassociation during the dissociation stage by means of an excess of unlabelled Ang1 was potentially less robust.

In order to determine the off rate for Ang1 binding to cell surface-anchored Tie2, Tie2-DT40 cells were incubated at room temperature in a His-tagged recombinant Ang1 concentration of more than ten times K_d, and subsequently labelled with anti-His-PE at 4°C. The cells were then incubated with an excess of room temperature His-tagged recombinant Ang1 for varying time points, until the dissociation was

stopped by significant dilution at 4°C. Mean fluorescence intensity of each sample was assayed by flow cytometry (section 2.7.6.3).

The expected rapid Ang1 dissociation was not observed. In order to clarify whether the data truly reflects slow dissociation of Ang1 or methodological problems, Ang2 dissociation was measured using the anti-His protocol. A similar phenomenon of slow Ang2 dissociation occurred (Figure 3.24) suggesting inaccuracy in the protocol and therefore an estimate of Ang1 K_{off} was not achieved.

Discussion

Data presented in this chapter demonstrate the construction of a system in which to conduct directed evolution of Tie2ECD by somatic hypermutation and FACS.

Selection of Tie2 residues 1 -441 for study, as opposed to the minimal binding domain, broadens the scope of the investigation. In order to permit integration of Tie2ECD into the Ig locus and subsequently allow selection by FACS, a Tie2-cell surface display construct was cloned and transferred into the pHypermut2 vector.

Arakawa *et al.* designed pHypermut2 vector for use in DT40-based SHM due to findings that pHypermut1, their original successful vehicle for transgene expression driven by the Ig light chain promoter, was prone to influence by mutations in the Ig locus itself (Arakawa et al. 2008). Expression of the transgene

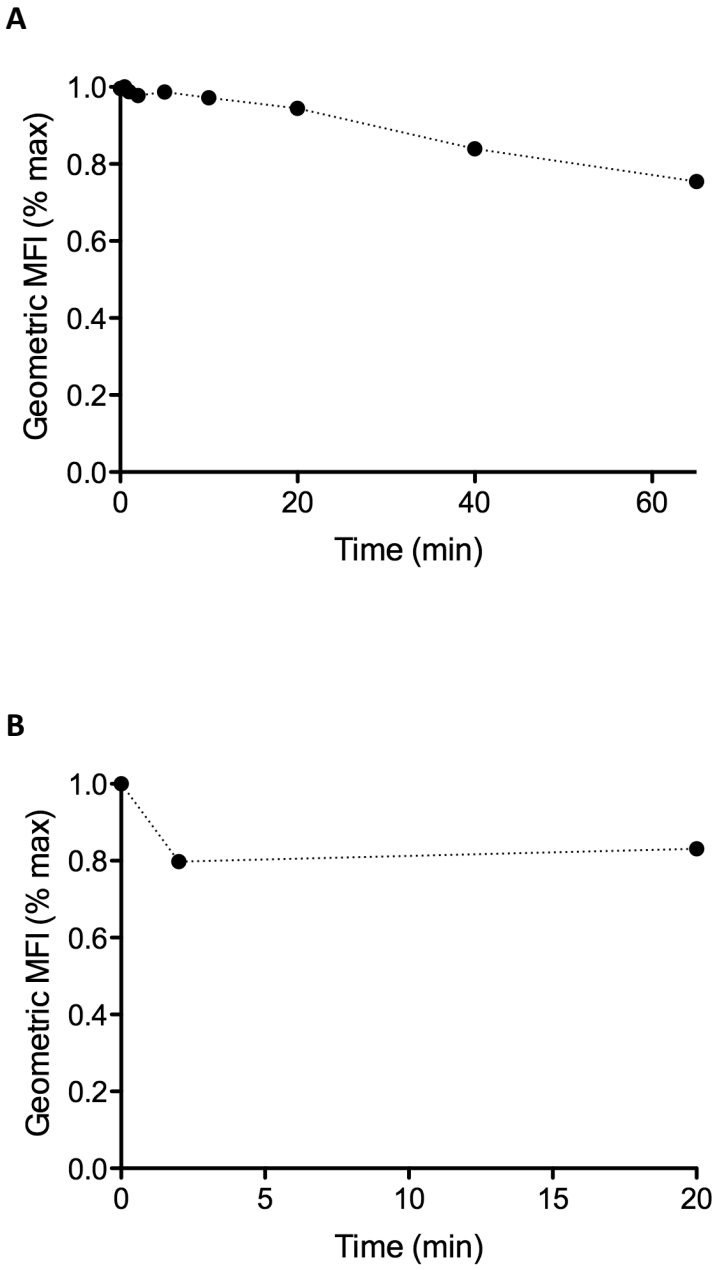

Figure 3.24: Dissociation of the angiopoietin-Tie2ECD binding interaction. Anti-His-PE-labelled angiopoietin was bound at excess to wild-type Tie2-DT40 cells and allowed to dissociate for varying time points, as described in section 2.7.6. The geometric Mean Fluorescence Intensity (MFI) was determined by flow cytometry. Raw data of single experiments is expressed (*n*=1).

a) Angiopoietin 1

b) Angiopoietin 2

in pHypermut2 is driven by its integral RSV promoter and integration into the Ig locus occurs in the opposite orientation to native genes.

Ligation of Tie2ECD-CSD into pHypermut2 proved more difficult than ligations with the TOPO expression vector despite smaller vector to insert size ratio and use of ultracompetent cells for transformation. Poor efficiency was multi-factorial and likely compounded in pHypermut2 due to its larger size and/or structural complexity. However cloning was successfully achieved as demonstrated by sequencing and expression in transfected HEK293 cells.

The DT40 cell line offers several advantages as a host for SHM, including short doubling time and high frequency of targeted integration of transgenes at the Ig locus. In addition, the 'ψV^- AID^R Cl4' modification supports SHM only and allows excision of highly expressed AID on demand, in contrast to the wild-type DT40 cell line where AID-dependent gene conversion occurs in addition to SHM and AID is expressed constitutively. The function of this cell line will be discussed in more detail in the next chapter.

DT40 cells are relatively difficult to transfect and low efficiencies are expected. At the time of investigation electroporation was the most frequently reported method of stable transfection with advertised efficiency of up to 20% (Wagner, Betzenhauser & Yule 2006). The Amaxa™ Nucleofector™ was frequently employed in transient transfection due to improved effectiveness over electroporation (Franklin, Sale 2006), but only occasionally as a means of stable transfection (Wagner, Betzenhauser & Yule 2006).

Attempts at stable transfection with the Amaxa™ Nucleofector™ were not successful, despite use of manufacturer's guidelines and published conditions (Franklin, Sale 2006). Optimisation of this technique would be hastened by cloning of a fluorescent protein-Hypermut2 plasmid, in order to observe protein expression over the period of culture subsequent to testing of different conditions.

Electroporation was pursued as a method of stable transfection due to the greater body of evidence for its success and ability to manipulate conditions. Stable transfection of Tie2ECD was achieved at an efficiency of 0.002%, assuming an average of fifty percent cell death during electroporation and origin of each colony from a single transfected cell. Although this frequency is extremely low the total number of colonies produced is inconsequential, as single clonal populations with a single site of Tie2ECD integration are required for further experimentation. Selected populations were maintained under puromycin selection and did not exhibit any loss of Tie2ECD expression based on immunofluorescent staining after a period of cell culture.

An alternative approach that should guarantee preferable transfection efficiency is retroviral transduction (Barreto et al. 2003, Randow, Sale 2006). Reports of fluorescent protein evolution by SHM have utilised retroviral infection of Ramos and 18-81 cell lines (Wang et al. 2004b, Wang, Yang & Wabl 2004, Wang, Harper & Wabl 2004). However this method carries the risk of introducing multiple copies of the transgene into the cell, such that each cell is not guaranteed of displaying a

single genotype. Transgene integration is also acknowledged to be random in this situation (Wang, Yang & Wabl 2004).

All three Tie2-DT40 clonal populations examined demonstrated correct targeted integration in the rearranged Ig locus, in agreement with the greater than 70% successful integration quoted by Arakawa *et al.* for pHypermut constructs (Arakawa et al. 2008). Blagodatski *et al.* reported a 50 – 500 times higher mutation rate in the Ig locus versus other genomic locations (Blagodatski et al. 2009) and hence these clonal populations were selected for study of somatic hypermutation.

The ability to detect cell-surface expressed Tie2ECD via the FLAG epitope and successful binding and fluorescent staining of angiopoietins confirm intact Tie2 confirmation and the success of PDGFRβ-TM as a mechanism of cell-surface display. No significant background signal was detected from untransfected DT40 cells indicating adequate specificity of the reagents. Attempted refinement of the binding steps reduced Mean Fluorescence Intensity (MFI), consequently diminishing sensitivity of the assay. Rationalisation of the protocol would therefore require a reduction in number of required reagents.

Binding characteristics for Ang1 and Ang2 binding to cell surface expressed wild-type Tie2ECD approximate to existing literature despite differences in materials and method. K_d of 0.456nM for Ang1 and 1.026nM for Ang2 are lower than the 3nM K_d observed by Davis for both interactions (Davis et al. 1996). Variation in technique for assessment of Ang1 and Ang2 was suboptimal, although comparative analysis of the anti-His-biotin labelling method offered a degree of validation.

Greater variation was observed between individual Ang1 K_d experiments, perhaps reflecting the insufficiency of biotin-conjugated His antibody in comparison to biotinylated ligand; however this is not reflected in the standard error of mean K_d. Ang2 appears to have lower binding affinity than Ang1, although the order of magnitude is far less than that reported by Yuan *et al.* (Yuan et al. 2009) and does not carry statistical significance.

Calculation of K_{off} for Ang1 and Ang2 binding to cell surface displayed wild-type Tie2ECD proved more challenging. Kinetic analysis of Ang2 dissociation was performed as described in the literature (Boder, Wittrup 1997), yielding a K_{off} value of 9.6×10^{-3} s^{-1} on analysis of the initial dissociation. This phase of dissociation however plateaued at 57.8% of maximal fluorescence, against a background cell autofluorescence of 1.9%. The subsequent more gradual phase of dissociation displayed considerable variation between experiments and did not progress to the level of cell autofluorescence. This apparent two-phase effect may be due to intrinsic oligomeric properties of recombinant angiopoietins. Incomplete loss of fluorescence reduces the ability to discriminate minor differences in K_{off} between one cell and another, and has implications for the success of FACS.

The dissociation rate for Ang1 binding to cell surface expressed Tie2ECD was not successfully measured. There is a vast difference in K_d between the interaction of His-tag with His-antibody and streptavidin with biotin, at 10^{-6} M (Nieba, Krebber & Pluckthun 1996) and 10^{-15} M (Weber et al. 1989) respectively. The kinetics of the particular PE-conjugated His antibody used in this context are not known, but even accounting for more favourable characteristics would not offer any match for

streptavidin-biotin. Anti-His-PE potentially has a lower affinity for Ang1 than the Ang1-Tie2 interaction itself and apparent loss of fluorescence could be attributable to anti-His-PE dissociation. In addition, the excess of unlabelled Ang1 present at the time of dissociation could inadvertently be labelled itself with dissociated anti-His-PE, although the intention was to prevent reassociation of PE-His-Ang1. These fundamental issues do not favour the success of the technique in any circumstances, and investment in development of biotinylated recombinant Ang1 would seem more prudent.

In this chapter Tie2ECD has been correctly inserted into a DT40 hypermutating cell line in a position of maximal mutability, and engineering of a cell surface display construct has allowed measurement of baseline Ang1 and Ang2 binding affinities by fluorescent on-cell labelling within the system of choice. Fluorescent staining protocols involve complex interactions and parameters, which require development to maximise assay specificity and sensitivity and will be further discussed in Chapter 5. The next chapter will focus on somatic hypermutation within the selected system.

CHAPTER FOUR

Generation of a mutagenic Tie2 library by somatic hypermutation in the DT40 'ψV^{-} AID^{R} Cl4' cell line

In order to utilise somatic hypermutation (SHM) as a method of genetic diversification in directed protein evolution, the frequency and spread of mutations must be sufficient to construct a credible library. The efficiency of the evolution process, in which iterative selection is performed on actively mutating cells, depends on a high mutation rate and can be optimised further by the ability to control the action of Activation Induced Deaminase (AID).

Use of SHM presents a challenge due to the fact that the mechanism of AID activity has not yet been fully characterised. However several relevant host cell and target gene properties have been identified, including AID expression, target gene location, accessibility of target gene DNA and target gene sequence.

In Chapter 3 the gene of interest for directed protein evolution, Tie2ECD, was successfully integrated into the rearranged Ig locus of the hypermutating ψV^- AID^R Cl4 DT40 cell line, which is a modified form of wild-type DT40.

SHM of Tie2ECD in the ψV^- AID^R Cl4 DT40 cell line is explored in this chapter, to include:

- AID expression in ψV^- AID^R Cl4 DT40;
- Scope of SHM in diversification of Tie2ECD;
- Observed mutagenesis in Tie2ECD;
- Optimisation mechanisms for SHM in ψV^- AID^R Cl4 DT40.

Introduction

The DT40 cell line diversifies immunoglobulin (Ig) genes by SHM and gene conversion, both of which are driven by the action of AID. SHM results in single point mutations, whereas gene conversion introduces new sequences derived from upstream pseudo V (ψV) Ig donors.

Deletion of ψV donors in the DT40 cell line abolishes gene conversion and increases the rate of SHM (Sale et al. 2001, Arakawa, Saribasak & Buerstedde 2004) . The extent of SHM in Ig and non-Ig genes is improved by AID overexpression (Martin, Scharff 2002, Wang et al. 2004b, Wang, Yang & Wabl 2004, Wang, Harper & Wabl 2004, Arakawa et al. 2008) and the mutation rate of transgenes is highest in the Ig locus (Blagodatski et al. 2009). The combination of vector and cell line utilised in this study addresses each of the above points: pHypermut2 encourages rearranged Ig locus integration; the ψV^{-} AID^{R} modification of the DT40 cell line, of which ψV^{-} AID^{R} Cl4 is a clonal population, features β-actin promoter driven AID transcription and ablation of all rearranged locus ψV donors. β-actin offers improved AID expression compared with the native DT40 promoter (Yang, Fugmann & Schatz 2006, Arakawa et al. 2008).

There is further complexity associated with AID expression in the ψV^{-} AID^{R} DT40 cell line. Endogenous AID is replaced by a floxed AID construct (Arakawa, Hauschild & Buerstedde 2002, Arakawa, Saribasak & Buerstedde 2004) composed of ggAID-IRES-gpt (*Gallus gallus* Activation Induced Deaminase-Internal Ribosome Entry Site-Guanine Phosphoribosyl Transferase). The ability to block AID action

via Cre recombinase induction and loxP mediated-cassette excision is advantageous once the desired mutant phenotype is reached, considering that diversification and selection will occur in live cells. The presence of gpt in the construct also permits selection of AID cassette-positive cells with mycophenolic acid (MPA). The control of this system will be assessed in this chapter.

The reported mutation rate for transgenes located in the rearranged Ig locus of ψV$^-$ AID^R DT40 cells is 1×10^{-5} per base pair per generation (Blagodatski et al. 2009). A healthy population of ψV$^-$ AID^R Cl4 DT40 cells, having undergone MPA selection for AID expression, should have a similar rate of mutation. Although mutation rates are expressed as a function of generation time, duration in cell cycle growth phase and splitting conditions seem to be important variables and chronological time could be argued as a more reliable measure (Faili et al. 2002, Wang, Wabl 2005). Higher culture temperature and optimal cell density shorten doubling time of DT40 cells, whereas genetic modifications may lengthen it (Simpson, Sale 2003, Nakamura et al. 2010). The doubling time of ψV$^-$ AID^R Cl4 DT40 cells and mutation frequency of Ig locus located Tie2ECD will be determined.

The probability of point mutation at any single nucleotide is not equal in SHM. The action of AID begins approximately 185 base pairs downstream from the transcription start site, preferentially targets C:G base pairs in the DT40 cell line and has a predilection for particular 'hotspot' sequence motifs (Lebecque, Gearhart 1990, Rada et al. 1997, Rogozin, Kolchanov 1992, Rogozin et al. 2001). Therefore potential diversity of Tie2 is dependent on its sequence and likely to involve 97% G:C base pair mutations and 55% of mutations within the D<u>G</u>YW/WR<u>C</u>H

consensus, with the underlined base indicating the mutable position (Arakawa, Saribasak & Buerstedde 2004, Rogozin, Diaz 2004) (section 1.4). Equally the type of mutation is influenced by DNA repair mechanisms and DT40 cells do not share the same predilection for transitions as germinal center B-cells (Sale et al. 2001, Barreto et al. 2003, Arakawa, Saribasak & Buerstedde 2004). The stem loop structure of its single stranded DNA may also influence mutation distribution (Wright, Schmidt & Minnick 2004), and additionally prevalence of *cis*-elements for transcription factors including E2A could influence the mutation frequency (Schoetz et al. 2006). The theoretical and actual Tie2 mutant library generated will be explored.

The requirement for single stranded DNA as an AID substrate dictates that the rate of SHM is proportional to transgene transcription (Bachl et al. 2001) and linked to DNA accessibility. Whilst the endogenous Ig promoter is not a prerequisite (Rada et al. 1997), a strong promoter is vital. In this system Tie2ECD transcription is driven by the RSV promoter, which is known to support SHM (Arakawa et al. 2008, Blagodatski et al. 2009). Accessibility of DNA can be improved by Trichostatin A (TSA)-mediated hyperacetylation to augment AID activity (Woo, Martin & Scharff 2003, Seo et al. 2005). Interestingly the eEF1α promoter does not support SHM in DT40 cells, despite satisfactory expression levels (Yang, Fugmann & Schatz 2006). It is however a potentially useful tool as the AID gene itself can be mutated when overexpressed (Martin, Scharff 2002) and therefore eEF1α promoter-driven AID transcription would eliminate the risk of inactivating mutations. Modification of AID activity will also be investigated.

4.1 Regulation of somatic hypermutation in the DT40 'ψV$^-$ AID^R' cell line

The 'ψV$^-$ AID^R' DT40 cell line is engineered to allow control of AID expression in addition to promotion of SHM. The mechanism of control is by means of a floxed AID-gpt gene: oestrogen derivatives should excise AID-gpt from the genome, whilst mycophenolic acid should kill cells that lack AID-gpt. It was necessary to verify this capability prior to exploiting it during iterative selection.

4.1.1 AID expression can be unintentionally lost in 'ψV$^-$ AID^R Cl4' DT40 cells

During development of an RT-PCR assay for transcribed AID, a whole population of 'ψV$^-$ AID^R Cl4' DT40 cells was found to have lost AID having undergone several rounds of cell passage in the absence of any exposure to exogenous oestrogen derivatives. Western immunoblotting for AID from whole cell lysate confirmed an absence of expressed protein (section 2.5) (Figure 4.1). Arakawa *et al.* report undesired excision of AID from a proportion of a cultured 'ψV$^-$ AID^R' DT40 cell population and attribute this to basal background activity of Cre recombinase (Arakawa et al. 2008). Periodic selection of AID-gpt positive cells is therefore crucial to maintain mutagenesis.

4.1.2 AID-expressing 'ψV$^-$ AID^R Cl4' DT40 cells can be selected

MPA-mediated selection of AID-gpt positive cells was performed by culture with 1.6μM MPA for 72 hours as described by Arakawa *et al.* (Arakawa et al. 2008).

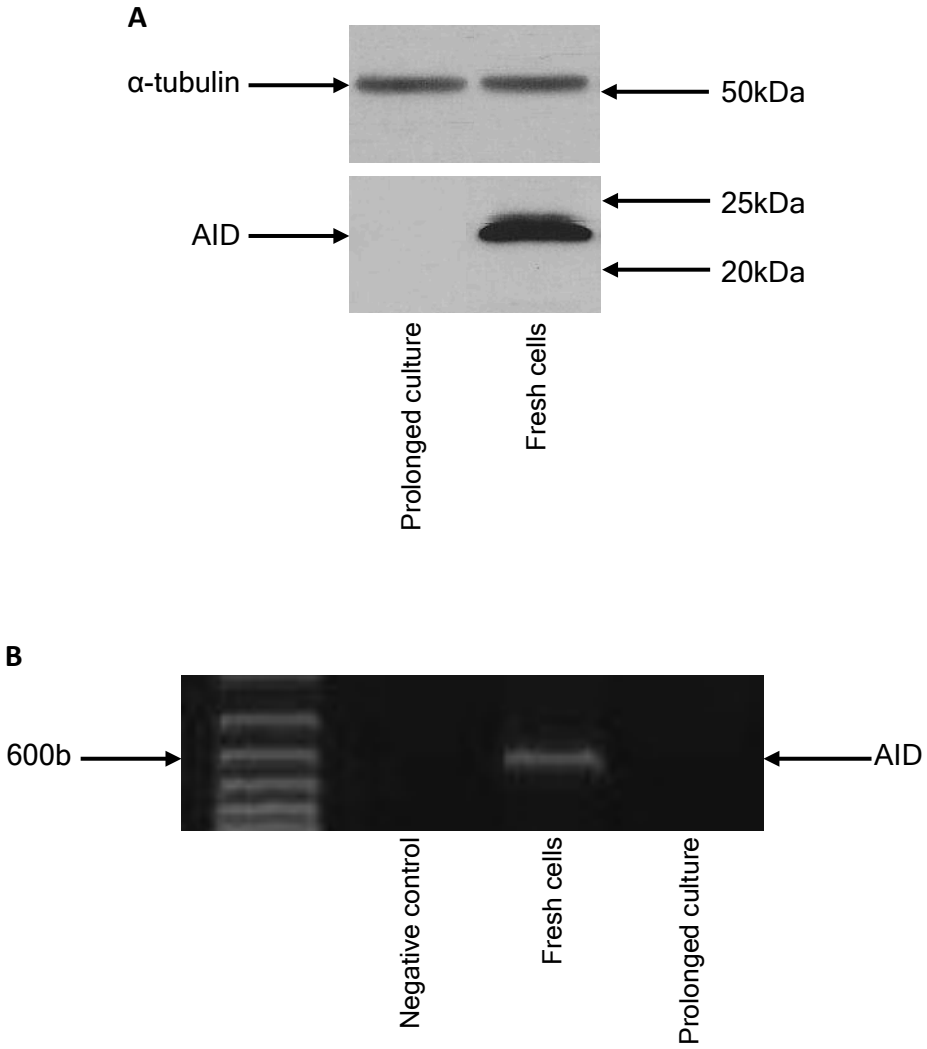

Figure 4.1: AID expression can be unintentionally lost in DT40 'ψV$^-$ AID^R Cl4' cells.

a) AID expression probe. Whole cell lysate was prepared from low and high passage DT40 'ψV$^-$ AID^R Cl4' cell cultures, and subjected to SDS-PAGE and Western blotting as described in section 2.5. Immunoblot analysis was performed with anti-AICDA polyclonal antibody. The position of molecular weight markers are indicated.

b) RT-PCR of AID. Total RNA was extracted from low and high passage DT40 'ψV$^-$ AID^R Cl4' cell cultures and subjected to RT-PCR as described in section 2.6. The 615bp product was resolved by electrophoresis on 1.2% agarose gel and visualised by UV illumination as described in section 2.2.5. The position of molecular size markers are indicated.

In order to test this selection, a low passage clonal population of 'ψV$^-$ AID^R Cl4' DT40 cells was treated with MPA and cultured for one month before being split. One culture was retreated with MPA prior to preparation of whole cell lysate from both cultures.

Western immunoblotting of SDS-PAGE-resolved proteins was performed with anti-AICDA antibody for AID, prior to assessment with anti-α-tubulin antibody as a loading control (section 2.5). A higher AID expression level was demonstrated in the culture more recently treated with MPA, indicating that AID negative cells had been removed by MPA selection (Figure 4.2). Consequently cells were treated with MPA at periodic intervals, and before any intervention such as transfection or assessment of mutagenesis was performed.

4.1.3 AID can be excised from the 'ψV$^-$ AID^R Cl4' DT40 cell genome on demand

It should be possible to excise AID-gpt from the genome with the oestrogen derivative 4-hydroxytamoxifen (4-OHT). To test this, DT40 'ψV$^-$ AID^R Cl4' cells were removed from liquid nitrogen and, when sufficiently recovered, treated with MPA. The culture was split into three parts and treated with serially diluted 1, 0.5 and 0.1 μM 4-OHT.

Total RNA was extracted from each cell population after 48, 96 and 144 hours of cell culture, 2μg of which was used for immediate cDNA synthesis by reverse transcription (section 2.6). PCR for a 615bp portion of AID was performed on each cDNA under the conditions specified in Appendix 2.1. 0.5μM 4-OHT was sufficient

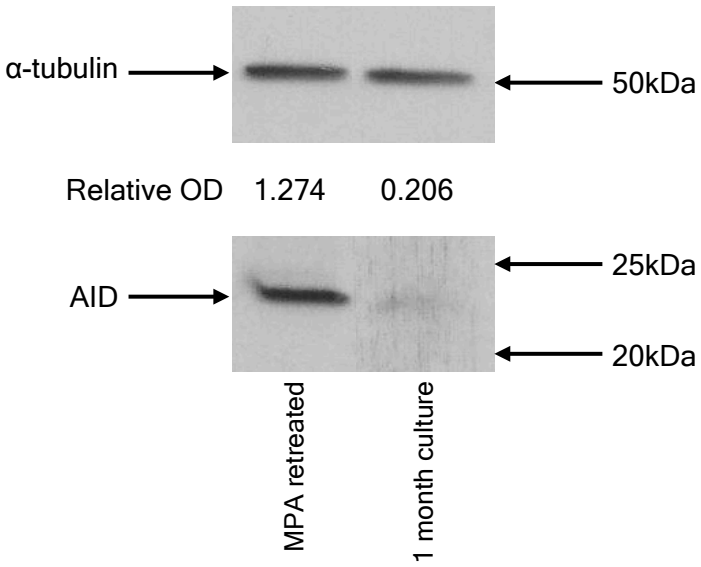

Figure 4.2: Expression of AID in MPA-selected DT40 'ψV$^-$ AID^R Cl4' cells. DT40 'ψV$^-$ AID^R Cl4' cells were treated with 1.6μM MPA and subsequently cultured for one month. The culture was split and one half retreated with 1.6μM MPA, prior to preparation of whole cell lysate from each. SDS-PAGE and Western blotting were performed as described in section 2.5. Following probing with anti-AICDA polyclonal antibody the membrane was stripped and re-probed with anti-α-tubulin monoclonal antibody. The position of molecular weight markers are indicated. Relative Optical Density (OD) was calculated as a ratio of AID to α-tubulin optical density for each culture and determined by ImageJ analysis of non-saturated films (*n*=1).

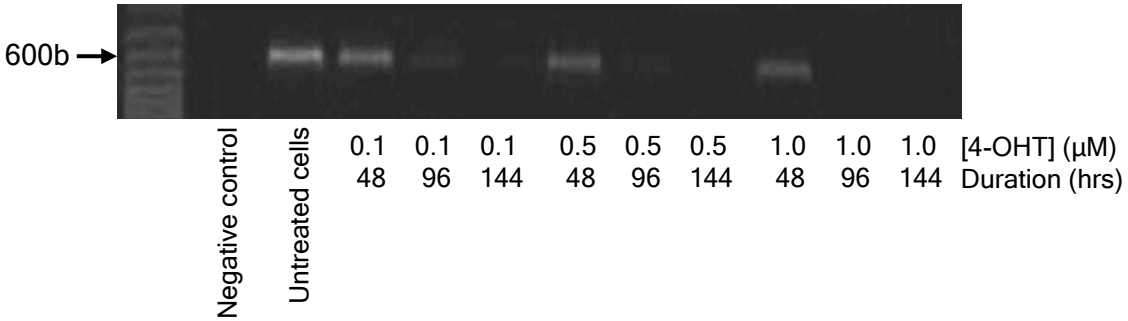

Figure 4.3: Excision of AID in MPA-selected DT40 'ψV$^-$ AID^R Cl4' cells. DT40 'ψV$^-$ AID^R Cl4' cells were split and cultured with varying concentrations of 4-hydroxytamoxifen (OHT). Total RNA was extracted from each culture at 48, 96 and 144 hours. RT-PCR for AID was performed as described in section 2.6. The 615bp product was resolved by electrophoresis on 1.2% agarose gel and visualised by UV illumination as described in section 2.2.5 (*n*=2). The position of molecular size markers are indicated.

to abolish detectable AID transcription by 144 hours and 1μM enabled excision by 96 hours (Figure 4.3). Whilst this technique of preventing further SHM should be effective the concentration and timing of 4-OHT exposure is important and therefore excision of floxed AID should be confirmed following 4-OHT treatment.

4.1.4 AID is differentially expressed in clonal populations of Tie2 ECD-transfected 'ψV^{-} AID^{R} Cl4' DT40 cells

The level of AID expression contributes to rate of SHM and therefore it was of interest to assess the quantity of AID in three separate MPA-treated Tie2-DT40 clones. Whole cell lysate was prepared from these Tie2-DT40 clones (A, B & C) on three separate occasions, and subjected to SDS-PAGE and Western blotting. Nitrocellulose membranes were first probed with anti-AICDA antibody prior to stripping and re-probing for α-tubulin as a loading control (section 2.5).

Figure 4.4 depicts an AID probe from a single representative experiment and a graphical representation of mean AID expression levels. Clone B had the highest mean level of AID expression, which was statistically significant when compared to Clone A. Clone C exhibited more variability between experiments. Therefore it may be important to assay AID expression levels when selecting a Tie2-DT40 population to take forward for SHM.

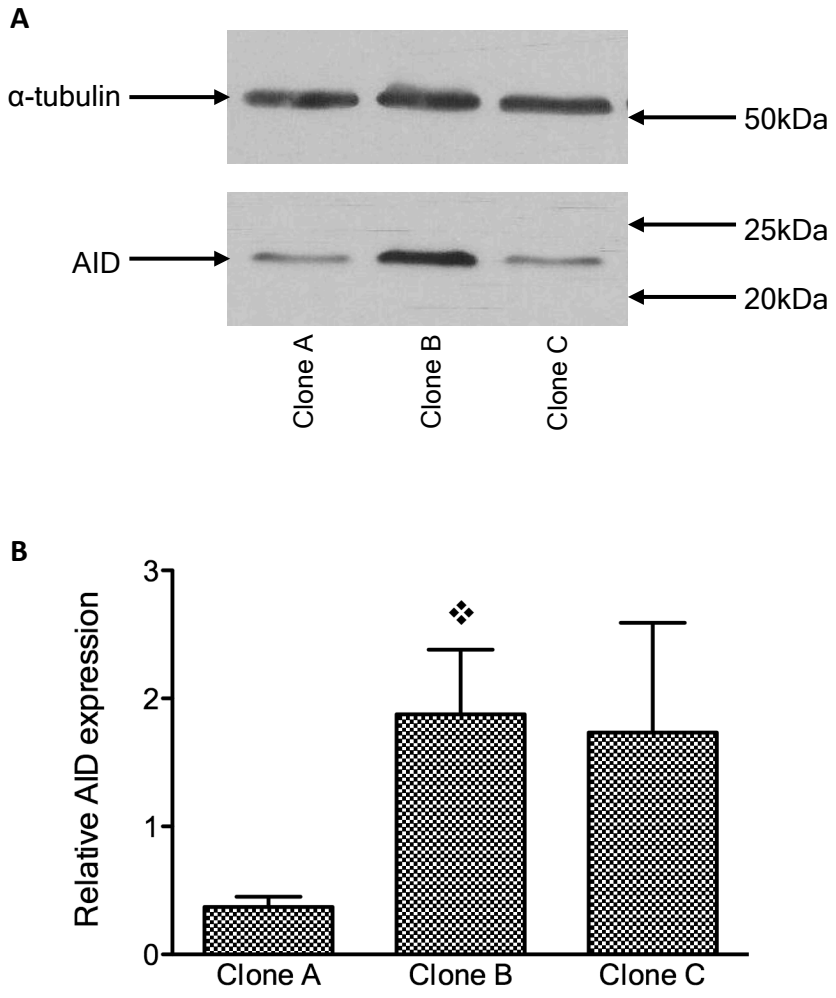

Figure 4.4: Expression of AID in Tie2-DT40 clones A, B & C.

a) AID expression probe. Tie2-DT40 clones A, B & C were treated with MPA prior to preparation of whole cell lysate from 1 million cells of each culture. SDS-PAGE and Western blotting were performed as described in section 2.5 (*n*=3). Following probing with anti-AICDA polyclonal antibody the membrane was stripped and re-probed with anti-α-tubulin monoclonal antibody. The position of molecular weight markers are indicated.

b) Optical Density comparison. Relative Optical Density (OD) was calculated as a ratio of AID to α-tubulin optical density for Tie2-DT40 clones A, B & C on three separate occasions. Graphed values represent mean of triplicate values. Data was analysed using the unpaired Student's two-tailed t-test.

❖ Clone B expresses more AID than Clone A (*p*= 0.04).

4.2 Scope of SHM-driven mutagenesis

The frequency with which different point mutations accumulate in DT40 cells according to the limited available literature is tabulated in Tables 1.1 & 4.1 and the predilection for 'hotspot' motifs is outlined above. This data was utilised to explore the theoretical distribution of mutations that SHM might generate in Tie2ECD in order to evaluate the suitability of SHM as a method of diversification for evolution of Tie2ECD.

4.2.1 Nucleotide diversity of potential Tie2 ECD mutants

To examine potential mutation sites the 1323bp Tie2ECD DNA sequence was examined for hotspots and corresponding amino acid mutations (Figure 4.5).

There are 87 G:C mutable bases within R<u>G</u>YW/WR<u>C</u>Y hotspots and an additional 54 G:C mutable bases if D<u>G</u>YW/WR<u>C</u>H is considered, where the underlined base indicates the mutable position. Of the total 141 highly mutable nucleotides, 47% are at D<u>G</u>YW and 53% are at WR<u>C</u>H, and these mutations cover a quarter of Tie2ECD amino acid residues excluding sequence-conserving mutations. If the whole four-nucleotide hotspot motif is considered to be more mutagenic than surrounding sequence, one third of the 1323bp nucleotide sequence is covered.

The 185 bases of Tie2 located immediately downstream of the transcription start site comprise the secretory leader sequence and approximately one third of the Ig1 domain (Barton, Tzvetkova & Nikolov 2005). These bases are unlikely to be

Table 4.1: Mutation patterns in DT40 cell lines. The studies featured in Table 1.1 were analysed to characterise type of mutations observed in DT40. The frequency of each mutation was calculated for each study. Studies were grouped according to the type of DT40 genetic modification: pseudo V donor ('ψV$^-$ AID^R')* and RAD51 paralogue ('XRCC 2/3$^-$')§ deletion. The tabulated results feature mean proportion of each mutation for these two groups and for the total from all five studies ('All'). Transitions are shaded. The mean total proportion of mutations at each nucleotide is shown in the left-hand column.

			TO:				
			A	G	C	T	
FROM:	A	0.0207		0.0190	0	0.0017	ψV$^-$ AID^R *
		0.0070		0	0.0035	0.0035	XRCC 2/3$^-$ §
		0.0152		**0.0114**	**0.0014**	**0.0024**	All
	G	0.4082	0.1220		0.2407	0.0455	ψV$^-$ AID^R *
		0.4336	0.1722		0.2140	0.0474	XRCC 2/3$^-$ §
		0.4184	**0.1421**		**0.2300**	**0.0463**	All
	C	0.5562	0.0729	0.2863		0.1970	ψV$^-$ AID^R *
		0.5366	0.0801	0.3268		0.1297	XRCC 2/3$^-$ §
		0.5484	**0.0758**	**0.3025**		**0.1701**	All
	T	0.0151	0.0108	0.0006	0.0037		ψV$^-$ AID^R *
		0.0145	0.0110	0	0.0035		XRCC 2/3$^-$ §
		0.0146	**0.0109**	**0.0001**	**0.0036**		All

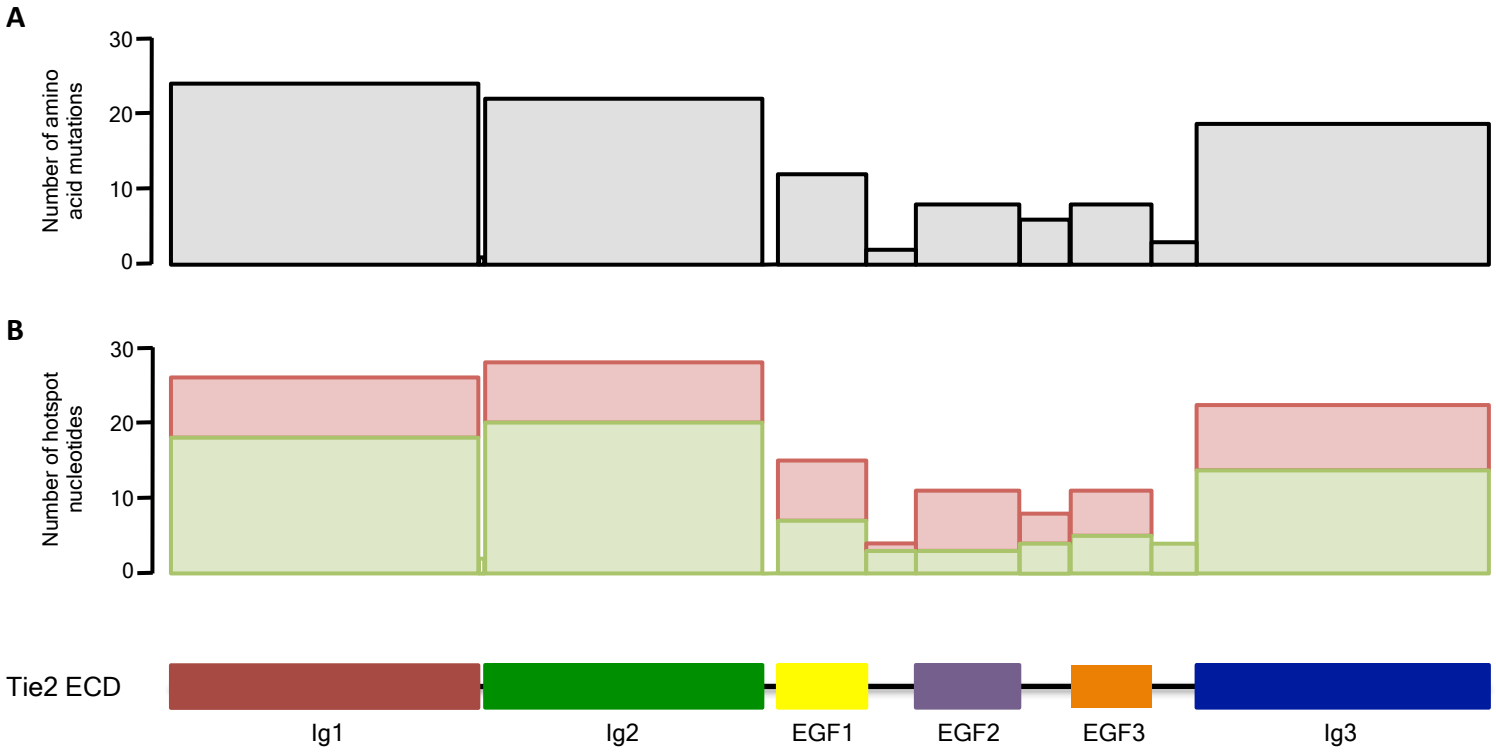

Figure 4.5: Distribution of hotspots in Tie2ECD. Schematic of Tie2ECD domains shown for reference.

a) Potential amino acid mutations. Histogram depicting total number of potential amino acid mutations distributed throughout regions of Tie2ECD. Refers to underlined base DGYW/WRCH hotspot positions.

b) Potential nucleotide mutations. Histogram depicting number of potential nucleotide mutations within underlined hotspot positions. RGYW/WRCY motifs coloured green. Additional DGYW/WRCH motifs coloured red.

mutated by SHM due to their location relative to the transcription initiation site (Rada et al. 1997). Whilst the Ig1 domain (23-120) is involved in hydrophobic and Van der Waals interactions with other domains, Ig2 (122-209) is the angiopoietin-binding domain and is certainly located within the mutable area. Ten percent of Tie2 DNA codons do not contain guanine or cytosine and thus are also unlikely to be mutated.

The CANNTG E-box motif occurs five times in Tie2ECD, and a further six times in the RSV promoter and the immediately upstream Ig locus homologous sequence combined. These sequences should be capable of recruiting E2A transcription factors, which appear to increase the rate of SHM (Schoetz et al. 2006).

4.2.2 Amino acid diversity of potential Tie2ECD mutants

To examine the range of amino acids that could be incorporated into Tie2ECD at mutation sites, the 141 hotspot mutation sites identified above were analysed for possible amino acid changes (Figure 4.6). There were three different possible substitutions in 55% of hotspot amino acids, and a range from one to a maximum of fourteen possible mutations in the remainder.

The probability of particular mutations can be estimated by reference to the incidence of individual nucleotide substitutions in existing literature (Table 4.2). To do this the average incidence of each nucleotide mutation in ψV^{-} AID^{R} was calculated from the three available studies (Arakawa, Saribasak & Buerstedde 2004, Schoetz et al. 2006, Blagodatski et al. 2009), and the probability of each

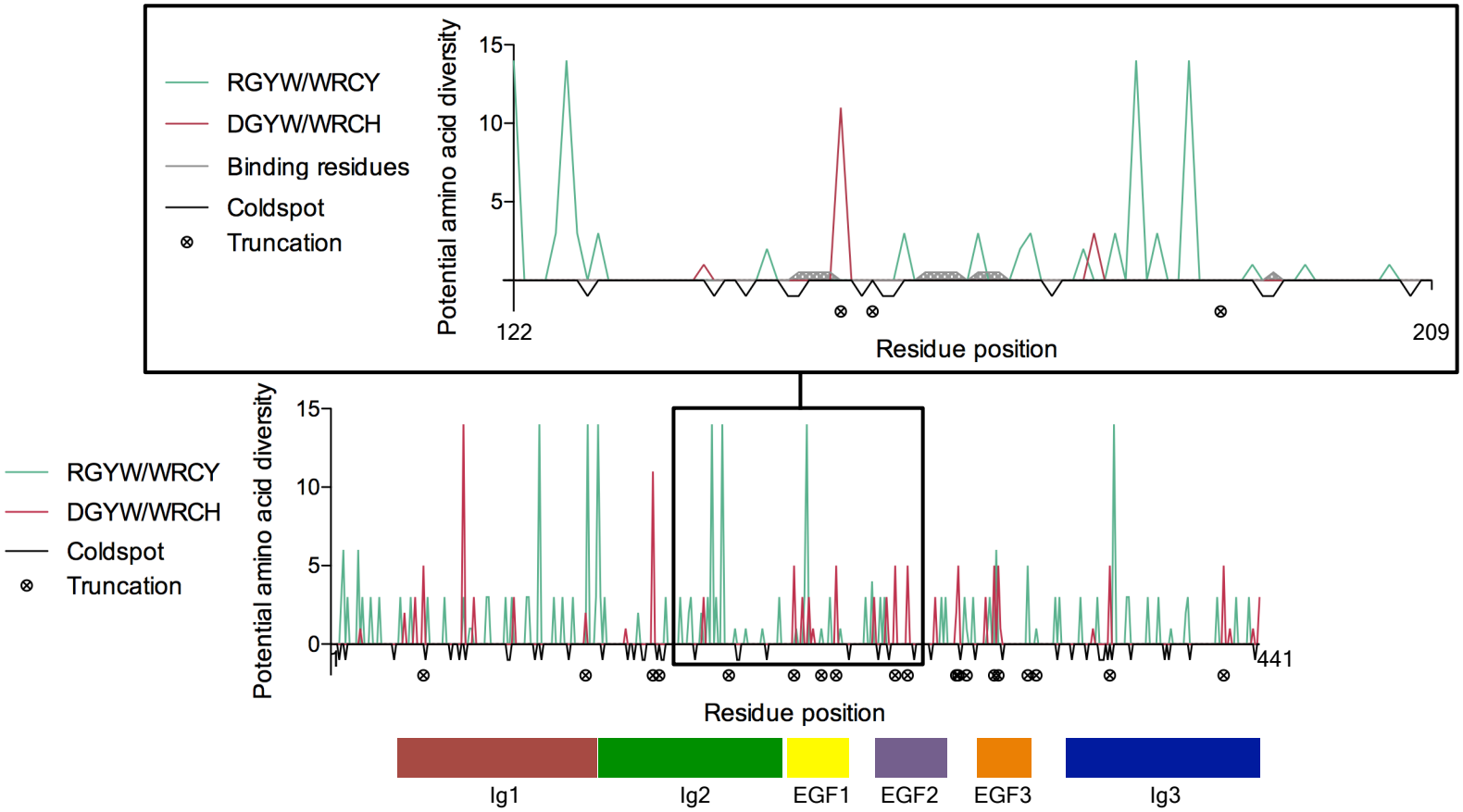

Figure 4.6: Potential amino acid diversity at Tie2ECD hotspots. Graphical representation of potential diversity of amino acid sequence. RGYW/WRCY and DGYW/WRCH hotspots were considered, where the underlined base indicates the mutable position. The number of possible resulting amino acid mutations relating to each hotspot is quantified on the positive axis. The baseline of zero represents all residues outside of hotspots containing a G/C base in the codon, with unknown probability of mutation. Residues assigned negative diversity (coldspot) are those containing A/T bases only. Truncation signifies potential mutation to premature stop codon. Relation of Tie2 domains to the sequence is shown. The detailed Ig2 graph also depicts the position of Ang2-binding residues (Barton06).

Table 4.2: Probability of individual base mutations in the ψV$^-$ AID^R DT40 cell line. The mean proportion of each mutation across pseudo V donor deletion DT40 studies is shown for reference ('ψV$^-$ AID^R *'- see Table 4.1). The probability of mutation outcome at each nucleotide ('Prob') was calculated according to the proportions observed at each nucleotide in these studies. Transitions are shaded.

			TO:				
			A	G	C	T	
FROM:	A	0.0207 1.0		0.0190 0.9179	0 0	0.0017 **0.0821**	ψV$^-$ AID^R * Prob
	G	0.4082 1.0	0.1220 **0.2989**		0.2407 **0.5897**	0.0455 **0.1115**	ψV$^-$ AID^R * Prob
	C	0.5562 1.0	0.0729 **0.1311**	0.2863 **0.5147**		0.1970 **0.3542**	ψV$^-$ AID^R * Prob
	T	0.0151 1.0	0.0108 **0.7152**	0.0006 **0.0397**	0.0037 **0.2450**		ψV$^-$ AID^R * Prob

mutation at a particular nucleotide was calculated as a proportion of incidence at that nucleotide. Hotspot mutations yield differing degrees of potential amino acid diversity depending on individual codons involved. Figure 4.7 characterises and qualifies potential amino acid diversity in the Ig2 domain according to probability. When the amino acids are classified according to type of side chain, probable significant mutations are possible at eighteen of twenty-three hotspot residues within Ig2.

4.3 Basal mutagenesis in the DT40 'ψV$^-$ AID^R Cl4' cell line

Although the analysis above suggests a potential range of mutations that could occur in Tie2ECD this may not necessarily correlate with experimental observations. It is therefore necessary to examine both the rate and characteristics of mutations in the DT40 cell line used in this study.

4.3.1 Estimation of generation time of ψV$^-$ AID^R Cl4 DT40 cells

Mutation rates are generally expressed as a function of generation time and generation time varies according to method of cell culture. To measure generation time for ψV$^-$ AID^R Cl4 DT40 cells under potential growth conditions three Tie2-DT40 clones were cultured in two different ways. Two 80cm^2 flasks were prepared containing 7 × 10^6 exponentially growing cells in 30ml complete DT40 medium. One culture was treated by passaging in a ratio of 1:3 as described by Wang *et al.* (Wang, Yang & Wabl 2004), and the other was treated by centrifugation and

Figure 4.7: Potential amino acid diversity at Tie2 Ig2 domain hotspots. Depicts the possible amino acid changes at DGYW/WRCH hotspot motifs in the Ig2 domain. Amino acids with two possible nucleotide mutations per codon are shown in the main sequence as double mutants, and above the sequence for single mutants. Size of letters corresponds to probability (Table 4.3). Letters are coloured according to amino acid side chain: *green = positively charged; blue = negatively charged; red = polar uncharged; purple = hydrophobic; orange = individual; black (X) = termination. No. = residue number; WT = wild-type sequence*.

refeeding to avoid loss of any potential mutants. Prior to each intervention, cells were counted on a haemocytometer.

Passaging proved to be a sustainable method of cell culture although cells were not maintained in the exponential growth phase throughout, presumably due to excessive cell density. More aggressive passaging would maintain a faster doubling time, but this needs to be balanced against the reduction of potential diversity associated with discarding a substantial proportion of potentially mutated cells and a lesser proportion of cell cycle spent in growth phase, when mutations are said to occur (Faili et al. 2002). The refeeding method resulted in rapid attainment of a plateau phase and is therefore unsuitable as a continued method of cell culture. Culture of clone A is graphically represented in Figure 4.8 as an example.

The initial 30 hours of cell culture by passaging appeared to represent the exponential phase. Doubling time was calculated using the formula:

$$T_d = t \times \frac{\log(2)}{\log\left(n_2/n_1\right)}$$

where T_d = doubling time; t = culture time; n_2 = final number of cells & n_1 = initial number of cells.

Generation time was also calculated for each time point in the passaging group and used to estimate a mean generation time for cells undergoing this method of cell culture.

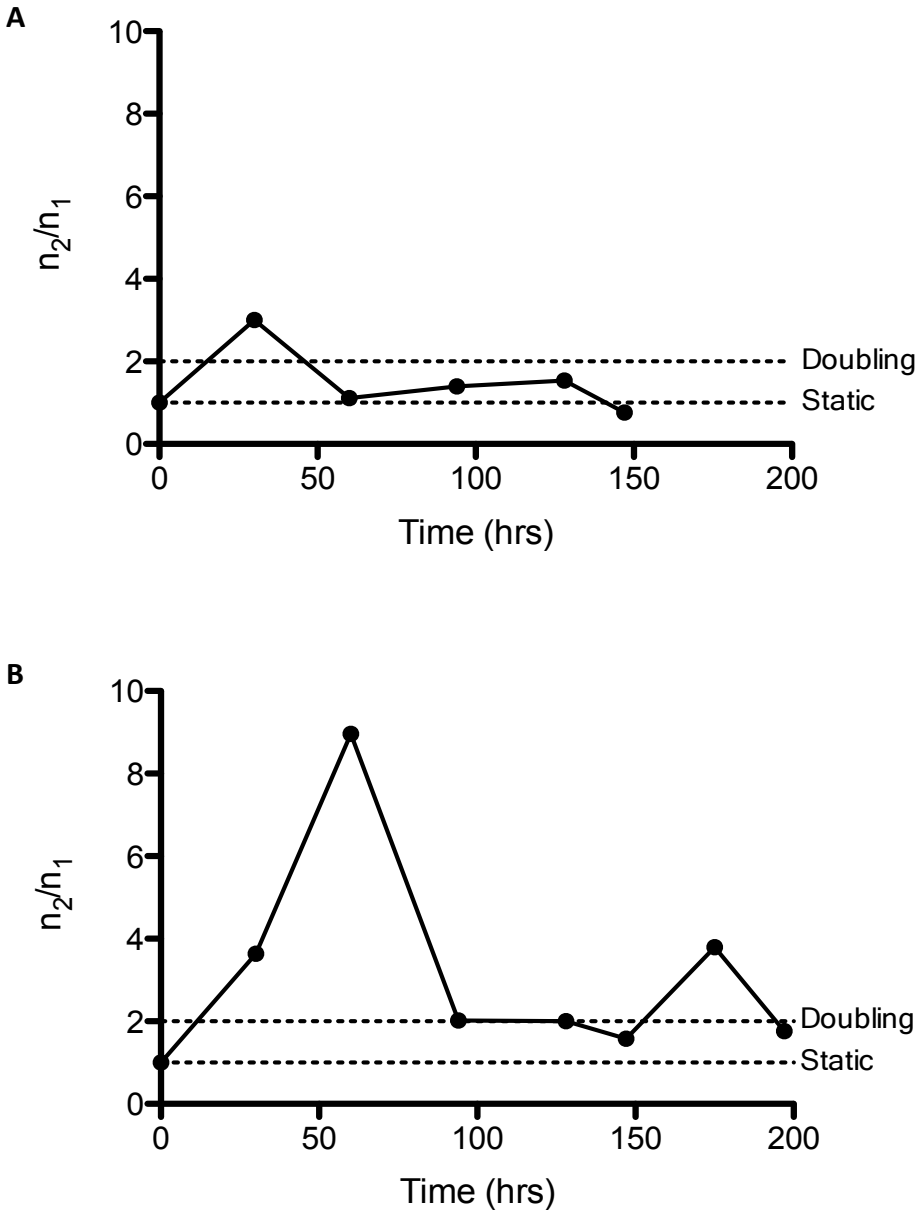

Figure 4.8: Growth of Tie2-DT40 clone A under test conditions. Tie2-DT40 cells were maintained via refeeding or passaging as described in section 2.4.11 (*n*=1). Cells were counted on a haemocytometer at intervals. Population size is represented as a function of n_2/n_1 where n_2 = number of cells at end of time point and n_1 = number of cells at start of time point.

a) Refeeding method. Clone A shown.

b) Passaging method. Clone A shown.

Mean generation time for the initial 30-hour period of culture was 16.58 hours. Average generation time for passaged cells thereafter was 23.34 hours for clone A, 21.07 hours for clone B and 24.3 hours for clone C, giving a mean of 22.87 hours.

4.3.2 Baseline frequency of genetic changes in Tie2ECD

In order to estimate baseline mutation rate in DT40, clonal populations that had been frozen down as soon as practicable following transfection of the cells with pTie2CSD-Hypermut2 were retrieved from liquid nitrogen in order to amplify and sequence the Tie2ECD gene. In addition, a Tie2-transfected AID-negative clone (4.1.1) was used as a control.

In brief, RT-PCR was performed on total RNA followed by TA cloning of the PCR product, allowing production of colonies with individual copies of the Tie2 gene as outlined in section 2.6. PCR for Tie2 was performed with proofreading polymerase, which has a published error rate of 4.4×10^{-7}, as specified in Appendix 2.1.

Sequencing of twelve random AID-positive 1323bp Tie2 segments revealed only one nucleotide point mutation of C414G, which produces an amino acid substitution of N138K and occurred in clone B. There were no mutations in the five AID-negative clone sequences. If the single mutation across all three clones were accurate, it would yield a mutation frequency of 0.083 per Tie2 sequence or 6.29×10^{-5} per base pair. The mutation frequency for clone B alone would be 0.25 per Tie2 sequence or 1.89×10^{-4} per base pair.

Presuming that each Tie2-DT40 clone originated from a single cell a maximum of 30.72 divisions would have occurred prior to sequencing, including growth up to approximately 40×10^6 cells per clone prior to freezing and three days of exponential culture after the point of defrosting. The baseline mutation rate across all three clones would be 2.1×10^{-6} mutations/bp/generation, or 6.1×10^{-6} mutations/bp/generation when considering clone B alone.

4.3.3 Distribution of mutations in Tie2ECD in the first 3 months of cell culture

In view of relatively elevated levels of AID expression and positive sequencing in clone B, this clone was taken forward for further analysis. The cells were cultured by the passaging method with periodic MPA treatment to select AID positive cells. A random sample of 1323bp Tie2ECD segments was sequenced as described above after one month and three months of cell culture.

At one month, a nucleotide point mutation was present, G671C, in one of five Tie2ECD segments. Assuming that a further 35.31 generations had occurred subsequent to baseline sequencing, the mutation rate in the 6615bp explored is reduced to 2.3×10^{-6} mutations/bp/generation.

After three months of culture however, eight of eleven sequences contained a single point mutation and a further two sequences contained two mutations. This equates to a mutation rate of 6.8×10^{-6} mutations/bp/generation, which is similar to that of the baseline clone B sample. However only three different mutations

were observed, C496T, G541T and C567G, and therefore the breadth of diversity could not be assessed from this relatively small number of sequences.

The number of Tie2 sequences examined does not yield sufficient power to produce an accurate mutation rate, but based on these random samples the mutation rate is likely to be lower than published estimates of 1×10^{-5} mutations/bp/generation (Blagodatski et al. 2009). Cells were maintained in culture, whilst efforts concentrated on improving mutation rate.

4.3.4 Distribution of mutations in Tie2 ECD at 9 months of culture

Cells were cultured as described in section 2.4.3, with periodic MPA treatment to select AID positive cells. After nine months of culture, Tie2 segments were sequenced as previously described (section 2.6). Of thirty sequences analysed all contained a genetic modification, verified by study of the chromatogram. There were point mutations in half of the sequences, and surprisingly, deletions in 25 of 30 sequences. In contrast to the 3-month culture, there were seventeen different point mutations. Individual events are mapped in Figure 4.9.

In total there were 23 point mutations in the 39690bp explored, giving a frequency of 0.8 per Tie2 sequence and 5.79×10^{-4} mutations per bp. In comparison a mutation rate of 1×10^{-3} mutations per bp was attained for a transgene inserted into the Ig locus of the ψV^{-} AID^{R} cell line after only six weeks of cell culture (Blagodatski et al. 2009), which is effectively eleven times greater than the rate observed in Tie2ECD. More mutations per sequence were also observed in the Ig V

Figure 4.9: Genetic events in Tie2ECD at nine months of cell culture. DNA sequence and translation is shown. Green DNA text identifies RGYW/WRCY hotspots. Red DNA text identifies additional DGYW/WRCH hotspots. Italics = non-mutable initial 185bp. DNA bases with reported mutability within hotspots are underlined, and corresponding amino acid residues are coloured according to DNA hotspot labelling system. Greyed out nucleotides and digits represent deletions and their corresponding frequencies. Nucleotide mutations and resulting amino acid translations are mapped onto the sequence in bold text, and subscript digits indicate multiple occurrences. ⊗ = stop codon.

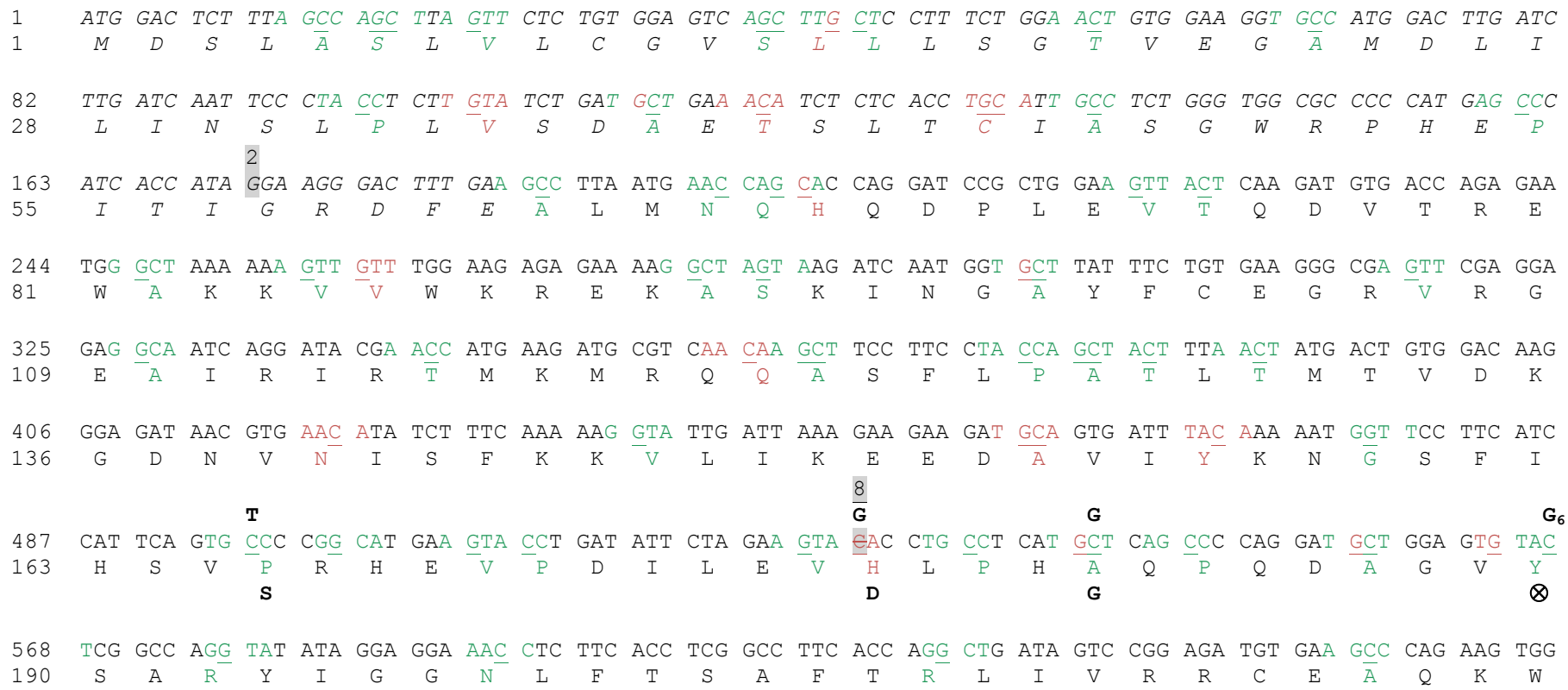


649 GGA CCT GAA TGC AAC CAT CTC TGT ACT GCT TGT ATG AAC AAT GGT GTC TGC CAT GAA GAT ACT GGA GAA TGC ATT TGC CCT
217 G P E C N H L C T A C M N N G V C H E D T G E C I C P
730 CCT GGG TTT ATG GGA AGG ACG TGT GAG AAG GCT TGT GAA CTG CAC ACG TTT GGC AGA ACT TGT AAA GAA AGG TGC AGT GGA
244 P G F M G R T C E K A C E L H T F G R T C K E R C S G
811 CAA GAG GGA TGC AAG TCT TAT GTG TTC TGT CTC CCT GAC CCC TAT GGG TGT TCC TGT GCC ACA GGC TGG AAG GGT CTG CAG
271 Q E G C K S Y V F C L P D P Y G C S C A T G W K G L Q
892 TGC AAT GAA GCA TGC CAC CCT GGT TTT TAC GGG CCA GAT TGT AAG CTT AGG TGC AGC TGC AAC AAT GGG GAG ATG TGT GAT
298 C N E A C H P G F Y G P D C K L R C S C N N G E M C D
973 CGC TTC CAA GGA TGT CTC TGC TCT CCA GGA TGG CAG GGG CTC CAG TGT GAG AGA GAA GGC ATA CCG AGG ATG ACC CCA AAG
325 R F Q G C L C S P G W Q G L Q C E R E G I P R M T P K
1054 ATA GTG GAT TTG CCA GAT CAT ATA GAA GTA AAC AGT GGT AAA TTT AAT CCC ATT TGC AAA GCT TCT GGC TGG CCG CTA CCT
352 I V D L P D H I E V N S G K F N P I C K A S G W P L P
1135 ACT AAT GAA GAA ATG ACC CTG GTG AAG CCG GAT GGG ACA GTG CTC CAT CCA AAA GAC TTT AAC CAT ACG GAT CAT TTC TCA
379 T N E E M T L V K P D G T V L H P K D F N H T D H F S
1216 GTA GCC ATA TTC ACC ATC CAC CGG ATC CTC CCC CCT GAC TCA GGA GTT TGG GTC TGC AGT GTG AAC ACA GTG GCT GGG ATG
406 V A I F T I H R I L P P D S G V W V C S V N T V A G M
1297 GTG GAA AAG CCC TTC AAC ATT TCT GTT
433 V E K P F N I S V

gene of the ψV^{-} AID^{R} cell line in another study (Arakawa, Saribasak & Buerstedde 2004) (Figure 4.10). Presuming mean generation time to be 21.07 hours in clone B, the mutation rate is 2×10^{-6} mutations per bp per generation. Therefore when the longer doubling time is considered the mutation frequency is six times lower than that of the literature.

The distribution of mutations is broadly in agreement with previous observations (Table 4.3). 91.3% of mutations occur at G:C base pairs as compared with 96.7% in the published ψV^{-} AID^{R} cell line literature (Arakawa, Saribasak & Buerstedde 2004, Schoetz et al. 2006, Blagodatski et al. 2009). However 43.5% of mutations are transitions, as compared with a mean of 34.2% from the above previous reports. Thirteen mutations occur at the underlined base within R<u>G</u>YW/WR<u>C</u>Y hotspots, and an additional seven within the D<u>G</u>YW/WR<u>C</u>H motif. Three mutations are not located within conventional hotspot positions, although two of these are T to C mutations where thymine is located within a four-nucleotide hotspot motif. Figure 4.11 depicts point mutations relative to hotspot distribution.

Although the frequency of G to C mutations is significantly lower than the published frequency at 4% versus 24%, the elevated level of C to G mutation at 52% compared with the literature mean of 29% yields a comparable total for G:C/C:G transversions. In total there are fourteen mutations at WR<u>C</u>H versus six mutations at D<u>G</u>YW, and this apparent preference for the coding strand may have skewed the data.

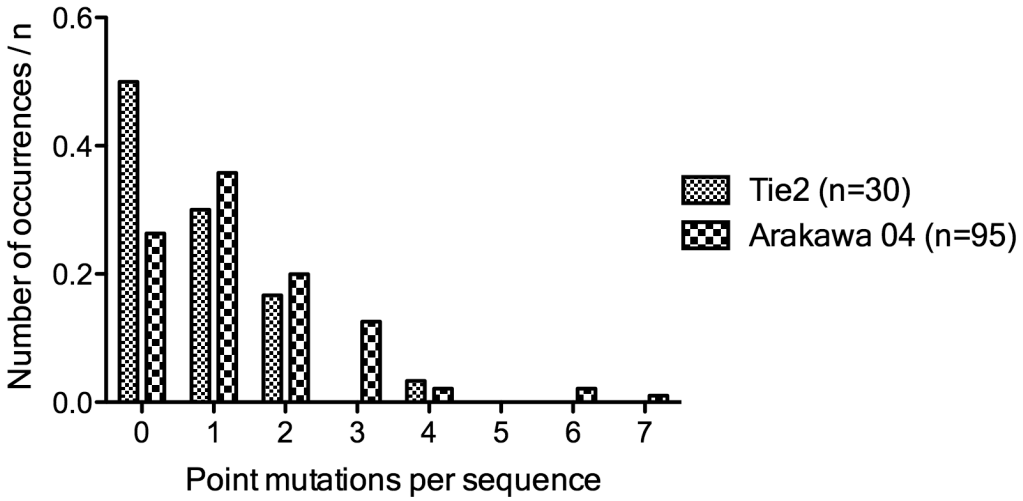

Figure 4.10: Point mutations per sequence. Tie2-DT40 cells were cultured for nine months with periodic MPA treatment. Individual random copies of the Tie2ECD gene were sequenced via RT-PCR and TA cloning as described in section 2.6 (*n*=30). The number of mutations per Tie2ECD sequence is graphed against that recorded for the VJ gene after six weeks of culture in a similar cell line (Arakawa, Saribasak & Buerstedde 2004). Both frequencies are expressed as a percentage of total number of sequences examined.

Table 4.3: Observed mutation frequency in Tie2-DT40 cells. Tie2-DT40 cells were cultured for nine months with periodic MPA treatment. Individual random copies of the Tie2ECD gene were sequenced via RT-PCR and TA cloning as described in section 2.6. The frequency of each mutation permutation is stated ('Actual'). The literature frequencies are also tabulated as a reference ('ψV$^-$ AID^R *' & 'All *§': see Table 4.1). Transitions are shaded.

			TO: A	TO: G	TO: C	TO: T	
FROM:		0		0	0	0	Actual
	A	0.0158		**0.0190**	0	0.0017	ψV$^-$ AID^R *
		0.0152		**0.0114**	0.0014	0.0024	All *§
		0.2609	0.2174		0.0435	0	Actual
	G	0.4317	0.1220		0.2407	0.0455	ψV$^-$ AID^R *
		0.4184	**0.1421**		**0.2300**	**0.0463**	All *§
		0.6522	0	0.5217		0.1304	Actual
	C	0.5355	0.0729	0.2863		0.1970	ψV$^-$ AID^R *
		0.5484	**0.0758**	**0.3025**		**0.1701**	All *§
		0.0870	0	0	0.0870		Actual
	T	0.0174	0.0108	0.0006	0.0037		ψV$^-$ AID^R *
		0.0146	**0.0109**	**0.0001**	**0.0036**		All *§

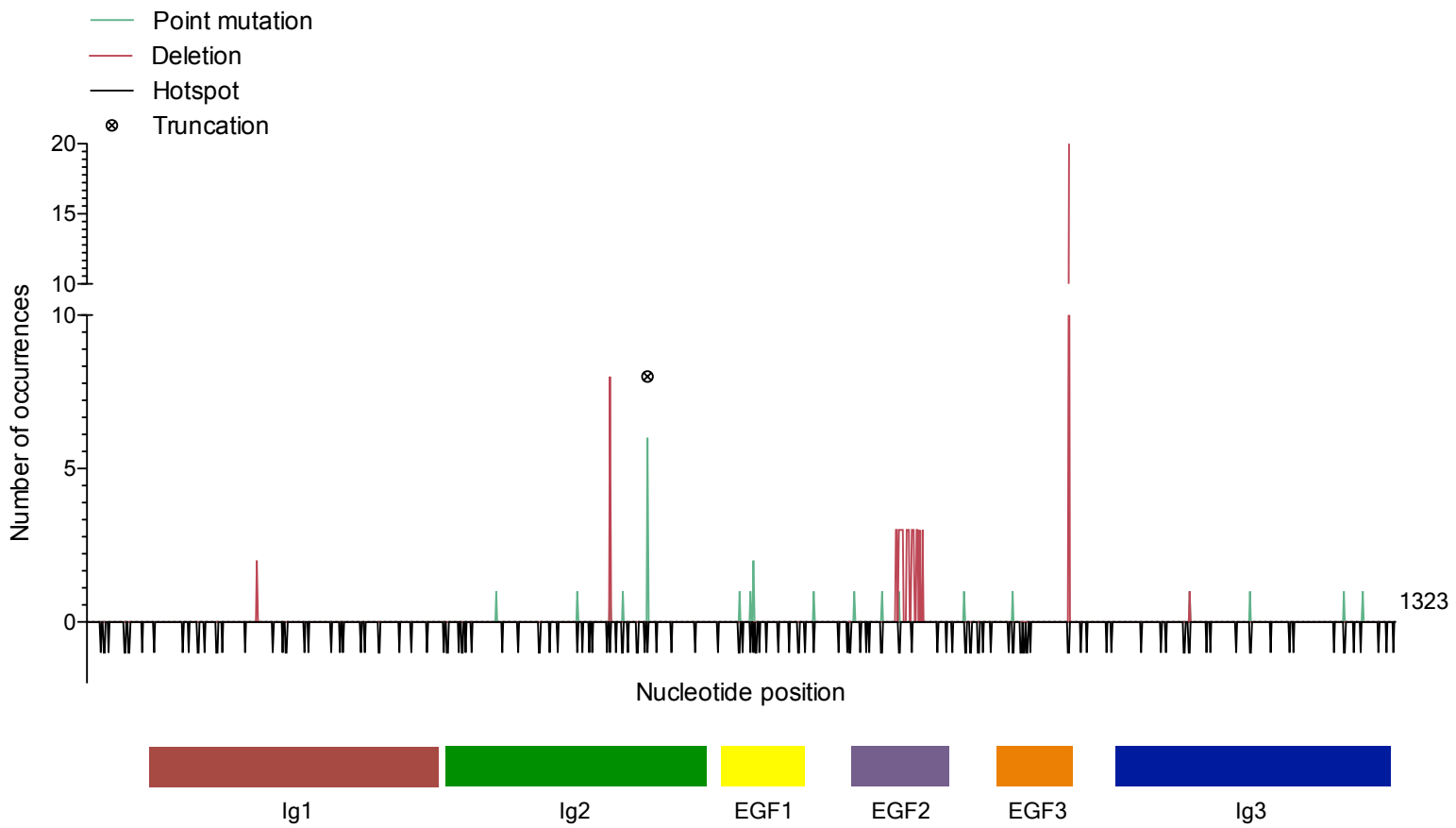

Figure 4.11: Observed nucleotide diversity in Tie2ECD. Graphical representation of diversity of nucleic acid sequence. RGYW/WRCY and DGYW/WRCH hotspots are marked. The number point mutations and deletions is quantified on the positive axis. Truncation signifies mutation to premature stop codon. Relation of Tie2 domains to the sequence is shown. Shown magnified overleaf.

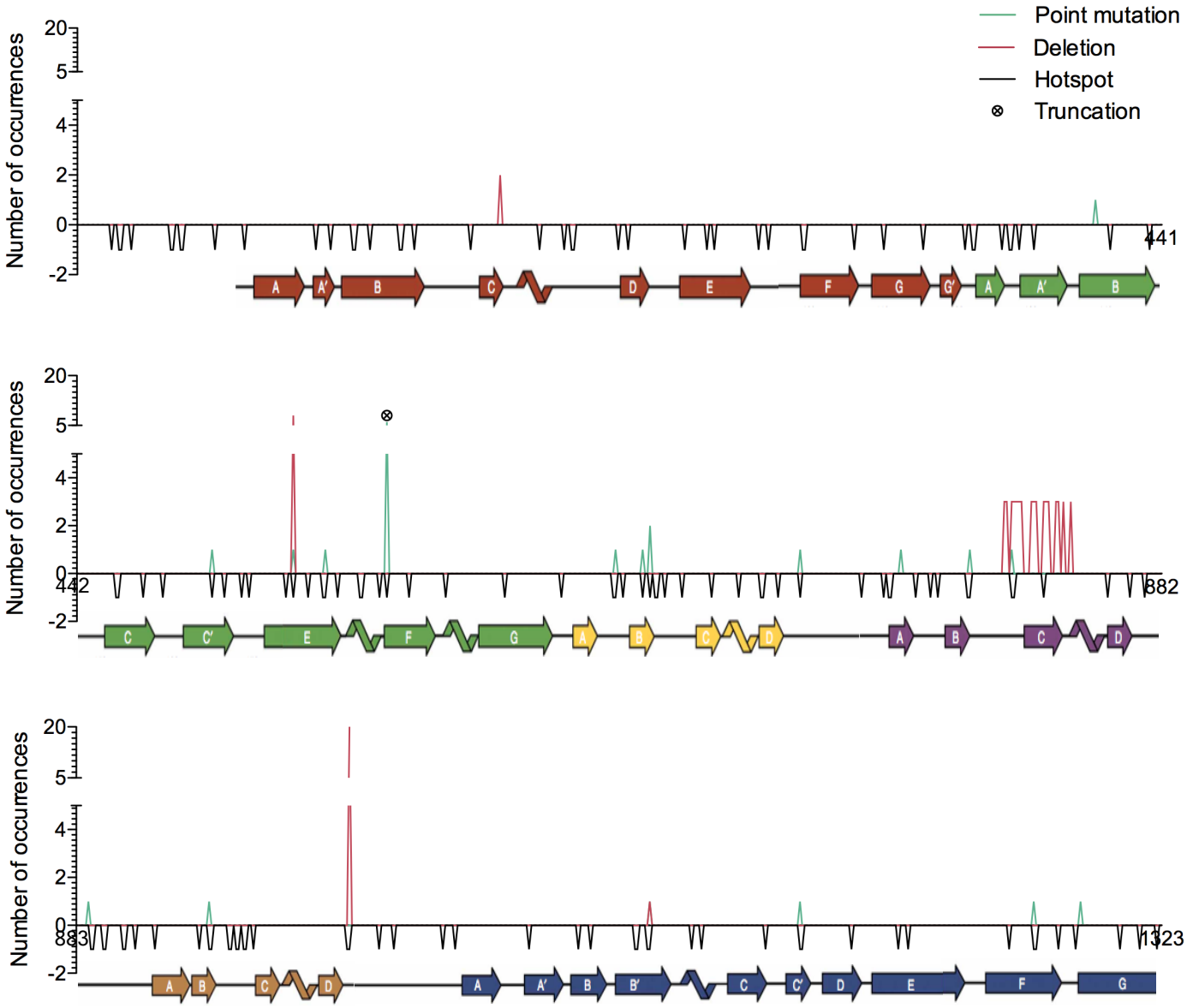
Point mutation
Deletion
Hotspot
Truncation
Number of occurrences
20
5
4
2
0
-2
441
442
882
883
1323
A
A'
B
C
D
E
F
G
G'
C'
B'

When considering all mutations in the DGYW nomenclature (Rogozin, Diaz 2004), the most frequently occurring mutations, in descending order, occur within AGTA, TGCA, TGTA and AGCT motifs. The 'D' position is occupied by adenine, guanine and thymine in a ratio of 11:2:7 respectively, and the occurrence of cytosine versus thymine at 'Y' is approximately equal (9:11). A pattern is observed on analysis of the two most frequent mutations: G to C transversions are more frequently flanked by adenine as opposed to guanine in the 5' position (11:1) and thymine rather than cytosine in the 3' position (9:3), whereas the 5' neighbour is likely to be thymine in preference to adenine (6:2) and the 3' neighbour cytosine rather than thymine (6:2) in G to A mutations (Figure 4.12).

Both single and multiple nucleotide deletions were observed. Of the single nucleotide incidents, C993, a WRCY motif, was the most frequently encountered, followed by C529, a WRCH hotspot. The non-hotspot G172 was deleted on two occasions and C1115, a WRCY motif, was deleted in one sequence. Multiple nucleotide deletions occurred between nucleotides 818 and 845 producing a frameshift. The density of hotspots within this sequence is 0.07 per base pair, as compared with an average Tie2ECD frequency of 0.11 per base pair. The hotspots are not located at the margins of the deleted section.

The most 5' genetic modification is a deletion of G172, and the most 5' point mutation occurred at C496. Point mutations are distributed throughout the Tie2 domains, totalling four in Ig3, three in Ig2 and EGF1, two in EGF2 and one in EGF3. Three of the mutations are located at residues believed to be involved in interdomain interactions and one is located at a residue involved in angiopoietin

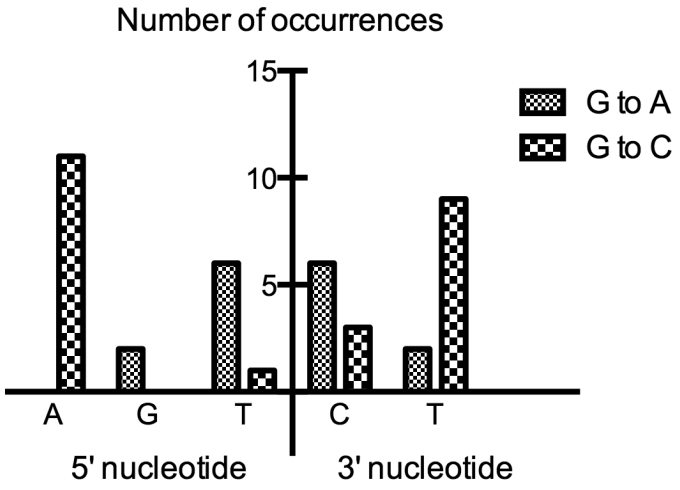

Figure 4.12: Nucleotides surrounding mutations. Tie2-DT40 cells were cultured for nine months with periodic MPA treatment. Individual random copies of the Tie2ECD gene were sequenced via RT-PCR and TA cloning as described in section 2.6 (*n*=30). The bases located immediately upstream and downstream of each mutation are graphed in terms of number of occurrences. All WRCH mutations are represented in the DGYW consensus.

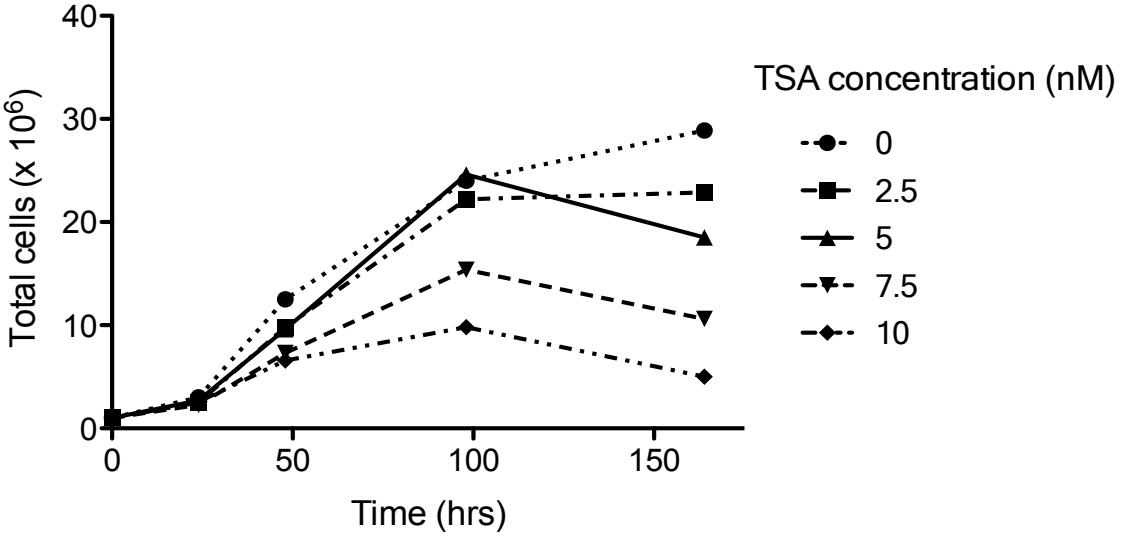

Figure 4.13: Effect of Trichostatin A on growth of Tie2-DT40 cells. Tie2-DT40 cells were cultured with varying concentrations of TSA via the refeeding method and counted on a haemocytometer at intervals. Data from a single experiment is shown to represent total population size (*n*=1).

binding. Of the seventeen different point mutations observed, five are silent and one inserts a premature stop codon. Three mutations, A181G, T225S and A372G, are relatively neutral. The remaining eight are likely to produce more significant changes: P166S; H177D; C224Y; T259R; C274Y; L296P; K312N; C424Y.

4.4 Optimisation of mutagenesis

Whilst AID activity within the DT40 'ψV$^-$ AID^R Cl4' cell line is sufficient to mutate Tie2ECD, the mutation frequency observed is substantially lower than that reported in the literature. Therefore strategies were investigated to potentiate SHM by elevation of AID expression levels and augmentation of existing AID activity in the 'ψV$^-$ AID^R Cl4' cell line.

4.4.1 Trichostatin A in the DT40 'ψV$^-$ AID^R Cl4' cell line

TSA is reported to enhance the action of AID by improving the accessibility of ssDNA. Woo *et al.* used 10nM TSA for 72 hours to elicit a 2.5-fold increase in mutation rate without impacting on cell viability (Woo, Martin & Scharff 2003), and Seo *et al.* used up to 8.27nM TSA for six weeks to elicit a significant increase in gene conversion events (Seo et al. 2005). In order to determine an appropriate level of TSA for ψV$^-$ AID^R Cl4 DT40 cells, the influence of TSA on cell growth was assessed.

1×10^6 mixed clonal Tie2-DT40 cells were cultured in 10ml complete DT40 medium with 0.5μg/ml puromycin and between 0 and 10nM TSA. Medium was changed approximately every 48 hours as required and cell numbers were determined by counting at intervals. A concentration of 5nM TSA was the maximum tolerated without significant growth arrest (Figure 4.13).

Tie2-DT40 clone B was cultured in 5nM TSA for a period of three months. Tie2ECD was sequenced as previously described on three separate occasions (section 2.6). Of a total of thirty independent clones examined, the majority produced artefact. Of four apparently accurate sequences, two were wild-type, one contained a single deletion and one contained a segment of multiple base deletions. Whilst the small number of sequences obtained is inadequate, it is unlikely that TSA stimulates increased SHM based on the comparison of these sequences with the 3-month culture sequences obtained in section 4.3.3.

4.4.2 Strategies for stable non-targeted transfection of human AID into Tie2 ECD transfected 'ψV$^-$ AID^R Cl4' DT40 cells

Whilst it is advantageous to have the ability to excise AID from the genome, the floxed AID-gpt construct appears to have a degree of instability in ψV$^-$ AID^R Cl4 DT40. Transfection of AID into Tie2-DT40 for ubiquitous expression should elevate AID expression levels.

Two variants of vector pRH125, containing FLAG-tagged human AID on an eEF1α promoter, were a kind gift from Sale *et al.* (MRC, University of Cambridge).

Transfection of either vector into Tie2-DT40 clones should improve constitutive AID expression and prevent mutation of the AID gene itself, at the expense of being unable to excise AID from the genome on demand. Selection of stable transfectants is via puromycin in vector #1678, and hygromycin B or puromycin in vector #1680 (Appendix 4.1).

Confirmation of AID expression was achieved by transient transfection of plasmids #1678 and #1680 into HEK293 cells (section 2.4.2) followed by SDS-PAGE of whole cell lysates at 24 hours and subsequent Western immunoblotting for FLAG and AID (section 2.5). Plasmid #1678 appeared to give preferable hsAID expression levels in a single experiment (Figure 4.14).

4.4.2.1 Hygromycin selection in Tie2ECD-transfected DT40 cells

Due to existing puromycin resistance in the Tie2-DT40 clones, a kill curve was performed with a mixed clonal population of cells to enable hygromycin B-based selection. Typical concentrations used for selection in DT40 cells range from 0.5 to 2 mg/ml. Cells were cultured in the presence of puromycin, without passaging or change of medium, to simulate conditions used during selection. 0.4mg/ml hygromycin B was sufficient to kill all cells by 124 hours despite initial growth, and 0.6mg/ml was sufficient to prevent significant growth (Figure 4.15). Hygromycin B is alkaline and activity is dependent on pH, but there were no adverse affects on cell growth with the pH produced by up to 1mg/ml concentration hygromycin (data not shown). On the basis of hygromycin and pH experiments, hygromycin concentrations of between 0.5 and 0.7 mg/ml were used for selection.

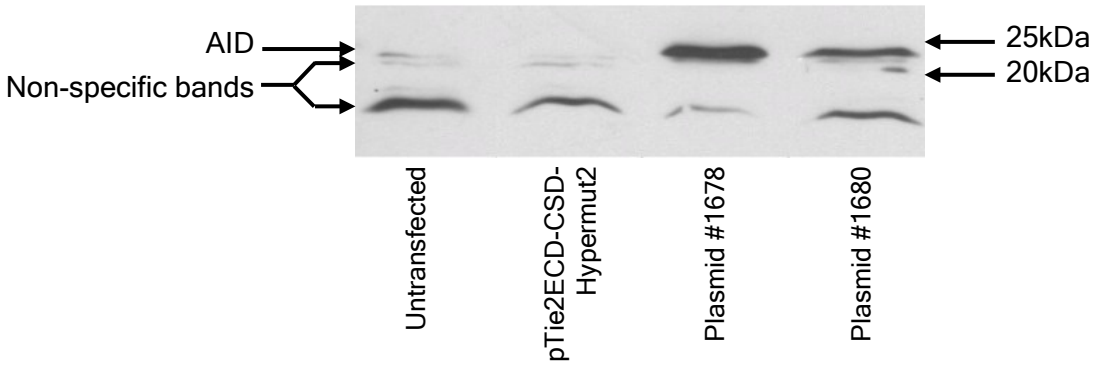

Figure 4.14: Expression of transfected pRH125 AID in HEK293 cells. HEK293cells were transiently transfected with two variants of pRH125, #1678 and #1680, via lipofection as described in 2.4.2. Whole cell lysate was prepared after 24 hours and subjected to SDS-PAGE and Western blotting as described in section 2.5 (*n*=1). Immunoblot analysis was performed with anti-AICDA polyclonal antibody. The position of molecular weight markers are indicated.

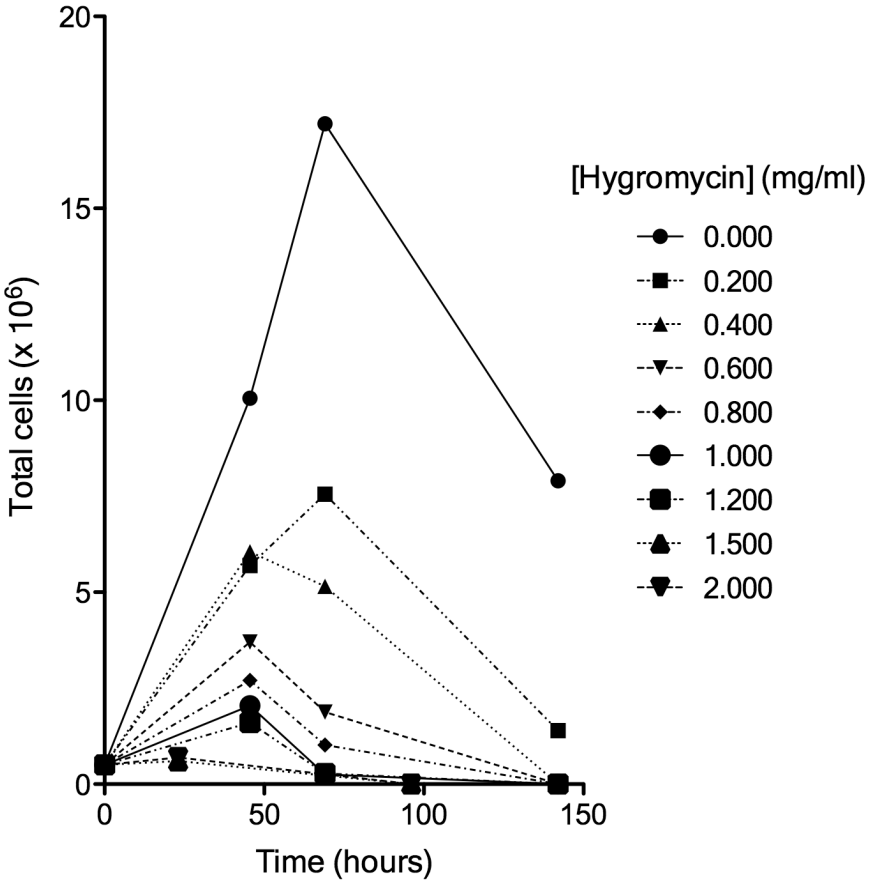

Figure 4.15: Hygromycin B kill curve in Tie2-DT40 cells. Tie2-DT40 cells were cultured with varying concentrations of hygromycin B without change of medium and cells were counted on a haemocytometer at intervals (*n*=1). Total population size is represented.

Tie2-DT40 clones A, B & C were transfected with 30 and 50μg ethanol precipitated #1680 plasmid as per published conditions (section 2.4.5). Selection was performed with 0.5mg/ml hygromycin and variation in cell density to allow for growth. After ten days, colonies had appeared for clone C in both the 30μg and 50μg transfections at a density of approximately four colonies per well. Clones A and B did not produce any colonies at 28 days.

Clone C colonies were picked and subcloned to produce single clonal populations. Their growth rate in hygromycin was at most a third of that previously experienced with puromycin selection. Expression of AID was not detectable in whole cell lysates on assessment by SDS-PAGE and Western immunoblotting with anti-FLAG probing (Figure 4.16). Therefore hygromycin does not produce clean selection in Tie2-DT40.

4.4.2.2 Antibiotic marker recycling in Tie2ECD-transfected DT40 cells

As puromycin-mediated selection is successful in Tie2-DT40 an alternative approach was to utilise plasmid #1678 for AID transfection. The puromycin resistance gene is flanked by loxP sites in pHypermut2, enabling excision of the integrated form from the Tie2-DT40 genome via Cre recombinase induction and therefore antibiotic marker recycling for #1678 selection. In addition ggAID would also be excised.

Clones A, B and C were cultured in progressively higher concentrations of 4-OHT. Cell death was incomplete on subsequent exposure to puromycin and therefore

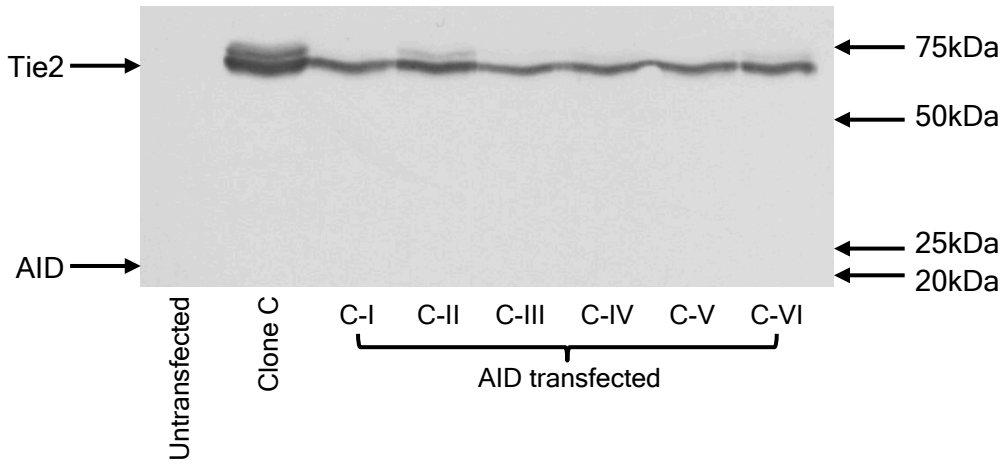

Figure 4.16: Probing for AID in pRH125-#1680-transfected Tie2-DT40. Clone C Tie2-DT40 cells were transfected with circular pRH125-#1680 via electroporation and selected with hygromycin B. Whole cell lysate was prepared from emerging colonies, and subjected to SDS-PAGE and Western blotting as described in section 2.5. Immunoblot analysis was performed with anti-FLAG monoclonal antibody. The position of molecular weight markers are indicated.

subcloning was performed as outlined in section 2.4.9 to isolate puromycin-sensitive cells. A series of #1678 plasmid transfections was performed in these subclones with manipulation of electroporation conditions (section 2.4.5).

Clones were recovered from two transfections, one in subclone A1 and one in subclone B2, which had utilised different conditions. Single colonies were expanded prior to preparation of whole cell lysate and Western immunoblotting for AID and FLAG epitope (section 2.5). There was no detectable FLAG-AID expression in either transfection and unexpectedly no Tie2 expression was seen in subclone A1 (Figure 4.17). Tie2 is not contained within a floxed cassette in pHypermut2 and should not be affected by 4-OHT. Expression of Tie2 was confirmed to be present in all 4-OHT-treated B-subclones and absent in all A-sublcones on assessment of whole cell lysate by SDS-PAGE and Western immunoblotting with anti-FLAG (Figure 4.18).

Transfection of pRH125 vector was abandoned as a strategy due to the ability to select antibiotic-resistant colonies that do not express the gene of interest and the complications experienced in using puromycin or hygromycin as selection tools.

4.4.3 Stable non-targeted transfection of human AID into Tie2ECD-transfected DT40 cells

As it was not possible to transfect pRH125 into Tie2-DT40, cloning of human AID into pEF6/V5-His-TOPO® was undertaken. This permits selection with the blasticidin resistance cassette, reported to give clean and rapid selection in DT40

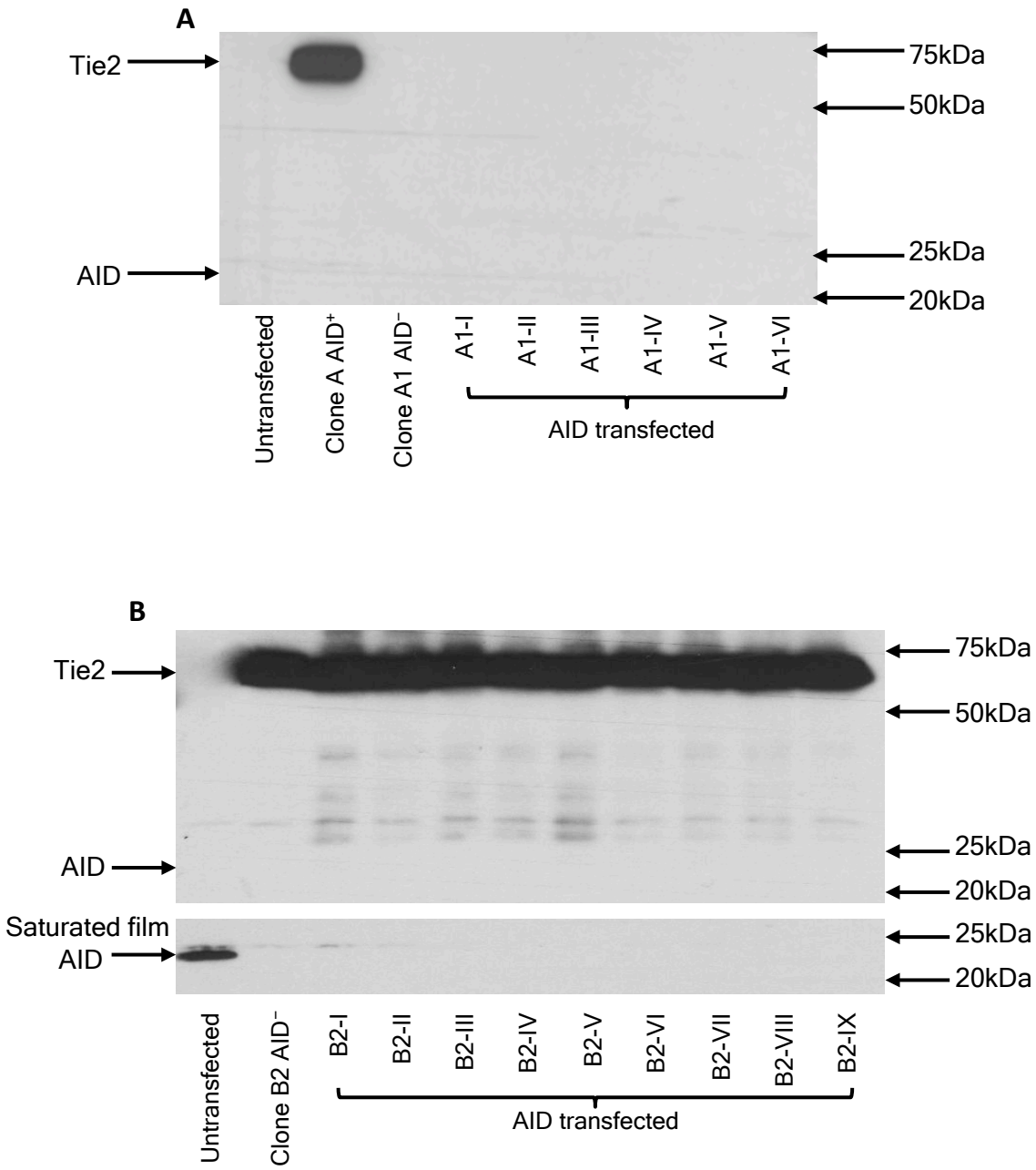

Figure 4.17: Probing for AID in pRH125-#1678-transfected Tie2-DT40. Subclone A and B Tie2-DT40 cells were transfected with circular pRH125-#1678 via electroporation and selected with puromycin. Whole cell lysate was prepared from emerging colonies, and subjected to SDS-PAGE and Western blotting as described in section 2.5. Immunoblot analysis was performed with anti-FLAG monoclonal antibody. The position of molecular weight markers are indicated.

a) Subclone A. 700µl cell suspension; 250V electroporation.

b) Sublcone B. 500µl cell suspension; 360V electroporation.

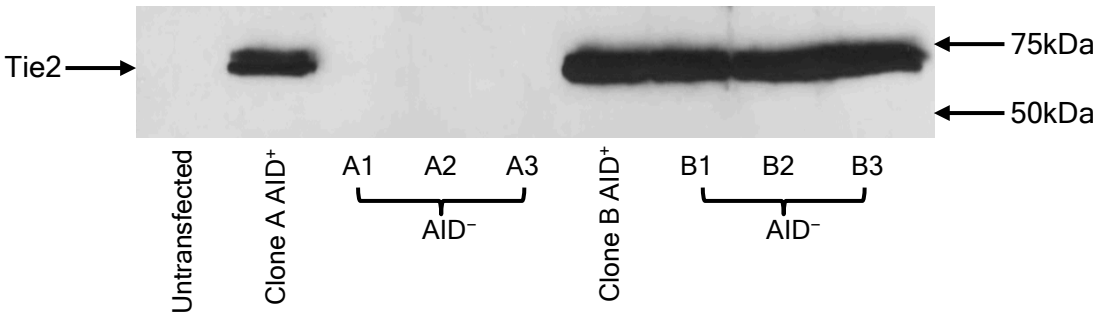

Figure 4.18: Probing for Tie2 in 4-OHT treated Tie2-DT40 subclones. Clone A and B Tie2-DT40 cells were treated with 4-hydroxytamoxifen (OHT) and subcultured for puromycin sensitivity. Whole cell lysate was prepared from resulting subclones (A1–3 and B1–3) and subjected to SDS-PAGE and Western blotting as described in section 2.5. Immunoblot analysis was performed with anti-FLAG monoclonal antibody. The position of molecular weight markers are indicated.

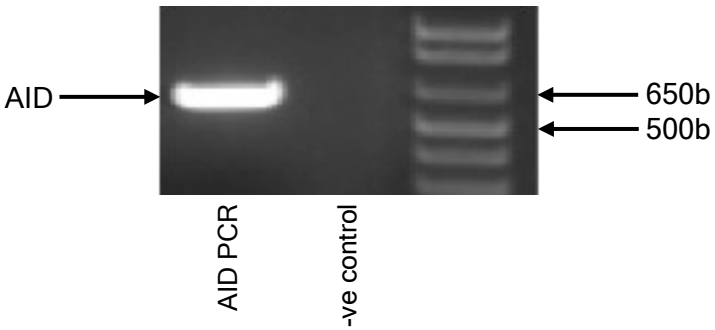

Figure 4.19: Verification of human AID PCR. PCR was performed as described in section 2.3.1 / Appendix 2.1. The 601bp product was resolved by electrophoresis on 1.2% agarose gel and visualised by UV illumination as described in section 2.2.5. The position of molecular size markers are indicated.

cells (Sale 2006), and maintains amplification of AID by the EF-1α promoter (Appendix 4.1). Primers were designed to amplify human AID from plasmid pRH125-#1678, and PCR was performed with proof-reading polymerase as specified in Appendix 2.1 (Figure 4.19). The product was cloned using the TA method (section 2.6.3) to create pAID-TOPOblast^r by Teonchit Nuamchit (University of Leicester).

Transfection of ggAID-positive clone B cells was performed in conjunction with Teonchit Nuamchit (University of Leicester) using the standard stable non-targeted transfection method outlined in section 2.4.5 and 20μg/ml blasticidin selection. Colonies appeared at a density of approximately 0.2 per well after ten days of selective pressure. Wells containing single colonies were selected for expansion.

4.4.4 Over-expression of human AID in Tie2ECD-transfected DT40 cells

To confirm successful transfection of pAID-TOPOblast^r and assess AID expression level relative to Tie2-DT40, whole cell lysate was prepared from seven separate hsAID-DT40 clones and subjected to SDS-PAGE and Western blotting. Clone B Tie2-DT40 cells and AID-negative subclone-B Tie2-DT40 cells were included as controls. Nitrocellulose membranes were first probed with anti-AID antibody prior to stripping and re-probing for α-tubulin as a loading control (section 2.5). AID expression ranged from equal to 100-times higher than levels in Tie2-DT40 clone B cells (Figure 4.20). It was not possible to assess the effect of AID expression on mutation rate within the time constraints of this study.

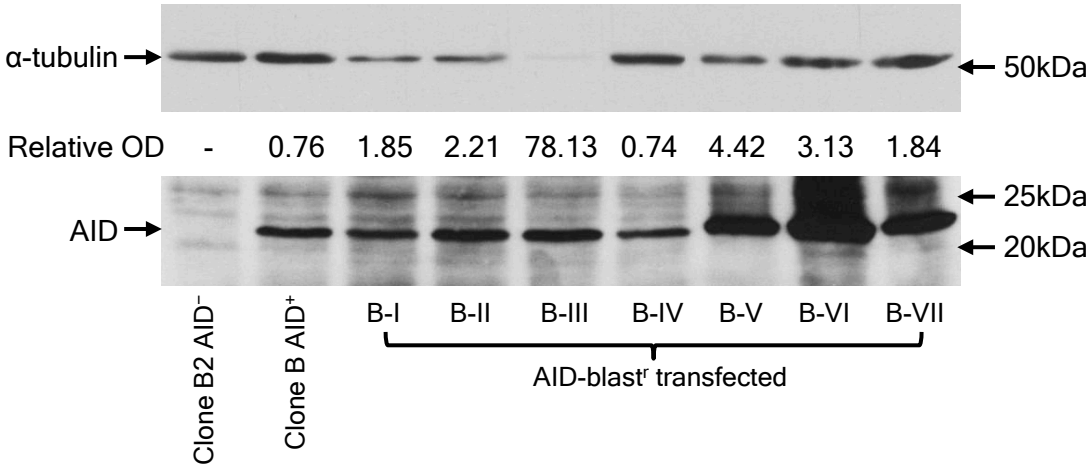

Figure 4.20: Probing for AID in AID-blast^r-transfected Tie2-DT40. Clone B Tie2-DT40 cells were transfected with circular pAID-TOPOblast^r by electroporation. Whole cell lysate was prepared from 1 × 10^6 cells of each emerging colony, and subjected to SDS-PAGE and Western blotting as described in section 2.5. Immunoblot analysis was performed with anti-AICDA polyclonal antibody and anti-α-tubulin monoclonal antibody. The position of molecular weight markers are indicated. Relative Optical Density (OD) was calculated as a ratio of AID to α-tubulin optical density for each culture and determined by ImageJ analysis of non-saturated films (*n*=1).

Discussion

The data presented in this chapter investigate the construction of a cell-based mutant library in which to conduct directed protein evolution.

The ψV^{-} AID^{R} DT40 cell line has previously been utilised as a vehicle for evolution of fluorescent proteins (Arakawa et al. 2008, Blagodatski et al. 2009). The purpose of this chapter was to explore the characteristics of the system, and to study the theoretical and actual mutation distribution in Tie2ECD as a basis for evolution. As a precursor, Tie2ECD was integrated into the rearranged Ig locus of the ψV^{-} AID^{R} DT40 cell line in order to maximise mutation frequency (Blagodatski et al. 2009).

The scope of SHM is partially dependent on the gene of interest (Bloom, Arnold 2009, Romero, Arnold 2009). Whilst the genetic sequence is fixed, an assessment of the sequence in question affords some insight into the likely success of SHM as a method of genetic diversification. In order to assess this the Tie2ECD sequence was explored with reference to existing literature.

Mutations have a predilection for nucleotide 'hotspots'. The principal hotspot nucleotides occupy one quarter of the Tie2ECD amino acid sequence, whereas only 21% of the Ig region screened by Arakawa *et al.* contains mutable hotspot residues (Arakawa, Saribasak & Buerstedde 2004). Given that the Ig gene has evolved as a mutable region, the sequence coverage in Tie2ECD should be satisfactory. Presuming that 45% of mutations may occur outside of these hotspots at random, and mainly at G:C base pairs (Arakawa, Saribasak & Buerstedde 2004), a total of

90% of the Tie2ECD sequence space is potentially covered. Resulting amino acid diversity is not infinite, but considering that the Tie2-angiopoietin interaction already has high affinity extensive mutagenesis is likely to disrupt function altogether.

During SHM the initial 185 bases downstream of the promoter are considered to be non-mutable (Rada et al. 1997), and therefore a significant portion of the Ig1 domain of Tie2ECD is unlikely to be mutated. Although mutations located outside active sites can modify protein activity (Shimotohno et al. 2001, Spiller et al. 1999), the binding domain, Ig2 in this case, is likely to be the most critical region (Morley, Kazlauskas 2005) and should attract maximal SHM activity. Therefore SHM is a reasonable mechanism by which to produce a mutant library for modulating Tie2ECD function.

Tie2-DT40 cells were cultured for a total of nine months without selection pressure in order to generate a mutant library. There are several features in the observed pattern of point mutation in these cells that differ from previous reports (Arakawa, Saribasak & Buerstedde 2004, Schoetz et al. 2006, Blagodatski et al. 2009) despite a general congruency. 87% of mutations are situated in mutable hotspot positions as compared with 55% observed by Arakawa *et al.* (Arakawa, Saribasak & Buerstedde 2004). There is apparent bias for the non-coding strand, and a transition frequency that approaches that of the B cell rather than hypermutating cell lines. The most 5' point mutation is located approximately 500 bases downstream of the RSV promoter, considerably further downstream than the initial 185 non-mutable bases attributed to the transition point between the

initiating and elongating forms of the transcription bubble in previous reports (Rada et al. 1997). The bases located immediately upstream and downstream of the mutated base do however comply with previous observations (Rogozin et al. 2001), and furthermore a pattern is observed when the resulting mutation is studied in relation to neighbouring nucleotides.

The principal point of difference in genetic modification observed in Tie2-DT40 cells is that nucleotide deletions were prevalent in 97% of Tie2ECD sequences tested after 9 months of cell culture, compared with no significant incidence of deletions in the literature (Arakawa, Saribasak & Buerstedde 2004, Schoetz et al. 2006, Blagodatski et al. 2009). It has been suggested that adjacent deoxycytosine deaminations may result in deletions depending on the action of DNA repair mechanisms (Wang, Wabl 2005). Whilst three of four single nucleotide deletions did occur at hotpots, multiple nucleotide deletions did not occur in a particularly hotspot dense area of Tie2ECD. It is possible that the specific clonal population of ψV^- AID^R DT40 utilised in this study has a predilection for deletions and other clonal populations of ψV^- AID^R DT40 should be tested for comparison. The high prevalence of deletions is a major concern, as the frameshift effect would render 97% of Tie2ECD sequences inactive in this cohort. Selection of Tie2-DT40 cells that actively bind angiopoietins would however discard cells harbouring nucleotide deletions.

Whilst changes to protein binding affinities are made in small steps and only 0.01% of single mutations are predicted to be beneficial (Bloom, Arnold 2009), the mutation rate must be sufficient to expediently produce a mutant library for

directed evolution and ensure that progressive mutations and phenotypical changes can occur between rounds of iterative selection. The mean mutation frequency of 0.8 per Tie2ECD sequence in the 9-month cell culture is ideal as a starting point for mutant library screening, but the time taken to generate this library is far from ideal.

The calculated mutation rate is significantly lower than that of the literature, particularly when considered in terms of real time as opposed to generation time. The generation time of Tie2-DT40 cells is longer than would be expected according to previous reports (Simpson, Sale 2003, Seo et al. 2007). Manipulation of the cell genome and high culture density created by the passaging method are likely to have slowed doubling time (Simpson, Sale 2003, Nakamura et al. 2010), although cells were maintained at a higher culture temperature to counteract this in part. However time spent in the G_1 and G_2/M phases is more critical than the S phase for SHM and potentially offers an improved mutation rate (Wang, Wabl 2005). Although mutation rates are often reported as a function of generation time, chronological time is the most critical function when considering feasibility of the method in manufacture of a mutant library and therefore it was necessary to investigate the characteristics of the ψV^- AID^R DT40 cell line.

Endogenous AID is replaced by a floxed AID-IRES-gpt cassette in ψV^- AID^R DT40. The proposed advantage of AID control relies on the ability of 4-hydroxytamoxifen (4-OHT) to successfully and cleanly excise AID from the genome when selection is complete. 4-OHT binds to the mutated oestrogen receptor with between ten and one hundred times more affinity than tamoxifen (Zhang et al. 1996) and

concentrations of 10nM to 100nM are reported to excise floxed cassettes by 48 hours (Buelow, Scharenberg 2008). When this was tested in Tie2-DT40, at least 1μM 4-OHT was required to reliably and promptly excise AID. The concentration required for Cre recombinase induction also varied between experiments, which may be due to poor solubility of 4-OHT in aqueous solution and consequent variation in concentration. Testing of individual mutant cells is not practical but population assay to assess excision of AID is advisable.

Although Arakawa *et al.* allude to minimal undesired excision of AID (Arakawa et al. 2008), AID expression was unintentionally lost from a whole population of cultured cells in this study. DNA was harvested from approximately 200,000 cells to confirm AID excision as compared with 500 cells utilised by Arakawa *et al.* (Arakawa, Lodygin & Buerstedde 2001), excluding the possibility of assay sensitivity as a contributor to the observation of AID loss. Leakage of the Cre-loxP system is a recognised phenomenon, although MerCreMer is more reliable than the single hormone-binding domain derived CreMer (Zhang et al. 1996). MPA selection of AID-gpt positive cells is certainly essential for population maintenance.

Mutation rate seems to relate to AID expression (Martin, Scharff 2002). AID transcription is stimulated by the exogenous β-actin promoter in ψV^- AID^R DT40, which allegedly produces preferable AID expression levels over endogenous AID (Arakawa et al. 2008). However the expression level of AID was observed to vary between different clonal populations of Tie2-DT40 cells despite the fact that the ψV^- AID^R Cl4 DT40 cell line was produced from a single clonal population following transfection of the floxed AID cassette and MerCreMer. The observed variation

could be explained by changes in individual cells prior to Tie2 transfection, including mutation of AID or its regulatory elements or background Cre recombinase activity. The effect of differing AID expression levels on the transgene mutation rate has not been formally documented and a far greater quantity of sequencing would be required to reach a definitive conclusion.

It is not known from the data presented whether the mutation rate remains equivocal throughout, or whether there is a trend of incremental reduction in frequency over time similar to a pattern previously observed in Ramos cells (Zhang et al. 2001). The ability to excise AID by Cre recombinase induction is advantageous in this SHM system, but background activity certainly contributes to reduction in AID expression levels. Alternative approaches to Cre recombinase-mediated AID switching are the inducible Tet-promoter and the auxin-inducible degron system. The Tet promoter is known to be effective in DT40 cells, although high cell density can limit switching to the Tet-off function (Wang, Takagaki & Manley 1996). The auxin-inducible degron system is however reported to be rapidly effective in DT40 cells (Nishimura et al. 2009). Utilisation of these technologies was beyond the limit of this investigation.

Alternative strategies were employed in an attempt to improve the mutation rate in Tie2-DT40. The first focused on accessibility of Tie2ECD for SHM. The required high level of Tie2ECD transcription would appear to be met based on protein expression analysis. Although the Tie2ECD sequence and stem-loop structure is fixed, Trichostatin A (TSA) was used in an attempt to improve accessibility of single stranded DNA for SHM. However sequencing of cells cultured for up to three

months did not demonstrate any benefit. A future line of investigation could involve increasing the density of E2A transcription factor binding sites adjacent to Tie2ECD.

A separate approach was to address the issue of AID expression. Transfection of AID for constitutive expression in Tie2-DT40, with no vulnerability to mutation, was eventually achieved in this chapter using blasticidin as a selection agent. However testing of the effect on mutation rate was beyond the temporal scope of this project and will be continued in future work. Significant difficulties were encountered with non-targeted transfection of AID into Tie2-DT40 cells, highlighting the importance of clean and rapid selection of cells. Although floxed puromycin marker recycling was achieved to enable puromycin-mediated selection of AID transfectants, the protracted route of increased 4-OHT exposure followed by subsequent subcloning and concurrent unexplained excision of Tie2ECD in one of the cell lines demonstrates another deficiency in the Cre-loxP system of genetic modification. In addition optimisation of transfection efficiency was hampered by poor sensitivity of detection assays. Co-transfection of GFP and retroviral transfection are strategies that should be considered to optimise this process.

The complexity and incomplete delineation of AID regulation and SHM mechanisms present challenges in engineering a successful biological tool for mutant library diversification. However new insights are published frequently and ultimately creation of an elegant effective system should be possible. The mutant library created in this chapter will be utilised for phenotype selection in Chapter 5.

CHAPTER FIVE

Isolation of mutant Tie2 phenotypes by Fluorescence Activated Cell Sorting (FACS) in the DT40 'ψV^{-} AID^{R} Cl4' cell line

In order to screen and select a desired mutant phenotype by Fluorescence Activated Cell Sorting (FACS), a sufficiently sensitive and robust fluorescent assay must be designed and the selection process must preserve cell viability.

FACS has been successfully employed for selection of mutant cell-surface displayed proteins with improved binding characteristics in a variety of non-mammalian host cells (Boder, Wittrup 1997, Georgiou et al. 1997). The process typically consists of a binding process between the cell library and fluorescent-labelled binding partner and selection of the brightest cells by FACS. Recovered cells are cultured prior to repetition of the process, which is continued until the desired phenotype is attained or no further improvements are made (Figure 1.4).

Chapters 3 and 4 describe engineering of Tie2ECD, the gene of interest, for cell surface display and its subsequent mutation by SHM in the ψV^{-} AID^{R} DT40 cell line. Baseline wild-type Tie2ECD 'on-cell' binding parameters for angiopoietins 1 and 2 have also been established by fluorescent labelling and flow cytometry.

Screening and selection of the cell-surface displayed mutant Tie2ECD library is performed in this chapter, to include:

- Exploration of screening methods;
- Definition of sorting parameters;
- Selection of Tie2ECD phenotypes;
- Sequencing of evolved proteins.

Introduction

Successful evolution of intrinsically fluorescent proteins via FACS-based screening and selection in the DT40 cell line (Arakawa et al. 2008, Blagodatski et al. 2009) illustrates that DT40 cells are robust enough to undergo iterative selection and culture.

The processes involved in screening of a cell-surface expressed binding protein are however more complex. The probability of recovering the target phenotype from the mutant population is dependent on several factors including: size of the screened population; sensitivity of the assay; selection within the sorted population; accuracy of the FACS apparatus and cell viability on completion of the process. A representation of the planned optimisation for FACS is shown in Figure 5.1.

In order to address accuracy the FACS apparatus will be calibrated regularly with beads to confirm discriminatory power and cleaned to maintain sterility. Cell viability will be optimised by minimal handling of cells during binding assays, maintenance at 4°C during sorting and collection directly into media to aid recovery. The issues of population screening and selection are more challenging.

Considering that the angiopoietin-Tie2 interaction has attained its high affinity by evolution and the expected number of beneficial mutations in directed evolution experiments is in the region of 0.01 – 0.5% (Bloom, Arnold 2009), the frequency of

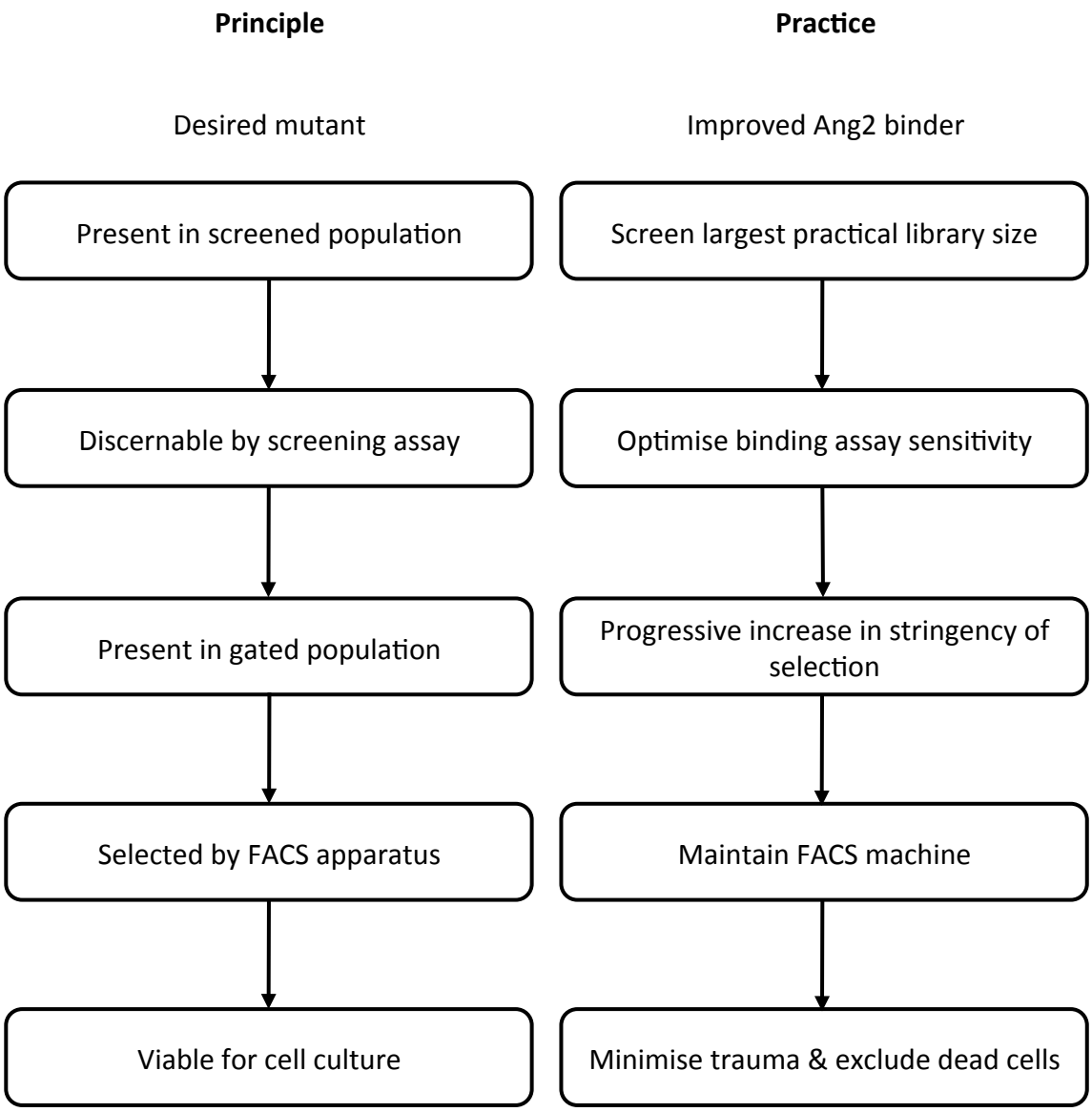

Figure 5.1: Approach to optimisation of FACS for evolution of binding proteins. General principles considered (left) and translation for this application (right).

cells in the Tie2ECD mutant library displaying increased affinity for angiopoietins is likely to be extremely low. A sensitive screening assay is therefore critical.

Two different methods of screening for improved affinity are described in the literature and applied in different circumstances. The first is equilibrium screening, which selects cells with greater binding affinity in an equilibrium reaction where the concentration of fluorescent-labelled ligand is below that of the wild-type K_d. The second method involves kinetic screening for cells with reduced binding dissociation rates when bound to saturation with fluorescent-labelled ligand.

It has been suggested that equilibrium screening is appropriate for interactions of K_d greater than 10nM (Boder, Wittrup 1998), and certainly not for interactions with K_d less than 1nM (Kieke et al. 1997). The difficulty in equilibrium screening of low K_d libraries lies in the large incubation volumes required to prevent ligand depletion. Conversely, dissociation rate may be impractically rapid in a high K_d library, limiting discrimination of kinetic variation. The practicalities of these methods for screening of the binding interaction between Tie2ECD and angiopoietins 1 and 2, which have dissociation constants of 0.46nM and 1.026nM respectively (section 3.4), will be tested in this chapter.

Published studies into competitive binding between two ligands also utilise equilibrium and dissociation concepts in assay design. Sensitivity can be maximised by variation in the ratio of ligand to competitor concentration and utilisation of the displacement method, whereby the fluorescent-labelled ligand

competes with pre-bound competitor for binding sites (Sklar et al. 1985, Waller et al. 2001). Relative concentrations and timing of the Ang1-Ang2 competition reaction will also be assessed for Tie2ECD.

It is also crucial to maximise differentiation between the mutant fluorescence emission signal and wild-type fluorescence, or 'background', and non-specific fluorescence, or 'noise'. The fluorescence profile of mutants will overlap with that of wild-type cells, and the size of DT40 cells, at approximately 10 microns, potentially limits the total fluorescence intensity. The signal to background ratio must therefore be optimised by utilisation of a competent fluorophore. R-phycoerythrin produces high fluorescence intensity (Kronick, Grossman 1983, Zola et al. 1990) and hence should offer preferable signal to background ratio in this study. Noise will be minimised by ensuring that fluorescent reagents do not produce non-specific staining, and by exclusion of non-viable cells and clumped cells via propidium iodide staining (section 3.3.1) and light scatter characteristics respectively.

Variation in expression level of Tie2ECD across the cell population further complicates the situation. High Tie2 expressors are likely to be more numerous and yield greater fluorescence intensity than higher affinity angiopoietin binders. In addition mutations conferring higher affinity may also decrease expression or viability, allowing overgrowth of non-target cells in the sorted population. It is therefore essential to delineate angiopoietin binding as a function of Tie2 expression. The addition of FLAG-peptide to the Tie2ECD construct enables dual

fluorescence assays for Tie2 expression and angiopoietin binding (section 3.3.5) and this method will be used for all sorting applications.

The relatively low predicted target cell frequency has implications for sorting criteria. The probability of encountering a rare target cell is 0.95 if three times more cells than the expected diversity are screened (Lowman et al. 1991). In theory there are 20^{441} different permutations of Tie2ECD, but in reality the mutation frequency in the proposed library is only 0.8 per cell (section 4.3.4). If the improved target cell frequency were assumed equal to 0.01% (Bloom, Arnold 2009) and only applied to the 80% of cells harbouring a mutation, only 1 in 12500 cells would possess an improved phenotype. This estimate can be further reduced to a frequency of 1 in 100,000 when the Tie2ECD mutation frequency is modified to exclude cells containing concomitant deletions (80%). It is likely that an initial sort for angiopoietin binders will remove cells containing deletions. Subsequent rounds of FACS will screen as many cells as practical, with gradual reduction in the proportion of cells selected to first allow enrichment and later specify purity.

5.1 Refinement of fluorophores

Concurrent anti-FLAG and angiopoietin binding reduces the amplitude of angiopoietin fluorescence (section 3.3.5). An alternative approach of minimising the reagents required was taken to streamline the staining process (Figure 5.2).

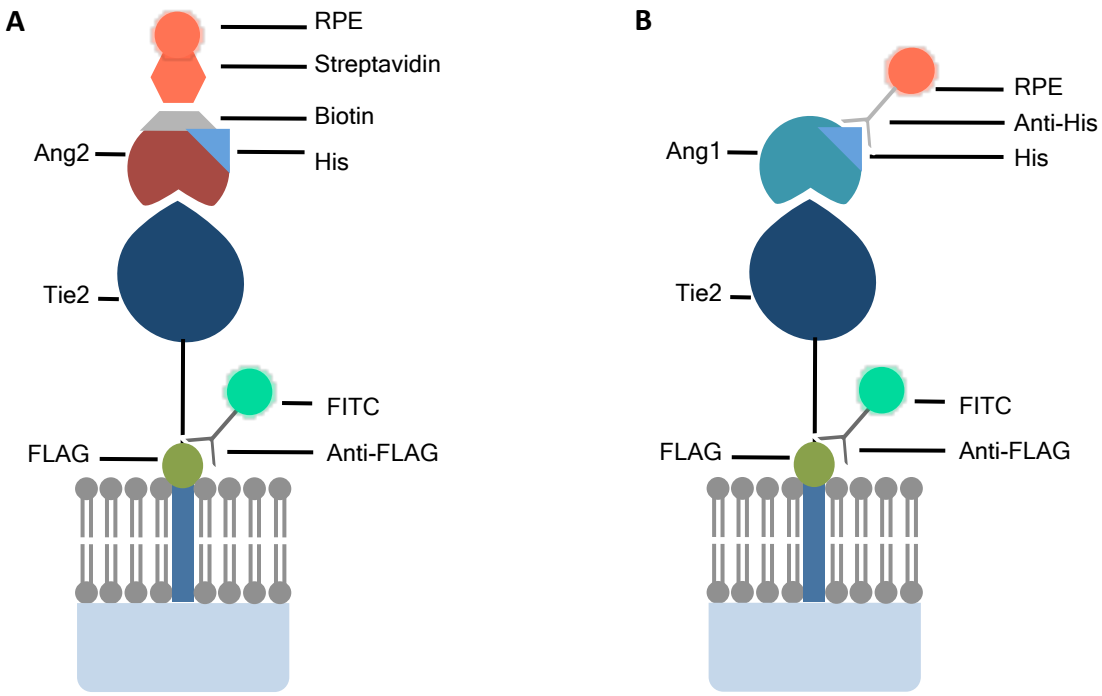

Figure 5.2: Immunofluorescent screening of cell surface expressed Tie2ECD.

a) Ang2 dual stain. Immunofluorescent FLAG detection and biotinylated Ang2 detection via streptavidin-R-phycoerythrin.

b) Ang1 dual stain. Immunofluorescent FLAG detection and Ang1 detection via anti-His-phycoerythrin.

Separate primary anti-FLAG and secondary fluorescent antibodies were replaced with anti-FLAG-FITC. Tie2-DT40 cells and untransfected DT40 cells were stained at concentrations above and including the recommended 1:200 dilution, with and without preceding Ang2 binding, and analysis by flow cytometry. A dilution of 1:100 produced the optimal signal to noise fluorescence (Figure 5.3a). Only 0.1% of untransfected DT40 cells emitted 530nm light above autofluorescence intensity of unlabelled cells.

Anti-His PE was utilised to label Ang1, as opposed to separate primary biotin and secondary fluorescent reagents. The optimal anti-His PE concentration was established by staining Tie2-DT40 cells at concentrations above and including the recommended 1:50 – 1:100 dilution, with and without preceding Ang1 binding, and analysis by flow cytometry. 1:25 anti-His PE dilution produced the maximum possible signal without presence of significant noise (Figure 5.3b). At this dilution five percent of unbound Tie2-DT40 cells emitted 582nm light above autofluorescence of unlabelled cells with GMFI of 50 versus 31 respectively, but this was accepted due to the 75% increase in signal gained from Ang1 bound Tie2-DT40cells with GMFI of 1950, as compared with 1110 for 1:50 anti-His-PE dilution.

The optimal streptavidin-R-PE concentration was previously ascertained by Dr S Sharma (University of Leicester). However the duration of exposure is relevant depending on whether the maximum possible signal or expediency is the prime concern. In order to characterise the association between streptavidin and biotin in this context, Tie2-DT40 cells were bound to 20nM Ang2-biotin and incubated with 1:25 4°C streptavidin-R-PE for varying times prior to screening by flow

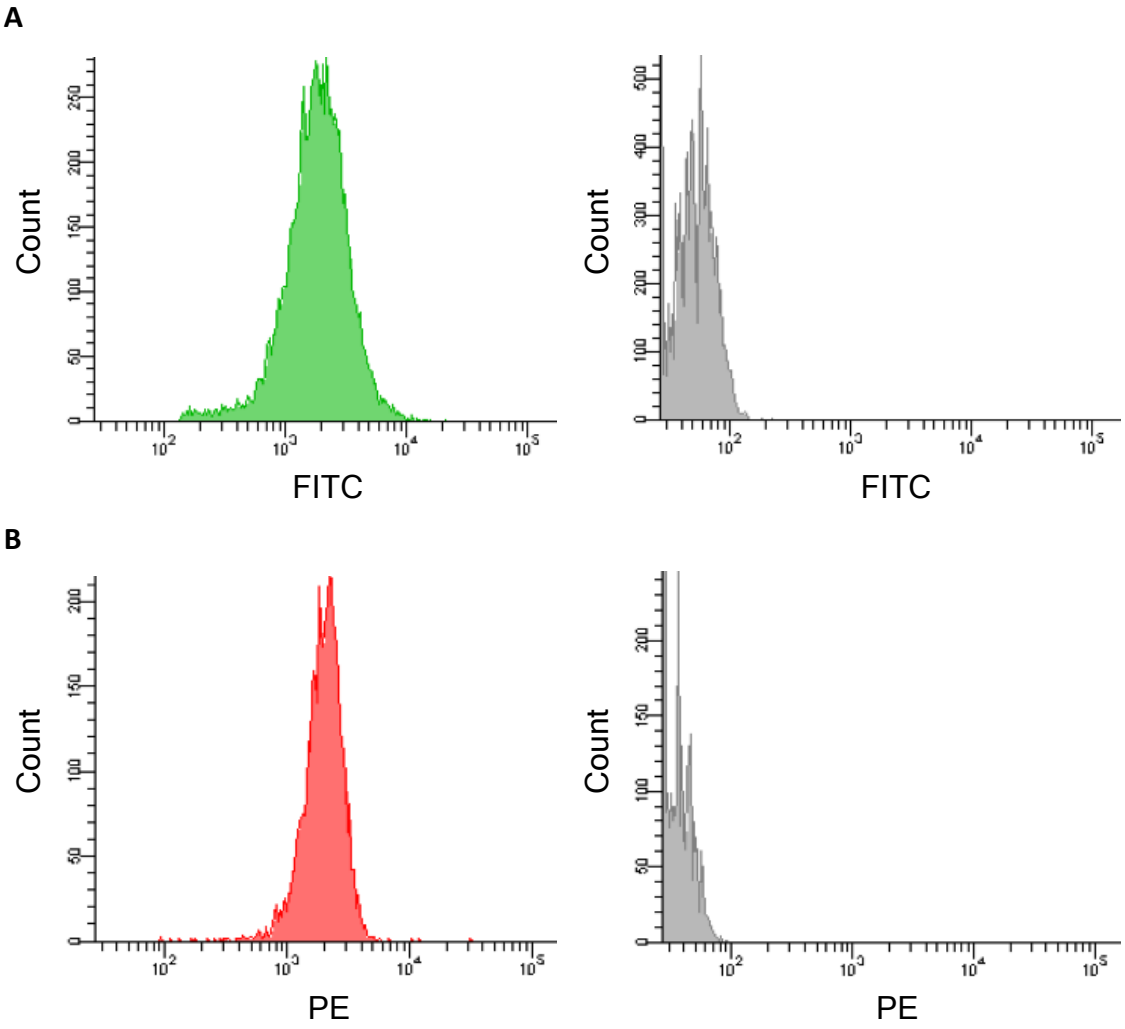

Figure 5.3: Refinement of fluorescent reagents for FLAG and Ang1 detection.

a) Anti-FLAG-FITC. Immunofluorescent FLAG detection with 1:100 anti-FLAG-FITC in Tie2-DT40 cells (left) versus untransfected DT40 cells (right). Parallel histograms are shown.

b) Anti-His-PE. Immunofluorescent Ang1 detection with 1:25 anti-His-PE in Ang1-bound Tie2-DT40 cells (left) and unbound Tie2-DT40 cells (right). Parallel histograms are shown.

cytometry. The emission signal gradually increases with time and is easily sufficient for detection at five minutes (Figure 5.4).

5.2 Exploration of kinetic screening for angiopoietin-Tie2 binding

The calculated K_d for Ang1 and Ang2 binding to Tie2ECD are 0.46nM and 1.03nM respectively (section 3.4). Therefore it was necessary to explore kinetic methods for the most sensitive screening of the mutant library.

5.2.1 Validation of K_{off} methodology

A 25°C reduction in temperature is reported to reduce off-rate by between fifty and a hundred times in the situation of antibody-antigen interactions (Boder, Wittrup 1998). Excluding ligand-receptor association and dissociation, all steps in the staining protocol were conducted at 4°C. If significant dissociation were occurring at 4°C, the signal to background and signal to noise ratios would be adversely affected.

In order to assess the validity of the assumption that reported observations can be translated into this context, cells were incubated in 4°C PBS for varying time periods following binding of 40nM RT Ang2-biotin and prior to five minutes of 4°C streptavidin-RPE labelling. A small gradual increase in MFI was observed with increasing 4°C dissociation time (Figure 5.5). When cells are incubated in RT PBS for 2 and 5 minutes following binding of 40nM RT Ang2-biotin and prior to 20

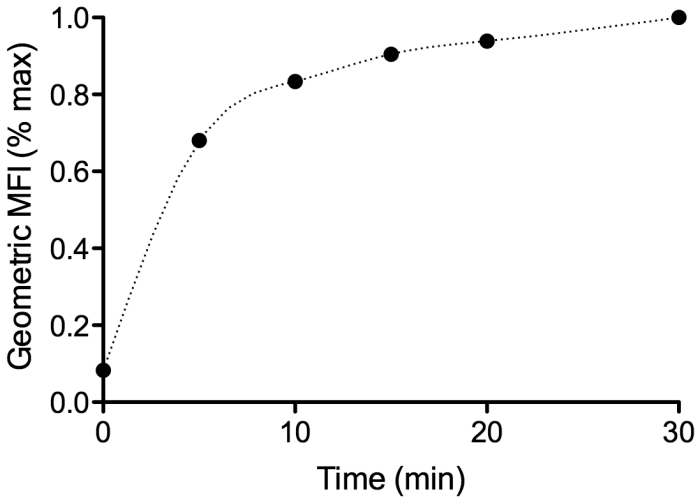

Figure 5.4: Association of streptavidin-R-PE at 4°C. Biotinylated Ang2 was bound at excess to wild-type Tie2-DT40 cells prior to incubation with streptavidin-R-PE for varying time points at 4°C, as described in section 2.7. The geometric Mean Fluorescence Intensity (MFI) was determined by flow cytometry. Raw data of a single experiment is expressed (*n*=1).

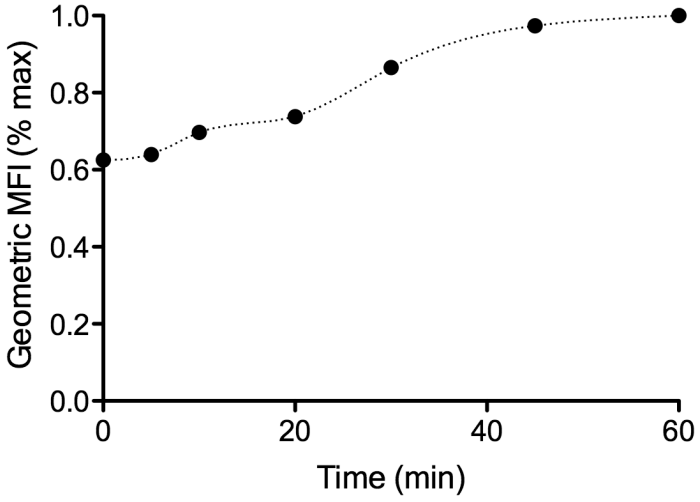

Figure 5.5: Dissociation of Ang2 at 4°C. Biotinylated Ang2 was bound at excess to wild-type Tie2-DT40 cells and incubated in PBS for varying time points at 4°C prior to rapid streptavidin-R-PE labelling. The geometric Mean Fluorescence Intensity (MFI) was determined by flow cytometry. Raw data of a single experiment is expressed (*n*=1).

minutes of 4°C streptavidin-RPE labelling, a reduction in MFI is seen from 3923 with no dissociation to 3101 for 5 minutes of dissociation, despite the possibility of Ang2-biotin reassociation in the absence of excess unlabelled Ang2. Therefore temperature is a reliable modulator of binding dissociation.

5.2.2 Dissociation of Ang2 (K_{off})

An estimation of the dissociation rate for Ang2 binding to cell-surface expressed Tie2ECD was made in section 3.4.4. However the fluorescence intensity achieved after forty minutes Ang2 dissociation time, or the apparent plateau phase, remained half that of Ang2 saturation (Figure 3.23). Incomplete dissociation lessens the maximal signal to background ratio and consequently reduces sensitivity of the method.

The technique utilised in section 3.4.4 involved streptavidin-R-PE labelling of the bound biotinylated-Ang2 prior to its dissociation. The streptavidin-biotin-Ang2 complex is likely to exhibit reduced dissociation over Ang2-biotin alone due to avidity effects of the multivalent streptavidin-biotin interaction. In addition to elevated background fluorescence and underestimation of the Ang2 off-rate, in this situation retention of Ang2-biotin-streptavidin-RPE on the mutant Tie2ECD expressing cell surface may be a function of spatial orientation as well as strength of the Tie2-Ang2 interaction.

In order to remedy this issue, triplicate experiments were performed in which Tie2-DT40-bound biotinylated-Ang2 was allowed to dissociate in the presence of

an excess of RT unlabelled Ang2 prior to streptavidin-RPE labelling at 4°C. Concentrations and quantities of reagents remained as outlined previously in sections 3.4.4/2.7.6.2. Variation of results between experiments and relative lack of dissociation limit credibility of the method (Figure 5.6).

A negative aspect of this method in comparison with 3.4.4 is that cells are split into aliquots prior to fluorescent labelling. Although they are theoretically treated in the same way thereafter with master-mixed reagents, labelling of each sample may not be absolutely identical. The coexistence of oligomeric recombinant Ang2-biotin and tetrameric streptavidin in a kinetic screening protocol for the Ang2-Tie2 interaction is extremely limiting. The number of molecules involved is unpredictable, such that the fluorescence intensity may not reflect the true level of Ang2-Tie2 binding.

5.2.3 Optimisation of signal:background ratio

A biotinylated Ang2 concentration of twenty times K_d should be sufficient to bind Tie2ECD to saturation. However, increasing the Ang2-biotin concentration could potentially improve the signal to background ratio. A two-phase effect was observed during Ang2 K_d determination, in which an initial increase in fluorescence intensity occurred between 0 and 5nM, with a second rise beyond 25nM Ang2 (data not shown). Recombinant Ang2 exists as trimers, tetramers and pentamers with few multimers (Procopio et al. 1999, Kim et al. 2005). It is possible that excessive Ang2 multimerises on the cell surface and rising fluorescence does not represent increased binding.

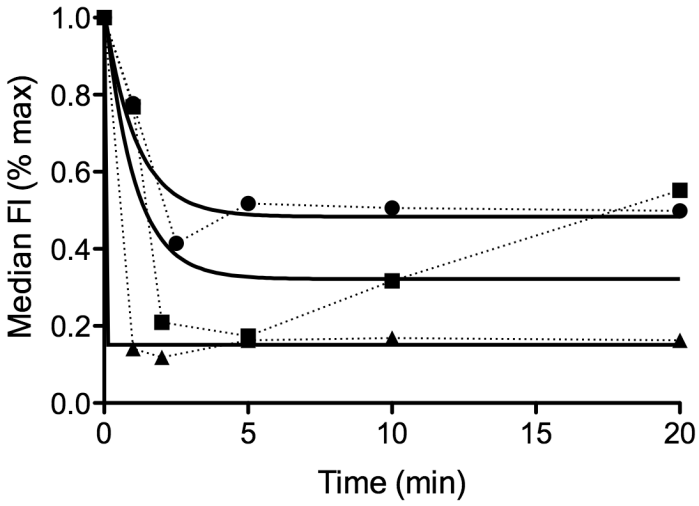

Figure 5.6: Dissociation of the biotinylated Ang2-Tie2ECD binding interaction. An excess of biotinylated Ang2 was bound to wild-type Tie2-DT40 cells and allowed to dissociate in the presence of an excess of recombinant Ang2 for varying time points at RT. Cells were labelled with streptavidin-R-PE at 4°C prior to determination of Median Fluorescence Intensity (FI) by flow cytometry, as described in section 2.7. Raw data from three separate experiments (broken lines) and respective non-linear regression analyses (solid lines) are shown.

Off-rate experiments were performed using the protocol outlined above, using 40nM and 200nM Ang2-biotin. Although the absolute MFI values were greater at 200nM Ang2, there was no significant difference in the pattern and percentage change between the two concentrations over the time course, negating concentration as a useful parameter in signal:background ratio (Figure 5.7). The higher Ang2 concentration did however improve signal:noise ratio by four times on comparison of maximal fluorescence emission for each Ang2 concentration and unstained cell autofluorescence.

Unexpectedly, the MFI increased after 2 minutes of dissociation time compared with no dissociation time, although a lower percentage of cells were contained within the stained population. When no dissociation time is allowed and cells are labelled with streptavidin-R-PE alone, as in the above techniques, versus streptavidin-R-PE with 200nM unconjugated Ang2, the median fluorescence intensity is less for streptavidin-R-PE alone at 979 compared with the presence of Ang2 at 1696. It is possible that unconjugated Ang2 produces a secondary binding response and affects streptavidin-R-PE labelling. In the above experiment two minutes' dissociation involves unconjugated Ang2 exposure whereas no dissociation does not, therefore increasing the fluorescence intensity in cells that have undergone dissociation.

5.2.4 Dissociation of Ang1 (K_{off})

His-tagged recombinant Ang1 and anti-His-PE fluorescent labelling were initially utilised to assay Ang1 K_{off} with poor results, as described in section 3.4.5. Briefly,

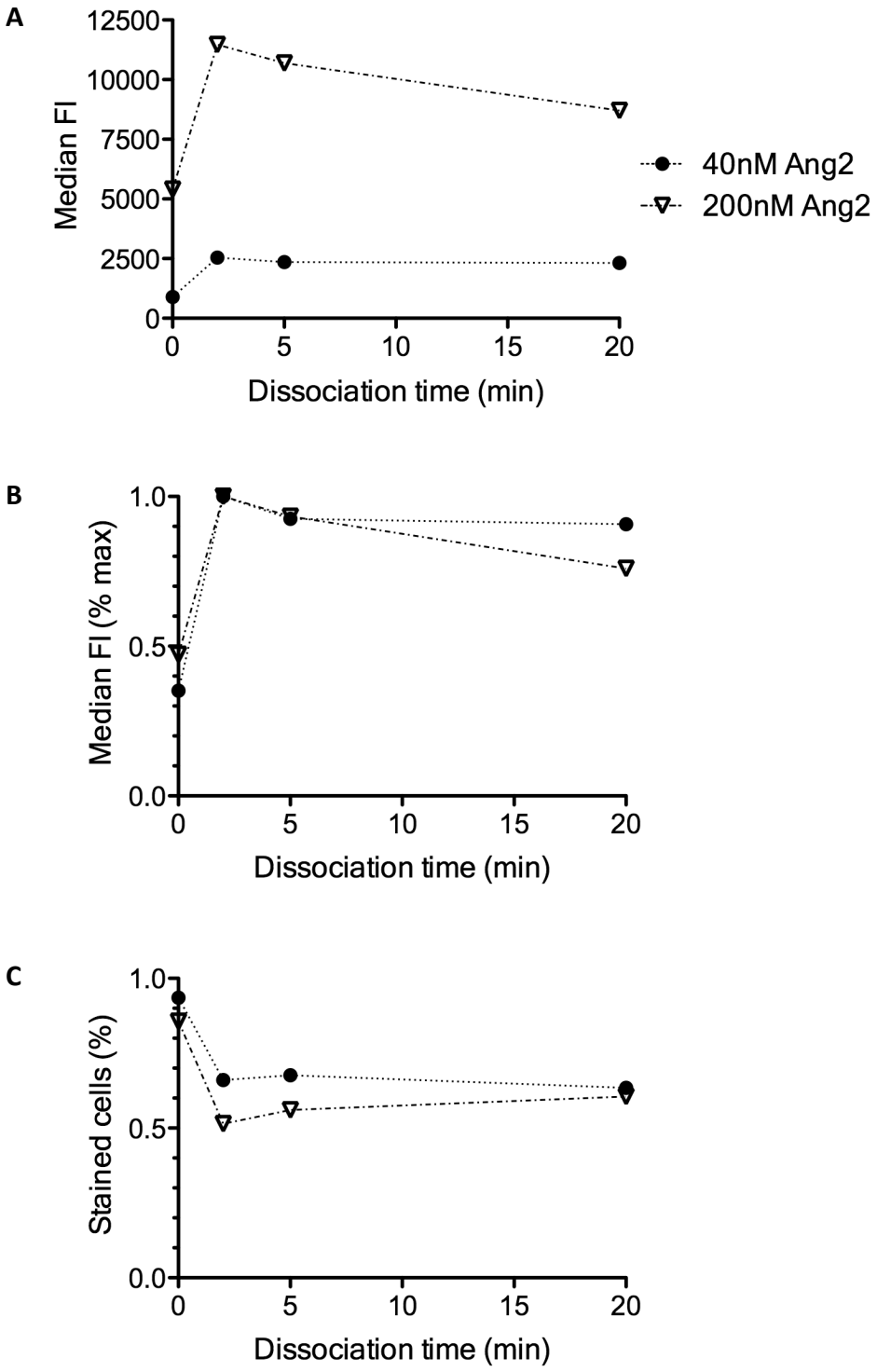

Figure 5.7: Dissociation of Ang2-Tie2ECD as a function of Ang2 concentration. An excess of biotinylated Ang2 was bound to wild-type Tie2-DT40 cells and allowed to dissociate in the presence of an excess of recombinant Ang2 for varying time points at RT. Cells were labelled with streptavidin-R-PE at 4°C prior to determination of Median Fluorescence Intensity (FI) by flow cytometry, as described in section 2.7 (*n*=1). Raw data from a single experiment is shown. Unstained cell median FI = 38.

a) Absolute fluorescence intensity.

b) Percentage of maximal fluorescence.

c) Percentage of cells stained.

Ang1 was bound to Tie2-DT40 cells and labelled with anti-HisPE prior to dissociation in the presence of an excess of Ang1. This method relies on negligible dissociation and avidity effect of the His tag-anti-His complex.

An alternative approach was tried, where Ang1 was bound to Tie2-DT40 cells and allowed to dissociate in a relatively large volume of PBS prior to labelling with anti-His-PE. Unfortunately this technique was also unsuccessful (Figure 5.8a), possibly due to reassociation of Ang1 during the dissociation stage despite the relatively dilute conditions and also potential avidity affects of anti-His-PE.

Inability to accurately quantify Ang1 binding was assumed secondary to reagents, evidenced by the fact that results for Ang2 binding assays deteriorate when the same method is employed (Figure 5.8b).

5.2.5 Biotinylation of Ang1

Initial experiments for Ang1 binding to Tie2DT40 have utilised His-tag as a mechanism of fluorescent labelling. Reported K_d values for the anti-His antibody-His tag interaction vary within the range 3–60 × 10^{-4} s^{-1} (Nieba, Krebber & Pluckthun 1996, Bates, Quake 2009), between 1000 and 20000 times higher than the biotin-streptavidin interaction. In equilibrium, His-tag detection produced similar results to biotin for Ang2 K_d measurement (section 3.4.3). Labelling of both Ang1 & Ang2 with biotin-streptavidin would clearly be preferable, particularly for kinetic assays. However biotinylated Ang1 is not currently commercially available.

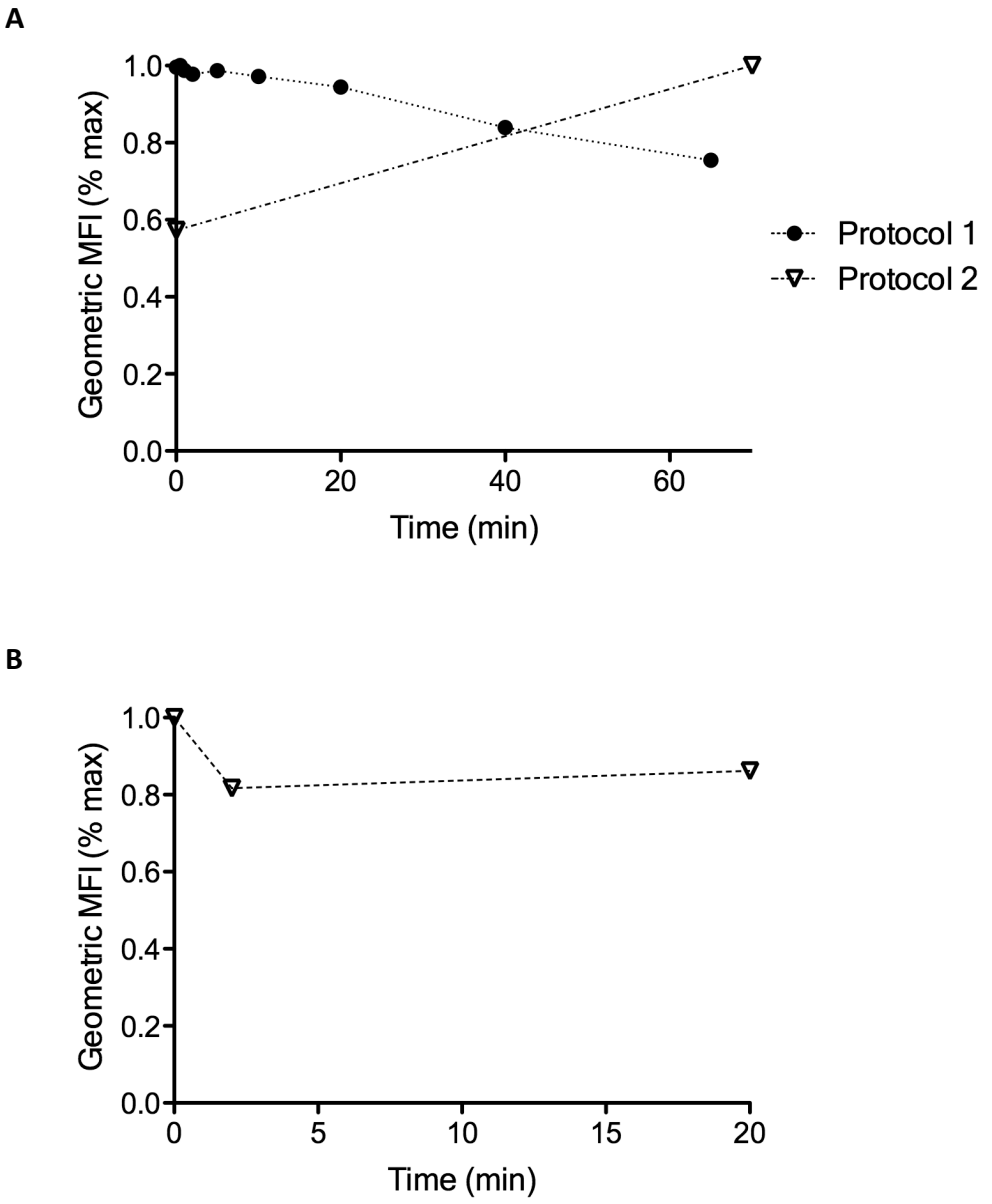

Figure 5.8: Dissociation of the angiopoietin-Tie2ECD binding interaction.

a) Ang1. An excess of Ang1 was bound to wild-type Tie2-DT40 cells and allowed to dissociate in the presence of an excess of PBS for varying time points at RT. Cells were labelled with anti-His-PE at 4°C prior to determination of Median Fluorescence Intensity (FI) by flow cytometry (Protocol 2; *n*=1). Protocol 1, in which dissociation occurred in an excess of Ang1 (section 3.4.5), is shown for reference.

b) Ang2. An excess of biotinylated Ang2 was bound to wild-type Tie2-DT40 cells and allowed to dissociate in the presence of an excess of PBS for varying time points at RT. Cells were labelled with streptavidin-R-PE at 4°C prior to determination of Median Fluorescence Intensity (FI) by flow cytometry (*n*=1).

Biotinylation of Ang1 was attempted via a commercial kit (Innova Biosciences) as per the manufacturer's instructions (section 2.5.7). The biotinylation reaction product and an equal quantity of non-biotinylated Ang1 were resolved by SDS-PAGE and assessed by Western immunoblotting with anti-His and streptavidin probes (section 2.5). In addition to biotinylated Ang1 the streptavidin probe revealed multiple higher molecular weight bands, which did not appear to contain Ang1 and therefore did not apparently represent multimers (Figure 5.9a).

In order to assess the quantity of Ang1 that was successfully biotinylated in the reaction, the product was immunoprecipitated with streptavidin beads against non-biotinylated Ang1 as a control (section 2.5.8). Probing for His and biotin was performed following SDS-PAGE and Western blotting. Minimal biotinylated Ang1 was immunoprecipitated, as detected by streptavidin-HRP, and Ang1 was able to bind non-specifically to streptavidin beads (Figure 5.9b).

Use of biotinylated Ang1 in kinetic experiments would require a pure protein sample with accurately determined concentration, and therefore this method of biotinylation was determined unsuitable for the desired application. Further investigation of Ang1 kinetics was not possible within the constraints of this study.

5.2.6 Association of Ang2 (K_{on})

Direct measurement of Ang1 binding is not necessary in a competition assay involving biotinylated Ang2. When considering a kinetics based competition screen whereby Ang1 is allowed to dissociate from Tie2-DT40 cells in the presence

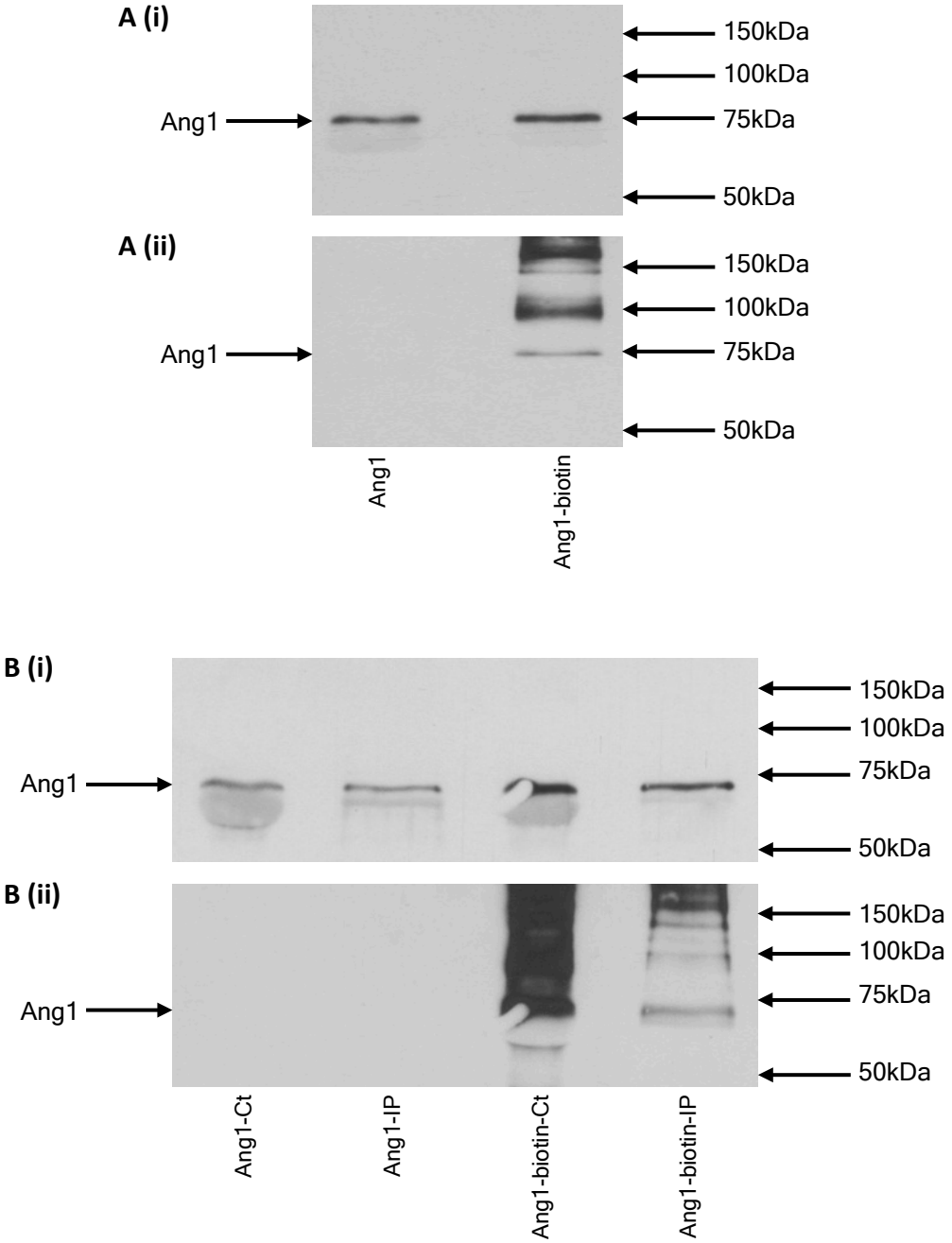

Figure 5.9: Biotinylation of Ang1. Ang1 was biotinylated as per the manufacturer's instructions (Innova Biosciences).

a) Biotin probe. Equal quantities of recombinant Ang1 and the biotinylation reaction product were resolved by SDS-PAGE and subjected to western immunoblotting as described in section 2.5 (*n*=1).

b) Quantification of biotinylation. Equal quantities of recombinant Ang1 and biotinylation reaction product were immunoprecipitated with streptavidin beads as described in section 2.5.8 (*n*=1). The assay products (IP) were resolved and transferred to nitrocellulose membrane along with non-IP controls (Ct).

Immunoblot analysis was performed with **(i) anti-His antibody** and **(ii) streptavidin-HRP**. The position of molecular weight markers are indicated.

of an equal or lesser relative concentration of biotinylated Ang2, a rapid on rate for Ang2 binding to Tie2-DT40 is essential assuming that the dissociation of Ang1 is relatively quick.

Tie2-DT40 cells were suspended in 2nM biotinylated Ang2 for varying lengths of time prior to labelling with streptavidin-R-PE and flow cytometry, as described in section 2.7.6.4. The initial phase of association occurred rapidly, and is likely to be an underestimate due to physical limitations of the experiment (Figure 5.10).

5.2.7 Ang1-Ang2 competition

A kinetics-based competition assay between Ang1 and Ang2 for Tie2-DT40 binding involves complex interactions. A potential protocol for such an experiment would involve saturation binding of Ang1 to Tie2-DT40 followed by a period of dissociation in the presence of biotinylated-Ang2, during which any dissociated free Ang1 would be present at relatively low concentration in relation to biotinylated-Ang2. Streptavidin-R-PE could then be used to stain cells that have dissociated from Ang1 and associated with Ang2. A serious limitation in designing this experiment is the unknown K_{off} for Ang1 binding.

Variables include the time allowed for dissociation of Ang1 and simultaneous association of Ang2, and the relative concentration of Ang1 in comparison to Ang2. When iterative sorting is implemented, reduction in Ang1 dissociation/Ang2 association time and reduction in Ang2 concentration relative to Ang1 could both be used to increase the stringency of the selection.

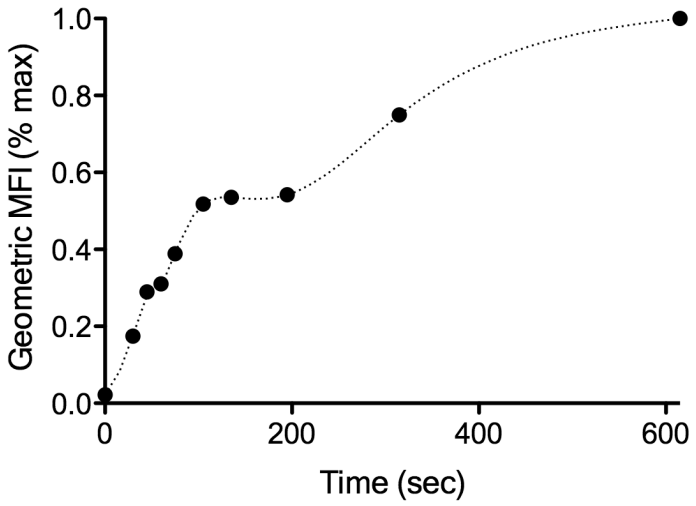

Figure 5.10: Association of the Ang2-Tie2ECD binding interaction. Wild-type Tie2-DT40 cells were incubated with 2nM biotinylated Ang2 for varying time points prior to labelling with steptavidin-R-PE at 4°C. Geometric MFI was determined via flow cytometry. Raw data from a single experiment (broken line) and non-linear regression analysis (solid line) are shown (*n*=1).

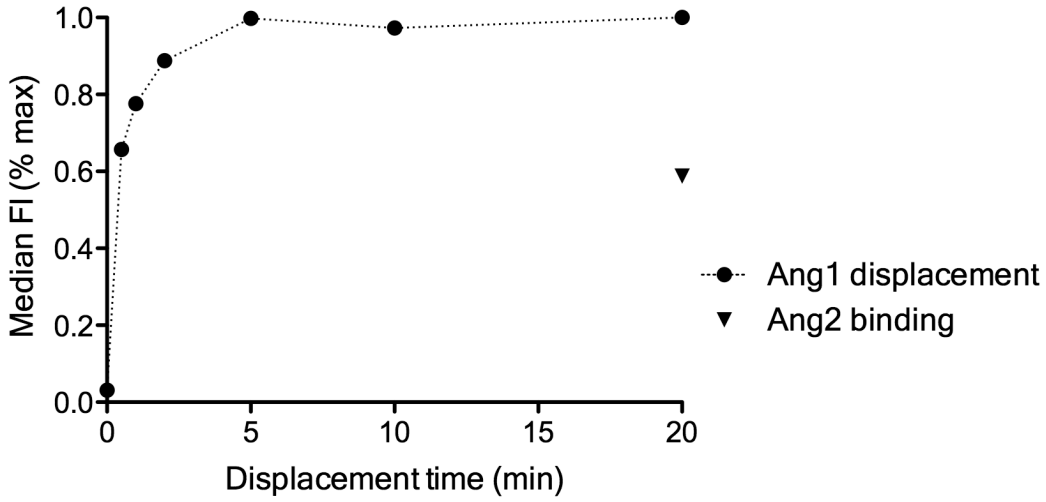

Figure 5.11: Displacement of Ang1-Tie2ECD binding by Ang2. Wild-type Tie2-DT40 cells were bound to saturation with 4nM Ang1 prior to incubation with 20nM biotinylated Ang2 for varying time points (Ang1 displacement). Concurrently Tie2-DT40 cells were incubated with 20nM biotinylated Ang2 for 20 minutes (Ang2 binding). Labelling was performed with steptavidin-R-PE at 4°C and median FI was determined via flow cytometry. Raw data from a single representative experiment are shown (*n*=3).

To visualise the time course of the Ang1 dissociation/Ang2 association, Ang1 was utilised at approximately half the relative concentration of Ang2. Tie2-DT40 cells were bound to 4nM RT Ang1 to equilibrium and washed prior to resuspension in 20nM RT biotinylated Ang2 for varying lengths of time. 20nM RT biotinylated Ang2 binding was also performed simultaneously for 20 minutes on a separate cell sample. Cells were then washed and labelled with steptavidin-R-PE. The experiment was performed twice and the median fluorescence intensity increased relatively rapidly on both occasions (Figure 5.11), limiting its practicality as a screening scenario for Ang1 dissociation. The median FI was also lower in independent Ang2 binding than the equivalent Ang1 displacement sample, suggesting that the interactions in this situation carry additional complications. The concentration effect is discussed separately below.

5.3 Exploration of equilibrium screening for angiopoietin-Tie2 binding

Both equilibrium and kinetic screening have successfully generated antibodies with improved binding characteristics. The dissociation constant is formed by the relationship between association and dissociation rates of the ligand-receptor complex:

$$K_d = \frac{K_{off}}{K_{on}} = \frac{[R][L]}{[C]}$$

where R = receptor; L = ligand and C = ligand-receptor complex

Thus the alternative strategy of equilibrium binding was explored.

5.3.1 Ang2 concentration

An expression for the fluorescence ratio between an improved mutant and wild-type cells was described by Boder & Wittrup (Boder, Wittrup 1998):

$$F_r = \frac{S_r K_r \left(\frac{[L]}{K_d^{wt}}\right)^2 + \left(S_r K_r + 1\right)\left(\frac{[L]}{K_d^{wt}}\right) + 1}{S_r K_r \left(\frac{[L]}{K_d^{wt}}\right)^2 + \left(S_r + K_r\right)\left(\frac{[L]}{K_d^{wt}}\right) + 1}$$

where $S_r = \frac{F_{\max}}{F_{bg}}$ $K_r = \frac{K_d^{wt}}{K_d^{mut}}$

The achievable reduction in K_d is unknown, but unlikely to be large given the strong affinity of the wild type interaction. For the purposes of this exercise K_r was assumed to equal 2. The mean fluorescence intensity ratio achieved during triplicate Ang2 K_d calculation was taken as representative of S_r at 45. A graphical representation of F_r using the stated parameters is displayed in Figure 5.12.

The fluorescence ratio peaks sharply at a relatively low concentration of Ang2 and decreases very gradually as Ang2 concentration increases. In the presence of an uncertain K_r value overestimation of the optimal Ang2 concentration is therefore preferable. The relative fluorescence improvement or signal to background ratio

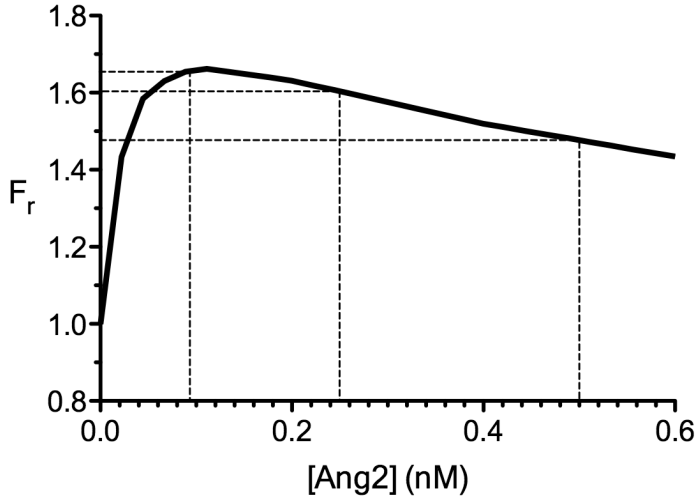

Figure 5.12: Mutant:wild-type fluorescence ratio (F_r) as a function of Ang2 concentration. Graphical representation of the expression:

$$F_r = \frac{S_r K_r \left(\frac{[L]}{K_d^{wt}}\right)^2 + (S_r K_r + 1)\left(\frac{[L]}{K_d^{wt}}\right) + 1}{S_r K_r \left(\frac{[L]}{K_d^{wt}}\right)^2 + (S_r + K_r)\left(\frac{[L]}{K_d^{wt}}\right) + 1}$$

where S_r = 45 and K_r = 2 (section 5.3.1).

S_r = maximal fluorescence to cell autofluorescence ratio.
K_r = wild-type K_d to mutant K_d ratio.
Predicted fluorescence ratios for Ang2 concentrations of 0.125, 0.25 and 0.5 nM are marked by broken lines.

for a two-fold reduction in K_d is relatively small, indicating that accuracy and sensitivity is paramount.

In order to test the feasibility of possible Ang2 concentrations, Tie2-DT40 cells were incubated to equilibrium with varying concentrations of biotinylated Ang2 prior to labelling with anti-FLAG-FITC and streptavidin-R-PE, and examined by flow cytometry. At 0.125nM Ang2, staining was barely above background. The higher concentrations selected, 0.25 and 0.5nM, were more discriminatory (Figure 5.13). A sorting protocol involving a higher concentration such as 0.5nM during the enrichment rounds, with later reduction when purity is required, should capture the majority of desired mutants.

5.3.2 Ang1-Ang2 competition

Competitive equilibrium sorting involving Ang1 and Ang2 requires determination of the concentrations at which the ligands compete for Tie2 binding sites. Wild-type Tie2-DT40 cells were incubated with a mixture of 2nM ($1.95 \cdot K_d$) biotinylated Ang2 and varying concentrations of serially diluted Ang1 at RT to equilibrium. Following staining with 4°C streptavidin-R-PE, cells were analysed by flow cytometry (Figure 5.14a). A precipitous drop in Ang2 binding, determined by fluorescence intensity, was seen between Ang1 concentrations of 20 and 30nM. The half maximal inhibitory concentration (IC50) of Ang1 occurred at 25nM ($54.8 \cdot K_d$).

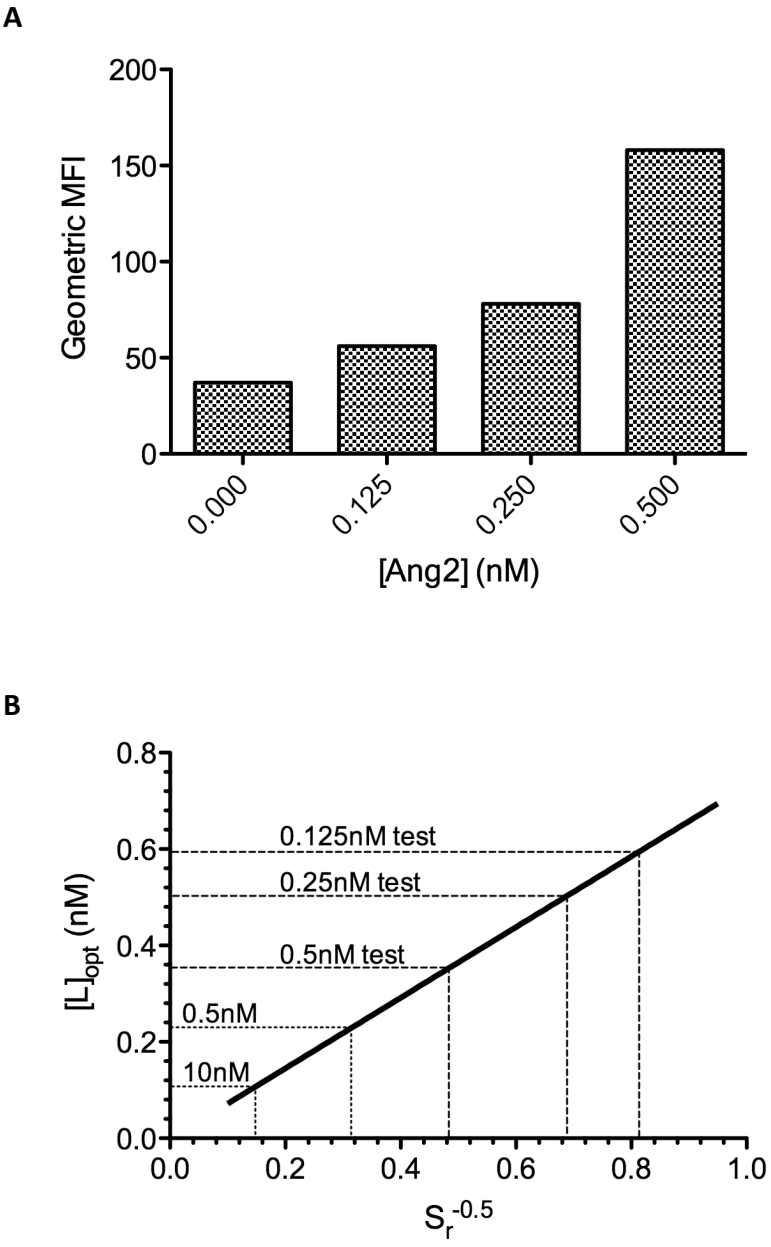

Figure 5.13: Fluorescence intensity by Ang2 concentration.

a) Observed fluorescence intensity. Wild-type Tie2-DT40 cells were bound to equilibrium with differing concentrations of biotinylated Ang2 prior to labelling with streptavidin-R-PE at 4°C. Geometric Mean FI was determined via flow cytometry. Raw data from a single experiment are shown (*n*=1).

b) Comparison to theoretical optimal ligand concentration. Assuming that an improved Ang2 mutant has a K_d of half the wild-type K_d (1.026nM), the optimal ligand concentration is dependent on the ratio of maximal to autofluorescence (S_r) at any given concentration. Dashed lines mark observed S_r from Fig 5.13a. Dotted lines mark S_r from Fig 3.19.

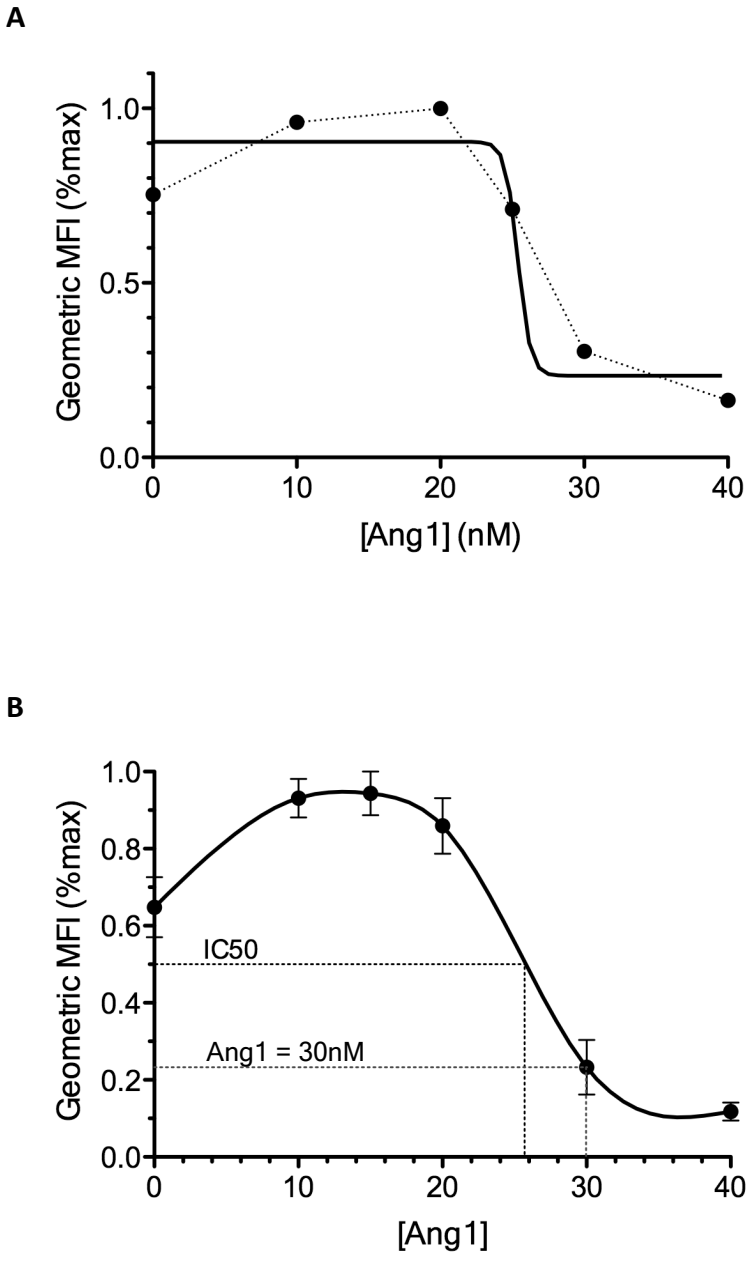

Figure 5.14: Competitive equilibrium of Ang1 versus Ang2. Wild-type Tie2-DT40 cells were bound to equilibrium with 2nM biotinylated Ang2 and varying concentrations of Ang1. Labelling was performed with steptavidin-R-PE at 4°C and Geometric Mean FI was determined via flow cytometry.

a) Single representative experiment. Raw data from a single representative experiment (broken line) and non-linear regression for one site competitive binding (solid line) are shown (*n*=3).

b) Mean. Standard error bars, curve-fit (solid line) and IC50 are shown. Remaining Ang2 binding at 30nM Ang1 concentration is marked.

In order to capture cells with improved Ang2 binding relative to Ang1 binding, a relatively high concentration of Ang1 is required. An Ang1 concentration of 30nM ($65.8 \cdot K_d$), maintaining Ang2 concentration at 2nM ($1.95 \cdot K_d$), would select the remaining 16% of Ang2 binders (Figure 5.14b). As with Ang2 equilibrium screening, the Ang1 concentration may need to be gradually increased for stringency in later rounds of sorting.

5.4 Determination of parameters for cell sorting

To ensure that DT40 cells could be sorted and recovered on the available FACS apparatus a test sort was performed. 2×10^6 Tie2-DT40 cells were bound to Ang2 and labelled with R-PE as previously described. The brightest 10% of R-PE stained cells were gated and sorted directly into 4°C compete medium in purity mode with a reported efficiency of 92%.

Cells were screened at a rate of 679 per second, significantly less than the manufacturer's recommended limit of 2000 per second. The process of sorting circa 1 million cells was 23.5 minutes in duration, although this could be reduced by an increase in sorting speed. Therefore approximately ten minutes of sorting time should be budgeted for each million cells.

Despite the conservative approach to sorting, the percentage of screened cells recovered was only 6.9% rather than the 10% gated. In addition the total number of cells screened was only half that of the number harvested for staining due to

viability issues. The recovered cells did however appear healthy post-sorting and culture was relatively rapid. There was no apparent difference in the fluorescence intensity of sorted and unsorted cells on repeat Ang2 fluorescent binding assay, as would be expected after a single enrichment sort (Figure 5.15).

The percentage of unstained cells located within the live cell gating in flow cytometry experiments is generally between 60% and 80%. This can be accounted for by exclusion of both non-viable and clumped cells. Light scatter data indicates that the relative proportions of each are 29% and 1% in unstained cells respectively. Therefore 1% of the 2×10^6 viable cells would have been excluded due to the assay requirement for single cells.

Conducting a staining procedure reduces cell viability by approximately 20% from that of unstained cells. Therefore the observed viability in stained cells is approximately 50% of the total cells screened. In an attempt to compensate for suboptimal cell viability a fluorescent angiopoietin binding assay was performed with 40×10^6 Tie2-DT40 cells, with the aim of retaining a reasonable number for sorting. This however resulted in a drastic reduction in cell viability, perhaps due to larger incubation volumes and additional centrifugation speed required. Health of cells is clearly paramount, and therefore all cultures were maintained at optimal cell density prior to sorting and handled with the utmost care. A range of 10-20 $\times 10^6$ cells was decided upon as a starting point for sorting applications to balance issues of time and viability against examinable diversity.

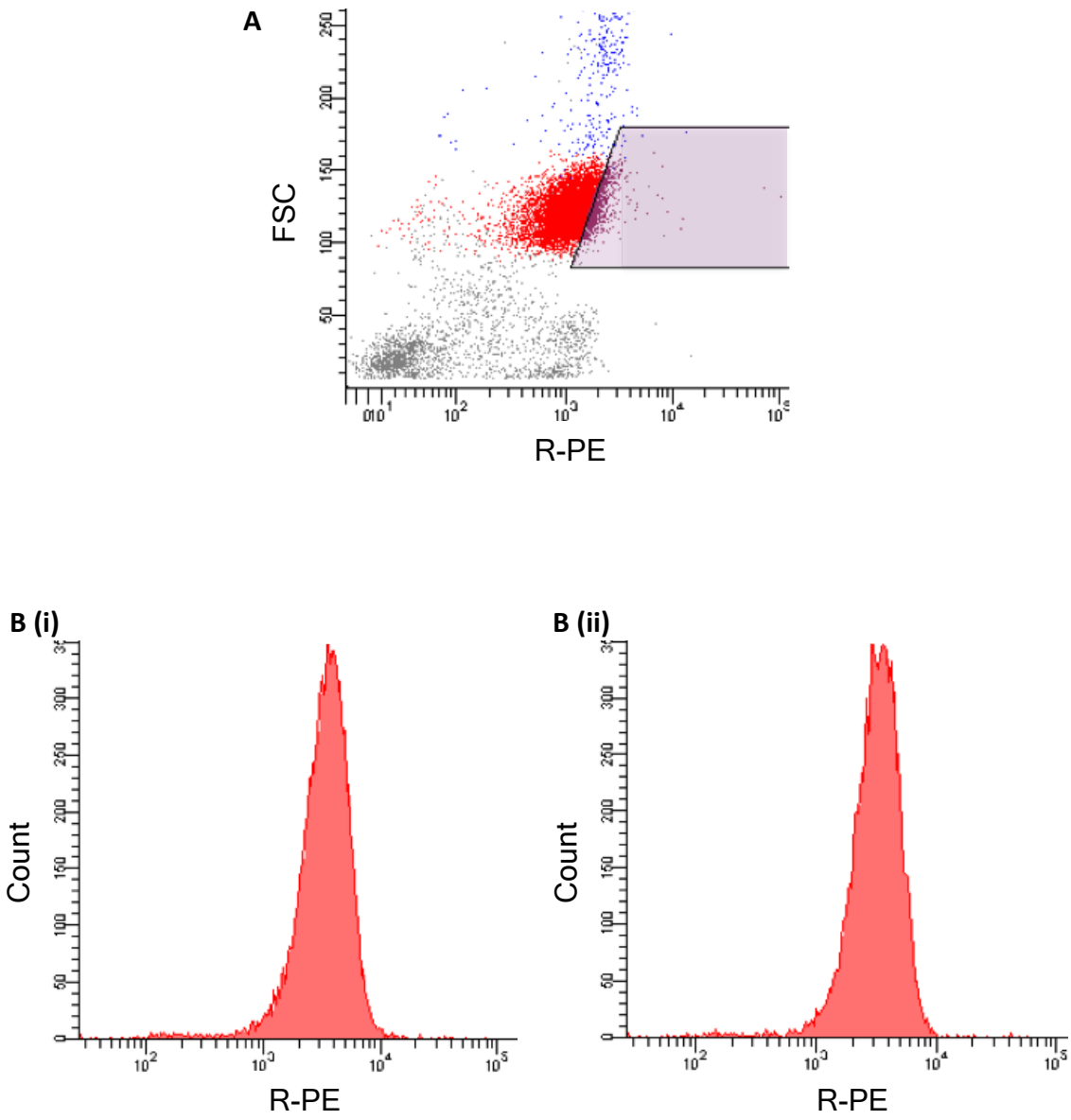

Figure 5.15: Test sorting Tie2-DT40 for Ang2 binding.

a) Sorting for highest Ang2 binders. 2 × 10^6 TIe2-DT40 cells were bound to equilibrium with 2nM biotinylated Ang2 prior to labelling with streptavidin-R-PE and flow cytometry. The highest 10% of Ang2 binders (coloured red) were sorted via 2-way purity as per shaded window in dot plot. Dead and unstained cells are coloured grey and clumped cells are coloured blue.

b) Screening of sorted population. 1 × 10^6 sorted cells (i) and unsorted cells (ii) were bound to equilibrium with 2nM biotinylated Ang2 prior to labelling with streptavidin-R-PE and flow cytometry. Parallel histograms are shown.

5.5 Selection of mutant populations for evolution

Sequencing of clone B after 9 months of culture demonstrated deletions in 96.67% of the population tested. Of the sequences with long segment deletions, none remained in-frame. Of the point deletions, only one sequence contained three separate deletions, which could result in a non-functional cell-surface expressed protein. Whilst some point deletions occurred downstream of the Ig2 binding domain with possible retention of angiopoietin binding capability, they would render the cell surface expression domain obsolete. However the diversity of mutations in the 9-month cultured population appeared to be greater than that of the 3-month population. It was therefore necessary to characterise these cells further.

5.5.1 Ang2 binding in mutant clone B populations

Cells were assessed for Ang2 binding by immunofluorescent staining and flow cytometry. Comparative dual staining of clone B cells cultured for 3 and 9 months was performed with an excess of Ang2 (40nM) (section 2.7.2). The proportion of cells fluorescing for Ang2 and FLAG was 27.7% in the 9-month culture versus 82.3% in the 3-month culture, indicating that the 9-month population has more genetic modifications (Figure 5.16).

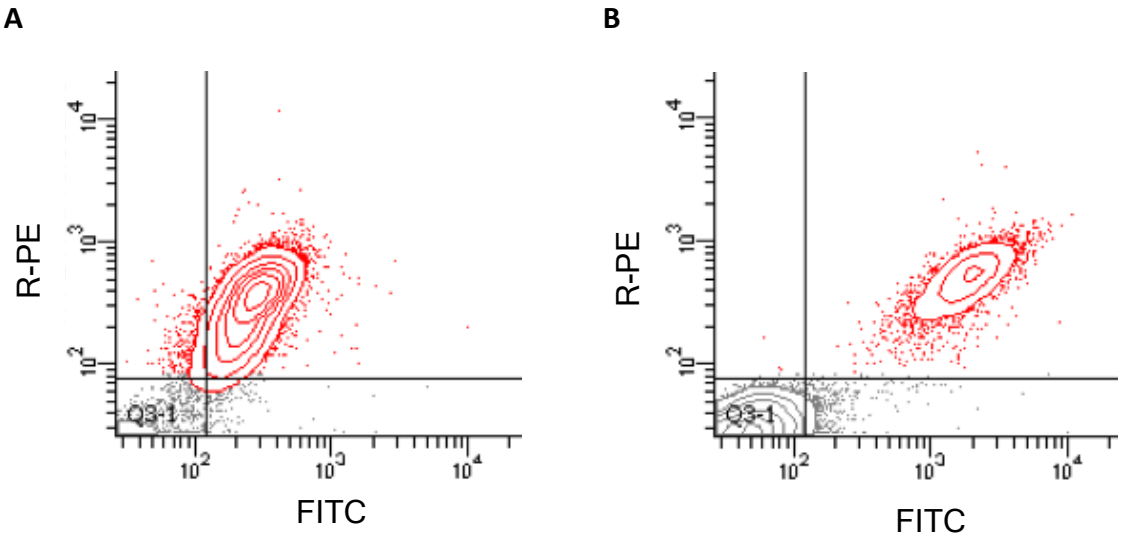

Figure 5.16: Ang2 binding in cultured mutant populations. 1 × 10^6 TIe2 DT40 cells were maintained in culture as below, and bound to saturation with 40nM biotinylated Ang2 prior to labelling with streptavidin-R-PE and flow cytometry. Contour plot is shown.

a) 3 month-culture.

b) 9 month-culture.

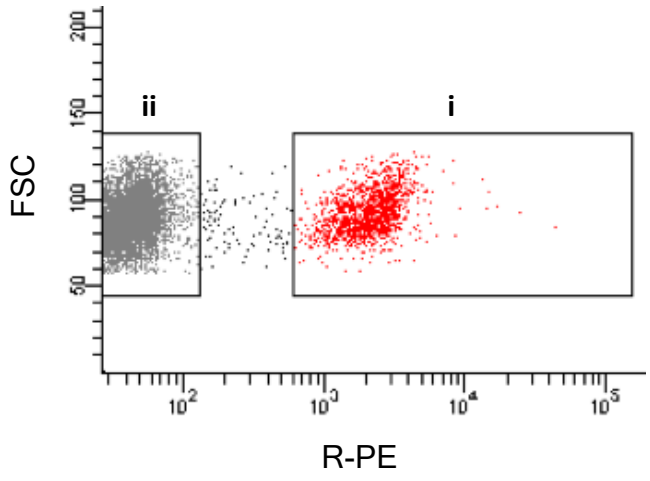

Figure 5.17: Sorting of 9-month Tie2-DT40 for Ang2 binding. 20 × 10^6 cells were bound to saturation with 40nM biotinylated Ang2 prior to labelling with streptavidin-R-PE. Ang2 bound cells and non-bound cells were sorted via 2-way purity as per windows (i) and (ii) respectively. Dot plot is shown.

5.5.2 Sorting of mutant clone B population for Ang2 binding

The 9-month culture was taken forward as a starting population. Ang2 binding and non-binding populations were differentiated by FACS. 20×10^6 cells were sequentially stained with RT 40nM biotinylated Ang2 and 4°C streptavidin-RPE prior to sorting of definite Ang2-binding and non-binding populations, amounting to 27% and 72% of live single cells respectively (Figure 5.17).

5.5.3 Tie2 expression in sorted Ang2 binding and non-binding populations

Total RNA was extracted from untransfected DT40 cells, the naïve 9-month clone B population and sorted Ang2 binding and non-binding populations; a 2μg quantity was used for immediate cDNA synthesis by reverse transcription. PCR of the 1323bp Tie2 gene was performed on each cDNA under the conditions specified in Appendix 2.1/section 2.6. There was no discernable difference in quantity of Tie2 between naïve and sorted clone B populations, indicating integrity of Tie2 transcription (Figure 5.18).

Whole cell lysate was also prepared from the same cell populations and subjected to SDS-PAGE and Western blotting. Probing for FLAG and Tie2 revealed that expression levels were highest in binders and lowest in non-binders (Figure 5.19). Frameshift deletions in the Tie2 gene would abolish FLAG expression given the downstream position of FLAG in the Tie2ECD-CSD structure. The Tie2 antibody is raised against residues 23 to 745 of full-length Tie2 receptor. Although the antibody clearly binds to a truncated segment of 23 to 441, many of the deletions

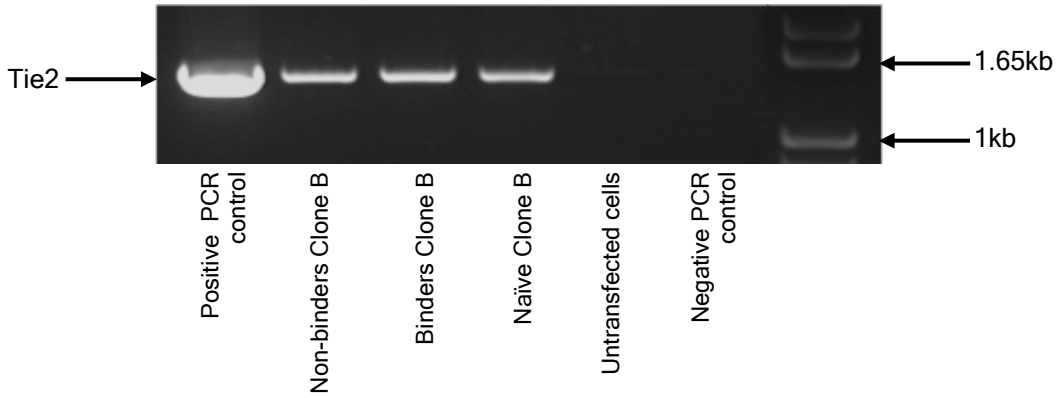

Figure 5.18: RT-PCR of Tie2ECD in Ang2 binding and non-binding sorted populations. Total RNA was extracted from untransfected DT40 cells and from naïve and sorted 9-month Tie2-DT40 cells, 2µg of which was subjected to RT-PCR as described in section 2.6 (*n*=1). pTie2ECD-TOPO plasmid was used as a positive PCR control. The 1342bp product was resolved by electrophoresis on 1% agarose gel and visualised by UV illumination as described in section 2.2.5. The position of molecular weight markers are indicated.

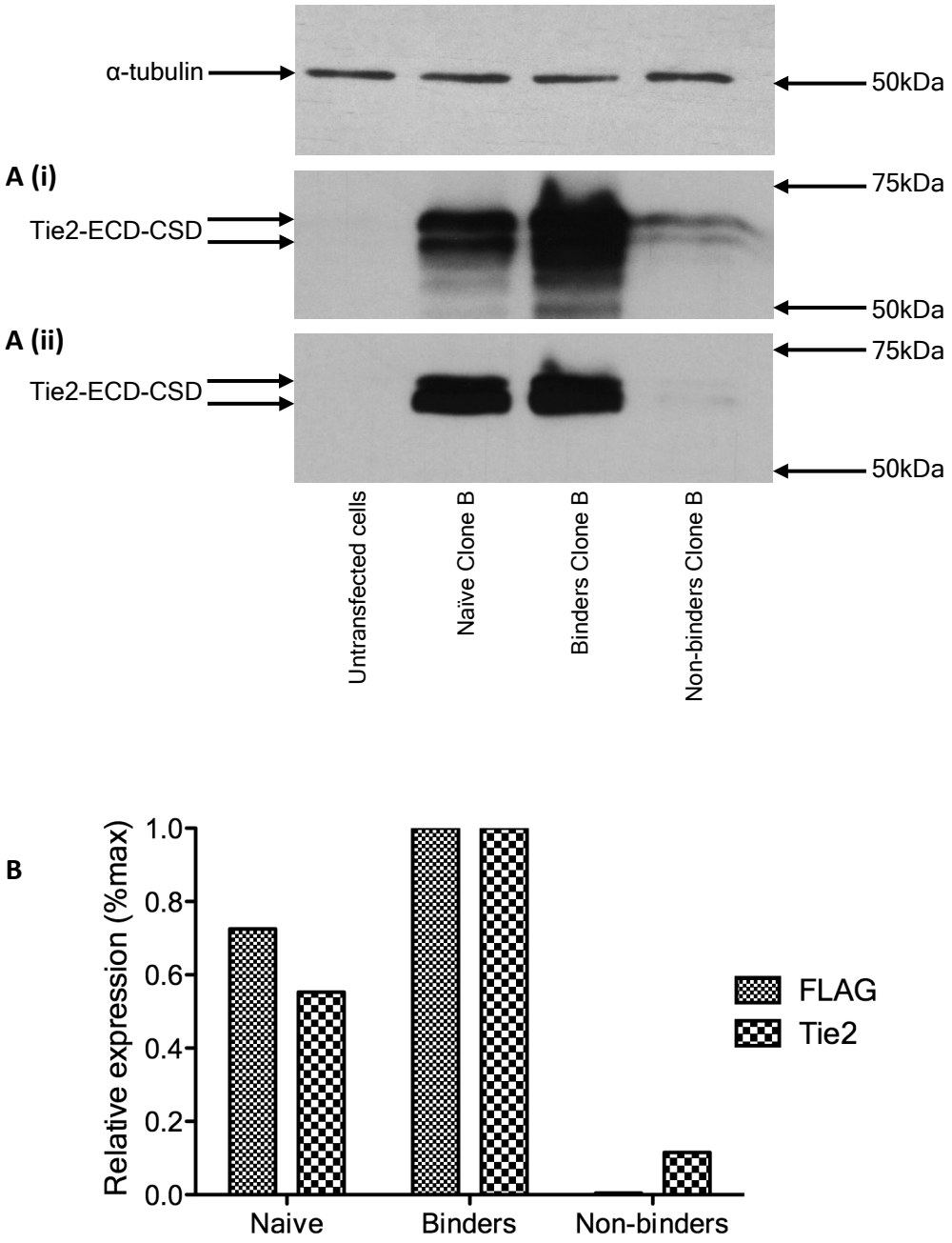

Figure 5.19: Expression of Tie2ECD in Ang2 binding and non-binding sorted populations.

a) Tie2 expression probe. Whole cell lysate was prepared from untransfected DT40 cells and from naïve and sorted 9-month Tie2-DT40 cells, and subjected to SDS-PAGE and Western blotting as described in section 2.5 (*n*=1). Immunoblot analysis was performed with anti-Tie2 (i) and anti-FLAG (ii) antibodies, in addition to anti-α-tubulin as a loading control. The position of molecular weight markers are indicated.

b) Optical Density comparison. Relative Optical Density (OD) was determined by ImageJ analysis of non-saturated films and calculated as a ratio of Tie2 to α-tubulin optical density for each antibody.

would result in frameshift from the residue 176, resulting in a segment that is possibly too short to bind to the antibody successfully.

5.5.4 Sequencing of Ang2 non-binding population

The Ang2-non-binding Tie2 PCR product was prepared for sequencing as described previously (sections 4.3.2 & 2.6). Of 32 sequences obtained, 30 contained a deletion. The remaining two sequences contained point mutations, including a double mutant involving a stop codon at position 189, and a single mutant, A146V. The amino acids alanine and valine are not significantly different in size, structure or side chain and therefore the substitution is theoretically conservative. Whilst the mutation could abolish binding, its inclusion may also represent a sorting error. Alternatively the cell in question could harbour a deleterious mutation in the downstream cell-surface expression domain, which was not sequenced, preventing expression of Tie2 on the cell surface.

The total number of point mutations in the 42432bp explored was 25, yielding a frequency of 5.89×10^{-4} mutations per bp or 0.78 per Tie2 sequence, which is very similar to the frequency attained in naïve clone B cells (section 4.3.4). There is however less variety in the distribution and type of mutation observed in comparison with naïve clone B cells (Table 5.1). All mutations occurred at G:C base pairs although only 16% were transitions, and 96% occurred in hotspots, 96% of which were at R<u>G</u>YW/WR<u>C</u>Y motifs as opposed to D<u>G</u>YW/WR<u>C</u>H (Figure 5.20).

			TO:				
			A	G	C	T	
FROM:	A	0		0	0	0	Non-binders
		0		0	0	0	Naive
		0.0158		**0.0190**	0	0.0017	ψV$^-$ AID^R *
	G	0.12	0.1200		0	0	Non-binders
		0.2609	0.2174		0.0435	0	Naive
		0.4317	0.1220		0.2407	0.0455	ψV$^-$ AID^R *
	C	0.88	0	0.8400		0.0400	Non-binders
		0.6522	0	0.5217		0.1304	Naive
		0.5355	0.0729	0.2863		0.1970	ψV$^-$ AID^R *
	T	0	0	0	0		Non-binders
		0.0870	0	0	0.0870		Naïve
		0.0174	0.0108	0.0006	0.0037		ψV$^-$ AID^R *

Table 5.1: Observed mutation frequency in angiopoietin-2 non-binding Tie2-DT40 cells. Tie2-DT40 cells were cultured for nine months to form a mutagenic library. Cells with no apparent Ang2 binding capability were selected by FACS. Random copies of the Tie2ECD gene were sequenced via RT-PCR and TA cloning as described in section 2.6. The frequency of each mutation permutation is stated ('Non-binders'). The frequency of mutations in the starting population ('Naïve': see Table 4.3) and literature frequencies ('ψV$^-$ AID^R *': see Table 4.1) are also tabulated as a reference. Transition mutations are shaded.

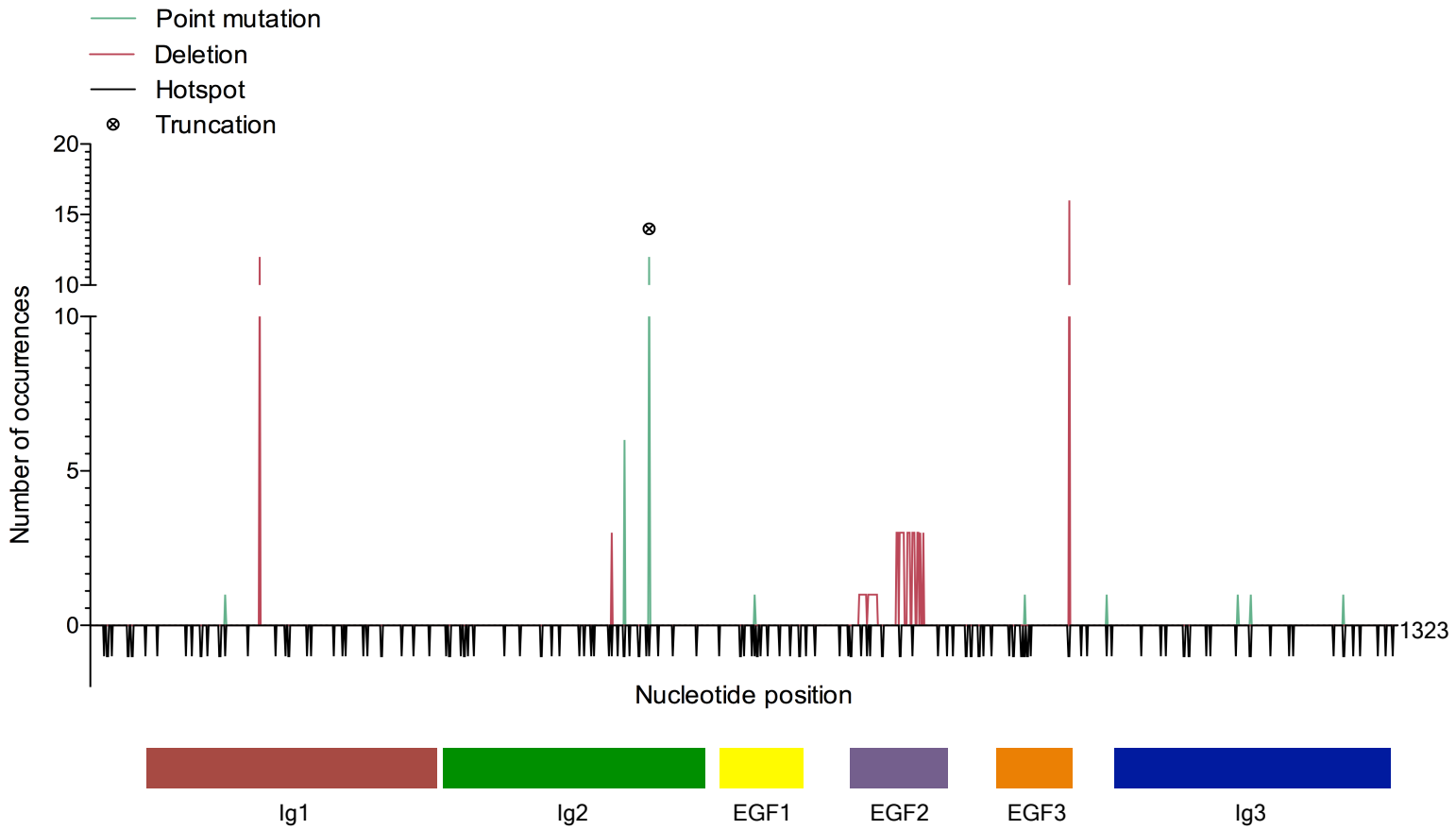

Figure 5.20: Observed nucleotide diversity in non-binding Tie2ECD. Graphical representation of nucleic acid sequence. DGYW/WRCH hotspots are marked on the negative axis, where the underlined base marks the mutable position. The number of point mutations and deletions is quantified on the positive axis. Truncation signifies mutation to premature stop codon. Relation of Tie2 domains to the sequence is shown.

5.5.5 Sequencing of Ang2 binding population

The Ang2-binding population was also sequenced as above. Of 32 sequences examined, there were no deletions and only three point mutations. The mutations C674G, G771T and G1299A result in only one translational change, T225S. Both threonine and serine have polar uncharged side chains and are similar in size, and hence the substitution, in the EGF1 domain, can be considered as conservative. One of the three mutations, G1299A, is outside of hotspot motifs.

5.6 Selection of lower affinity Ang2 binding cells

96.67% of Ang2 non-binding cells sequenced in section 5.5 displayed deletions, and in one case a mutation, that would prevent cell-surface display of the severely altered Tie2 protein completely. Establishing a library of Tie2 point mutations that reduce or prevent angiopoietin binding is a useful mechanism for studying Ang-Tie2 interactions.

The selection of Ang2 non-binding cells in section 5.5.2 did not take account of FLAG expression. Further sorting and sequencing of cells expressing Tie2 but with reduced or absent binding to Ang2 and/or Ang1 would create a useful analytical library.

5.6.1 Sorting for lower affinity Ang2 binding

The Ang2 non-binding population developed in 5.5.2 was put through three rounds of iterative sorting. In brief, 10^7 cells were bound to RT 40nM biotinylated Ang2 prior to staining with anti-FLAG-FITC and streptavidin-R-PE at 4°C. In the first round all cells expressing FLAG were selected, amounting to 0.6% of the population. In the second round 0.8% of the population was selected, constituting all FLAG-expressing cells displaying background levels of phycoerythrin fluorescence. The third round entailed selection of the lowest selectable population on the 582/15nm filter axis, totalling 10.4% of the population (Figure 5.21).

Immediately after the first sort it was noted that approximately 10% of sorted cells were in fact lysed. In subsequent rounds propidium iodide was added to the final cell suspension. Angiopoietin binding and lysed cells were excluded together as propidium iodide and phycoerythrin have emission spectra detectable by the 582/15nm filter (Figure 5.22).

Despite exclusion of Ang2-binding cells, sorted populations showed reversion to an Ang2-binding phenotype (Figure 5.21). A distinct cluster of cells with significant levels of Ang2 binding is discernable in the first sorted population, where 95.2% of cells did not bind anti-FLAG or Ang2. It is possible that some apparently non-binding cells were not fully exposed to Ang2 or streptavidin-R-PE during the staining process in sort 1. Equally, some of the FLAG binding could be attributable to a background effect, estimated at 16.67% of cells selected based on control anti-

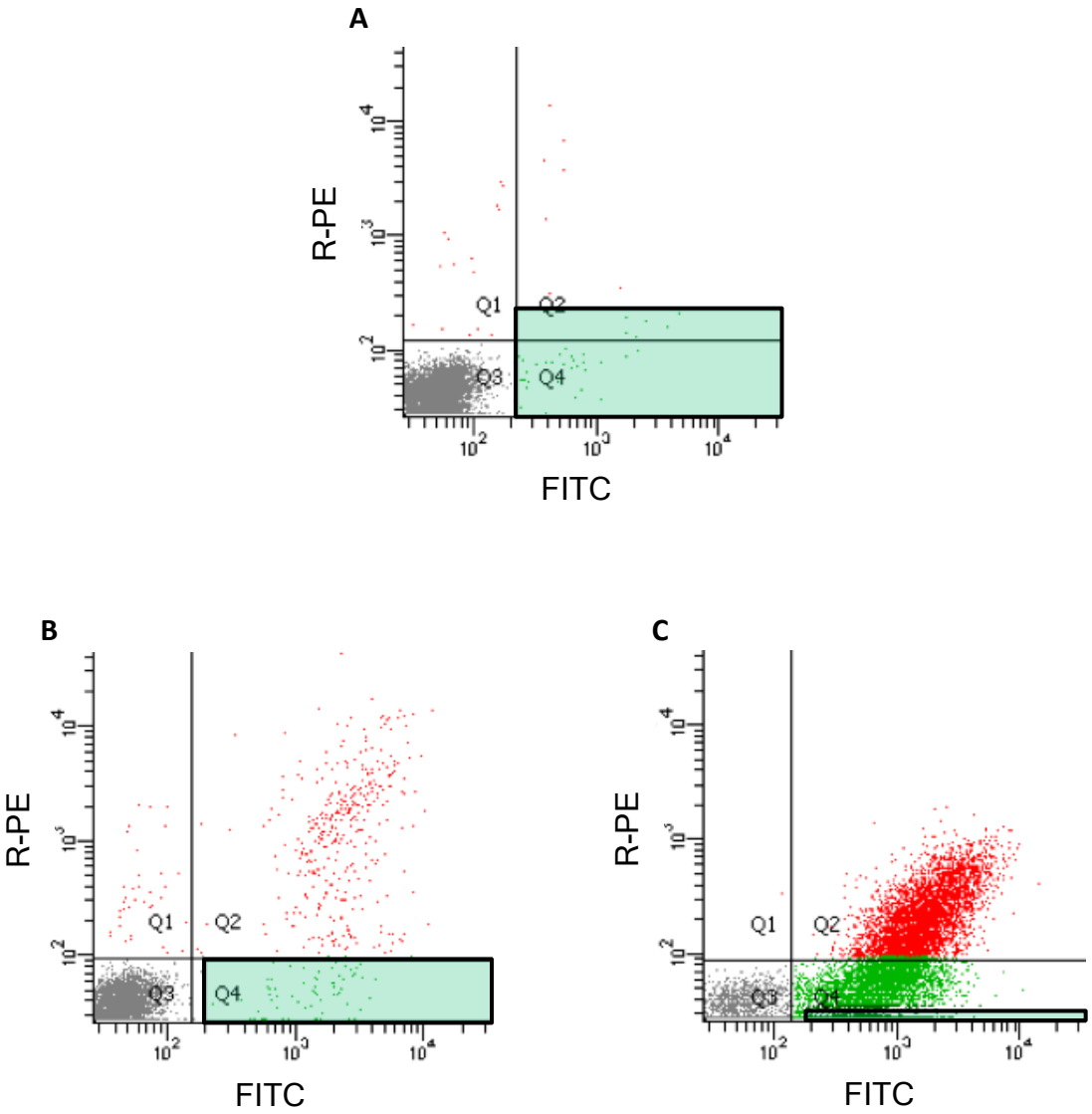

Figure 5.21: Sorting for lower affinity Ang2 binders. 10 × 10^6 non-binding DT40 cells were bound to saturation with 40nM biotinylated Ang2 prior to labelling with streptavidin-R-PE and anti-FLAG-FITC. Ang2 non-bound cells were sorted via 2-way purity as per shaded windows in dot plots.

a) First sort.

b) Second sort.

c) Third sort.

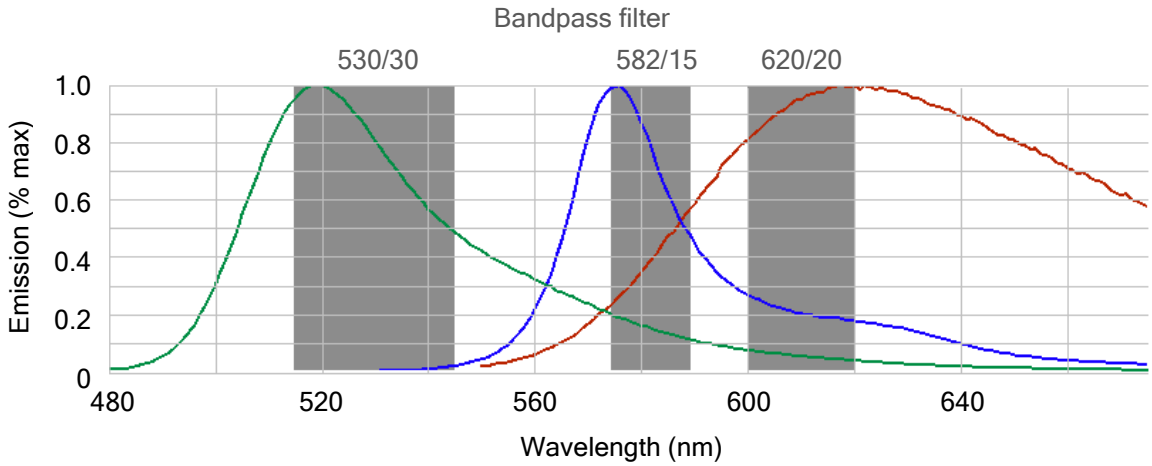

Figure 5.22: Emission spectra of fluorescent reagents. FITC emission is coloured green; PE emission is coloured blue; PI emission is coloured red. Detection by bandpass filters is shaded grey. From Invitrogen Fluorescence Spectra Viewer.

FLAG-FITC background staining. Given that the initial sort selected only 0.6% of the population the number of cells involved could be significant.

Subsequent sorts involving selection of cells with no apparent Ang2 binding capability resulted in attainment of dense populations with lower than average Ang2 binding and a progressively decreased proportion of completely unstained cells. No apparent improvement was seen between the second and third sorted populations. Decreased Ang2 binding was confirmed by flow cytometry assay in which Ang2 binders (section 5.5.2) and third sorted Ang2 non-binders were bound to 0.5nM biotinylated Ang2 prior to anti-FLAG-FITC and streptavidin-R-PE staining (Figure 5.23).

5.6.2 Sequencing of lower affinity Ang2 binders

Genomic DNA was extracted from the sorted low affinity Ang2 binding population and PCR of the 1323bp Tie2 gene and adjoining cell surface display (CSD) domain was performed under the conditions specified in Appendix 2.1/section 2.6. The PCR product was prepared for sequencing as described previously (sections 4.3.2 & 2.6).

Ten of eleven sequences obtained contained a point mutation C496T, which is located within an RGYW/WRCY motif in the Ig2 domain and produces a significant mutation within a known Ang2 binding residue, P166S (Figure 5.24). In addition one of the sequences concurrently contained a mutation in the PDGFR transmembrane domain, which translates to P529S. Although this is also a

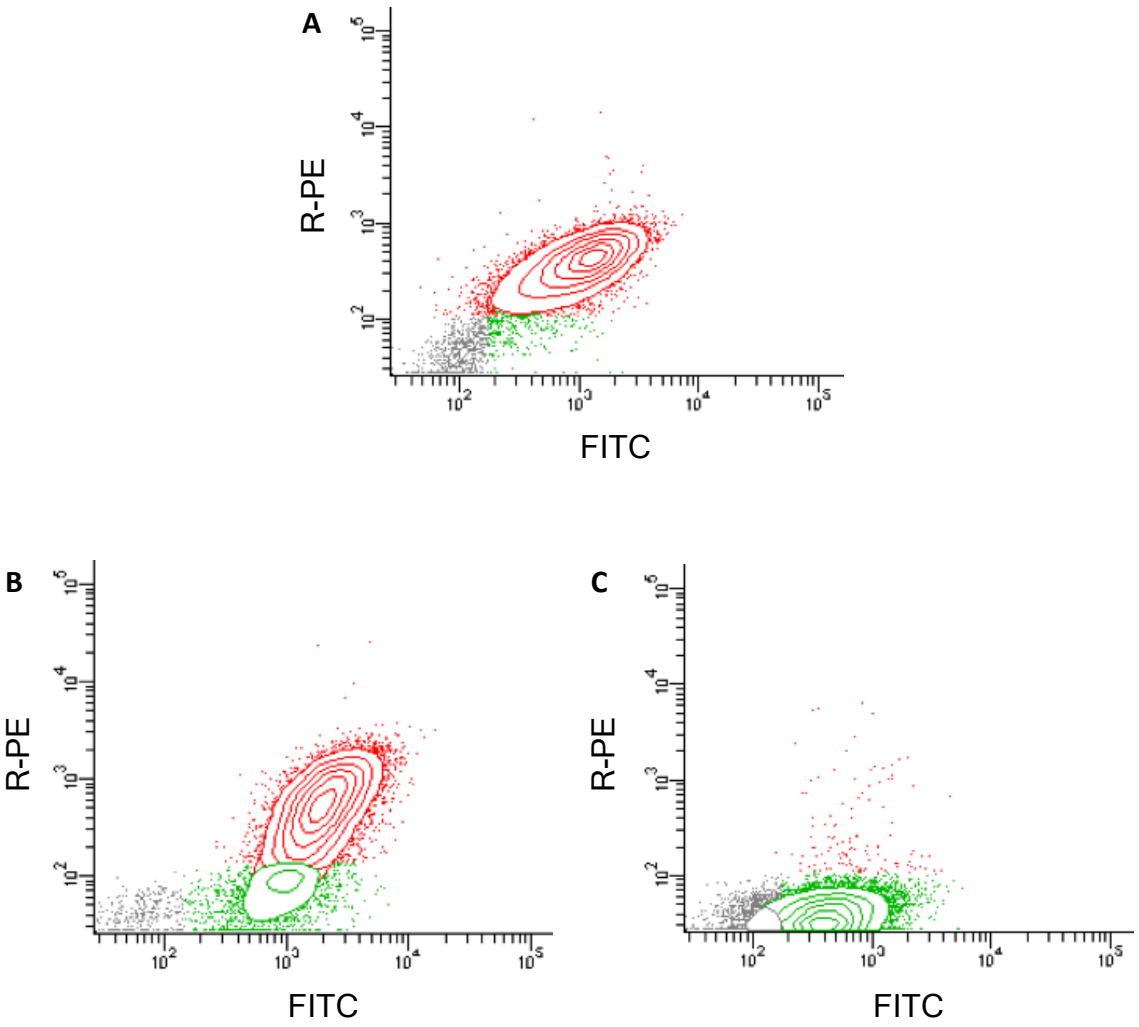

Figure 5.23: Attainment of lower affinity Ang2 binders. The original Ang2-binding population and sorted lower affinity Ang2-binding population was bound to equilibrium with biotinylated Ang2 prior to labelling with anti-FLAG-FITC and steptavidin-R-PE at 4°C (*n*=1). Contour plots of 10,000 cells are shown.

a) Original Ang2 binding population. 0.5nM Ang2.

b) Sorted lower affinity Ang2 binders. 25nM Ang2.

c) Sorted lower affinity Ang2 binders. 0.5nM Ang2.

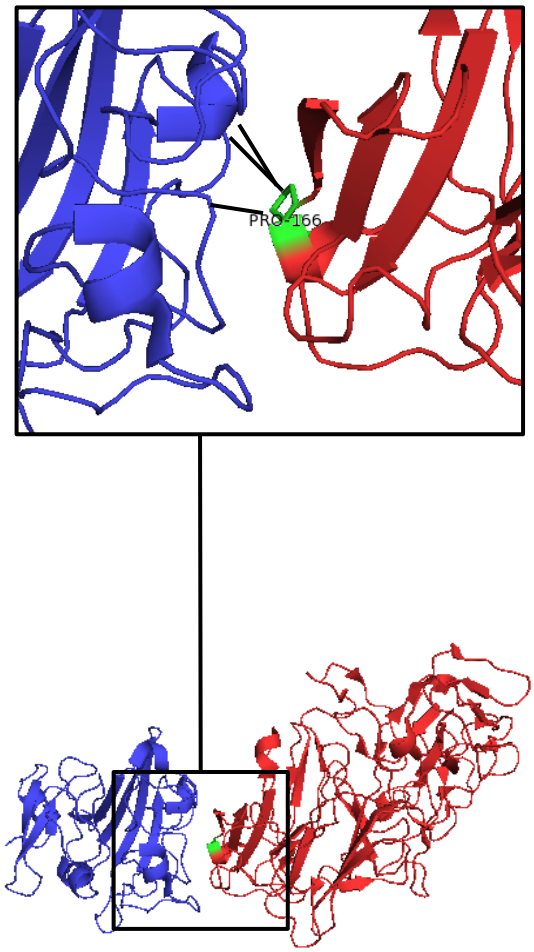

Figure 5.24: Proline-166 is involved in Ang2 binding. The P166S substitution is positioned at the Ang-Tie ligand-receptor interface. P166 contacts multiple Ang2 residues including P452, Y475 and Y476 (shown as solid lines). Ang2 is coloured blue and Tie2 is coloured red. P166 is shown in green. Modelled on PDB accession 2GY7 (Barton et al. 2006).

significant mutation it did not apparently abolish Tie2ECD expression. One of the eleven sequences appeared to be wild-type.

5.7 Selection of higher affinity Ang2 binding cells

The original objective of producing a mutant form of Tie2ECD that preferentially binds Ang2 and not Ang1 could be achieved via different routes. The option of kinetic screening was excluded due to assay inaccuracy. The complexity involved with dual ligand binding assays also requires further characterisation. The remaining options of equilibrium screening include sequential selection of differing angiopoietin binding affinities, starting with either reduced Ang1 affinity or improved Ang2 affinity. Given that Ang1 and Ang2 are thought to bind Tie2 in a similar manner, it seems likely that the majority of mutations deleterious to Ang1 binding would be equally deleterious to Ang2 binding, creating a very small mutant pool in which to select preserved Ang2 binding. Therefore selection for improved Ang2 binding is a reasonable initial target.

5.7.1 Sorting for higher affinity Ang2 binding

An Ang2 concentration of 0.5nM was determined to be suitable for the early rounds of equilibrium sorting (section 5.3.1). Setting of sort windows for highest binders took account of Ang2 binding relative to Tie2 expression levels (Figure 5.25). Propidium iodide was not used to confirm cell viability as its emission spectrum crosses with that of phycoerythrin and therefore desired cells.

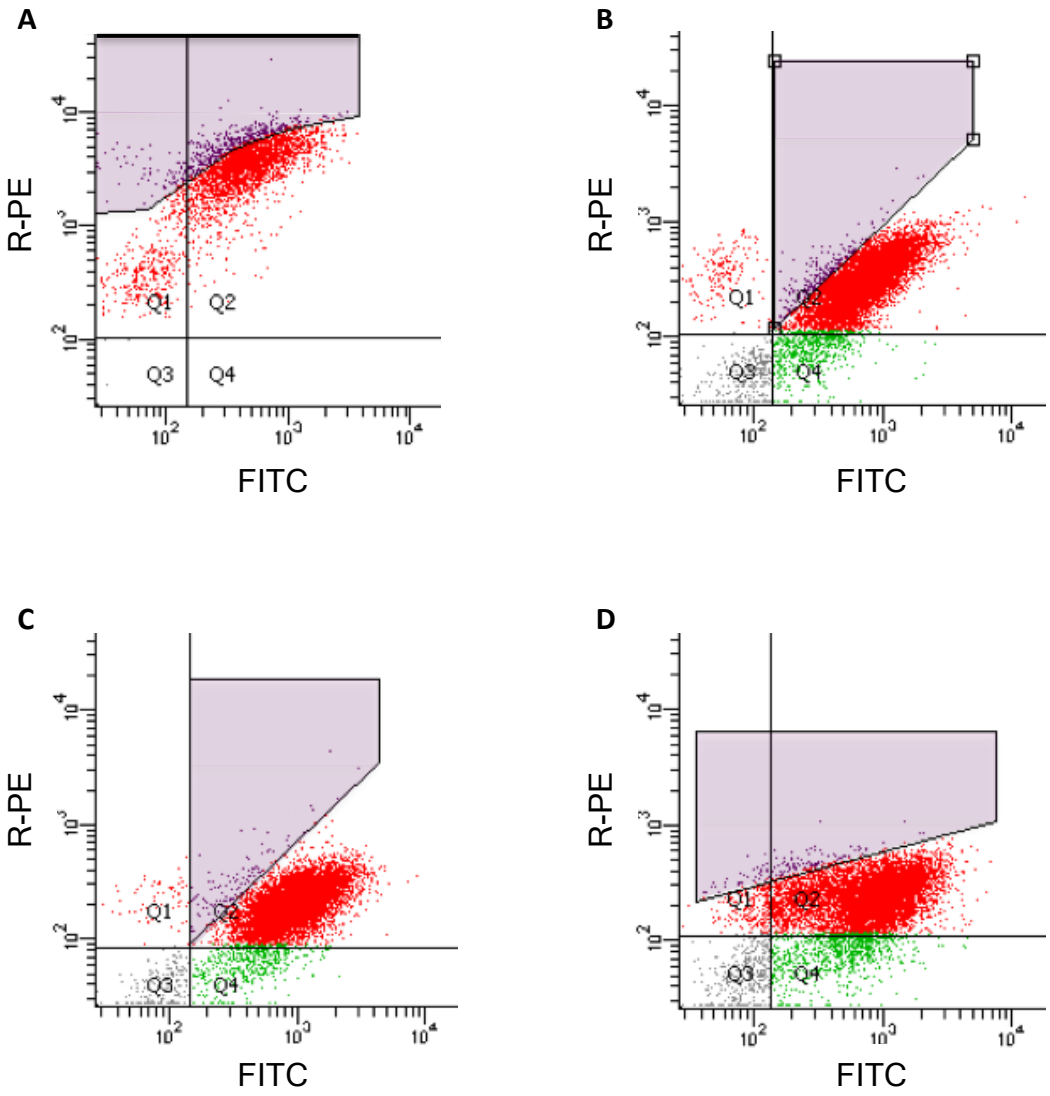

Figure 5.25: Sorting for higher affinity Ang2 binders. 10×10^6 cells were bound to equilibrium with 0.5nM biotinylated Ang2 piror to labelling with anti-FLAG-FITC and streptavidin-R-PE. The strongest binding, lowest expressing cells were sorted via 2-way purity as per shaded windows in dot plots.

a) First sort.
b) Second sort.
c) Third sort.
d) Fourth sort.

The Ang2-binding population developed in 5.4.2 was bound to RT 0.5nM biotinylated Ang2 prior to anti-FLAG-FITC and streptavidin-R-PE staining at 4°C. For enrichment, the initial round selected the top 11.7% of Ang2 binders. In the second and third rounds a purity strategy was employed, selecting 2% and 1% of the population respectively. In the fourth round the Ang2 concentration was reduced to 0.25nM and the top 1.3% was selected.

Gradual emergence of a distinct population with lower Tie2 expression and high Ang2 binding was achieved (Figure 5.26).

5.7.2 Sequencing of higher affinity Ang2 binders

Genomic DNA extraction, PCR and sequencing of the 1542bp Tie2ECD-CSD gene in the sorted high affinity Ang2 binding population was performed as described previously.

Of six sequences obtained, five contained a single mutation in the FLAG peptide. The point mutation occurred at an RGYW/WRCY hotspot and converted the terminal residue from lysine to asparagine. It is likely that the majority of cells in the higher Ang2 binder sort window represent abnormal FLAG detection rather than any improvement in Ang2 binding relative to Tie2 expression. The sixth sequence contained a point mutation within the EGF2 domain, G791A, which is located at a DGYW/WRCH motif. The resulting mutation, C264Y, is potentially significant in a conformational context as it is located close to residues that are involved in interdomain interactions.

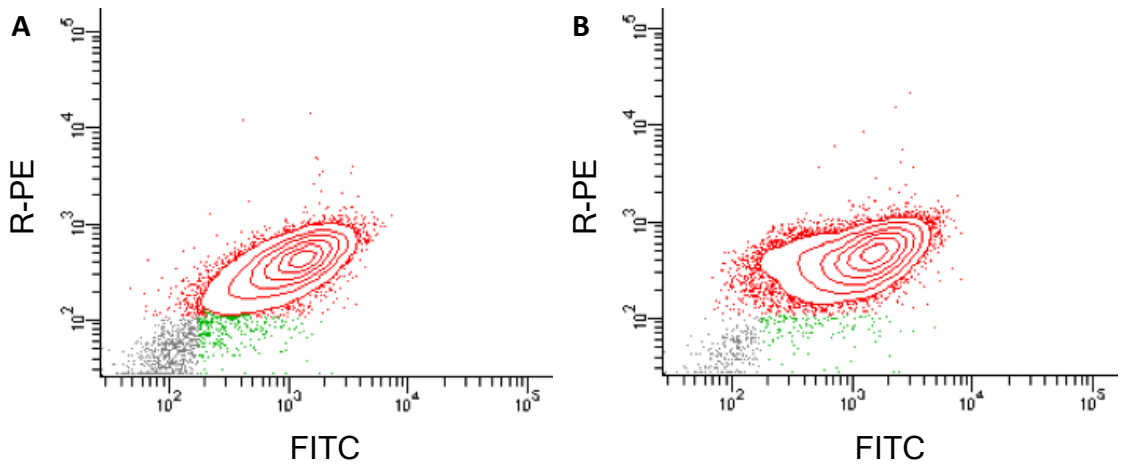

Figure 5.26: Attainment of higher affinity Ang2 binders. The original Ang2-binding population and sorted higher affinity Ang2-binding population was bound to equilibrium with 0.5nM biotinylated Ang2 prior to labelling with anti-FLAG-FITC and steptavidin-R-PE at 4°C (*n*=1). Contour plots of 10,000 cells are shown.
a) Original Ang2 binding population.
b) Sorted higher affinity Ang2 binders.

Iterative sorting was not continued due to the high proportion of FLAG mutants and anticipated low frequency of new mutations.

Discussion

The above data illustrate utilisation of cell surface display in screening a mutant protein library to permit selection of discrete mutant phenotypes.

The original motivation for developing this method was in generation of variants of Tie2 ectodomain with higher affinity for angiopoietins generally, and to create a variant with improved Ang2 affinity but lesser Ang1 binding capability. Although Ang1 and Ang2 appear to bind Tie2 in a similar manner, the complexities of this interaction and differences in consequent signalling are not understood. Therefore directed evolution should carry more success than rationally designed mutations in manipulation of this interface.

Whilst the evolution of proteins for novel functions is considered the most difficult task in protein engineering, improvement on a naturally high affinity interaction nonetheless requires serious precision. The use of flow cytometry to quantify the wild-type interaction between angiopoietins and cell surface displayed Tie2 ectodomain yielded dissociation constants in the region of 1nM, a relatively high affinity scenario (section 3.4). It is therefore crucial that the screening and selection methods employed are robust.

Cell surface display and FACS have successfully generated antibodies with improved femtomolar binding affinities (Boder, Midelfort & Wittrup 2000). Published data suggests that a kinetic assay would be most successful in obtaining Tie2 mutants with higher angiopoietin binding affinity (Boder, Wittrup 1998). Therefore the initial approach was to design a discriminative assay based on the dissociation rate of the angiopoietin-Tie2 interaction. It was not possible to obtain any plausible estimation of the Ang1 dissociation rate, and the Ang2 dissociation rate could not be accurately measured within the constraints of available reagents.

Attempts to biotinylate Ang1 to improve Ang1 binding assays were complicated by poor yield and possible impurities. Adjustments to the accepted protocol for dissociation rate determination did not produce consistent or reliable data in the case of Ang2. The variable oligomerisation states of recombinant angiopoietins combined with multivalency of streptavidin in the case of Ang2 and suboptimal affinity of the His-tag-antibody interaction with Ang1 created particular difficulties in the logistics of kinetic screening. Engineering of fluorescent-tagged angiopoietin monomers would revolutionise screening in this regard.

The alternative approach of equilibrium screening was described for assay of interactions with dissociation constants as low as 1nM (Kieke et al. 1997). The optimal Ang2 concentration for use in this method was initially estimated based on mathematical models and verified by flow cytometry. A concentration of 0.5nM Ang2 required an achievable incubation volume of 2ml per million cells. Experimental determination of the number of Tie2 molecules expressed on each

DT40 cell surface may allow this volume to be reduced. Avidity effects of reagents have diminished significance in this context.

In order to screen for differential Ang1 and Ang2 binding characteristics a competitive dual screen would be ideal. Accurate estimates of the competitive inhibitory concentration of Ang2 versus Ang1 were achieved. Experiments to compare the time course of the interaction between the two ligands were considered invalid for the same reasons that kinetic screening of individual angiopoietin-Tie2 interactions failed. The literature suggests that a kinetic component is necessary to exert sufficient selection pressure in this type of situation and further study would be required to produce a viable screening process (Sklar et al. 1985, Waller et al. 2001).

Equilibrium screening based on Ang2 binding affinity was the selected strategy. Given the sequence conservation between Ang1 and Ang2, a high proportion of mutations are likely to affect the binding of both ligands similarly. The approach employed was therefore to select for improved Ang2 binding, with subsequent assessment for Ang1 binding. In addition the mutant library was also screened for lower affinity Ang2 binding with the aim of creating a starting point to investigate residues in and around the binding interface.

In preparation for FACS-based selection, reagents were rationalised to refine the number of staining steps required and potentially improve viability and signal. Phycoerythrin was selected as the binding reporter due to wide reports of high intensity signal in flow cytometry applications, although it is sensitive to

photobleaching on microscopy (Kronick, Grossman 1983, Glazer 1988, Zola et al. 1990). Dead cells were characterised and eliminated by a combination of light scatter characteristics and propidium iodide staining where possible. Concurrent FLAG detection was utilised to quantify Tie2 expression, though not included during the angiopoietin binding phase to minimise interference.

Whilst selection of cells expressing wild-type Tie2 or harbouring neutral mutations may initially limit enrichment, it increases the likelihood of epistatic coupling between mutations. The 9-month cell culture was chosen as a starting point for sorting based on this neutral drift hypothesis. Although a high proportion of cells did not bind Ang2 or express Tie2, the remaining binding population was potentially more diverse than that of the 3-month culture. When this population was sorted into Ang2 binding and non-binding subpopulations, the non-binding cells emerged as being poor Tie2 expressors with a high percentage of frameshift deletions. The binding cells conversely carried a disappointing number of genetic modifications. When Bershtein *et al.* tested the neutral drift hypothesis, regular low pressure selections were performed to purge deleterious mutations, which although limits the possible diversity and epistasis, would in hindsight have been beneficial in this scenario (Bershtein, Goldin & Tawfik 2008).

There is a practical limit to the number of cells that can be screened and therefore the maximum diversity cannot be tested. Improvement of cell viability during the staining process would partially address this issue, though in practice may be difficult to achieve given the trauma involved in centrifugation yet the need to wash cells free of any unbound label. Magnetic sorting has been advocated as an

option for conducting panning rounds on larger cell populations and could be investigated further (Wentzel et al. 1999).

In the case of high affinity selection, the sorted percentage of the population was reduced from an enrichment format of 10% to a purity strategy at 1%. In addition the concentration of Ang2 was also reduced during the process. A distinct population of high binding, low expressing cells was cultivated. Sequencing of a small sample revealed a single deleterious mutation in FLAG peptide rather than Ang2 mutation. It is likely that the mutation rate was not high enough to support iterative sorting for improved Ang2 binding and hence the selection was prematurely concluded.

Evolution of the non-binding population was also performed, selecting cells that apparently expressed Tie2 but did not bind Ang2. The expectation would be for this population to contain deleterious mutations rather than deletions. Since the initial percentage of such cells was low, enrichment was not possible in a conventional sense. This approach is likely to have contributed to the finding that most of the cells reverted to an Ang2-binding phenotype, and were perhaps Ang2 binders from the outset but were not identified due to experimental error. Ultimately however, when compared with the unsorted Ang2-binding subpopulation, the sorted cells did exhibit lower binding affinity and 91% of sequences contained a single mutation, P166S. This residue in the Ig2 domain is known to interact with Ang2 (Barton, Tzvetkova & Nikolov 2005), but its mutation does not appear to completely abolish binding.

The possibilities for screening and selection of cell surface displayed libraries are wide-ranging and only a fraction has been tested here. In crude terms, equilibrium screening was successful as a means of identifying new phenotypes of Tie2ECD. The remaining challenge is to hone and perfect this process to permit its exploitation.

CHAPTER SIX

General Discussion

The potential of anti-angiogenic therapies, not only in providing an additional treatment modality in cancers, but also in modulating an array of other conditions whose pathology involves endothelial activation such as sepsis, chronic inflammatory disorders and retinopathy remains largely undiscovered. The guarded success of anti-VEGF therapies has highlighted a range of issues, not least in terms of acquired resistance, which were unexpected despite the prominence of VEGF as the best characterised of all angiogenic growth factors. Whilst there is a need for more effective pre-clinical simulation models in which to test such therapies, there is also a requirement for a multi-targeted approach and improved comprehension of the interplay between individual angiogenic players.

The angiopoietin-Tie2 system has long been identified as a suitable target to adjunct VEGF antagonism (Oliner et al. 2004). Initial data concerning blockade of Ang2 plus or minus Ang1 in animal tumour models confirms a synergistic action when combined with VEGF antagonism (Falcon et al. 2009, Koh et al. 2010, Hashizume et al. 2010). The question of selective Ang2 blockade versus pan-angiopoietin blockade is unlikely to be answered for some time due to the paucity of animal models available for studying the array of pathologies and long-term effects. However Ang2 is certainly the key effector molecule and maintenance of Ang1 pro-quiescent activity is likely to reduce systemic adverse effects.

Since the discovery of protein structure-function data, appreciation of the sophistication of natural proteins and advancement in molecular biological techniques, proteins have been a focus for development of new therapeutics. The two major methods of rational design and directed evolution have progressed

considerably during this time, but each approach retains significant obstacles. Directed evolution, as an imperfect imitator of natural evolution, represents the best option for evolving binding proteins when detailed protein interaction data is not available and expectations are complex. It is limited however by the protracted techniques involved in iteratively mutating, screening and selecting the protein, and the constraints of utilising non-mammalian and inequitable protein expression systems.

Somatic hypermutation is a mechanism of natural evolution that has recently been utilised to engineer intrinsically fluorescent proteins for unique emission spectra by means of a single transfection into a mammalian cell line. The possibility of combining this system with existing cell surface display and Fluorescence Activated Cell Sorting (FACS) techniques presents an innovative method of rationalising directed evolution.

To address the stated hypotheses, the data formerly presented has demonstrated the generation of a mutant Tie2 library by means of somatic hypermutation in the DT40 cell line, the possibilities of screening cell-surface displayed-Tie2 for angiopoietin binding affinities and that mutant Tie2 phenotypes can be selected by FACS. Each of the hypotheses is discussed in detail below.

6.1 Somatic hypermutation as a mechanism of mammalian mutagenic library generation

Traditional methods of directed evolution usually employ error-prone PCR or DNA shuffling as a means of mutant library generation (Mullis, Faloona 1987, Stemmer 1994). DNA must be transferred into a vehicle for expression of the resulting protein in order to screen and select the desired mutants, and the whole process requires several rounds of repetition to achieve the evolutionary goal. The resulting diversity is more far reaching than it is possible to test with current high throughput screening methods.

In this study the chicken bursal lymphoma DT40 cell line was utilised as the vehicle for SHM. The outstanding advantage of this mechanism lies not only in the fact that mutant proteins are directly expressed in a higher eukaryotic context, but also with the possibility of cell surface display to allow completion of the iterative mutation, screening and selection process in one cohort of cells.

The principal benefit of the DT40 cell line over other hypermutating cell lines is that single exogenous genes can be targeted with high frequency to integrate into the Ig locus, where the highest level of mutation occurs (Blagodatski et al. 2009). The pHypermut2 homologous recombination vector was indeed successful in correctly integrating Tie2 into the rearranged Ig locus in all of the three clonal populations tested post-transfection. Although this finding does not exclude the possibility of integration of multiple copies of Tie2 per cell, the probability of concurrent randomly integrated Tie2 genes is predictably low given the difficulties

encountered with non-targeted stable transfections in general. Singular Tie2 integration is required to ensure expression of one mutant protein per cell.

Theoretical SHM-generated library diversity in currently available hypermutating cell lines is inferior to that of B-lymphocyte antibody diversification when hotspot predilection is considered, or indeed to traditional methods of library generation in directed evolution such as error-prone PCR. However considering the limitation in number of mutants that can be screened and selected, SHM is not an unreasonable choice. Future developments in high-throughput screening may increase the scope for testing larger libraries, and likewise advancement in our knowledge of the action of AID and its control mechanisms is likely to generate possibilities for its manipulation in order to expand SHM-generated libraries.

Previous reports of the mutation pattern for transgenes in DT40 cells are relatively few in number, particularly in terms of serious detail (Arakawa, Saribasak & Buerstedde 2004). The pattern of mutation observed in Tie2-DT40 cells did not entirely agree with published material. In particular the percentage of mutations occurring at hotspots was significantly higher than expected, and the number of transitions was similar to that seen in human B-lymphocytes rather than hypermutating cell lines. The most surprising observation was the high frequency of deletions, which has not been reported previously. There were however no episodes of gene conversion activity, as expected for the ψV knockout cell line, and the majority of mutations did occur at C:G base pairs. Patterns were also observed that link the type of mutation to the surrounding sequence, although the number of mutations assessed was not sufficiently high in number to make a definitive

conclusion. It is possible that deletions confer a growth advantage to cells and therefore there is a propensity of such cells to overgrow and become over-represented in the population. Equally the unexpected patterns of genetic modification in Tie2ECD may be due to suboptimal AID expression, although the observed changes cannot be definitively classified as atypical given the paucity of literature.

It is clear that SHM possesses species-specific properties, with different patterns of mutation being observed in human B-lymphocytes versus chicken lymphoma. Delineation of the reasons behind this would improve our ability to manipulate SHM in the experimental context. A recent study has utilised a C-terminal truncated form of AID, known to exhibit greater nuclear localisation, in order to increase the mutation rate in DT40 cells despite a lower total expression level (Magari et al. 2010). The active site of AID can also be engineered to produce alternative mutation spectra (Wang, Rada & Neuberger 2010), potentially creating greater diversity when used in combination with wild-type AID.

The rate of mutation observed in the ψV^{-} AID^{R} Cl4 DT40 cell line was significantly inferior to that of published reports for ψV^{-} AID^{R} DT40, whether assessed as a function of generation or chronological time. There is no published data to assess how the clone 'Cl4', utilised here, compares with other similar clones or indeed ψV knockouts retaining endogenous AID. Despite this a starting population with a mutation frequency of 0.8 per sequence was produced, before the loss of diversity secondary to deletions was accounted for.

The major disappointments with such a mutation rate are that generation of a mutant library is a time-consuming process and the probability of generating new mutations between rounds of screening and selection is relatively low, challenging the concept of perpetual improvements. The contributing factors are analysed below.

The RSV promoter was successful in producing high and reliable Tie2 expression in DT40 cells. Tie2 was successfully integrated into the Ig locus where mutation rates are reported to be highest. The mutability of the Tie2 ectodomain gene itself appeared promising, given the improved number of hotspots over the Ig gene and multiple E-box motifs. Only ten percent of residues were considered to be relatively non-mutable.

Passaging conditions contributed to a long cell doubling time, though this was thought to be preferable to rapid divisions and consequent greater proportion of time spent in the S-phase of the cell cycle (Wang, Wabl 2005). Further investigation of the links between passaging conditions, cell cycle and mutation rate in DT40 cells are required to verify the significance of generation time.

It was observed early in the investigation that AID could be unintentionally lost from ψV^{-} AID^{R} Cl4 DT40 cells, which was attributed to incompetence of the Cre recombinase-loxP system. Background activity of MerCreMer is a known complication in the use of such systems (Zhang et al. 1996) but excision of floxed cassettes from a whole population nevertheless seems extreme. The additional finding of variation in AID expression level between different clonal populations of

Tie2-DT40 supports the notion that Cre recombinase activity or other regulators of AID are involved, given that the cell line was developed from a single clone following AID transfection and therefore the AID integration site is not variable. Unstable AID activity has also been reported in the Ramos cell line, particularly after prolonged culture (Zhang et al. 2001). The temporal effect of AID expression requires characterisation.

The system of Cre recombinase regulated AID expression was initially considered an advantage of this cell-based evolutionary model. Considering the ability to PCR Tie2ECD from a small number of FACS-recovered cells, the ability to terminate AID activity is not essential and certainly of lower precedence than the rate of SHM. The possibility of utilising TSA to augment AID activity was not successful in this study. As such, a strategy to transfect AID into Tie2-DT40 cells for constitutive expression was undertaken. The difficulties in achieving non-targeted transfection prevented assessment of the effect of AID overexpression over a suitable time course, but this together with transfection efficiency should be examined further.

The ability to perform targeted integration of transgenes at the Ig locus confers a great advantage to DT40 cells as opposed to any other hypermutating cell line. An ideal SHM-driven system may consist of ψV^- knockout DT40 cells with more reliably inducible expression of multiple forms of AID, such as via the auxin-inducible degron system and to include C-terminal truncated native AID and engineered forms that offer different mutation spectra. However ψV deletion may not be necessary for transgenes that have no homology to the IgV region and the effects of expressing multiple variants of AID in a single cell line have not yet been

tested. It is equally possible that wild-type DT40 may offer a more efficient system for transgene SHM than the ψV^{-} AID^{R} Cl4 DT40 cell line utilised here.

6.2 Discrimination of angiopoietin-Tie2 binding via cell surface display

Flow cytometry of cell surface displayed proteins and immunoglobulins is an accurate and reliable method by which binding affinities can be determined (Lofblom et al. 2007). In a protein evolution context, the majority of studies have involved yeast and bacterial surface expression of single chain antibodies. Provided that the protein in question is orientated into the extracellular environment, any ligand-receptor binding assay can be designed.

It is vital that screening assays for altered binding affinities are both sensitive and specific given the low frequency of target cells in the mutant population (Boder, Wittrup 1998, Daugherty, Iverson & Georgiou 2000, Bloom, Arnold 2009). In addition to a robust method for assay of binding itself, individual components of the screening process must be optimised to maximise the probability of discerning the desired cell.

In this study Tie2 was successfully coupled to the transmembrane domain of PDGF receptor β chain to permit orientation of Tie2 ectodomain with its N-terminus and binding domain positioned most extracellularly. Initial flow cytometry confirmed cell surface locality by means of FLAG epitope detection. The ability to measure

Tie2 expression was essential in developing angiopoietin affinity screening as the quantity of Tie2 is directly liked to levels of angiopoietin binding.

The concentration and type of reagents were optimised to provide the best possible signal as compared to noise levels. Some layers of complexity in staining protocols were necessary to avoid simultaneous spatial competition between different reagents for binding sites. The number of Tie2 molecules per cell was estimated at 5×10^4. As a reference, *S. aureus* displays 10^4 proteins per cell and has a size of up to 1.5μm diameter (Andreoni et al. 1997). DT40 cells are approximately 10μm in diameter and therefore 45 times larger in surface area if each cell is approximated to a sphere. It is possible that the number of surface receptors was underestimated and therefore ligand depletion could be an issue. In addition cells that appeared non-viable on microscopy were not included in the cell count for each binding assay, although reagents have a propensity to bind to permeable cells and this could create a steal phenomenon.

Dissociation constants (K_d) for Ang1 and Ang2 binding interactions with Tie2 receptor were determined as previously described (Lofblom et al. 2007). The resulting values of 0.46nM and 1.03nM respectively are similar to the previously reported figures of 3.7nM and 3nM, which were derived by different methodology (Davis et al. 1996, Maisonpierre et al. 1997). It does appear that Ang1 may have slightly greater binding affinity than Ang2, although the result was not statistically significant and does not approach the twenty-fold discrepancy reported by Yuan *et al.* (Yuan et al. 2009).

Dissociation rates (K_{off}) for the angiopoietin-Tie2 interaction proved more difficult to determine. Dissociation of Ang1 was not measurable with a His-tag based labelling approach and an attempt to rectify this by biotinylation of Ang1 did not yield a product of the necessary purity. Although an approximation of the initial dissociation of Ang2 was gained despite a high level of apparent residual binding, theoretical improvements to the methodology merely confused the picture. Multivalency of both ligand and labelling agent certainly contributed to this predicament, in that dissociation of a ligand from the receptor-binding site may not translate into loss of the fluorescent marker if that marker were bound to other ligands. The level of accuracy required to measure K_{off} could not be achieved with the available reagents.

There is general agreement that kinetic-based screening assays are more sensitive for high affinity interactions (K_d < 1nM), whereas equilibrium screens are certainly more appropriate for interactions with K_d greater than 10nM. The method of screening interactions of intermediate affinities is more debatable. Due to difficulties encountered with measurement of K_{off}, kinetic screening was not a viable option in providing a sensitive or specific screening assay for the angiopoietin-Tie2 interaction.

Equilibrium binding was therefore pursued as a screening method. The avidity and variable oligomerisation issues should affect all cells equally in the equilibrium model and the consequence is therefore negligible. Equilibrium screening demands that the ligand is used at a concentration below its K_d. An appropriate concentration was determined by means of mathematical models and

experimental testing. Estimation of improvements in angiopoietin binding was conservative in this process due to pre-existing high affinity of the wild-type interaction. Consequently the ratio of maximal to background fluorescence was not ideal and alternative fluorophores could be explored to improve this.

The competitive equilibrium between Ang1 versus Ang2 yielded consistent results. However the likelihood of added complexities in the dynamic between the two ligands and Tie2 meant that a sensitive and screening method could not be confidently designed.

Limitations of screening methodology are the most significant obstacle to the success of directed evolution, both in this study and in general. The ideal model for screening of the angiopoietin-Tie2 interaction would consist of fluorophore conjugated-monomeric angiopoeitins in a kinetic displacement assay, and engineering of such molecules should be considered for future work.

6.3 Evolution of new Tie2 phenotypes by FACS-based iterative selection

There is much debate concerning the best way to conduct directed evolution. The premise of the technique is that it mimics natural evolution over a shorter timescale, in randomly mutating a gene and selecting the best variant for a given purpose. Whilst it is possible to experimentally accelerate the initial mutation process, a high mutation rate does not necessarily correlate with improved phenotypes due to the predilection for deleterious mutations. In addition, the

process of iterative screening and selection is far from natural, given that it is generally only the top performing section of the library that is selected and this limits the pool of variation significantly.

Studies of fitness landscapes and neutral drift in protein evolution suggest that there are many routes by which a protein can be evolved for a given function and experience in enzyme studies suggests that mutations outside the active site can influence binding capability (Bloom, Arnold 2009, Bershtein, Goldin & Tawfik 2008, Romero, Arnold 2009, Shimotohno et al. 2001, Spiller et al. 1999). The majority of Tie2 ectodomain was selected for evolution as opposed to the specific Ig2 binding domain to expand evolutionary potential. The mutation rate in this experimental system did not permit early population screening, but in addition the idea that the population may neutrally drift was thought to enhance the prospect of epistasis and improve diversity.

The discovery of a high prevalence of deletions in the 9-month cultured population necessitated an initial panning round in order to separate binding and non-binding populations. It was not surprising to discover that the non-binders contained multiple deletions and Tie2 expression levels were very low. It was however disappointing to discover a low mutation frequency in the binding population, and this somewhat limited the potential of the study by reducing the target cell frequency further and consequently placing more emphasis on the competence of the binding assay. The prevalence of deletions in cells subjected to prolonged culture could be potentially avoidable in future studies by intermittently sorting for Tie2 expression.

There is a practical limit to the number of cells that can be screened and therefore the maximum diversity cannot be tested. Improvement of cell viability during the staining process would partially address this issue, though in practice may be difficult to achieve given the trauma involved in centrifugation yet the need to wash cells free of any unbound label. Magnetic sorting has been advocated as an option for conducting panning rounds on larger cell populations and could be investigated further (Wentzel et al. 1999).

The chosen approach for evolution of an Ang2-binding protein was to initially select improved Ang2 binders, followed by subsequent screening for Ang1 binding affinity. The stringency of selection was gradually increased through Ang2 concentration and percentage of population selected. This yielded a population with improved Ang2 binding relative to Tie2 expression, yet initial sequencing after four rounds of selection revealed that the majority of cells harboured a deleterious FLAG mutation as opposed to a positive Tie2 mutation.

The outcome of this evolution successfully demonstrates a genotype that directly links to the observed phenotype, but the population was not taken forward for further selection given the rarity of the improved Ang2-binding target cell and low probability of generating significant diversity between rounds of sorting. Optimisation of the mutation frequency is necessary to produce an appropriate library in which to search for improved Ang2-binding and/or reduced Ang1 binding affinity.

The probability of selecting mutants with reduced binding affinity may be greater than selecting improved mutants, and as such Tie2 was also evolved for reduced Ang2 binding. Evolution of a Tie2-DT40 population with reduced Ang2 binding affinity was achieved by selecting cells that did not apparently bind Ang2 despite expressing Tie2. When compared with the unsorted Ang2-binding subpopulation, the evolved cells exhibited reduced Ang2-binding affinity. A single mutation encountered in the majority of sorted cells, P166S, was responsible for this phenotypical change. The residue in question is known to contact Ang2 during binding, though its mutation does not abolish binding altogether in this study.

The combinatorial effect of further mutations for reduced angiopoietin binding would provide useful insight into angiopoietin-Tie2 interactions. However the accumulation of mutations between rounds of selection was intrinsically limited and a prolonged period of culture between rounds would be necessary to address this issue. Contrarily, it is important to re-sort libraries as soon as the desired population size is reached to prevent loss of existing diversity through cell passaging. The identification of a single congruent mutation as opposed to multiple different mutations in the selected cells suggests that the mutation rate in Tie2-DT40 was too limiting to consider further iterative selections.

The ability to identify a mutant form of Tie2ECD with different Ang2 binding capability by screening and selection of a DT40-based library represents proof of concept in this method. In order to achieve the original goal of creating a form of Tie2ECD that preferentially binds Ang2 and not Ang1, the mutation rate and screening assay must be optimised. However the success in evolving Tie2 for a

new phenotype presented here suggests that SHM combined with cell surface display is a suitable approach to achieve such an objective.

6.4 Conclusion

It is ironic yet predictable that this technology requires evolution in order to acquire the necessary sophistication for its own application of directed evolution. The preliminary work presented in this thesis demonstrates that the combination of vertebrate cell based somatic hypermutation and cell surface display enables directed evolution of binding proteins. The proposed advantages of this method over traditional protein engineering techniques justify investment in its future development.

APPENDICES

Appendix 2.1: PCR

a) Primers

Name	Sequence 5' → 3'	T_m (°C)
Tie2 Fwd	CACCGCTAGCATGGACTCTTTAGCCAGCTT	69.5
Tie2 Rev	GGAATTCTTAACAGAAATGTTGAAGGGCT	62.4
PDGFR Fwd	CACCAAGAATTCCCCCGCCGCCGCCGCCGCCATGGACTACAAGGACGACGACGAC AAGCTGGTGGGCCAGGACACGCAGGA	88.6
PDGFR Rev	AGATCTTCAGTAACGTGGCTTCTTCTGCC	66.7
GW Fwd	TTTCCGAAAAAAATGACAAAATATT	51.5
GW Rev	GGTCAAGCCTTGCCTTGTTGTAGCTTAAATTTTGC	69.3
P5 Fwd	GGGGGATCCAGATCTGTGACCGGTGCAAGTGATAGAAACT	74.6
P4 Rev	TACAAAAACCTCCTGCCAGTGCAAGGAGCAGCTGATGGTTTTTACTGTCT	75.2
ggAID Fwd	AGAAGATCTATGGACAGCCTCTTGATGAAGAGG	68.2
ggAID Rev	GCAGAATTCTCAAAGTCCCAGAGTTTTAAAGGC	67.0
hsAID Fwd	CACCATGGACAGCCTCTTGATGAACCGG	69.5
hsAID Rev	TCAAAGTCCCAAAGTACGAAATGCGTC	63.4

T_m was estimated according to the formula:

$$T_m = 69.3 + \frac{41(n_G + n_C)}{N} - \frac{650}{N}$$

n_G = number guanine bases
n_C = number cytosine bases
N = total number bases

b) Amplification conditions

	Section	3.1.1 4.3.2 5.4.4 5.4.5	3.1.2	3.1.3 3.1.4 3.2.2	3.2.3	3.2.4	4.1.3	4.4.3	5.4.3	5.5.2 5.6.2
	Fwd primer	Tie2	PDGFR	Tie2	GW	P5	ggAID	hsAID	Tie2	Tie2
	Rev primer	Tie2	PDGFR	PDGFR	GW	P4	ggAID	hsAID	Tie2	PDGFR
Initial denaturation	Temp (°C)	94	94	94	94	94	95	98	94	94
	Duration (min)	3	3	3	3	5	3	0.5	3	3
Denaturation	Temp (°C)	94	94	94	94	94	95	98	94	94
	Duration (min)	1	1	1	0.5	1	1	0.5	0.5	1
Annealing	Temp (°C)	60	65	60	60	68	55	60	60	60
	Duration (min)	1	1	1	0.5	1	1	0.5	1	1
Extension	Temp (°C)	72	72	72	70	72	72	72	72	72
	Duration (min)	1	1	1.5	0.5	0.5	1	0.5	1	1.5
	Cycles	30	30	25	35	35	30	30	30	30
Final extension	Temp (°C)	72	72	72	70	72	72	72	72	72
	Duration (min)	10	10	10	10	10	10	10	10	10

c) Reaction components

	Section	3.1.1 4.3.2 5.4.4 5.4.5	3.1.2	3.1.3 3.1.4 3.2.2	3.2.3	3.2.4	4.1.3	4.4.3	5.4.3	5.5.2 5.6.2
	Fwd primer	Tie2	PDGFR	Tie2	GW	P5	ggAID	hsAID	Tie2	Tie2
	Rev primer	Tie2	PDGFR	PDGFR	GW	P4	ggAID	hsAID	Tie2	PDGFR
BIOTAQ	10x NH_4 buffer	-	-	2.5 µl	2.5 µl	2.5 µl	2.5 µl	-	2.5 µl	-
	50mM $MgCl_2$	-	-	2.0 µl	2.0 µl	2.0 µl	2.0 µl	-	2.0 µl	-
	Biotaq	-	-	0.5 µl	0.5 µl	0.5 µl	0.25 µl	-	0.5 µl	-
Phusion	5x HF buffer	10.0 µl	10.0 µl	-	-	-	-	10.0 µl	-	10.0 µl
	Phusion	0.5 µl	0.5 µl	-	-	-	-	0.5 µl	-	0.5 µl
All	10mM dNTPs	1.0 µl	1.0 µl	0.5 µl	1.0 µl	0.5 µl	0.5 µl	0.75 µl	0.5 µl	1.0 µl
	Primer	0.5 µl	0.5 µl	0.5 µl	0.5 µl	0.5 µl	0.5 µl	0.5 µl	0.5 µl	0.5 µl
	Primer	0.5 µl	0.5 µl	0.5 µl	0.5 µl	0.5 µl	0.5 µl	0.5 µl	0.5 µl	0.5 µl
	100% DMSO	0.5 µl[§]	-	0.5 µl	0.5 µl	0.5 µl	0.5 µl	-	0.5 µl	0.5 µl
	DNA	30ng P 5 µl C[§]	30ng P	5 µl C	300 ng G	100 ng G	5 µl C	20ng P	5 µl C	5 µl C
	H_2O	to 50.0 µl	to 50.0 µl	to 25.0 µl	to 25.0 µl	to 25.0 µl	to 25.0 µl	to 50.0 µl	to 25.0 µl	to 50.0 µl

Appendix 2.2: Volumes and dilutions for angiopoietin binding assays

a) Ang2 dissociation constant (K_d)

Molarity (nM)	Volume (µl)	No. ligands	200nM Ang2 (µl)
100	50	3.0×10^{12}	25
50	50	1.5×10^{12}	12.5
25	50	7.5×10^{11}	6.25
10	100	6.02×10^{11}	5
5	200	6.02×10^{11}	5
2.5	400	6.02×10^{11}	5
1	1000	6.02×10^{11}	5
0.5	2000	6.02×10^{11}	5
0	50	-	-

b) Ang1 dissociation constant (K_d)

Molarity (nM)	Volume (µl)	No. ligands	1µM Ang1 (µl)
50	50	1.5×10^{12}	2.5
25	50	7.5×10^{11}	1.25
10	100	6.02×10^{11}	1
5	200	6.02×10^{11}	1
2.5	400	6.02×10^{11}	1
1	1000	6.02×10^{11}	1
0.5	2000	6.02×10^{11}	1
0	50	-	-

Appendix 3.1: Cloning

3.1.1: Cloning of Tie2ECD into pcDNA ™3.1D/V5-His-TOPO® expression vector

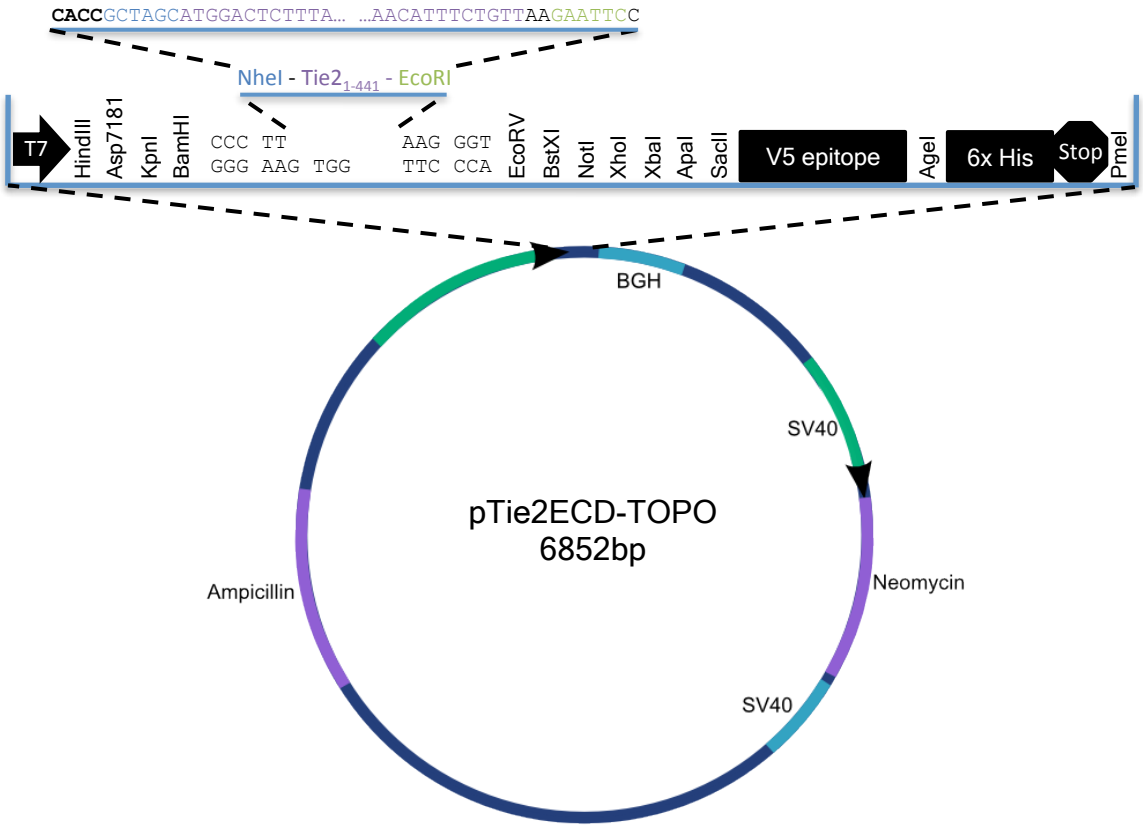

3.1.2: Cloning of cell surface display system into pcDNA ™3.1D/V5-His-TOPO® expression vector

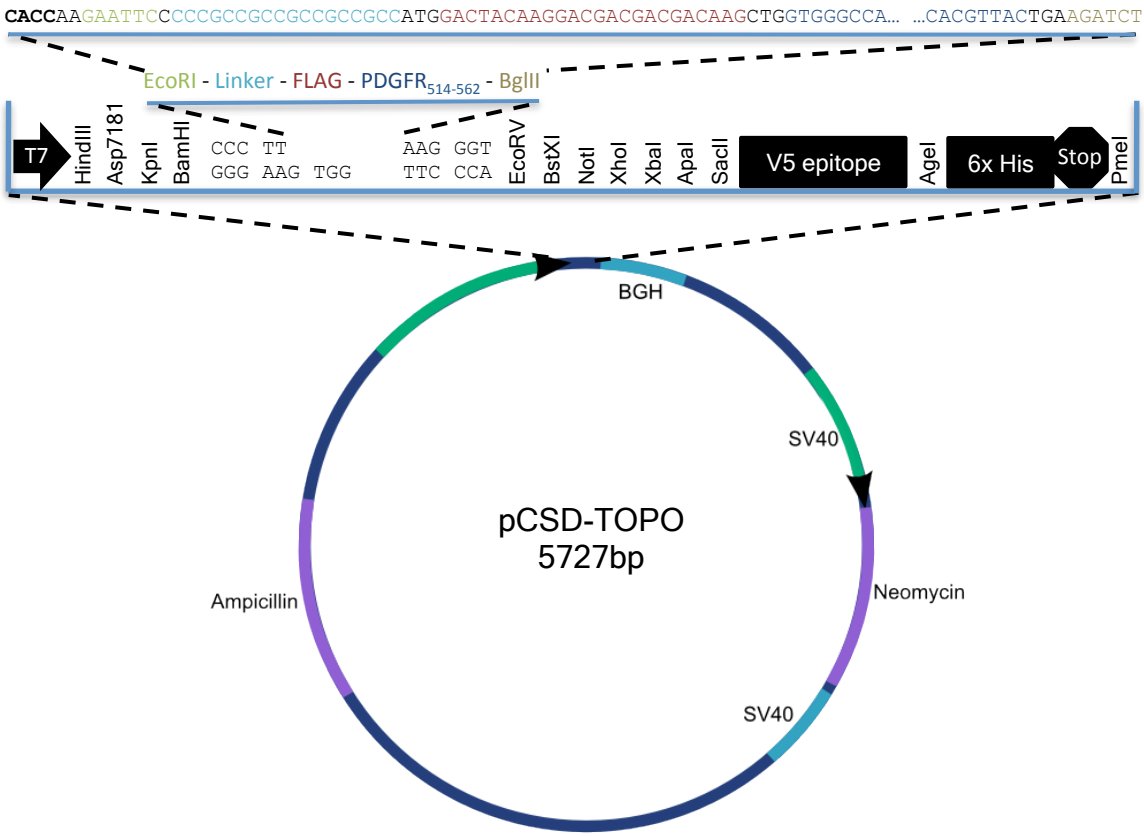

3.1.3: Cloning of cell-surface displayed Tie2ECD in pcDNA™3.1D/V5-His-TOPO® expression vector

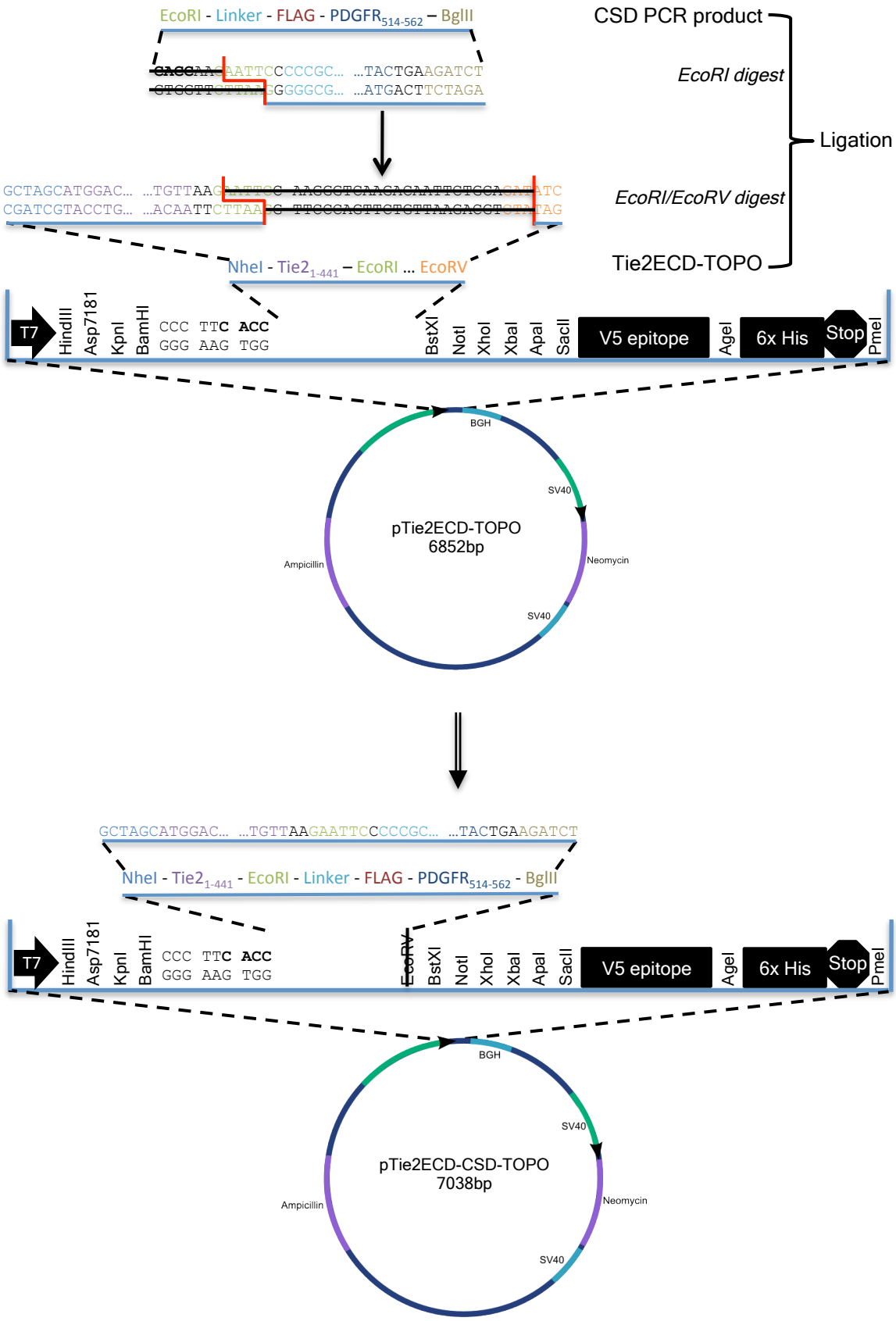

3.1.4: Cloning of cell-surface displayed Tie2 ECD into pHypermut2 vector

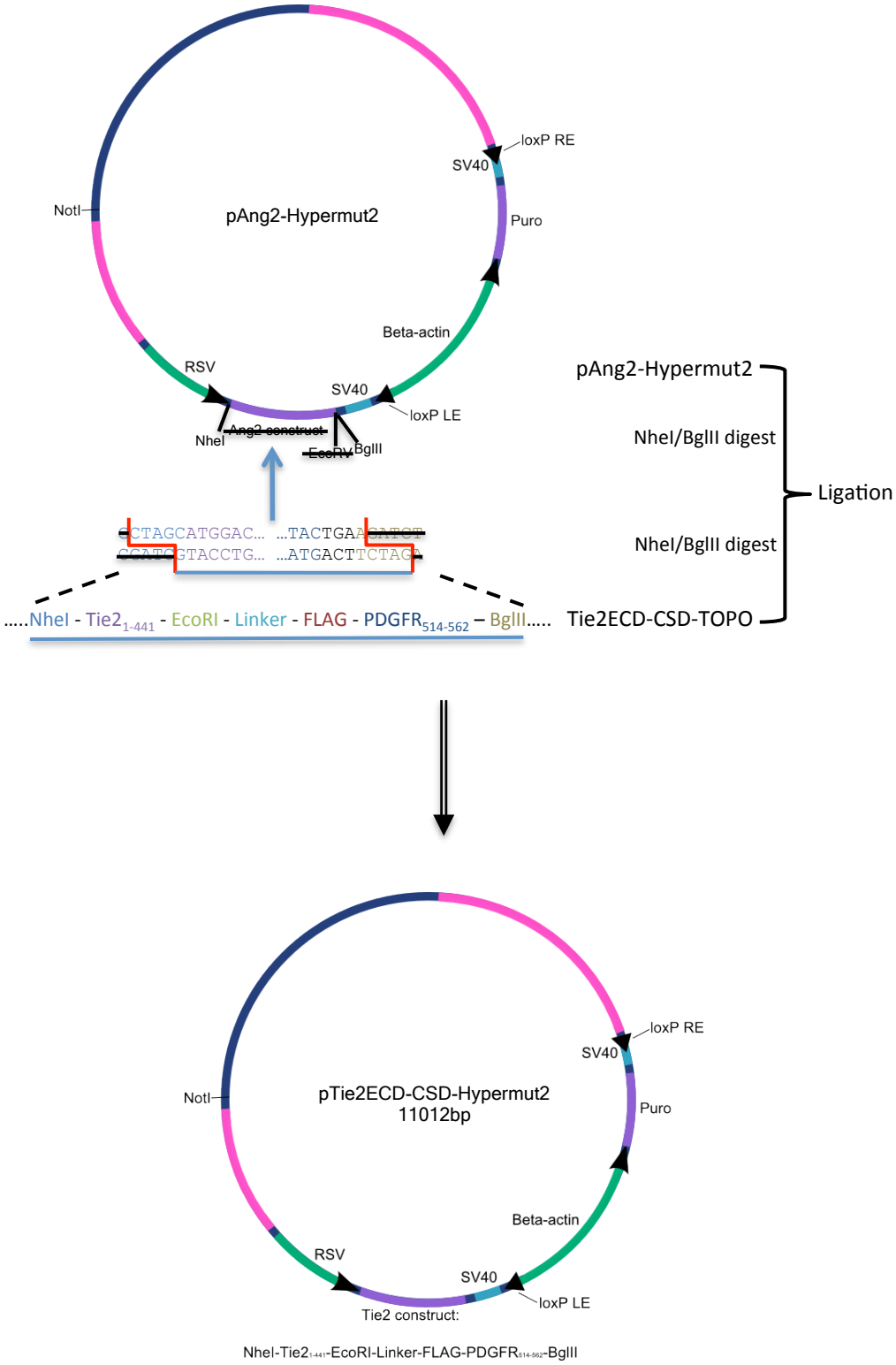

Appendix 4.1: AID vectors

4.4.2: pRH125 vectors

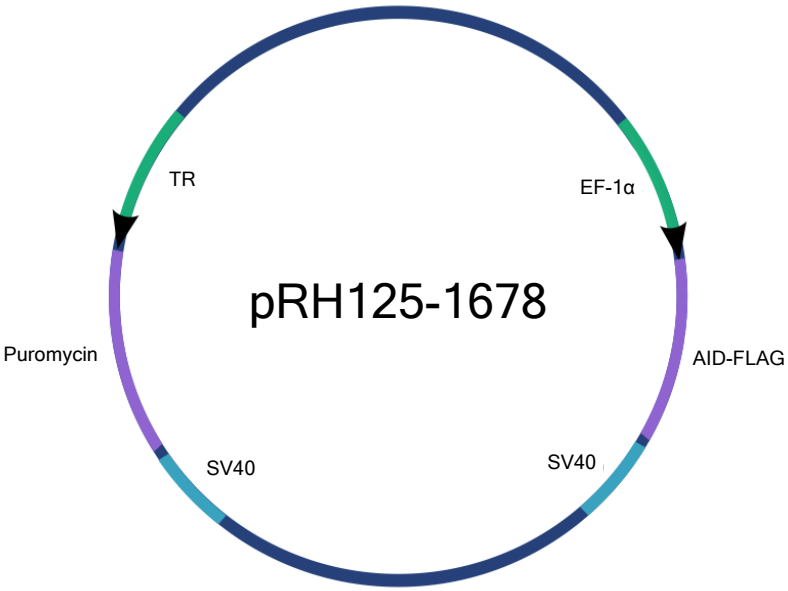

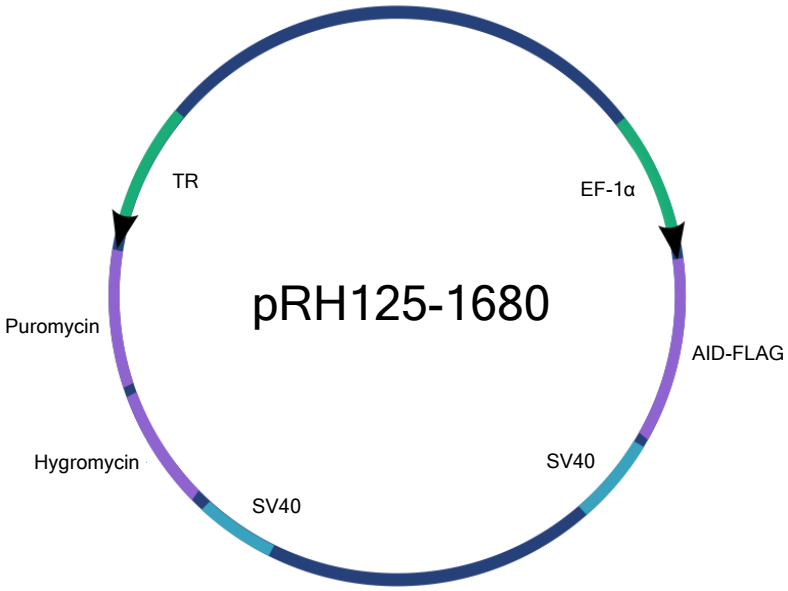

4.4.3: Cloning of AID into pEF6/V5-His-TOPO®

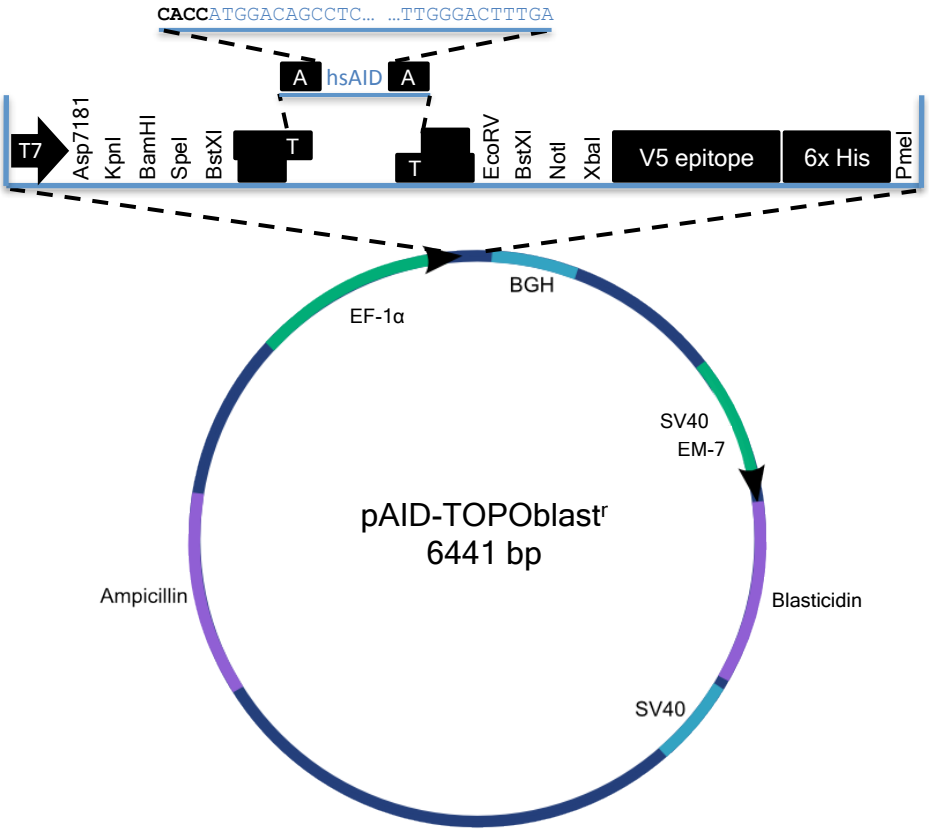

BIBLIOGRAPHY

Ahmad, S.A., Liu, W., Jung, Y.D., Fan, F., Wilson, M., Reinmuth, N., Shaheen, R.M., Bucana, C.D. & Ellis, L.M. 2001, "The effects of angiopoietin-1 and -2 on tumor growth and angiogenesis in human colon cancer", *Cancer research,* vol. 61, no. 4, pp. 1255-1259.

Andreoni, C., Goetsch, L., Libon, C., Samuelson, P., Nguyen, T.N., Robert, A., Uhlen, M., Binz, H. & Stahl, S. 1997, "Flow cytometric quantification of surface-displayed recombinant receptors on staphylococci", *BioTechniques,* vol. 23, no. 4, pp. 696-702, 704.

Arakawa, H. & Buerstedde, J.M. 2004, "Immunoglobulin gene conversion: insights from bursal B cells and the DT40 cell line", *Developmental dynamics : an official publication of the American Association of Anatomists,* vol. 229, no. 3, pp. 458-464.

Arakawa, H., Hauschild, J. & Buerstedde, J.M. 2002, "Requirement of the activation-induced deaminase (AID) gene for immunoglobulin gene conversion", *Science (New York, N.Y.),* vol. 295, no. 5558, pp. 1301-1306.

Arakawa, H., Kudo, H., Batrak, V., Caldwell, R.B., Rieger, M.A., Ellwart, J.W. & Buerstedde, J.M. 2008, "Protein evolution by hypermutation and selection in the B cell line DT40", *Nucleic acids research,* vol. 36, no. 1, pp. e1.

Arakawa, H., Lodygin, D. & Buerstedde, J.M. 2001, "Mutant loxP vectors for selectable marker recycle and conditional knock-outs", *BMC biotechnology,* vol. 1, pp. 7.

Arakawa, H., Saribasak, H. & Buerstedde, J.M. 2004, "Activation-induced cytidine deaminase initiates immunoglobulin gene conversion and hypermutation by a common intermediate", *PLoS biology,* vol. 2, no. 7, pp. E179.

Axe, D.D., Foster, N.W. & Fersht, A.R. 1998, "A search for single substitutions that eliminate enzymatic function in a bacterial ribonuclease", *Biochemistry,* vol. 37, no. 20, pp. 7157-7166.

Bachl, J., Carlson, C., Gray-Schopfer, V., Dessing, M. & Olsson, C. 2001, "Increased transcription levels induce higher mutation rates in a hypermutating cell line", *Journal of immunology (Baltimore, Md.: 1950),* vol. 166, no. 8, pp. 5051-5057.

Bachl, J. & Wabl, M. 1996, "An immunoglobulin mutator that targets G.C base pairs", *Proceedings of the National Academy of Sciences of the United States of America,* vol. 93, no. 2, pp. 851-855.

Baffert, F., Thurston, G., Rochon-Duck, M., Le, T., Brekken, R. & McDonald, D.M. 2004, "Age-related changes in vascular endothelial growth factor dependency and angiopoietin-1-induced plasticity of adult blood vessels", *Circulation research,* vol. 94, no. 7, pp. 984-992.

Barreto, V., Reina-San-Martin, B., Ramiro, A.R., McBride, K.M. & Nussenzweig, M.C. 2003, "C-terminal deletion of AID uncouples class switch recombination from somatic hypermutation and gene conversion", *Molecular cell,* vol. 12, no. 2, pp. 501-508.

Barton, W.A., Tzvetkova, D. & Nikolov, D.B. 2005, "Structure of the angiopoietin-2 receptor binding domain and identification of surfaces involved in Tie2 recognition", *Structure (London, England : 1993),* vol. 13, no. 5, pp. 825-832.

Barton, W.A., Tzvetkova-Robev, D., Miranda, E.P., Kolev, M.V., Rajashankar, K.R., Himanen, J.P. & Nikolov, D.B. 2006, "Crystal structures of the Tie2 receptor ectodomain and the angiopoietin-2-Tie2 complex", *Nature structural & molecular biology,* vol. 13, no. 6, pp. 524-532.

Basu, U., Chaudhuri, J., Alpert, C., Dutt, S., Ranganath, S., Li, G., Schrum, J.P., Manis, J.P. & Alt, F.W. 2005, "The AID antibody diversification enzyme is regulated by protein kinase A phosphorylation", *Nature,* vol. 438, no. 7067, pp. 508-511.

Bates, S.R. & Quake, S.R. 2009, "Highly parallel measurements of interaction kinetic constants with a microfabricated optomechanical device", *Applied Physics Letters,* vol. 95, no. 7, pp. 73705.

Bergers, G. & Hanahan, D. 2008, "Modes of resistance to anti-angiogenic therapy", *Nature reviews.Cancer,* vol. 8, no. 8, pp. 592-603.

Bershtein, S., Goldin, K. & Tawfik, D.S. 2008, "Intense neutral drifts yield robust and evolvable consensus proteins", *Journal of Molecular Biology,* vol. 379, no. 5, pp. 1029-1044.

Blagodatski, A., Batrak, V., Schmidl, S., Schoetz, U., Caldwell, R.B., Arakawa, H. & Buerstedde, J.M. 2009, "A cis-acting diversification activator both necessary and sufficient for AID-mediated hypermutation", *PLoS genetics,* vol. 5, no. 1, pp. e1000332.

Bloom, J.D. & Arnold, F.H. 2009, "In the light of directed evolution: pathways of adaptive protein evolution", *Proceedings of the National Academy of Sciences of the United States of America,* vol. 106 Suppl 1, pp. 9995-10000.

Bloom, J.D., Romero, P.A., Lu, Z. & Arnold, F.H. 2007, "Neutral genetic drift can alter promiscuous protein functions, potentially aiding functional evolution", *Biology direct,* vol. 2, pp. 17.

Boder, E.T., Midelfort, K.S. & Wittrup, K.D. 2000, "Directed evolution of antibody fragments with monovalent femtomolar antigen-binding affinity", *Proceedings of the National Academy of Sciences of the United States of America,* vol. 97, no. 20, pp. 10701-10705.

Boder, E.T. & Wittrup, K.D. 1998, "Optimal screening of surface-displayed polypeptide libraries", *Biotechnology progress,* vol. 14, no. 1, pp. 55-62.

Boder, E.T. & Wittrup, K.D. 1997, "Yeast surface display for screening combinatorial polypeptide libraries", *Nature biotechnology,* vol. 15, no. 6, pp. 553-557.

Bogdanovic, E., Nguyen, V.P. & Dumont, D.J. 2006, "Activation of Tie2 by angiopoietin-1 and angiopoietin-2 results in their release and receptor internalization", *Journal of cell science,* vol. 119, no. Pt 17, pp. 3551-3560.

Bowers, P.M., Horlick, R.A., Neben, T.Y., Toobian, R.M., Tomlinson, G.L., Dalton, J.L., Jones, H.A., Chen, A., Altobell, L.,3rd, Zhang, X., Macomber, J.L., Krapf, I.P., Wu, B.F., McConnell, A., Chau, B., Holland, T., Berkebile, A.D., Neben, S.S., Boyle, W.J. & King, D.J. 2011, "Coupling mammalian cell surface display with somatic hypermutation for the discovery and maturation of human antibodies", *Proceedings of the National Academy of Sciences of the United States of America,* vol. 108, no. 51, pp. 20455-20460.

Brannigan, J.A. & Wilkinson, A.J. 2002, "Protein engineering 20 years on", *Nature reviews.Molecular cell biology,* vol. 3, no. 12, pp. 964-970.

Brindle, N.P., Saharinen, P. & Alitalo, K. 2006, "Signaling and functions of angiopoietin-1 in vascular protection", *Circulation research,* vol. 98, no. 8, pp. 1014-1023.

Buelow, B. & Scharenberg, A.M. 2008, "Characterization of parameters required for effective use of tamoxifen-regulated recombination", *PloS one,* vol. 3, no. 9, pp. e3264.

Buerstedde, J.M. & Takeda, S. 1991, "Increased ratio of targeted to random integration after transfection of chicken B cell lines", *Cell,* vol. 67, no. 1, pp. 179-188.

Carlson, T.R., Feng, Y., Maisonpierre, P.C., Mrksich, M. & Morla, A.O. 2001, "Direct cell adhesion to the angiopoietins mediated by integrins", *The Journal of biological chemistry,* vol. 276, no. 28, pp. 26516-26525.

Cascone, I., Napione, L., Maniero, F., Serini, G. & Bussolino, F. 2005, "Stable interaction between alpha5beta1 integrin and Tie2 tyrosine kinase receptor regulates endothelial cell response to Ang-1", *The Journal of cell biology,* vol. 170, no. 6, pp. 993-1004.

Chao, G., Lau, W.L., Hackel, B.J., Sazinsky, S.L., Lippow, S.M. & Wittrup, K.D. 2006, "Isolating and engineering human antibodies using yeast surface display", *Nature protocols,* vol. 1, no. 2, pp. 755-768.

Chesnut, J.D., Baytan, A.R., Russell, M., Chang, M.P., Bernard, A., Maxwell, I.H. & Hoeffler, J.P. 1996, "Selective isolation of transiently transfected cells from a mammalian cell population with vectors expressing a membrane anchored single-chain antibody", *Journal of immunological methods,* vol. 193, no. 1, pp. 17-27.

Cho, C.H., Kammerer, R.A., Lee, H.J., Yasunaga, K., Kim, K.T., Choi, H.H., Kim, W., Kim, S.H., Park, S.K., Lee, G.M. & Koh, G.Y. 2004, "Designed angiopoietin-1 variant, COMP-Ang1, protects against radiation-induced endothelial cell apoptosis", *Proceedings of the National Academy of Sciences of the United States of America,* vol. 101, no. 15, pp. 5553-5558.

Cho, C.H., Kim, K.E., Byun, J., Jang, H.S., Kim, D.K., Baluk, P., Baffert, F., Lee, G.M., Mochizuki, N., Kim, J., Jeon, B.H., McDonald, D.M. & Koh, G.Y. 2005, "Long-term and sustained COMP-Ang1 induces long-lasting vascular enlargement and enhanced blood flow", *Circulation research,* vol. 97, no. 1, pp. 86-94.

Chou, W.C., Liao, K.W., Lo, Y.C., Jiang, S.Y., Yeh, M.Y. & Roffler, S.R. 1999, "Expression of chimeric monomer and dimer proteins on the plasma membrane of mammalian cells", *Biotechnology and bioengineering,* vol. 65, no. 2, pp. 160-169.

Coffelt, S.B., Tal, A.O., Scholz, A., De Palma, M., Patel, S., Urbich, C., Biswas, S.K., Murdoch, C., Plate, K.H., Reiss, Y. & Lewis, C.E. 2010, "Angiopoietin-2 regulates gene expression in TIE2-expressing monocytes and augments their inherent proangiogenic functions", *Cancer research,* vol. 70, no. 13, pp. 5270-5280.

Coxon, A., Bready, J., Min, H., Kaufman, S., Leal, J., Yu, D., Lee, T.A., Sun, J.R., Estrada, J., Bolon, B., McCabe, J., Wang, L., Rex, K., Caenepeel, S., Hughes, P., Cordover, D., Kim, H., Han, S.J., Michaels, M.L., Hsu, E., Shimamoto, G., Cattley, R., Hurh, E., Nguyen, L., Wang, S.X., Ndifor, A., Hayward, I.J., Falcon, B.L., McDonald, D.M., Li, L., Boone, T., Kendall, R., Radinsky, R. & Oliner, J.D. 2010, "Context-dependent role of angiopoietin-1 inhibition in the suppression of angiogenesis and tumor growth: implications for AMG 386, an angiopoietin-1/2-neutralizing peptibody", *Molecular cancer therapeutics,* vol. 9, no. 10, pp. 2641-2651.

Cumbers, S.J., Williams, G.T., Davies, S.L., Grenfell, R.L., Takeda, S., Batista, F.D., Sale, J.E. & Neuberger, M.S. 2002, "Generation and iterative affinity maturation of antibodies in vitro using hypermutating B-cell lines", *Nature biotechnology,* vol. 20, no. 11, pp. 1129-1134.

Daugherty, P.S., Chen, G., Olsen, M.J., Iverson, B.L. & Georgiou, G. 1998, "Antibody affinity maturation using bacterial surface display", *Protein engineering,* vol. 11, no. 9, pp. 825-832.

Daugherty, P.S., Iverson, B.L. & Georgiou, G. 2000, "Flow cytometric screening of cell-based libraries", *Journal of immunological methods,* vol. 243, no. 1-2, pp. 211-227.

Davis, S., Aldrich, T.H., Jones, P.F., Acheson, A., Compton, D.L., Jain, V., Ryan, T.E., Bruno, J., Radziejewski, C., Maisonpierre, P.C. & Yancopoulos, G.D. 1996, "Isolation of angiopoietin-1, a ligand for the TIE2 receptor, by secretion-trap expression cloning", *Cell,* vol. 87, no. 7, pp. 1161-1169.

Davis, S., Papadopoulos, N., Aldrich, T.H., Maisonpierre, P.C., Huang, T., Kovac, L., Xu, A., Leidich, R., Radziejewska, E., Rafique, A., Goldberg, J., Jain, V., Bailey, K., Karow, M., Fandl, J., Samuelsson, S.J., Ioffe, E., Rudge, J.S., Daly, T.J., Radziejewski, C. & Yancopoulos, G.D. 2003, "Angiopoietins have distinct modular domains essential for receptor binding, dimerization and superclustering", *Nature structural biology,* vol. 10, no. 1, pp. 38-44.

De Palma, M., Venneri, M.A., Galli, R., Sergi Sergi, L., Politi, L.S., Sampaolesi, M. & Naldini, L. 2005, "Tie2 identifies a hematopoietic lineage of proangiogenic monocytes required for tumor vessel formation and a mesenchymal population of pericyte progenitors", *Cancer cell,* vol. 8, no. 3, pp. 211-226.

Di Noia, J. & Neuberger, M.S. 2002, "Altering the pathway of immunoglobulin hypermutation by inhibiting uracil-DNA glycosylase", *Nature,* vol. 419, no. 6902, pp. 43-48.

Dumont, D.J., Gradwohl, G., Fong, G.H., Puri, M.C., Gertsenstein, M., Auerbach, A. & Breitman, M.L. 1994, "Dominant-negative and targeted null mutations in the endothelial receptor tyrosine kinase, tek, reveal a critical role in vasculogenesis of the embryo", *Genes & development,* vol. 8, no. 16, pp. 1897-1909.

Dumont, D.J., Yamaguchi, T.P., Conlon, R.A., Rossant, J. & Breitman, M.L. 1992, "Tek, a Novel Tyrosine Kinase Gene Located on Mouse Chromosome 4, is Expressed in Endothelial Cells and their Presumptive Precursors", *Oncogene,* vol. 7, no. 8, pp. 1471-1480.

Economides, A.N., Carpenter, L.R., Rudge, J.S., Wong, V., Koehler-Stec, E.M., Hartnett, C., Pyles, E.A., Xu, X., Daly, T.J., Young, M.R., Fandl, J.P., Lee, F., Carver, S., McNay, J., Bailey, K., Ramakanth, S., Hutabarat, R., Huang, T.T., Radziejewski, C., Yancopoulos, G.D. & Stahl, N. 2003, "Cytokine traps: multi-component, high-affinity blockers of cytokine action", *Nature medicine,* vol. 9, no. 1, pp. 47-52.

England, J.L. & Shakhnovich, E.I. 2003, "Structural determinant of protein designability", *Physical Review Letters,* vol. 90, no. 21, pp. 218101.

Faili, A., Aoufouchi, S., Flatter, E., Gueranger, Q., Reynaud, C.A. & Weill, J.C. 2002, "Induction of somatic hypermutation in immunoglobulin genes is dependent on DNA polymerase iota", *Nature,* vol. 419, no. 6910, pp. 944-947.

Falcon, B.L., Hashizume, H., Koumoutsakos, P., Chou, J., Bready, J.V., Coxon, A., Oliner, J.D. & McDonald, D.M. 2009, "Contrasting actions of selective inhibitors of angiopoietin-1 and angiopoietin-2 on the normalization of tumor blood vessels", *The American journal of pathology,* vol. 175, no. 5, pp. 2159-2170.

Felcht, M., Luck, R., Schering, A., Seidel, P., Srivastava, K., Hu, J., Bartol, A., Kienast, Y., Vettel, C., Loos, E.K., Kutschera, S., Bartels, S., Appak, S., Besemfelder, E., Terhardt, D., Chavakis, E., Wieland, T., Klein, C., Thomas, M., Uemura, A., Goerdt, S. & Augustin, H.G. 2012, "Angiopoietin-2 differentially regulates

angiogenesis through TIE2 and integrin signaling", *The Journal of clinical investigation,* vol. 122, no. 6, pp. 1991-2005.

Fiedler, U., Krissl, T., Koidl, S., Weiss, C., Koblizek, T., Deutsch, U., Martiny-Baron, G., Marme, D. & Augustin, H.G. 2003, "Angiopoietin-1 and angiopoietin-2 share the same binding domains in the Tie-2 receptor involving the first Ig-like loop and the epidermal growth factor-like repeats", *The Journal of biological chemistry,* vol. 278, no. 3, pp. 1721-1727.

Fiedler, U., Reiss, Y., Scharpfenecker, M., Grunow, V., Koidl, S., Thurston, G., Gale, N.W., Witzenrath, M., Rosseau, S., Suttorp, N., Sobke, A., Herrmann, M., Preissner, K.T., Vajkoczy, P. & Augustin, H.G. 2006, "Angiopoietin-2 sensitizes endothelial cells to TNF-alpha and has a crucial role in the induction of inflammation", *Nature medicine,* vol. 12, no. 2, pp. 235-239.

Fiedler, U., Scharpfenecker, M., Koidl, S., Hegen, A., Grunow, V., Schmidt, J.M., Kriz, W., Thurston, G. & Augustin, H.G. 2004, "The Tie-2 ligand angiopoietin-2 is stored in and rapidly released upon stimulation from endothelial cell Weibel-Palade bodies", *Blood,* vol. 103, no. 11, pp. 4150-4156.

Fischer, C., Jonckx, B., Mazzone, M., Zacchigna, S., Loges, S., Pattarini, L., Chorianopoulos, E., Liesenborghs, L., Koch, M., De Mol, M., Autiero, M., Wyns, S., Plaisance, S., Moons, L., van Rooijen, N., Giacca, M., Stassen, J.M., Dewerchin, M., Collen, D. & Carmeliet, P. 2007, "Anti-PlGF inhibits growth of VEGF(R)-inhibitor-resistant tumors without affecting healthy vessels", *Cell,* vol. 131, no. 3, pp. 463-475.

Franklin, R. & Sale, J.E. 2006, "Transient transfection of DT40", *Sub-cellular biochemistry,* vol. 40, pp. 379-382.

Freeman, G.J., Gray, G.S., Gimmi, C.D., Lombard, D.B., Zhou, L.J., White, M., Fingeroth, J.D., Gribben, J.G. & Nadler, L.M. 1991, "Structure, expression, and T cell costimulatory activity of the murine homologue of the human B lymphocyte activation antigen B7", *The Journal of experimental medicine,* vol. 174, no. 3, pp. 625-631.

Gale, N.W., Thurston, G., Hackett, S.F., Renard, R., Wang, Q., McClain, J., Martin, C., Witte, C., Witte, M.H., Jackson, D., Suri, C., Campochiaro, P.A., Wiegand, S.J. & Yancopoulos, G.D. 2002, "Angiopoietin-2 is required for postnatal angiogenesis and lymphatic patterning, and only the latter role is rescued by Angiopoietin-1", *Developmental cell,* vol. 3, no. 3, pp. 411-423.

Georgiou, G., Stathopoulos, C., Daugherty, P.S., Nayak, A.R., Iverson, B.L. & Curtiss, R.,3rd 1997, "Display of heterologous proteins on the surface of microorganisms: from the screening of combinatorial libraries to live recombinant vaccines", *Nature biotechnology,* vol. 15, no. 1, pp. 29-34.

Glazer, A.N. 1988, "Phycobiliproteins", *Methods in enzymology,* vol. 167, pp. 291-303.

Grimm, S., Salahshour, S. & Nygren, P.A. 2012, "Monitored whole gene in vitro evolution of an anti-hRaf-1 affibody molecule towards increased binding affinity", *New biotechnology,* vol. 29, no. 5, pp. 534-542.

Gronwald, R.G., Grant, F.J., Haldeman, B.A., Hart, C.E., O'Hara, P.J., Hagen, F.S., Ross, R., Bowen-Pope, D.F. & Murray, M.J. 1988, "Cloning and expression of a cDNA coding for the human platelet-derived growth factor receptor: evidence for more than one receptor class", *Proceedings of the National Academy of Sciences of the United States of America,* vol. 85, no. 10, pp. 3435-3439.

Guo, H.H., Choe, J. & Loeb, L.A. 2004, "Protein tolerance to random amino acid change", *Proceedings of the National Academy of Sciences of the United States of America,* vol. 101, no. 25, pp. 9205-9210.

Hashizume, H., Falcon, B.L., Kuroda, T., Baluk, P., Coxon, A., Yu, D., Bready, J.V., Oliner, J.D. & McDonald, D.M. 2010, "Complementary actions of inhibitors of angiopoietin-2 and VEGF on tumor angiogenesis and growth", *Cancer research,* vol. 70, no. 6, pp. 2213-2223.

Hayes, A.J., Huang, W.Q., Yu, J., Maisonpierre, P.C., Liu, A., Kern, F.G., Lippman, M.E., McLeskey, S.W. & Li, L.Y. 2000, "Expression and function of angiopoietin-1 in breast cancer", *British journal of cancer,* vol. 83, no. 9, pp. 1154-1160.

He, M. & Taussig, M.J. 2007, "Eukaryotic ribosome display with in situ DNA recovery", *Nature methods,* vol. 4, no. 3, pp. 281-288.

Heine, D., Muller, R. & Brusselbach, S. 2001, "Cell surface display of a lysosomal enzyme for extracellular gene-directed enzyme prodrug therapy", *Gene therapy,* vol. 8, no. 13, pp. 1005-1010.

Helfrich, I., Edler, L., Sucker, A., Thomas, M., Christian, S., Schadendorf, D. & Augustin, H.G. 2009, "Angiopoietin-2 levels are associated with disease progression in metastatic malignant melanoma", *Clinical cancer research : an official journal of the American Association for Cancer Research,* vol. 15, no. 4, pp. 1384-1392.

Hellinga, H.W. 1997, "Rational protein design: Combining theory andâ€‰experiment", *Proceedings of the National Academy of Sciences of the United States of America,* vol. 94, no. 19, pp. 10015-10017.

Ho, M., Nagata, S. & Pastan, I. 2006, "Isolation of anti-CD22 Fv with high affinity by Fv display on human cells", *Proceedings of the National Academy of Sciences of the United States of America,* vol. 103, no. 25, pp. 9637-9642.

Holopainen, T., Saharinen, P., D'Amico, G., Lampinen, A., Eklund, L., Sormunen, R., Anisimov, A., Zarkada, G., Lohela, M., Helotera, H., Tammela, T., Benjamin, L.E., Yla-Herttuala, S., Leow, C.C., Koh, G.Y. & Alitalo, K. 2012, "Effects of angiopoietin-2-blocking antibody on endothelial cell-cell junctions and lung

metastasis", *Journal of the National Cancer Institute,* vol. 104, no. 6, pp. 461-475.

Hu, B., Jarzynka, M.J., Guo, P., Imanishi, Y., Schlaepfer, D.D. & Cheng, S.Y. 2006, "Angiopoietin 2 induces glioma cell invasion by stimulating matrix metalloprotease 2 expression through the alphavbeta1 integrin and focal adhesion kinase signaling pathway", *Cancer research,* vol. 66, no. 2, pp. 775-783.

Huang, C. 2009, "Receptor-Fc fusion therapeutics, traps, and MIMETIBODY technology", *Current opinion in biotechnology,* vol. 20, no. 6, pp. 692-699.

Huang, H., Lai, J.Y., Do, J., Liu, D., Li, L., Del Rosario, J., Doppalapudi, V.R., Pirie-Shepherd, S., Levin, N., Bradshaw, C., Woodnutt, G., Lappe, R. & Bhat, A. 2011, "Specifically targeting angiopoietin-2 inhibits angiogenesis, Tie2-expressing monocyte infiltration, and tumor growth", *Clinical cancer research : an official journal of the American Association for Cancer Research,* vol. 17, no. 5, pp. 1001-1011.

Hurwitz, H. 2004, "Integrating the anti-VEGF-A humanized monoclonal antibody bevacizumab with chemotherapy in advanced colorectal cancer", *Clinical colorectal cancer,* vol. 4 Suppl 2, pp. S62-8.

Hyre, D.E., Le Trong, I., Freitag, S., Stenkamp, R.E. & Stayton, P.S. 2000, "Ser45 plays an important role in managing both the equilibrium and transition state energetics of the streptavidin-biotin system", *Protein science : a publication of the Protein Society,* vol. 9, no. 5, pp. 878-885.

Imanishi, Y., Hu, B., Jarzynka, M.J., Guo, P., Elishaev, E., Bar-Joseph, I. & Cheng, S.Y. 2007, "Angiopoietin-2 stimulates breast cancer metastasis through the alpha(5)beta(1) integrin-mediated pathway", *Cancer research,* vol. 67, no. 9, pp. 4254-4263.

Iwamoto, F.M., Abrey, L.E., Beal, K., Gutin, P.H., Rosenblum, M.K., Reuter, V.E., DeAngelis, L.M. & Lassman, A.B. 2009, "Patterns of relapse and prognosis after bevacizumab failure in recurrent glioblastoma", *Neurology,* vol. 73, no. 15, pp. 1200-1206.

Jones, P.F. 2003, "Not just angiogenesis--wider roles for the angiopoietins", *The Journal of pathology,* vol. 201, no. 4, pp. 515-527.

Joussen, A.M., Poulaki, V., Tsujikawa, A., Qin, W., Qaum, T., Xu, Q., Moromizato, Y., Bursell, S.E., Wiegand, S.J., Rudge, J., Ioffe, E., Yancopoulos, G.D. & Adamis, A.P. 2002, "Suppression of diabetic retinopathy with angiopoietin-1", *The American journal of pathology,* vol. 160, no. 5, pp. 1683-1693.

Karlan, B.Y., Oza, A.M., Richardson, G.E., Provencher, D.M., Hansen, V.L., Buck, M., Chambers, S.K., Ghatage, P., Pippitt, C.H.,Jr, Brown, J.V.,3rd, Covens, A., Nagarkar, R.V., Davy, M., Leath, C.A.,3rd, Nguyen, H., Stepan, D.E., Weinreich,

D.M., Tassoudji, M., Sun, Y.N. & Vergote, I.B. 2012, "Randomized, double-blind, placebo-controlled phase II study of AMG 386 combined with weekly paclitaxel in patients with recurrent ovarian cancer", *Journal of clinical oncology : official journal of the American Society of Clinical Oncology,* vol. 30, no. 4, pp. 362-371.

Kieke, M.C., Cho, B.K., Boder, E.T., Kranz, D.M. & Wittrup, K.D. 1997, "Isolation of anti-T cell receptor scFv mutants by yeast surface display", *Protein engineering,* vol. 10, no. 11, pp. 1303-1310.

Kieke, M.C., Shusta, E.V., Boder, E.T., Teyton, L., Wittrup, K.D. & Kranz, D.M. 1999, "Selection of functional T cell receptor mutants from a yeast surface-display library", *Proceedings of the National Academy of Sciences of the United States of America,* vol. 96, no. 10, pp. 5651-5656.

Kim, H.Z., Jung, K., Kim, H.M., Cheng, Y. & Koh, G.Y. 2009, "A designed angiopoietin-2 variant, pentameric COMP-Ang2, strongly activates Tie2 receptor and stimulates angiogenesis", *Biochimica et biophysica acta,* vol. 1793, no. 5, pp. 772-780.

Kim, K.T., Choi, H.H., Steinmetz, M.O., Maco, B., Kammerer, R.A., Ahn, S.Y., Kim, H.Z., Lee, G.M. & Koh, G.Y. 2005, "Oligomerization and multimerization are critical for angiopoietin-1 to bind and phosphorylate Tie2", *The Journal of biological chemistry,* vol. 280, no. 20, pp. 20126-20131.

Kioi, M., Vogel, H., Schultz, G., Hoffman, R.M., Harsh, G.R. & Brown, J.M. 2010, "Inhibition of vasculogenesis, but not angiogenesis, prevents the recurrence of glioblastoma after irradiation in mice", *The Journal of clinical investigation,* vol. 120, no. 3, pp. 694-705.

Koga, N., Tatsumi-Koga, R., Liu, G., Xiao, R., Acton, T.B., Montelione, G.T. & Baker, D. 2012, "Principles for designing ideal protein structures", *Nature,* vol. 491, no. 7423, pp. 222-227.

Koh, Y.J., Kim, H.Z., Hwang, S.I., Lee, J.E., Oh, N., Jung, K., Kim, M., Kim, K.E., Kim, H., Lim, N.K., Jeon, C.J., Lee, G.M., Jeon, B.H., Nam, D.H., Sung, H.K., Nagy, A., Yoo, O.J. & Koh, G.Y. 2010, "Double antiangiogenic protein, DAAP, targeting VEGF-A and angiopoietins in tumor angiogenesis, metastasis, and vascular leakage", *Cancer cell,* vol. 18, no. 2, pp. 171-184.

Kontermann, R.E. & Muller, R. 1999, "Intracellular and cell surface displayed single-chain diabodies", *Journal of immunological methods,* vol. 226, no. 1-2, pp. 179-188.

Kothapalli, N., Norton, D.D. & Fugmann, S.D. 2008, "Cutting edge: a cis-acting DNA element targets AID-mediated sequence diversification to the chicken Ig light chain gene locus", *Journal of immunology (Baltimore, Md.: 1950),* vol. 180, no. 4, pp. 2019-2023.

Kronick, M.N. & Grossman, P.D. 1983, "Immunoassay techniques with fluorescent phycobiliprotein conjugates", *Clinical chemistry,* vol. 29, no. 9, pp. 1582-1586.

Kuboki, S., Shimizu, H., Mitsuhashi, N., Kusashio, K., Kimura, F., Yoshidome, H., Ohtsuka, M., Kato, A., Yoshitomi, H. & Miyazaki, M. 2008, "Angiopoietin-2 levels in the hepatic vein as a useful predictor of tumor invasiveness and prognosis in human hepatocellular carcinoma", *Journal of gastroenterology and hepatology,* vol. 23, no. 7 Pt 2, pp. e157-64.

Lander, E.S., Linton, L.M., Birren, B., Nusbaum, C., Zody, M.C., Baldwin, J., Devon, K., Dewar, K., Doyle, M., FitzHugh, W., Funke, R., Gage, D., Harris, K., Heaford, A., Howland, J., Kann, L., Lehoczky, J., LeVine, R., McEwan, P., McKernan, K., Meldrim, J., Mesirov, J.P., Miranda, C., Morris, W., Naylor, J., Raymond, C., Rosetti, M., Santos, R., Sheridan, A., Sougnez, C., Stange-Thomann, N., Stojanovic, N., Subramanian, A., Wyman, D., Rogers, J., Sulston, J., Ainscough, R., Beck, S., Bentley, D., Burton, J., Clee, C., Carter, N., Coulson, A., Deadman, R., Deloukas, P., Dunham, A., Dunham, I., Durbin, R., French, L., Grafham, D., Gregory, S., Hubbard, T., Humphray, S., Hunt, A., Jones, M., Lloyd, C., McMurray, A., Matthews, L., Mercer, S., Milne, S., Mullikin, J.C., Mungall, A., Plumb, R., Ross, M., Shownkeen, R., Sims, S., Waterston, R.H., Wilson, R.K., Hillier, L.W., McPherson, J.D., Marra, M.A., Mardis, E.R., Fulton, L.A., Chinwalla, A.T., Pepin, K.H., Gish, W.R., Chissoe, S.L., Wendl, M.C., Delehaunty, K.D., Miner, T.L., Delehaunty, A., Kramer, J.B., Cook, L.L., Fulton, R.S., Johnson, D.L., Minx, P.J., Clifton, S.W., Hawkins, T., Branscomb, E., Predki, P., Richardson, P., Wenning, S., Slezak, T., Doggett, N., Cheng, J.F., Olsen, A., Lucas, S., Elkin, C., Uberbacher, E., Frazier, M., Gibbs, R.A., Muzny, D.M., Scherer, S.E., Bouck, J.B., Sodergren, E.J., Worley, K.C., Rives, C.M., Gorrell, J.H., Metzker, M.L., Naylor, S.L., Kucherlapati, R.S., Nelson, D.L., Weinstock, G.M., Sakaki, Y., Fujiyama, A., Hattori, M., Yada, T., Toyoda, A., Itoh, T., Kawagoe, C., Watanabe, H., Totoki, Y., Taylor, T., Weissenbach, J., Heilig, R., Saurin, W., Artiguenave, F., Brottier, P., Bruls, T., Pelletier, E., Robert, C., Wincker, P., Smith, D.R., Doucette-Stamm, L., Rubenfield, M., Weinstock, K., Lee, H.M., Dubois, J., Rosenthal, A., Platzer, M., Nyakatura, G., Taudien, S., Rump, A., Yang, H., Yu, J., Wang, J., Huang, G., Gu, J., Hood, L., Rowen, L., Madan, A., Qin, S., Davis, R.W., Federspiel, N.A., Abola, A.P., Proctor, M.J., Myers, R.M., Schmutz, J., Dickson, M., Grimwood, J., Cox, D.R., Olson, M.V., Kaul, R., Raymond, C., Shimizu, N., Kawasaki, K., Minoshima, S., Evans, G.A., Athanasiou, M., Schultz, R., Roe, B.A., Chen, F., Pan, H., Ramser, J., Lehrach, H., Reinhardt, R., McCombie, W.R., de la Bastide, M., Dedhia, N., Blocker, H., Hornischer, K., Nordsiek, G., Agarwala, R., Aravind, L., Bailey, J.A., Bateman, A., Batzoglou, S., Birney, E., Bork, P., Brown, D.G., Burge, C.B., Cerutti, L., Chen, H.C., Church, D., Clamp, M., Copley, R.R., Doerks, T., Eddy, S.R., Eichler, E.E., Furey, T.S., Galagan, J., Gilbert, J.G., Harmon, C., Hayashizaki, Y., Haussler, D., Hermjakob, H., Hokamp, K., Jang, W., Johnson, L.S., Jones, T.A., Kasif, S., Kaspryzk, A., Kennedy, S., Kent, W.J., Kitts, P., Koonin, E.V., Korf, I., Kulp, D., Lancet, D., Lowe, T.M., McLysaght, A., Mikkelsen, T., Moran, J.V., Mulder, N., Pollara, V.J., Ponting, C.P., Schuler, G., Schultz, J., Slater, G., Smit, A.F., Stupka, E., Szustakowski, J., Thierry-Mieg, D., Thierry-Mieg, J., Wagner, L., Wallis, J., Wheeler, R., Williams, A., Wolf, Y.I., Wolfe, K.H., Yang, S.P., Yeh, R.F., Collins, F., Guyer, M.S., Peterson, J., Felsenfeld, A., Wetterstrand, K.A., Patrinos, A., Morgan,

M.J., de Jong, P., Catanese, J.J., Osoegawa, K., Shizuya, H., Choi, S., Chen, Y.J. & International Human Genome Sequencing Consortium 2001, "Initial sequencing and analysis of the human genome", *Nature,* vol. 409, no. 6822, pp. 860-921.

Lebecque, S.G. & Gearhart, P.J. 1990, "Boundaries of somatic mutation in rearranged immunoglobulin genes: 5' boundary is near the promoter, and 3' boundary is approximately 1 kb from V(D)J gene", *The Journal of experimental medicine,* vol. 172, no. 6, pp. 1717-1727.

Lofblom, J., Sandberg, J., Wernerus, H. & Stahl, S. 2007, "Evaluation of staphylococcal cell surface display and flow cytometry for postselectional characterization of affinity proteins in combinatorial protein engineering applications", *Applied and Environmental Microbiology,* vol. 73, no. 21, pp. 6714-6721.

Lowman, H.B., Bass, S.H., Simpson, N. & Wells, J.A. 1991, "Selecting high-affinity binding proteins by monovalent phage display", *Biochemistry,* vol. 30, no. 45, pp. 10832-10838.

Macdonald, P.R., Progias, P., Ciani, B., Patel, S., Mayer, U., Steinmetz, M.O. & Kammerer, R.A. 2006, "Structure of the extracellular domain of Tie receptor tyrosine kinases and localization of the angiopoietin-binding epitope", *The Journal of biological chemistry,* vol. 281, no. 38, pp. 28408-28414.

Machein, M.R., Knedla, A., Knoth, R., Wagner, S., Neuschl, E. & Plate, K.H. 2004, "Angiopoietin-1 promotes tumor angiogenesis in a rat glioma model", *The American journal of pathology,* vol. 165, no. 5, pp. 1557-1570.

Magari, M., Kanehiro, Y., Todo, K., Ikeda, M., Kanayama, N. & Ohmori, H. 2010, "Enhancement of hypermutation frequency in the chicken B cell line DT40 for efficient diversification of the antibody repertoire", *Biochemical and biophysical research communications,* vol. 396, no. 2, pp. 353-358.

Maisonpierre, P.C., Suri, C., Jones, P.F., Bartunkova, S., Wiegand, S.J., Radziejewski, C., Compton, D., McClain, J., Aldrich, T.H., Papadopoulos, N., Daly, T.J., Davis, S., Sato, T.N. & Yancopoulos, G.D. 1997, "Angiopoietin-2, a natural antagonist for Tie2 that disrupts in vivo angiogenesis", *Science (New York, N.Y.),* vol. 277, no. 5322, pp. 55-60.

Majors, B.S., Chiang, G.G. & Betenbaugh, M.J. 2009, "Protein and genome evolution in Mammalian cells for biotechnology applications", *Molecular biotechnology,* vol. 42, no. 2, pp. 216-223.

Majors, B.S., Chiang, G.G., Pederson, N.E. & Betenbaugh, M.J. 2012, "Directed evolution of mammalian anti-apoptosis proteins by somatic hypermutation", *Protein engineering, design & selection : PEDS,* vol. 25, no. 1, pp. 27-38.

Marron, M.B., Hughes, D.P., Edge, M.D., Forder, C.L. & Brindle, N.P. 2000, "Evidence for heterotypic interaction between the receptor tyrosine kinases TIE-1 and TIE-2", *The Journal of biological chemistry,* vol. 275, no. 50, pp. 39741-39746.

Marron, M.B., Singh, H., Tahir, T.A., Kavumkal, J., Kim, H.Z., Koh, G.Y. & Brindle, N.P. 2007, "Regulated proteolytic processing of Tie1 modulates ligand responsiveness of the receptor-tyrosine kinase Tie2", *The Journal of biological chemistry,* vol. 282, no. 42, pp. 30509-30517.

Martin, A. & Scharff, M.D. 2002, "Somatic hypermutation of the AID transgene in B and non-B cells", *Proceedings of the National Academy of Sciences of the United States of America,* vol. 99, no. 19, pp. 12304-12308.

Mazzieri, R., Pucci, F., Moi, D., Zonari, E., Ranghetti, A., Berti, A., Politi, L.S., Gentner, B., Brown, J.L., Naldini, L. & De Palma, M. 2011, "Targeting the ANG2/TIE2 axis inhibits tumor growth and metastasis by impairing angiogenesis and disabling rebounds of proangiogenic myeloid cells", *Cancer cell,* vol. 19, no. 4, pp. 512-526.

McConnell, A.D., Do, M., Neben, T.Y., Spasojevic, V., Maclaren, J., Chen, A.P., Altobell, L.,3rd, Macomber, J.L., Berkebile, A.D., Horlick, R.A., Bowers, P.M. & King, D.J. 2012, "High Affinity Humanized Antibodies without Making Hybridomas; Immunization Paired with Mammalian Cell Display and In Vitro Somatic Hypermutation", *PloS one,* vol. 7, no. 11, pp. e49458.

McKean, D., Huppi, K., Bell, M., Staudt, L., Gerhard, W. & Weigert, M. 1984, "Generation of antibody diversity in the immune response of BALB/c mice to influenza virus hemagglutinin", *Proceedings of the National Academy of Sciences of the United States of America,* vol. 81, no. 10, pp. 3180-3184.

Morley, K.L. & Kazlauskas, R.J. 2005, "Improving enzyme properties: when are closer mutations better?", *Trends in biotechnology,* vol. 23, no. 5, pp. 231-237.

Mullis, K.B. & Faloona, F.A. 1987, "Specific synthesis of DNA in vitro via a polymerase-catalyzed chain reaction", *Methods in enzymology,* vol. 155, pp. 335-350.

Muramatsu, M., Kinoshita, K., Fagarasan, S., Yamada, S., Shinkai, Y. & Honjo, T. 2000, "Class switch recombination and hypermutation require activation-induced cytidine deaminase (AID), a potential RNA editing enzyme", *Cell,* vol. 102, no. 5, pp. 553-563.

Muramatsu, M., Sankaranand, V.S., Anant, S., Sugai, M., Kinoshita, K., Davidson, N.O. & Honjo, T. 1999, "Specific expression of activation-induced cytidine deaminase (AID), a novel member of the RNA-editing deaminase family in germinal center B cells", *The Journal of biological chemistry,* vol. 274, no. 26, pp. 18470-18476.

Nakamura, K., Kogame, T., Oshiumi, H., Shinohara, A., Sumitomo, Y., Agama, K., Pommier, Y., Tsutsui, K.M., Tsutsui, K., Hartsuiker, E., Ogi, T., Takeda, S. & Taniguchi, Y. 2010, "Collaborative action of Brca1 and CtIP in elimination of covalent modifications from double-strand breaks to facilitate subsequent break repair", *PLoS genetics,* vol. 6, no. 1, pp. e1000828.

Nakamura, T. & Matsumoto, K. 2005, "Angiogenesis inhibitors: from laboratory to clinical application", *Biochemical and biophysical research communications,* vol. 333, no. 2, pp. 289-291.

Nambu, H., Nambu, R., Oshima, Y., Hackett, S.F., Okoye, G., Wiegand, S., Yancopoulos, G., Zack, D.J. & Campochiaro, P.A. 2004, "Angiopoietin 1 inhibits ocular neovascularization and breakdown of the blood-retinal barrier", *Gene therapy,* vol. 11, no. 10, pp. 865-873.

Nambu, Y., Sugai, M., Gonda, H., Lee, C.G., Katakai, T., Agata, Y., Yokota, Y. & Shimizu, A. 2003, "Transcription-coupled events associating with immunoglobulin switch region chromatin", *Science (New York, N.Y.),* vol. 302, no. 5653, pp. 2137-2140.

Neuberger, M.S. & Rada, C. 2007, "Somatic hypermutation: activation-induced deaminase for C/G followed by polymerase eta for A/T", *The Journal of experimental medicine,* vol. 204, no. 1, pp. 7-10.

Nieba, L., Krebber, A. & Pluckthun, A. 1996, "Competition BIAcore for measuring true affinities: large differences from values determined from binding kinetics", *Analytical Biochemistry,* vol. 234, no. 2, pp. 155-165.

Nishimura, K., Fukagawa, T., Takisawa, H., Kakimoto, T. & Kanemaki, M. 2009, "An auxin-based degron system for the rapid depletion of proteins in nonplant cells", *Nature methods,* vol. 6, no. 12, pp. 917-922.

Novotny, N.M., Lahm, T., Markel, T.A., Crisostomo, P.R., Wang, M., Wang, Y., Tan, J. & Meldrum, D.R. 2009, "Angiopoietin-1 in the treatment of ischemia and sepsis", *Shock (Augusta, Ga.),* vol. 31, no. 4, pp. 335-341.

Oliner, J., Min, H., Leal, J., Yu, D., Rao, S., You, E., Tang, X., Kim, H., Meyer, S., Han, S.J., Hawkins, N., Rosenfeld, R., Davy, E., Graham, K., Jacobsen, F., Stevenson, S., Ho, J., Chen, Q., Hartmann, T., Michaels, M., Kelley, M., Li, L., Sitney, K., Martin, F., Sun, J.R., Zhang, N., Lu, J., Estrada, J., Kumar, R., Coxon, A., Kaufman, S., Pretorius, J., Scully, S., Cattley, R., Payton, M., Coats, S., Nguyen, L., Desilva, B., Ndifor, A., Hayward, I., Radinsky, R., Boone, T. & Kendall, R. 2004, "Suppression of angiogenesis and tumor growth by selective inhibition of angiopoietin-2", *Cancer cell,* vol. 6, no. 5, pp. 507-516.

Orencia, M.C., Yoon, J.S., Ness, J.E., Stemmer, W.P. & Stevens, R.C. 2001, "Predicting the emergence of antibiotic resistance by directed evolution and structural analysis", *Nature structural biology,* vol. 8, no. 3, pp. 238-242.

Orengo, C.A., Jones, D.T. & Thornton, J.M. 1994, "Protein superfamilies and domain superfolds", *Nature,* vol. 372, no. 6507, pp. 631-634.

Orfanos, S.E., Kotanidou, A., Glynos, C., Athanasiou, C., Tsigkos, S., Dimopoulou, I., Sotiropoulou, C., Zakynthinos, S., Armaganidis, A., Papapetropoulos, A. & Roussos, C. 2007, "Angiopoietin-2 is increased in severe sepsis: correlation with inflammatory mediators", *Critical Care Medicine,* vol. 35, no. 1, pp. 199-206.

Park, J.H., Park, K.J., Kim, Y.S., Sheen, S.S., Lee, K.S., Lee, H.N., Oh, Y.J. & Hwang, S.C. 2007, "Serum angiopoietin-2 as a clinical marker for lung cancer", *Chest,* vol. 132, no. 1, pp. 200-206.

Partanen, J., Puri, M.C., Schwartz, L., Fischer, K.D., Bernstein, A. & Rossant, J. 1996, "Cell autonomous functions of the receptor tyrosine kinase TIE in a late phase of angiogenic capillary growth and endothelial cell survival during murine development", *Development (Cambridge, England),* vol. 122, no. 10, pp. 3013-3021.

Peters, K.G., Kontos, C.D., Lin, P.C., Wong, A.L., Rao, P., Huang, L., Dewhirst, M.W. & Sankar, S. 2004, "Functional significance of Tie2 signaling in the adult vasculature", *Recent progress in hormone research,* vol. 59, pp. 51-71.

Procopio, W.N., Pelavin, P.I., Lee, W.M. & Yeilding, N.M. 1999, "Angiopoietin-1 and -2 coiled coil domains mediate distinct homo-oligomerization patterns, but fibrinogen-like domains mediate ligand activity", *The Journal of biological chemistry,* vol. 274, no. 42, pp. 30196-30201.

Rada, C., Ehrenstein, M.R., Neuberger, M.S. & Milstein, C. 1998, "Hot spot focusing of somatic hypermutation in MSH2-deficient mice suggests two stages of mutational targeting", *Immunity,* vol. 9, no. 1, pp. 135-141.

Rada, C., Yelamos, J., Dean, W. & Milstein, C. 1997, "The 5' hypermutation boundary of kappa chains is independent of local and neighbouring sequences and related to the distance from the initiation of transcription", *European journal of immunology,* vol. 27, no. 12, pp. 3115-3120.

Rajewsky, K., Forster, I. & Cumano, A. 1987, "Evolutionary and somatic selection of the antibody repertoire in the mouse", *Science (New York, N.Y.),* vol. 238, no. 4830, pp. 1088-1094.

Ramiro, A.R., Stavropoulos, P., Jankovic, M. & Nussenzweig, M.C. 2003, "Transcription enhances AID-mediated cytidine deamination by exposing single-stranded DNA on the nontemplate strand", *Nature immunology,* vol. 4, no. 5, pp. 452-456.

Ramsauer, M. & D'Amore, P.A. 2002, "Getting Tie(2)d up in angiogenesis", *The Journal of clinical investigation,* vol. 110, no. 11, pp. 1615-1617.

Randow, F. & Sale, J.E. 2006, "Retroviral transduction of DT40", *Sub-cellular biochemistry,* vol. 40, pp. 383-386.

Rennel, E.S., Regula, J.T., Harper, S.J., Thomas, M., Klein, C. & Bates, D.O. 2011, "A human neutralizing antibody specific to Ang-2 inhibits ocular angiogenesis", *Microcirculation (New York, N.Y.: 1994),* vol. 18, no. 7, pp. 598-607.

Roberts, R.W. & Szostak, J.W. 1997, "RNA-peptide fusions for the in vitro selection of peptides and proteins", *Proceedings of the National Academy of Sciences of the United States of America,* vol. 94, no. 23, pp. 12297-12302.

Rogozin, I.B. & Diaz, M. 2004, "Cutting edge: DGYW/WRCH is a better predictor of mutability at G:C bases in Ig hypermutation than the widely accepted RGYW/WRCY motif and probably reflects a two-step activation-induced cytidine deaminase-triggered process", *Journal of immunology (Baltimore, Md.: 1950),* vol. 172, no. 6, pp. 3382-3384.

Rogozin, I.B. & Kolchanov, N.A. 1992, "Somatic hypermutagenesis in immunoglobulin genes. II. Influence of neighbouring base sequences on mutagenesis", *Biochimica et biophysica acta,* vol. 1171, no. 1, pp. 11-18.

Rogozin, I.B., Pavlov, Y.I., Bebenek, K., Matsuda, T. & Kunkel, T.A. 2001, "Somatic mutation hotspots correlate with DNA polymerase eta error spectrum", *Nature immunology,* vol. 2, no. 6, pp. 530-536.

Romero, P.A. & Arnold, F.H. 2009, "Exploring protein fitness landscapes by directed evolution", *Nature reviews.Molecular cell biology,* vol. 10, no. 12, pp. 866-876.

Roopenian, D.C. & Akilesh, S. 2007, "FcRn: the neonatal Fc receptor comes of age", *Nature reviews.Immunology,* vol. 7, no. 9, pp. 715-725.

Saharinen, P., Eklund, L., Miettinen, J., Wirkkala, R., Anisimov, A., Winderlich, M., Nottebaum, A., Vestweber, D., Deutsch, U., Koh, G.Y., Olsen, B.R. & Alitalo, K. 2008, "Angiopoietins assemble distinct Tie2 signalling complexes in endothelial cell-cell and cell-matrix contacts", *Nature cell biology,* vol. 10, no. 5, pp. 527-537.

Sale, J.E. 2006, "Stable non-targeted transfection of DT40", *Sub-cellular biochemistry,* vol. 40, pp. 341-344.

Sale, J.E., Calandrini, D.M., Takata, M., Takeda, S. & Neuberger, M.S. 2001, "Ablation of XRCC2/3 transforms immunoglobulin V gene conversion into somatic hypermutation", *Nature,* vol. 412, no. 6850, pp. 921-926.

Sale, J.E. & Neuberger, M.S. 1998, "TdT-accessible breaks are scattered over the immunoglobulin V domain in a constitutively hypermutating B cell line", *Immunity,* vol. 9, no. 6, pp. 859-869.

Saribasak, H. & Arakawa, H. 2006, "Targeted transfection of DT40 cells", *Sub-cellular biochemistry,* vol. 40, pp. 419-421.

Sato, T.N., Qin, Y., Kozak, C.A. & Audus, K.L. 1993, "Tie-1 and tie-2 define another class of putative receptor tyrosine kinase genes expressed in early embryonic vascular system", *Proceedings of the National Academy of Sciences of the United States of America,* vol. 90, no. 20, pp. 9355-9358.

Sato, T.N., Tozawa, Y., Deutsch, U., Wolburg-Buchholz, K., Fujiwara, Y., Gendron-Maguire, M., Gridley, T., Wolburg, H., Risau, W. & Qin, Y. 1995, "Distinct roles of the receptor tyrosine kinases Tie-1 and Tie-2 in blood vessel formation", *Nature,* vol. 376, no. 6535, pp. 70-74.

Scharpfenecker, M., Fiedler, U., Reiss, Y. & Augustin, H.G. 2005, "The Tie-2 ligand angiopoietin-2 destabilizes quiescent endothelium through an internal autocrine loop mechanism", *Journal of cell science,* vol. 118, no. Pt 4, pp. 771-780.

Schnurch, H. & Risau, W. 1993, "Expression of tie-2, a member of a novel family of receptor tyrosine kinases, in the endothelial cell lineage", *Development (Cambridge, England),* vol. 119, no. 3, pp. 957-968.

Schoetz, U., Cervelli, M., Wang, Y.D., Fiedler, P. & Buerstedde, J.M. 2006, "E2A expression stimulates Ig hypermutation", *Journal of immunology (Baltimore, Md.: 1950),* vol. 177, no. 1, pp. 395-400.

Seo, H., Masuoka, M., Murofushi, H., Takeda, S., Shibata, T. & Ohta, K. 2005, "Rapid generation of specific antibodies by enhanced homologous recombination", *Nature biotechnology,* vol. 23, no. 6, pp. 731-735.

Seo, H., Yamada, T., Hashimoto, S., Lin, W. & Ohta, K. 2007, "Modulation of immunoglobulin gene conversion in chicken DT40 by enhancing histone acetylation, and its application to antibody engineering", *Biotechnology & genetic engineering reviews,* vol. 24, pp. 179-193.

Shafikhani, S., Siegel, R.A., Ferrari, E. & Schellenberger, V. 1997, "Generation of large libraries of random mutants in Bacillus subtilis by PCR-based plasmid multimerization", *BioTechniques,* vol. 23, no. 2, pp. 304-310.

Shim, A.H., Liu, H., Focia, P.J., Chen, X., Lin, P.C. & He, X. 2010, "Structures of a platelet-derived growth factor/propeptide complex and a platelet-derived growth factor/receptor complex", *Proceedings of the National Academy of Sciences of the United States of America,* vol. 107, no. 25, pp. 11307-11312.

Shim, W.S., Teh, M., Bapna, A., Kim, I., Koh, G.Y., Mack, P.O. & Ge, R. 2002, "Angiopoietin 1 promotes tumor angiogenesis and tumor vessel plasticity of human cervical cancer in mice", *Experimental cell research,* vol. 279, no. 2, pp. 299-309.

Shimotohno, A., Oue, S., Yano, T., Kuramitsu, S. & Kagamiyama, H. 2001, "Demonstration of the importance and usefulness of manipulating non-active-site residues in protein design", *Journal of Biochemistry,* vol. 129, no. 6, pp. 943-948.

Shyu, K.G., Manor, O., Magner, M., Yancopoulos, G.D. & Isner, J.M. 1998, "Direct intramuscular injection of plasmid DNA encoding angiopoietin-1 but not angiopoietin-2 augments revascularization in the rabbit ischemic hindlimb", *Circulation,* vol. 98, no. 19, pp. 2081-2087.

Simpson, L.J. & Sale, J.E. 2003, "Rev1 is essential for DNA damage tolerance and non-templated immunoglobulin gene mutation in a vertebrate cell line", *The EMBO journal,* vol. 22, no. 7, pp. 1654-1664.

Singh, H., Hansen, T.M., Patel, N. & Brindle, N.P. 2012, "The molecular balance between receptor tyrosine kinases Tie1 and Tie2 is dynamically controlled by VEGF and TNFalpha and regulates angiopoietin signalling", *PloS one,* vol. 7, no. 1, pp. e29319.

Sklar, L.A., Sayre, J., McNeil, V.M. & Finney, D.A. 1985, "Competitive binding kinetics in ligand-receptor-competitor systems. Rate parameters for unlabeled ligands for the formyl peptide receptor", *Molecular pharmacology,* vol. 28, no. 4, pp. 323-330.

Spiess, M., Schwartz, A.L. & Lodish, H.F. 1985, "Sequence of human asialoglycoprotein receptor cDNA. An internal signal sequence for membrane insertion", *The Journal of biological chemistry,* vol. 260, no. 4, pp. 1979-1982.

Spiller, B., Gershenson, A., Arnold, F.H. & Stevens, R.C. 1999, "A structural view of evolutionary divergence", *Proceedings of the National Academy of Sciences of the United States of America,* vol. 96, no. 22, pp. 12305-12310.

Stemmer, W.P. 1994, "Rapid evolution of a protein in vitro by DNA shuffling", *Nature,* vol. 370, no. 6488, pp. 389-391.

Sullivan, C.C., Du, L., Chu, D., Cho, A.J., Kido, M., Wolf, P.L., Jamieson, S.W. & Thistlethwaite, P.A. 2003, "Induction of pulmonary hypertension by an angiopoietin 1/TIE2/serotonin pathway", *Proceedings of the National Academy of Sciences of the United States of America,* vol. 100, no. 21, pp. 12331-12336.

Suri, C., Jones, P.F., Patan, S., Bartunkova, S., Maisonpierre, P.C., Davis, S., Sato, T.N. & Yancopoulos, G.D. 1996, "Requisite role of angiopoietin-1, a ligand for the TIE2 receptor, during embryonic angiogenesis", *Cell,* vol. 87, no. 7, pp. 1171-1180.

Thomas, M. & Augustin, H.G. 2009, "The role of the Angiopoietins in vascular morphogenesis", *Angiogenesis,* vol. 12, no. 2, pp. 125-137.

Tian, S., Hayes, A.J., Metheny-Barlow, L.J. & Li, L.Y. 2002, "Stabilization of breast cancer xenograft tumour neovasculature by angiopoietin-1", *British journal of cancer,* vol. 86, no. 4, pp. 645-651.

Tokuriki, N. & Tawfik, D.S. 2009, "Stability effects of mutations and protein evolvability", *Current opinion in structural biology,* vol. 19, no. 5, pp. 596-604.

Tsiamis, A.C., Morris, P.N., Marron, M.B. & Brindle, N.P. 2002, "Vascular endothelial growth factor modulates the Tie-2:Tie-1 receptor complex", *Microvascular research,* vol. 63, no. 2, pp. 149-158.

Valenzuela, D.M., Griffiths, J.A., Rojas, J., Aldrich, T.H., Jones, P.F., Zhou, H., McClain, J., Copeland, N.G., Gilbert, D.J., Jenkins, N.A., Huang, T., Papadopoulos, N., Maisonpierre, P.C., Davis, S. & Yancopoulos, G.D. 1999, "Angiopoietins 3 and 4: diverging gene counterparts in mice and humans", *Proceedings of the National Academy of Sciences of the United States of America,* vol. 96, no. 5, pp. 1904-1909.

Venter, J.C., Adams, M.D., Myers, E.W., Li, P.W., Mural, R.J., Sutton, G.G., Smith, H.O., Yandell, M., Evans, C.A., Holt, R.A., Gocayne, J.D., Amanatides, P., Ballew, R.M., Huson, D.H., Wortman, J.R., Zhang, Q., Kodira, C.D., Zheng, X.H., Chen, L., Skupski, M., Subramanian, G., Thomas, P.D., Zhang, J., Gabor Miklos, G.L., Nelson, C., Broder, S., Clark, A.G., Nadeau, J., McKusick, V.A., Zinder, N., Levine, A.J., Roberts, R.J., Simon, M., Slayman, C., Hunkapiller, M., Bolanos, R., Delcher, A., Dew, I., Fasulo, D., Flanigan, M., Florea, L., Halpern, A., Hannenhalli, S., Kravitz, S., Levy, S., Mobarry, C., Reinert, K., Remington, K., Abu-Threideh, J., Beasley, E., Biddick, K., Bonazzi, V., Brandon, R., Cargill, M., Chandramouliswaran, I., Charlab, R., Chaturvedi, K., Deng, Z., Di Francesco, V., Dunn, P., Eilbeck, K., Evangelista, C., Gabrielian, A.E., Gan, W., Ge, W., Gong, F., Gu, Z., Guan, P., Heiman, T.J., Higgins, M.E., Ji, R.R., Ke, Z., Ketchum, K.A., Lai, Z., Lei, Y., Li, Z., Li, J., Liang, Y., Lin, X., Lu, F., Merkulov, G.V., Milshina, N., Moore, H.M., Naik, A.K., Narayan, V.A., Neelam, B., Nusskern, D., Rusch, D.B., Salzberg, S., Shao, W., Shue, B., Sun, J., Wang, Z., Wang, A., Wang, X., Wang, J., Wei, M., Wides, R., Xiao, C., Yan, C., Yao, A., Ye, J., Zhan, M., Zhang, W., Zhang, H., Zhao, Q., Zheng, L., Zhong, F., Zhong, W., Zhu, S., Zhao, S., Gilbert, D., Baumhueter, S., Spier, G., Carter, C., Cravchik, A., Woodage, T., Ali, F., An, H., Awe, A., Baldwin, D., Baden, H., Barnstead, M., Barrow, I., Beeson, K., Busam, D., Carver, A., Center, A., Cheng, M.L., Curry, L., Danaher, S., Davenport, L., Desilets, R., Dietz, S., Dodson, K., Doup, L., Ferriera, S., Garg, N., Gluecksmann, A., Hart, B., Haynes, J., Haynes, C., Heiner, C., Hladun, S., Hostin, D., Houck, J., Howland, T., Ibegwam, C., Johnson, J., Kalush, F., Kline, L., Koduru, S., Love, A., Mann, F., May, D., McCawley, S., McIntosh, T., McMullen, I., Moy, M., Moy, L., Murphy, B., Nelson, K., Pfannkoch, C., Pratts, E., Puri, V., Qureshi, H., Reardon, M., Rodriguez, R., Rogers, Y.H., Romblad, D., Ruhfel, B., Scott, R., Sitter, C., Smallwood, M., Stewart, E., Strong, R., Suh, E., Thomas, R., Tint, N.N., Tse, S., Vech, C., Wang, G., Wetter, J., Williams, S., Williams, M., Windsor, S., Winn-Deen, E., Wolfe, K., Zaveri, J., Zaveri, K., Abril, J.F., Guigo, R., Campbell, M.J., Sjolander, K.V., Karlak, B., Kejariwal, A., Mi, H., Lazareva, B., Hatton, T., Narechania, A., Diemer, K., Muruganujan, A., Guo, N., Sato, S., Bafna, V., Istrail, S., Lippert, R., Schwartz, R.,

Walenz, B., Yooseph, S., Allen, D., Basu, A., Baxendale, J., Blick, L., Caminha, M., Carnes-Stine, J., Caulk, P., Chiang, Y.H., Coyne, M., Dahlke, C., Mays, A., Dombroski, M., Donnelly, M., Ely, D., Esparham, S., Fosler, C., Gire, H., Glanowski, S., Glasser, K., Glodek, A., Gorokhov, M., Graham, K., Gropman, B., Harris, M., Heil, J., Henderson, S., Hoover, J., Jennings, D., Jordan, C., Jordan, J., Kasha, J., Kagan, L., Kraft, C., Levitsky, A., Lewis, M., Liu, X., Lopez, J., Ma, D., Majoros, W., McDaniel, J., Murphy, S., Newman, M., Nguyen, T., Nguyen, N., Nodell, M., Pan, S., Peck, J., Peterson, M., Rowe, W., Sanders, R., Scott, J., Simpson, M., Smith, T., Sprague, A., Stockwell, T., Turner, R., Venter, E., Wang, M., Wen, M., Wu, D., Wu, M., Xia, A., Zandieh, A. & Zhu, X. 2001, "The sequence of the human genome", *Science (New York, N.Y.),* vol. 291, no. 5507, pp. 1304-1351.

Wabl, M., Burrows, P.D., von Gabain, A. & Steinberg, C. 1985, "Hypermutation at the immunoglobulin heavy chain locus in a pre-B-cell line", *Proceedings of the National Academy of Sciences of the United States of America,* vol. 82, no. 2, pp. 479-482.

Wagner, L.E.,2nd, Betzenhauser, M.J. & Yule, D.I. 2006, "ATP binding to a unique site in the type-1 S2- inositol 1,4,5-trisphosphate receptor defines susceptibility to phosphorylation by protein kinase A", *The Journal of biological chemistry,* vol. 281, no. 25, pp. 17410-17419.

Waller, A., Pipkorn, D., Sutton, K.L., Linderman, J.J. & Omann, G.M. 2001, "Validation of flow cytometric competitive binding protocols and characterization of fluorescently labeled ligands", *Cytometry,* vol. 45, no. 2, pp. 102-114.

Wang, C.L., Harper, R.A. & Wabl, M. 2004, "Genome-wide somatic hypermutation", *Proceedings of the National Academy of Sciences of the United States of America,* vol. 101, no. 19, pp. 7352-7356.

Wang, C.L. & Wabl, M. 2005, "Hypermutation rate normalized by chronological time", *Journal of immunology (Baltimore, Md.: 1950),* vol. 174, no. 9, pp. 5650-5654.

Wang, C.L., Yang, D.C. & Wabl, M. 2004, "Directed molecular evolution by somatic hypermutation", *Protein engineering, design & selection : PEDS,* vol. 17, no. 9, pp. 659-664.

Wang, G., Brennan, C., Rook, M., Wolfe, J.L., Leo, C., Chin, L., Pan, H., Liu, W.H., Price, B. & Makrigiorgos, G.M. 2004a, "Balanced-PCR amplification allows unbiased identification of genomic copy changes in minute cell and tissue samples", *Nucleic acids research,* vol. 32, no. 9, pp. e76.

Wang, J., Takagaki, Y. & Manley, J.L. 1996, "Targeted disruption of an essential vertebrate gene: ASF/SF2 is required for cell viability", *Genes & development,* vol. 10, no. 20, pp. 2588-2599.

Wang, L., Jackson, W.C., Steinbach, P.A. & Tsien, R.Y. 2004b, "Evolution of new nonantibody proteins via iterative somatic hypermutation", *Proceedings of the National Academy of Sciences of the United States of America,* vol. 101, no. 48, pp. 16745-16749.

Wang, M., Rada, C. & Neuberger, M.S. 2010, "Altering the spectrum of immunoglobulin V gene somatic hypermutation by modifying the active site of AID", *The Journal of experimental medicine,* vol. 207, no. 1, pp. 141-153.

Weber, P.C., Ohlendorf, D.H., Wendoloski, J.J. & Salemme, F.R. 1989, "Structural origins of high-affinity biotin binding to streptavidin", *Science (New York, N.Y.),* vol. 243, no. 4887, pp. 85-88.

Wentzel, A., Christmann, A., Kratzner, R. & Kolmar, H. 1999, "Sequence requirements of the GPNG beta-turn of the Ecballium elaterium trypsin inhibitor II explored by combinatorial library screening", *The Journal of biological chemistry,* vol. 274, no. 30, pp. 21037-21043.

White, R.R., Shan, S., Rusconi, C.P., Shetty, G., Dewhirst, M.W., Kontos, C.D. & Sullenger, B.A. 2003, "Inhibition of rat corneal angiogenesis by a nuclease-resistant RNA aptamer specific for angiopoietin-2", *Proceedings of the National Academy of Sciences of the United States of America,* vol. 100, no. 9, pp. 5028-5033.

Witzenbichler, B., Westermann, D., Knueppel, S., Schultheiss, H.P. & Tschope, C. 2005, "Protective role of angiopoietin-1 in endotoxic shock", *Circulation,* vol. 111, no. 1, pp. 97-105.

Woo, C.J., Martin, A. & Scharff, M.D. 2003, "Induction of somatic hypermutation is associated with modifications in immunoglobulin variable region chromatin", *Immunity,* vol. 19, no. 4, pp. 479-489.

Wright, B.E., Schmidt, K.H. & Minnick, M.F. 2004, "Mechanisms by which transcription can regulate somatic hypermutation", *Genes and immunity,* vol. 5, no. 3, pp. 176-182.

Yang, S.Y., Fugmann, S.D. & Schatz, D.G. 2006, "Control of gene conversion and somatic hypermutation by immunoglobulin promoter and enhancer sequences", *The Journal of experimental medicine,* vol. 203, no. 13, pp. 2919-2928.

Yoshikawa, K., Okazaki, I.M., Eto, T., Kinoshita, K., Muramatsu, M., Nagaoka, H. & Honjo, T. 2002, "AID enzyme-induced hypermutation in an actively transcribed gene in fibroblasts", *Science (New York, N.Y.),* vol. 296, no. 5575, pp. 2033-2036.

Yu, Q. & Stamenkovic, I. 2001, "Angiopoietin-2 is implicated in the regulation of tumor angiogenesis", *The American journal of pathology,* vol. 158, no. 2, pp. 563-570.

Yuan, H.T., Khankin, E.V., Karumanchi, S.A. & Parikh, S.M. 2009, "Angiopoietin 2 is a partial agonist/antagonist of Tie2 signaling in the endothelium", *Molecular and cellular biology,* vol. 29, no. 8, pp. 2011-2022.

Yuan, L., Kurek, I., English, J. & Keenan, R. 2005, "Laboratory-directed protein evolution", *Microbiology and molecular biology reviews : MMBR,* vol. 69, no. 3, pp. 373-392.

Zahnd, C., Amstutz, P. & Pluckthun, A. 2007, "Ribosome display: selecting and evolving proteins in vitro that specifically bind to a target", *Nature methods,* vol. 4, no. 3, pp. 269-279.

Zhang, W., Bardwell, P.D., Woo, C.J., Poltoratsky, V., Scharff, M.D. & Martin, A. 2001, "Clonal instability of V region hypermutation in the Ramos Burkitt's lymphoma cell line", *International immunology,* vol. 13, no. 9, pp. 1175-1184.

Zhang, Y., Riesterer, C., Ayrall, A.M., Sablitzky, F., Littlewood, T.D. & Reth, M. 1996, "Inducible site-directed recombination in mouse embryonic stem cells", *Nucleic acids research,* vol. 24, no. 4, pp. 543-548.

Zhou, Y.Z., Fang, X.Q., Li, H., Diao, Y.T., Yang, Y.F., Zhao, D.L., Wu, K. & Li, H.Q. 2007, "Role of serum angiopoietin-2 level in screening for esophageal squamous cell cancer and its precursors", *Chinese medical journal,* vol. 120, no. 14, pp. 1216-1219.

Zimmermann, K., Ahrens, K., Matthes, S., Buerstedde, J.M., Stratling, W.H. & Phi-van, L. 2002, "Targeted disruption of the GAS41 gene encoding a putative transcription factor indicates that GAS41 is essential for cell viability", *The Journal of biological chemistry,* vol. 277, no. 21, pp. 18626-18631.

Zola, H., Neoh, S.H., Mantzioris, B.X., Webster, J. & Loughnan, M.S. 1990, "Detection by immunofluorescence of surface molecules present in low copy numbers. High sensitivity staining and calibration of flow cytometer", *Journal of immunological methods,* vol. 135, no. 1-2, pp. 247-255.

Publications from this thesis

Brindle, N.P.J., Sale, J.E., Arakawa, H., Buerstedde, J-M., Nuamchit, T., Sharma, S., Steele, K.H. 2013, "Directed evolution of an angiopoietin-2 ligand trap by somatic hypermutation and cell surface display", submitted to *Proceedings of the National Academy of Sciences of the United States of America*